

https://dspace.org/

Can a -adrenergic receptor blocker reverse or at least attenuate left ventricular remodelling due to chronic non-ischaemic(primary) mitral regurgitation?

McCutcheon, Keir Robert Gregor

2018

https://hdl.handle.net/10539/28182

McCutcheon, Keir Robert Gregor (2018) Can a ß-adrenergic receptor blocker reverse or at least attenuate left ventricular remodeling due to chronic non-ischaemic mitral regurgitation, University of the Witwatersrand, Johannesburg, <http://hdl.handle.net/10539/28182>

Downloaded from a DSpace repository. https://dspace.org/

Can a β-adrenergic receptor blocker reverse or at least attenuate left ventricular remodelling due to chronic non-ischaemic (primary) mitral regurgitation?



Keir Robert Gregor McCutcheon

A thesis submitted to the Faculty of Health Sciences, University of the Witwatersrand, in fulfilment of the requirements for the degree of PhD.

Johannesburg, 2018

Declaration

I declare that this thesis is my own, unaided work. It is being submitted for the degree of Doctor of Philosophy of Science at the University of the Witwatersrand, Johannesburg. It has not been submitted before for any degree or examination in any other university.

_____

Keir Robert Gregor McCutcheon

_____ day of _____ 2018

To

Lindsay, Emma & Cameron.

&

My patients.

Abstract

Rheumatic Heart Disease (RHD) is one of the main causes of heart failure in Africa. One of the major manifestations of RHD is chronic primary mitral regurgitation (CPMR), which causes an abnormal volume overload on the left ventricle (LV) resulting in adverse LV remodelling. Currently, no medical therapy has been proven to attenuate this adverse remodelling or to improve outcomes in patients with CPMR. Beta-adrenergic receptor blockers have been found to attenuate LV adverse remodelling in animal models of CPMR and in humans with heart failure due to systolic dysfunction, but no prior study has prospectively examined the LV response to carvedilol in patients with CPMR. The current study was divided in to three components. Firstly, clinical, echocardiographic and serum markers of LV remodelling were measured in CPMR patients in response to carvedilol therapy. Secondly, the expression of genes, important in LV remodelling, was compared between patients with CPMR and tissue from normal hearts in order to establish baseline abnormalities in gene expression levels in CPMR. Lastly, changes in LV remodelling gene expression were measured in response to carvedilol therapy in the patients with CPMR. Twenty consecutive patients with isolated CPMR, who met pre-specified inclusion and exclusion criteria, were recruited to the study over a five-year period. Seven patients did not complete the study. Following baseline investigations including clinical evaluation, transthoracic echocardiography (TTE), serum analysis and LV endomyocardial biopsy (EMB), thirteen patients with severe CPMR awaiting mitral valve surgery were randomized to carvedilol therapy (n=7) or standard of care (n=6). At the time of surgery (at a median of 10 and 7 months after baseline in the two groups, respectively), non-invasive investigations and EMB were repeated. Baseline expression levels of 109 genes important in volume-overload LV remodelling were compared with levels in normal hearts (n=5). To account for the small sample size, patients were used as their own controls in order to counter heterogeneity within the two groups. Carvedilol failed to improve serum or echocardiographic measures of LV remodelling. In particular, in patients treated with carvedilol TTE measures of LV function did not improve while measures of right ventricular function deteriorated. Furthermore, serum markers of adverse cardiac function, including MMP-2, Fas and NT-pro-BNP increased in patients treated with carvedilol. At baseline, compared with normal hearts, patients with severe CPMR displayed abnormal expression of a number of genes important in β-adrenergic signalling, calcium handling, cell survival, apoptosis and extra-cellular matrix regulation. This is the first study to demonstrate significant down-regulation the β-adrenergic receptor-1 and the angiotensin-II-receptor-1 genes in patients with severe CPMR. Subsequently, after treatment with carvedilol, there was significant down-regulation of cardio-protective *β-arrestin2*, *PDE1A*, and *PDGFα* and a trend towards significant down-regulation of cardio-protective *PDE4D*. Significant up-regulation of *PLN*, which has previously been found to be associated with abnormal calcium regulation, contractile dysfunction and premature cardiac death, was noted in patients treated with carvedilol. Taken together, these findings suggest that carvedilol fails to attenuate adverse remodelling in patients with severe chronic primary mitral regurgitation.

Abstracts and publications arising from this thesis.

Abstracts

McCutcheon K, Grinter S, Mkhwanazi L, Vachiat A, Ramjee R, Moosa J, Tsabedze N, Maluleke T & Manga P. 2014. Carvedilol use in patients with severe rheumatic mitral regurgitation awaiting mitral valve surgery. 2014. *SAHJ* 11 (4): 190.

McCutcheon K, Dickens C, Dix-Peek T, Grinter S, McCutcheon L, Patel A, Vachiat A, Tsabedze N, Duarte R & Manga P. 2017. Carvedilol causes down-regulation of cardio-protective *STAT3*, *PDGFα* and *PDE4D* in patients with severe chronic primary mitral regurgitation. *SAHJ* 14 (4): 242.

McCutcheon K, Grinter S, McCutcheon L, Patel A, Vachiat A, Tsabedze N & Manga P. 2017. Carvedilol fails to attenuate adverse remodelling in patients with severe chronic primary mitral regurgitation. *SAHJ* 14 (4): 242.

Publications

McCutcheon K & Manga P. 2014. Delayed heart failure due to mitral valve perforation after stab chest. *European Heart Journal: Cardiovascular Imaging*, 15(3): 315.

McCutcheon K & Manga P. 2018. Left ventricular remodelling in chronic primary mitral regurgitation: implications for medical therapy. *Cardiovasc J Africa,* 29;51-65.

McCutcheon K, Dickens C, Van Pelt J, Dix-Peek T, Grinter S, McCutcheon L, Patel A, Hale M, Tsabedze N, Vachiat A, Zachariah D, Duarte R & Manga P. 2018. Effect of long-term carvedilol therapy on echocardiographic, serum and molecular markers of left ventricular remodelling in patients with severe chronic primary mitral regurgitation. *In submission*.

Acknowledgements

Firstly, I would like to thank my supervisor, Professor Pravin Manga, who from the very beginning (in 2010) gave me unconditional support and mentorship. The overall study concept was his and I am glad that he put his faith in me to carry out this important work. He ensured that I had access to the latest echocardiographic technology, personally carried out the left ventricular biopsies with me, provided critical counsel throughout the study and patiently read and criticized various versions of this work. At the same time, it was a privilege to have had my cardiology training under Professor Manga. I would also like to thank Drs Raquel Duarte and Caroline Dickens for their valuable advice and mentorship during the planning and execution of this work.

Secondly, I would like to thank my patients, who put their full trust in me despite the potential risks. I hope that, for those who completed the study, they continue to enjoy good health and long life after mitral valve surgery. For all the other patients, many of whom I screened but could not be included, I hope that they continue to enjoy excellent treatment at Charlotte Maxeke Johannesburg Academic hospital.

Thirdly, I would like to thank my colleagues and fellow contributors. I would like to thank the staff of the Division of Cardiology, Charlotte Maxeke Johannesburg Academic Hospital, for assistance in the non-invasive and cardiac catheterization laboratories. Drs Ahmed Vachiat, Nqoba Tsabedze, Don Zachariah, Themba Maluleke, Gloria Mukishimana, Rohan Ramjee, Jameel Moosa, Riaz Garda and Lance Mkhwanazi all provided help with patient recruitment and critical comment during the study and with paper preparation. I could not have completed this work without expert echocardiographic assistance from Sacha Grinter. I would also like to thank my colleagues from cardiothoracic surgery for help with surgical endomyocardial biopsies, in particular Dr Atul Patel. Thanks also to Professor Martin Hale (Anatomical Pathology) for patient help with histopathology. In the laboratory, I would like to thank Drs Raquel Duarte, Caroline Dickens and Therese Dix-Peek. In particular, I would like to thank Caroline for her massive help with statistical analysis and graph generation. I would also like to thank Dr Lindsay McCutcheon for assistance with laboratory work, table and figure generation, and thesis preparation. Further, more recently, I would particularly like to thank Professor Jos Van Pelt of the KU Leuven. I really appreciate all your help with the bioinformatics analysis.

Fourthly, I would like to thank the Discovery Foundation and The University of the Witwatersrand, Johannesburg, for funding this research, without which none of this would have been possible.

Lastly, and importantly, I would like to thank my family for always supporting me. My parents, Carol and Robert, have always believed in and supported me. Lindsay, Emma and Cameron, I hope that the afterhours and weekends that have been dedicated to this work will be worthwhile for us and for the medical community.

Contents

		Page
Declaration		ii
Abstract		iv
Abstracts and publications arising from this thesis		v
Acknowledgements		vi
Contents		vii
List of Figures		xii
List of Tables		xiv
List of Abbreviations		xv
Chapter 1	**Left ventricular remodelling in chronic primary mitral regurgitation: implications for medical therapy**	**1**
1.1	Introduction	2
1.2	Pathophysiological changes in the LV in chronic primary MR	4
1.2.1	MR causes mechanical stretch, which triggers mechanoreceptors and activates signal-transduction pathways	6
1.2.2	CPMR increases cardiac reactive oxidative stress	9
1.2.3	CPMR triggers an inflammatory response	9
1.2.4	Myocyte loss in chronic primary MR	12
1.2.5	ECM changes in chronic primary MR	13
1.2.6	CPMR activates the neurohormonal system: implications for beta-blocker therapy	17
1.3	Beta-blocker therapy improves β_1-AR signalling and clinical outcomes in HF	20
1.4	β-AR blockade in MR counters adverse adrenergic effects	22
1.5	β-AR blockade therapy for CPMR	23
1.6	Conclusion	31
1.7	References	32
Chapter 2	**Overall study rationale, aims, materials and methods**	**44**
2.1	Study rationale	45
2.2	Aim	46
2.3	Inclusion criteria	46
2.4	Exclusion criteria	46
2.5	Study methods	47
2.5.1	Enrolment	47
2.5.2	Study protocol	47
2.6	Data collection	49
2.6.1	Six-minute walk test (6MWT)	49
2.6.2	Heart Failure Questionnaire	50
2.6.3	Echocardiographic assessment of left ventricular function	50
2.6.3.1	Determining the severity of MR	51
2.6.3.2	Assessment of LV function by echocardiography	53
2.6.4	Serum	55
2.6.4.1	BNP	56
2.6.4.2	CRP	56

2.6.4.3 TNF-α, IL-1β, IL-6, IL-33, ST2, Fas-Ligand, Fas, MMP-1, -2, and -9 & TIMP-1 and -4 quantification 57
2.6.4.3.1. TNF-α, IL-1β, IL-6, IL-33, ST2, Fas-Ligand and Fas serum quantification 57
2.6.4.3.2. MMP-1, -2, and -9 & TIMP-1 and -4 quantification 58
2.6.5 Cardiac catheterization & Endomyocardial Biopsy 60
2.6.5.1 Endomyocardial biopsy 61
2.6.6 Gene expression analysis 63
2.6.6.1 RNA extraction and quantification 63
2.6.6.2 Gene expression (GX) 65
2.6.6.3 Selection of genes for analysis 66
2.7 Data Entry 68
2.8 Statistics 69
2.9 References 71

Chapter 3 Clinical, echocardiographic and serum markers of left ventricular remodelling in response to treatment with carvedilol in patients with chronic primary mitral regurgitation 75

3.1 Introduction 76
3.2 Methods 78
3.2.1 Study subjects 78
3.2.2 Echocardiography 79
3.2.3 Serum 79
3.2.3.1 Selection of serum tests 79
3.3 Results 81
3.3.1 Study population 81
3.3.2 Baseline characteristics 82
3.3.2.1 Baseline demographic and general characteristics 82
3.3.2.2 Baseline echocardiographic parameters 84
3.3.2.3 Baseline cardiac catheterization findings 85
3.3.2.4 Baseline serum results 88
3.3.2.5 Comparison of the two groups after removal of EM 89
3.3.2.6 Comparison of the two groups after including only those with EF >60% 89
3.3.3 Changes in clinical, echocardiographic and serum parameters from baseline to final (in response to treatment with carvedilol) 90
3.3.3.1 Change in heart rate (measured by resting ECG) over time 90
3.3.3.2 Change in systolic blood pressure (at rest) over time 92
3.3.3.3 Change in distance walked in 6 minutes from baseline to final 92
3.3.3.4 Change in Minnesota Living with Heart Failure Questionnaire Score 93
3.3.3.5 Changes in dosing of furosemide and digoxin over time 94
3.3.3.6 Changes in echocardiographic and serum markers in response to carvedilol therapy 94
3.3.3.6.1 Ejection fraction 94
3.3.3.6.2 LVEDDI (LV end diastolic dimension indexed to BSA) 95
3.3.3.6.3 LVESDI (LV end systolic dimension indexed to BSA) 96

3.3.3.6.4 LVEDVI (LV end diastolic volume indexed to BSA) 96
3.3.3.6.5 LVESVI (LV end systolic volume indexed to BSA) 96
3.3.3.6.6 LV dp/dt 97
3.3.3.6.7 Cardiac output indexed to body surface area 98
3.3.3.6.8 Global longitudinal strain (GLS) 98
3.3.3.6.9 Left atrial volume indexed to BSA 98
3.3.3.6.10 Vena contracta 99
3.3.3.6.11 Effective regurgitant orifice 99
3.3.3.6.12 MR volume 100
3.3.3.6.13 Right ventricular base diameter 101
3.3.3.6.14 Tricuspid annular plane systolic excursion (TAPSE) 101
3.3.3.6.15 Right ventricular tissue Doppler velocity (S') (cm/s) 102
3.3.3.6.16 TR Vmax 103
3.3.3.6.17 NT-pro-BNP 103
3.3.3.6.18 CRP 104
3.3.3.6.19 Changes in TNF-α over time 104
3.3.3.6.20 IL-1β 105
3.3.3.6.21 IL-6 105
3.3.3.6.22 Fas 105
3.3.3.6.23 Fas Ligand 106
3.3.3.6.24 ST2 106
3.3.3.6.25 IL-33 107
3.3.3.6.26 MMP-1 107
3.3.3.6.27 MMP-2 107
3.3.3.6.28 MMP-9 108
3.3.3.6.29 TIMP-1 108
3.3.3.6.30 TIMP-4 108
3.3.3.6.31 Changes in the MMP/TIMP ratios over time 109
3.3.3.6.31.1 MMP-1/TIMP-1 ratio 109
3.3.3.6.31.2 MMP-1/TIMP-4 ratio 109
3.3.3.6.31.3 MMP-2/TIMP-1 ratio 109
3.3.3.6.31.4 MMP-2/TIMP-4 ratio 109
3.3.3.6.31.5 MMP-9/TIMP-1 ratio 110
3.3.3.6.31.6 MMP-9/TIMP-4 ratio 110
3.4 Discussion 111
3.5 Conclusion 117
3.6 References 118

Chapter 4 Gene expression changes in patients with chronic primary mitral regurgitation compared with normal hearts 122

4.1 Introduction 123
4.2 Methods 125
4.2.1 Study subjects 125
4.2.2 RNA isolation 126
4.2.3 Gene selection 126
4.2.4 Gene expression analysis 127
4.2.5 Statistical analysis 127
4.3 Results 129

4.4 Discussion 134
4.4.1 Animal models of mitral regurgitation versus human CPMR 134
4.4.2 Gene expression in patients with CPMR compared with normal hearts 137
4.5 Conclusion 150
4.6 References 153

Chapter 5 Effect of long-term carvedilol therapy on molecular markers of left ventricular remodelling in patients with severe chronic primary mitral regurgitation 158
5.1 Introduction 159
5.2 Methods 161
5.2.1 Study subjects 161
5.2.2 Echocardiography 162
5.2.3 RNA isolation 162
5.2.4 Gene selection 162
5.2.5 Gene expression analysis 163
5.2.6 Statistical analysis 164
5.3 Results 165
5.3.1 Baseline results 165
5.3.2 Gene expression changes in response to carvedilol treatment 166
5.4 Discussion 171
5.5 Conclusion 181
5.6 References 182

Chapter 6 Concluding remarks 186
6.1 Introduction 187
6.2 Major highlights of this work 189
6.3 Study limitations 192
6.4 Future studies 194
6.5 Conclusion 197
6.6 References 198

Appendices 201
1 Human Research Ethics Committee (HREC) Certificate 202
2A Certificate for total heart RNA from Donor 1 203
2B Certificate for pooled total heart RNA from Donors 2-4 204
2C Certificate for total heart RNA from Donor 5 205
3 Minnesota Living with Heart Failure Questionnaire 206
4A Selected pages from R&D serum handbook 207
4B Certificate of Analysis for IL-33, ST2, Fas and Fas ligand 208
4C Certificate of Analysis for TNF-α, IL-1β and IL-6 209
5A Selected pages from MMP Panel instructions 210
5B Selected pages from TIMP-1 and -4 Panel instructions 211
6 Selected pages from mRNAeasy mini handbook 212
7 RNA quantification using Nanodrop Spectrophotometry 214
8A Selected pages from Agilent RNA 6000 Nano Kit 215

8B	RNA quality assessment using Agilent RNA 6000 Nano kit	217
8C	Agilent RNA Integrity Analysis	218
9	Nanostring project report	219
10	Genes selected for analysis	221
11	Genes selected from Zheng *et al.* (2014)	229
12	Gene expression in patients with CPMR compared with normal hearts	230
13	Gene Ontology analysis with DAVID bioinformatics	233
14	Gene expression in patients with CPMR versus normal hearts: comparison with previously published data	239
15	Correlation between animal and human studies	240
16	Baseline expression of genes in the two CPMR groups	243
17	Changes in expression of genes in response to treatment with carvedilol	246
18	Turnitin report	249
19	Printed copy of publication. McCutcheon K & Manga P. 2014. Delayed heart failure due to mitral valve perforation after stab chest. *European Heart Journal: Cardiovascular Imaging*, 15(3): 315.	250
20	Printed copy of publication. McCutcheon K & Manga P. 2018. Left ventricular remodelling in chronic primary mitral regurgitation: implications for medical therapy. *Cardiovasc J Africa*, 29;51-65.	251

List of Figures

		Page
Figure 1.1	Left ventricular remodelling in chronic primary mitral regurgitation	5
Figure 1.2	Schematic representation of gene regulation in response to myocyte sarcomere stretch via signal transduction through MLP and TK	8
Figure 1.3a	Proposed time-dependent changes in various remodelling pathways including changes in measured prevalence of mast cells	11
Figure 1.3b	Proposed overall time-dependent changes in remodelling pathway activation	12
Figure 1.4	Signalling pathways involved in sustained β-AR-stimulated cardiac myocyte apoptosis	19
Figure 1.5	Proposed mechanisms of action of carvedilol	21
Figure 2.1	Flow diagram of study	49
Figure 2.2	Important protein components of TNF and FAS apoptotic pathways	68
Figure 3.1	Flow diagram of study	82
Figure 3.2	Baseline left ventricular dimensions and volumes in the two study groups	84
Figure 3.3	Absolute change in median ECG HR	90
Figure 3.4	Change in distance (in meters) walked by patients during six minute walk test	93
Figure 3.5	Change in ejection fraction in patients treated with carvedilol (CRV) versus standard of care (NIL)	95
Figure 3.6	Change in left ventricular end systolic dimension (indexed to body surface area) in patients treated with carvedilol (CRV) versus standard of care (NIL)	97
Figure 3.7	Change in median effective regurgitant orifice	100
Figure 3.8	Change in median mitral regurgitant volume	101
Figure 3.9	Change in tricuspid annular plane systolic excursion in patients treated with carvedilol (CRV) versus standard of care (NIL)	102
Figure 3.10	Change in right ventricular S' in patients treated with carvedilol (CRV) versus standard of care (NIL)	103
Figure 3.11	Change in serum NT-pro BNP in patients treated with carvedilol (CRV) versus standard of care (NIL)	104
Figure 3.12	Absolute change in median serum Fas	106
Figure 3.13	Change in serum MMP-2 in patients treated with carvedilol (CRV) versus standard of care (NIL)	108
Figure 4.1	Heat map highlighting significant changes in expression levels of several genes important in left ventricular remodelling in normal heart tissue (Control), patients with CPMR at Baseline and Final (after treatment with carvedilol)	131
Figure 4.2	Schematic highlighting significant changes in gene expression levels in patients with severe CPMR compared with normal hearts in the current study	132

Figure 4.3	PDE4D is important in β1 adrenergic receptor regulation and signalling	140
Figure 4.4	*STAT3* is activated by β1-AR signalling resulting in the transcription of both excitation-contraction gene products such as the ryanodine receptor (*RyR2*) and *SERCA2* and non-EC genes such as the β1-AR gene itself (*Adrb1*)	143
Figure 4.5	Basic relationship between renin-angiotensin-aldosterone system and extra-cellular matrix remodelling	147
Figure 4.6	Effects of TGF-β on fibroblast phenotype and function	149
Figure 5.1	Change in levels of *ARRB2* gene expression in CRV and Nil groups	166
Figure 5.2	Change in levels of *COL5A2* gene expression in CRV and Nil groups	167
Figure 5.3	Change in levels of *PDGFA* gene expression in CRV and Nil groups	167
Figure 5.4	Change in levels of *PDE1A* gene expression in CRV and Nil groups	168
Figure 5.5	Change in levels of *PDE4D* gene expression in CRV and Nil groups	168
Figure 5.6	Change in levels of *PLN* gene expression in CRV and Nil groups	169
Figure 5.7	Molecular analysis of effect of carvedilol therapy on markers of left ventricular remodelling in patients with severe chronic primary mitral regurgitation	170
Figure 5.8	Schematic highlighting the significant changes in patients treated with carvedilol versus patients not treated	172
Figure 5.9	β-adrenergic receptor production, phosphorylation, internalization and degradation	173
Figure 5.10	Role of cardiomyocyte PAI-1 in TGF-β mediated cardiac fibrosis	177

List of Tables

		Page
Table 1.1	Studies of beta-blocker therapy & LV function in primary MR	29
Table 3.1	Baseline clinical characteristics	83
Table 3.2	Baseline echocardiographic and invasive hemodynamic data	87
Table 3.3	Baseline serum data	88
Table 3.4	Changes in clinical, echocardiographic and serum parameters in response to carvedilol treatment	91
Table 4.1	Comparison of results from dogs and humans with MR from Dell'Italia research group	135

List of Abbreviations

2D	two-dimensional
3D	three-dimensional
6MWT	six minute walk test
7TMR	seven-transmembrane receptor
ACEI	angiotensin converting enzyme inhibitor
ACC	American College of Cardiology
ACF	aorto-caval fistula
AHA	American Heart Association
AKAP	A-kinase anchoring protein
AKT	protein kinase B
AMP	adenosine monophosphate
ANF	atrial natriuretic factor
AR	aortic regurgitation
ATP	adenosine triphosphate
β-AR	beta-adrenergic receptor
BB	beta-adrenergic receptor blocker
Bmode	brightness mode
BNP	brain natriuretic peptide
BSA	body surface area
CI	confidence interval
C.I.	cardiac output indexed to body surface area
CO	cardiac output
CMJAH	Charlotte Maxeke Johannesburg Academic Hospital
CPMR	chronic primary mitral regurgitation
CRP	C-reactive protein
CRV	carvedilol
CSA	cross-sectional area
CTGF	connective tissue growth factor
CW	continuous wave
DAVID	database for annotation, visualisation, and integrated discovery
ECG	electrocardiogram
ECM	extra-cellular matrix
EF	ejection fraction
EMB	endomyocardial biopsy
ERK	extracellular signal-regulated kinase
ERO	effective regurgitant orifice
EROA	effective regurgitant orifice area
ESC	European Society of Cardiology
ESD	end systolic dimension/diameter
FADD	FAS-associated protein with death domain
FAS	first apoptosis signal
FDR	false discovery rate
FSV	forward stroke volume
GLS	global longitudinal strain
GO	gene ontology
GPCR	G protein-coupled receptor

GRK	G protein-coupled receptor kinase
GX	gene expression
HF	heart failure
HR	heart rate
IL	interleukin
JAK	janus kinase
JNK	c-Jun N-terminal kinases
LA	left atrium/left atrial
LV	left ventricle/left ventricular
LVEDD	left ventricular end diastolic diameter/dimension
LVEDDI	LVEDD indexed to BSA
LVEDP	left ventricular end diastolic pressure
LVEDV	left ventricular end diastolic volume
LVEDVI	LVEDV indexed to BSA
LVESD	left ventricular end systolic diameter/dimension
LVESDI	LVESDD indexed to BSA
LVESP	left ventricular end systolic pressure
LVESV	left ventricular end systolic volume
LVESVI	LVESV indexed to BSA
LVEF	left ventricular ejection fraction
LVOT	left ventricular outflow tract
MAPK	mitogen-activated protein kinase
MLHFQ	Minnesota Living with Heart Failure Questionnaire
MLP	muscle LIM protein
MMode	motion-mode
MMP	matrix metalloproteinase
MR	mitral regurgitation
mRNA	messenger RNA
MVP	mitral valve prolapse
NE	norepinephrine
NO	nitric oxide
NS	not significant
NYHA	New York Heart Association
PAI-1	plasminogen activator inhibitor-1
PAP	pulmonary artery pressure
PASP	pulmonary artery systolic pressure
PCR	polymerase chain reaction
PDE	phosphodiesterase
PDGF	platelet-derived growth factor
PE	pulmonary embolism
PLN	phospholamban
PI3K	phosphoinositide-3 kinase
PISA	proximal isovelocity surface area
PKA	protein kinase A
PPM	parts per million
QOL	quality of life
RAAS	renin-angiotensin-aldosterone system
RCT	randomized controlled trial

RHD	rheumatic heart disease
RIN	RNA Integrity Numbers
RNA	ribonucleic acid
ROS	reactive oxygen species
RV	right ventricle/right ventricular
RVol	regurgitant volume
STAT	signal transducer and activator of transcription
ST2	suppression of tumorigenicity 2
TAPSE	tricuspid annular plane systolic excursion
TGF-β	transforming growth factor-beta
TIMP	tissue inhibitor of metalloproteinase
TK	titin kinase
TNF-α	tumour necrosis factor-alpha
TRAIL	TNF-related apoptosis-inducing ligand
TSV	total stroke volume
VC	vena contracta
VCW	vena contracta width
VTI	velocity time integral
WebGestalt	web-based gene set analysis toolkit

Chapter 1

Left ventricular remodelling in chronic primary mitral regurgitation: implications for medical therapy.

1.1. Introduction

Mitral regurgitation (MR) is caused by failure of adequate coaptation of the anterior and posterior mitral leaflets during left ventricular (LV) contraction resulting in various degrees of regurgitation of blood from the LV into the left atrium (LA). The result of this regurgitation is twofold. Firstly, there is a reduction in forward stroke volume (FSV) into the aorta with subsequent reduction in perfusion. Secondly, there is an increase in LA blood volume during ventricular systole which results in an increase in left ventricular preload - the so-called 'volume overloaded' state.

MR is classified as either primary (organic) or secondary (functional) and acute or chronic.[1,2] Causes of acute MR include infective endocarditis and spontaneous cordal rupture and will not be discussed further in this review. Chronic secondary MR can be ischemic and/or non-ischemic in nature and therapies for secondary MR range from medical to surgical.[3] In contrast, chronic primary MR (CPMR) is predominantly caused by degenerative disease in developed countries[4] and rheumatic heart disease (RHD) in developing countries.[5] RHD is one of the major contributors to the aetiology of heart failure in Africa, where it remains the most common form of acquired cardiovascular disease in children and adults.[5]

Current therapy for patients with severe CPMR as recommended by guidelines comprises surgical repair or replacement in patients who are surgical candidates or conservative (i.e. palliative) therapy in patients with very poor left ventricular function who are deemed to be poor surgical candidates. At present, there is no recommendation for drug therapy in patients with any degree of CPMR. However, once heart failure develops angiotensin

converting enzyme-inhibitors (ACEIs), beta-blockers and spironolactone may be considered.[6]

Although there have been several recent reviews focusing on ventricular remodelling in ischemic heart disease, hypertensive heart disease and aortic stenosis, there have been few recent reviews on pathological left ventricular remodelling in patients with CPMR.[7-9] In this review we focus in particular on the pathophysiological changes seen in the myocardium of the left ventricle due to volume overload caused by CPMR. We also discuss medical interventions, which may attenuate or reverse the adverse changes seen in CPMR focusing on data related to the use of beta-blockers in these patients.

1.2. Pathophysiological changes in the LV in chronic primary MR

Primary MR may present acutely, as a slowly progressive disease or as chronic progressive MR with sudden deterioration related to acute changes in mitral valve anatomy such as a ruptured cord. Acute MR is usually a medical emergency requiring emergent surgery and is not the focus of this review.

Patients with CPMR are often asymptomatic for long periods of time before presenting at a late stage in heart failure. During this period there is development of progressive left ventricular dysfunction as the LV is remodelled in an attempt to produce an adequate forward stroke volume.[10,11] Ten-year cardiovascular mortality varies between 10-15% with worse prognosis for patients with severe MR.[12,13]

Alterations in the global structure of the LV in response to CPMR have been reviewed in detail previously.[10] Briefly, MR results in increases in LA volume, a reduction in FSV and an increase in LV preload. By mechanisms that are unclear but are discussed in more detail below, the LV responds to the increased preload by eccentric hypertrophy with a serial increase in myocyte sarcomeres and myofibril slippage (Figure 1.1).[14-19] Eccentric hypertrophy normalizes afterload as estimated by mean systolic stress, compared to patients with aortic regurgitation (AR), leading to a period of so-called 'compensation'.[20] However, the hypertrophy that develops is actually insufficient to fully compensate for the wall stress that develops. This is due to inadequate protein synthesis triggered by MR compared to pressure overload[17,21] and progressive deterioration in myocardial function.[22] There is no clear explanation for this phenomenon but it has been proposed that the lower systolic load in the case of MR may result in an insufficient hypertrophy response at a time

when there is a marked demand for an increased stroke volume.[22] Altered cytoskeletal changes, such as microtubular density, may also play a role.[23] With time, in the face of inadequate hypertrophy and a dilating LV, systolic wall stress increases (based on the LaPlace effect where wall stress is directly related to the pressure within the ventricle and its radius, and inversely related to the wall thickness; $\sigma = Pr/2h$) due to the increases in LV dimensions and inadequate hypertrophy.[22,24,25]

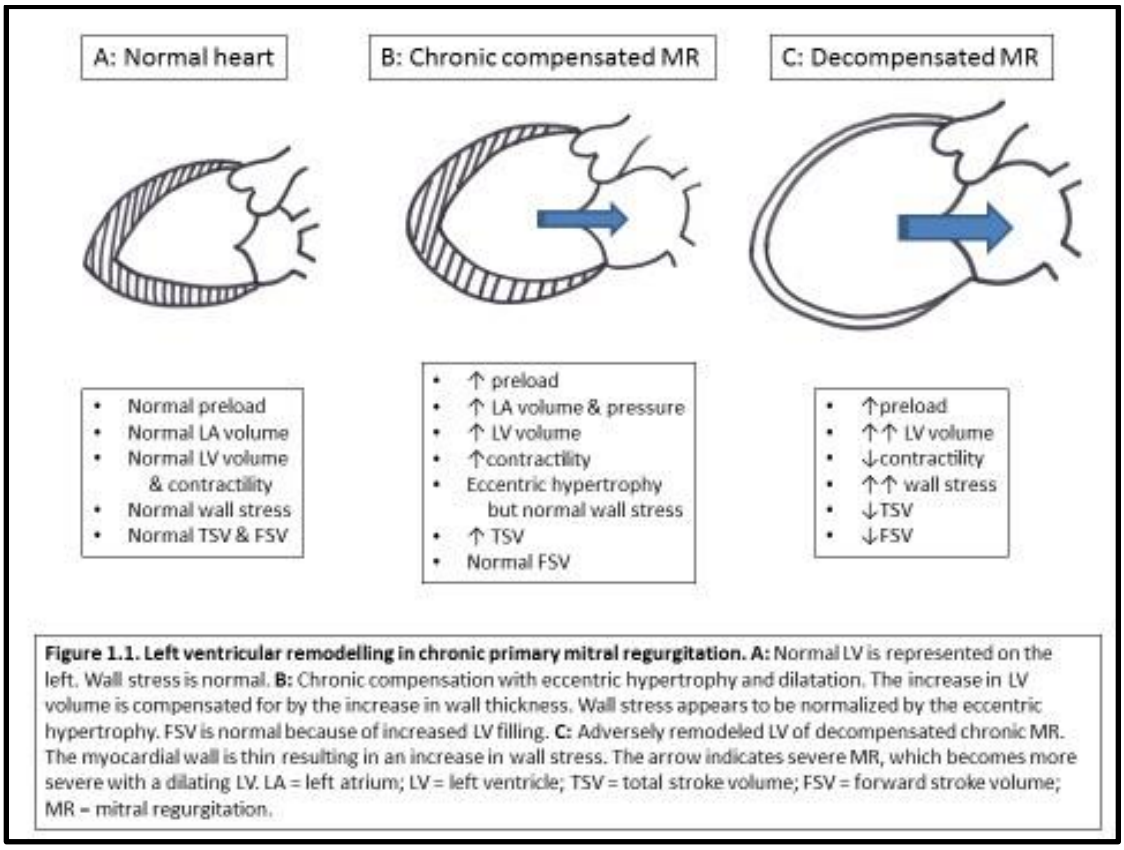

Figure 1.1. Left ventricular remodelling in chronic primary mitral regurgitation. A: Normal LV is represented on the left. Wall stress is normal. **B:** Chronic compensation with eccentric hypertrophy and dilatation. The increase in LV volume is compensated for by the increase in wall thickness. Wall stress appears to be normalized by the eccentric hypertrophy. FSV is normal because of increased LV filling. **C:** Adversely remodeled LV of decompensated chronic MR. The myocardial wall is thin resulting in an increase in wall stress. The arrow indicates severe MR, which becomes more severe with a dilating LV. LA = left atrium; LV = left ventricle; TSV = total stroke volume; FSV = forward stroke volume; MR = mitral regurgitation.

Chronic increases in wall stress are detrimental to the myocardium resulting in activation of a number of complex inflammatory and apoptotic pathways in a similar manner to heart failure from other causes. Ultimately, there is myocyte loss and sliding displacement of cardiomyocytes, or cell slippage, caused by disruption of the myocardial extracellular matrix (ECM)-integrin linkages.[8,26] Various lines of evidence point to time-dependent changes in the up-regulation and down-regulation of remodelling pathways in chronic

primary MR.[27] This process is initiated by diastolic mechanical stretch due to an increase in end-diastolic wall stress leading to an early increase in reactive oxygen species (ROS) generation, inflammatory cytokine expression and neurohormonal activation with increases in angiotensin II and catecholamines. Early in the remodelling process there is interstitial collagen loss and cell slippage. But with time there is myocyte apoptosis and pathological ECM fibrosis.[28] Chronic decompensated MR ensues, and the LV resembles end-stage dilated cardiomyopathy.

1.2.1. MR causes mechanical stretch, which triggers mechanoreceptors and activates signal-transduction pathways

Myocardial mechanoreception is currently poorly understood.[29-31] There is no evidence that specialized mechanosensory cells exist in the myocardium and the role of stretch-activated channels in sensing stretch is debatable.[30] Two systems appear to be particularly important in mechanoreception in the cardiomyocyte: the collagen-integrin-cytoskeleton connections[26,32] and sarcomere-related signalling.[31]

The contraction-relaxation cycle of the myocyte depends on the coordinated interaction between the thin actin filament and the thick myosin filament within the myocyte sarcomere.[33] Actin is bound directly to the Z-disc while myosin is bound indirectly to the Z-disc via the giant elastic protein titin.[34,35] In the normal heart, titin is responsible for restoring the stretched sarcomere to its resting length following active contraction.[34,35] However, another important role for titin is in mechanoreception and the activation of a number of signal transduction pathways when there is chronic myocyte stretch.[29,30,34,36-38]

It does this by changes in the expression of various genes involved in adaptation to the increased load and, ultimately, to the activation of various maladaptive pathways.[39-41]

Titin complexes with a number of potential 'signalosomes' (a mechanosensitive signalling complex) including the Z-disc-localized protein MLP (muscle LIM protein), which has been shown to be responsible for hypertrophy and cardiomyopathy in MLP-deficient animals.[42,43] MLP, aside from its structural role in the Z-disk and its interaction with signal transduction proteins, is able to translocate to the nucleus and thereby act as a transcription factor modifying gene expression depending on mechanical stretch.[44] MLP may be responsible for control of other transcription factors coordinating alterations in the expression of genes responsible for ventricular remodelling. Another important titin signalosome that controls muscle gene expression is the sarcomere M-band-associated protein titin kinase (TK), which is activated by myocyte stretch.[39,41] TK may primarily respond to diastolic stretch,[30] which is particularly relevant in the case of pathological volume overload caused by chronic MR (Figure 1.2).

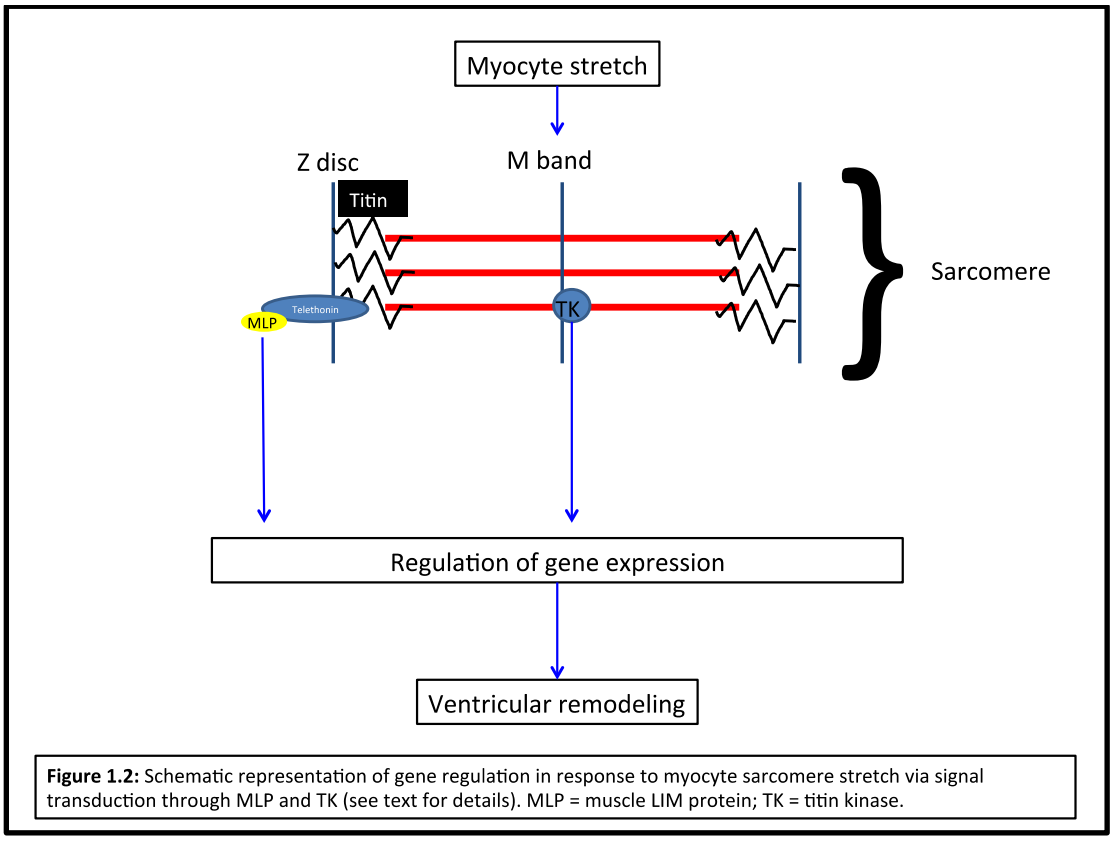

Figure 1.2: Schematic representation of gene regulation in response to myocyte sarcomere stretch via signal transduction through MLP and TK (see text for details). MLP = muscle LIM protein; TK = titin kinase.

Pathological volume overload-induced mechanical stretch has a number of other effects on the cardiomyocyte. For example, in *in vitro*[45] and *in vivo*[46] rat experiments, Tumour Necrosis Factor alpha (TNF-α) is produced by cardiomyocytes resulting in an inflammatory response to stretch, suggesting that TNF-α is an important component in the pathophysiological response of the myocardium to volume overload. Mechanical stretch also results in the local production of angiotensin II[47] and ROS[48] which, via transcription factors, such as TRAIL (TNF-related apoptosis-inducing ligand) and NFκB,[48] result in local increases in pro-inflammatory cytokines further contributing to activation of remodelling signal transduction pathways.[49,50] Finally, as discussed in more detail below, mechanical stretch is transmitted through the ECM to cardiomyocyte integrins, which trigger a number of intracellular signal transduction pathways involved in hypertrophy and apoptosis.[32,40]

1.2.2. CPMR increases cardiac reactive oxidative stress

ROS play an important role in signal transduction and physiologic regulation in vascular and myocardial cells. However, under pathological conditions, such as excessive myocyte stretch or excessive inflammatory signals, ROS have been shown to activate maladaptive remodelling signal transduction pathways.[51,52] These signal transduction pathways include (but are not limited to) protein phosphorylation pathways leading to cell growth or apoptosis (depending on ROS levels and other factors); matrix metalloproteinase activation;[53] cell cycle protein pathways leading to apoptosis; and pathways leading to the activation of inflammatory transcription factors such as NFκB.[54]

ROS are increased in patients with congestive heart failure[55] and there is evidence of pathological increases in ROS in patients with chronic isolated MR who still have LV ejection fractions above 60%.[56] This data suggests that there is an increase in oxidative stress even before the LV starts to develop systolic dysfunction, which supports the notion that wall stress is present throughout the evolution of LV remodelling in primary MR.[57] This oxidative stress appears to be present as long as the volume-overload persists (Figure 1.3).[58]

1.2.3. CPMR triggers an inflammatory response

TNF-α, interleukin-1 (IL-1) and interleukin-6 (IL-6) are produced by all nucleated cells including cardiac myocytes.[59] Cytokines are responsible for beneficial adaptation to short-term stresses, such as hemodynamic overload, within the myocardium. These molecules may play an important role in protecting the heart from oxidative injury and there are

several lines of evidence supporting their beneficial role in short-term stress.[60] However, the role of cytokines in remodelling is complicated and not easily predictable. For example, TNF-α can have both a protective and an adverse effect on the myocardium depending on which TNF-receptors are activated.[61] Furthermore, prolonged elevation of tissue cytokines has been found to have deleterious effects on the LV.[62,63]

Chronic elevation of cytokines has an effect on left ventricular remodelling by blunting of β-adrenergic signalling[59] and activation of apoptotic pathways.[64-66] TNF-α also increases cardiomyocyte apoptosis[65,67] by activating mitogen-activated protein kinase (MAPK)-1 (p38) and NFκB and by down-regulating MAPK-3 (ERK-1).[68] Overexpression of TNF-α has also been shown to increase tissue matrix metalloproteinase (MMP) activity with resultant acute loss in myocardial fibrillar collagen and LV dilatation.[69-71] However, with continuing TNF-α overexpression there is an increase in TIMP-1 expression and reduction in MMP expression leading to abnormal increases in fibrillar collagen[69,70] suggesting a time-dependent effect of chronic exposure to elevated myocardial TNF-α.

Cytokines are elevated in patients with heart failure,[72] in patients with pressure and volume overload[73] and in other forms of heart disease.[74,75] Several lines of evidence suggest that the myocardial response to TNF-α is similar regardless of aetiology. Gene expression analysis by microarray suggests that there is a time-dependent inflammatory response to volume overload (Figure 1.3).[27,46] Very early after the initiation of volume overload in aortocaval fistula rats there is a marked increase in expression of inflammatory pathway genes followed by relative normalization during the chronic ‘compensated’ period of volume overload.[27] This is supported by earlier studies that demonstrate that myocyte

stretch induces TNF-α secretion from myocytes[45,76] and mast cell-deficient rats with volume overload were protected from TNF-α-dependent LV remodelling.[71] Similarly, during compensated CPMR in humans with normal LV ejection fraction (LVEF), there is a down-regulation of inflammatory pathways.[58]

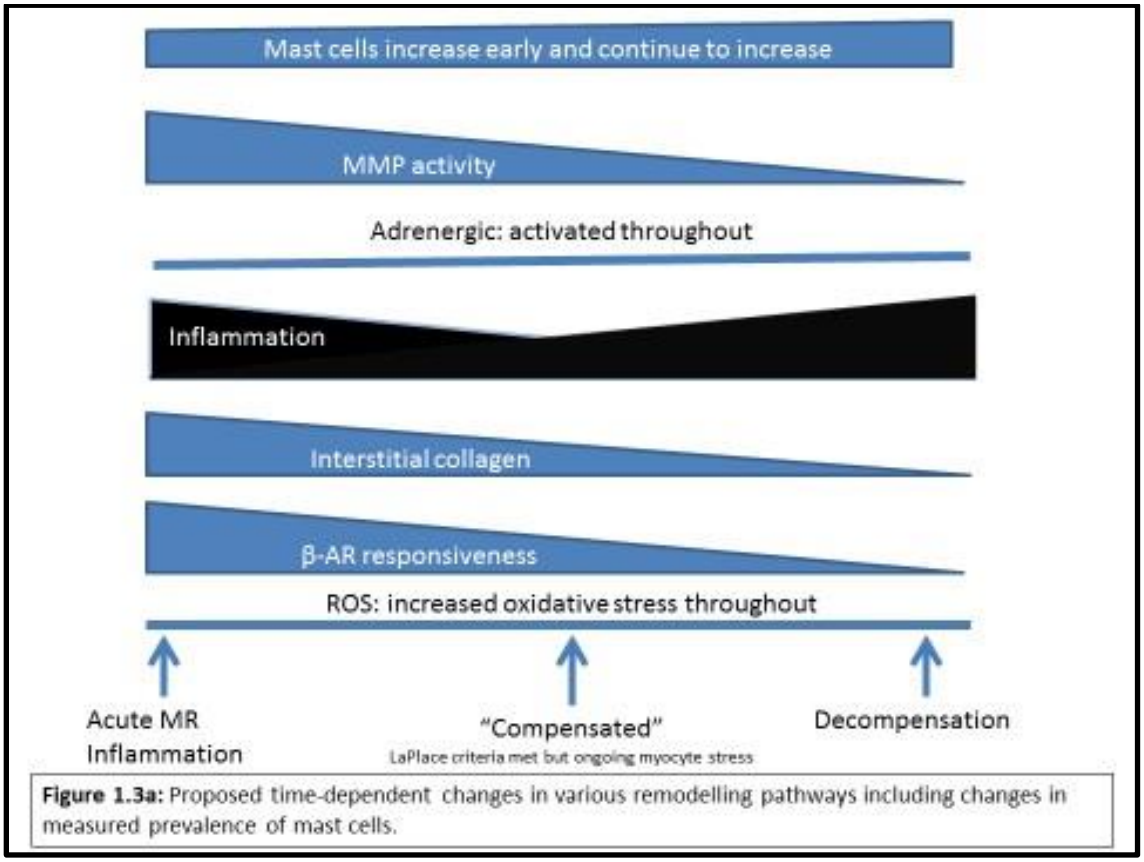

Figure 1.3a: Proposed time-dependent changes in various remodelling pathways including changes in measured prevalence of mast cells.

Figure 1.3b: Proposed overall time-dependent changes in remodelling pathway activation.

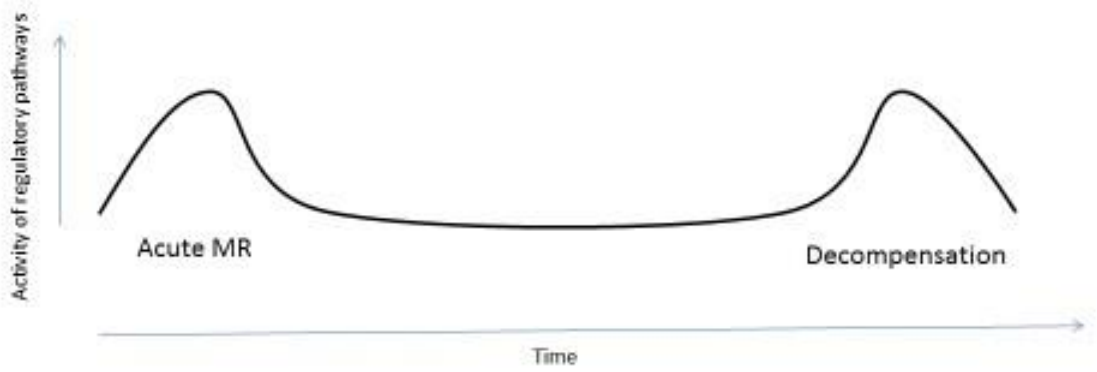

Figures 1.3a & 1.3b: Proposed time-dependent changes in various remodelling pathways including changes in measured prevalence of mast cells. MMP = matrix metalloproteinases; β-AR = β-adrenergic; ROS = reactive oxidative species. See text for details.

As the LV becomes dilated and dysfunctional there is an increase in inflammatory pathway gene expression,[27] which is supported by clinical work in patients with severe CPMR[73,77] and severe rheumatic aortic regurgitation.[78] Overall, there appears to be a biphasic elevation in the inflammatory response to mitral regurgitation with early volume overload activating the expression of numerous inflammatory pathways and decompensation triggering a second inflammatory response (Figure 1.3).

1.2.4. Myocyte loss in chronic primary MR

Apoptosis is activated by several extracellular death signals including myocyte stretch,[79] catecholamines[26,80-82] and inflammatory cytokines,[59] and various intracellular death signals.[83-87] These death signals[26] activate transcription factors[88] ultimately resulting in

activation of the caspase cascade.[89] Loss of myocytes will increase the stress on remaining myocytes. This leads to further increases in ROS[90], cytokine release,[45] increases in adrenergic activation[91]; perpetuating loss of myocytes in a down-ward spiraling process. Time-dependent apoptosis of non-myocyte cells has been described in volume-loaded rats[27] and there is evidence that CPMR causes a reduction in contractile elements.[22,84,92] Based on this evidence and evidence from studies in myocardial remodelling due to other causes, it is probable that cell loss is an important component in left ventricular dilatation and dysfunction in CPMR.

1.2.5. ECM changes in chronic primary MR

Myocyte arrangement and myocardial integrity is highly organized to enable the continuously moving myocardium to produce coordinated contraction resulting in stroke volume.[93] The structural integrity is provided by the ECM, which is comprised of a basement membrane, proteoglycans and glycosaminoglycans, and ECM proteins such as type I, III and V collagen of which approximately 85% is type I collagen.[8] This collagen framework serves to maintain cardiac myocyte alignment without which the myocytes would 'slip' altering the shape and size of the cardiac chambers.[93] The ECM is a highly dynamic part of the myocardium that changes depending on the degree and type of mechanical stress, neurohormonal activation, inflammation and oxidative stress. These stressors on the ECM result in changes in the expression and activation of the proteins responsible for ECM turnover and, ultimately, alterations in collagen deposition and degradation.

Matrix metalloproteinases (MMPs) are a heterogeneous family of enzymes responsible for the proteolysis of various protein-based extracellular substances. They include the collagenases (MMP-1, MMP-8 and MMP-13), stromelysins (MMP-3 and MMP-10) and the gelatinases (MMP-2 and MMP-9). They are expressed and secreted into the extracellular space by a variety of cells including cardiac myocytes, cardiac fibroblasts and macrophages.[94] However, the roles of each MMP and the control of their activity are not yet clearly elucidated and is an area of on-going research[8]. Some studies have demonstrated a correlation between MMP expression and cardiomyopathy phenotypes[95-97] and some studies have demonstrated that serum levels of MMPs have prognostic value in heart failure.[98,99]

Tissue inhibitors of metalloproteinases (TIMPs) are low-molecular-weight proteins that bind to the catalytic domain of active MMPs preventing substrate binding. There are 4 species of TIMPs with overlapping functions within the myocardium, which are not restricted to MMP inhibition. Other pleomorphic effects have been described. For example, TIMP-2 increases collagen production by fibroblasts whereas TIMP-3 is responsible for fibroblast apoptosis.[100]

Biological and/or mechanical stimuli trigger various signal transduction pathways resulting in the production of MMP transcription factors and the secretion of these enzymes into the ECM.[94,101-103] Mechanical stimuli, such as stretch,[104] are transduced through the ECM, which, via collagen-integrin-cytoskeleton connections, is connected to and activates a number of intra-myocyte signal transduction pathways involved in ECM remodelling.[32,47,105-108] Local ROS, endothelin-1, angiotensin II and catecholamines, via α-

and β-adrenergic receptors, are also responsible for increases in MMP expression.[53,91,109,110] Cytokines, such as TNF-α and IL-1, have been found to increase MMP expression,[69,104] promoting matrix degradation and ventricular dilatation.[8] On the other hand, MMP-9 production can be suppressed by TGF-β-activated NFκB binding in some experiments[111] whereas its expression is up regulated by Angiotensin II-activated NFκB in other experiments.[112] Angiotensin II[109] and aldosterone both increase ECM remodelling mainly through TGF-β[113] although the effects of this protein are multiple and often opposing depending on circumstances.[114] TGF-β stimulation induces maturation of fibroblasts to myofibroblasts and enhances ECM protein synthesis via induction of TIMP expression and inhibition of certain MMPs expression.[113] However, this is dependent on the load on the myocardium and there is clear evidence that volume overload results in reduction in TGF-β and loss of interstitial collagen,[115] whereas pressure overload increases TGF-β.[116] The result is increased detection of markers of collagen types I and III turnover in the serum,[117] pathological decreases in interstitial collagen[16,118,119] and left ventricular dilatation.

In response to different hemodynamic overloads (pressure versus volume), the ECM undergoes different patterns of remodelling.[28] Volume overload results in loss of collagen fibrils surrounding individual myocytes[16,118,120] with resultant wall thinning and ventricular dilatation changing the geometrical shape of the LV, whereas excess matrix deposition is observed in pressure overload.[121,122] Despite similar fibrotic molecular pathways and cellular effectors, the pathophysiological mechanisms leading to fibrotic remodelling are different depending on the load on the heart.[8] For example, ACEIs reduce remodelling and collagen accumulation in pressure overload,[123] but not in CPMR.[16,124] Furthermore, the expression of integrins, which are important in ECM-myocyte connectivity and ECM

remodelling, are reduced in MR[115] but increased in pressure overload.[125] Similarly, profibrotic TGF-β expression is increased in mice with pressure overload[116] but is decreased in dogs with experimental MR[115] and expression of plasminogen activator inhibitor-1 (PAI-1), is increased in a swine model of early pressure overload[126] but decreased in chronic MR.[115]

There appears to be a time-dependent increase and decrease in MMP activity during the evolution of LV remodelling in response to CPMR (Figure 1.3).[27,119] Myocardial mast cells have been found to be instrumental in increases in MMP activity in early volume overload[71,119,127,128] and are increased in number in response to volume overload-induced increases in myocardial TNF-α.[46] In animal models there is an early rise in myocardial MMP levels after the volume-loaded state is created but this seems to normalize after the acute phase.[129,130] MMP gene expression in dogs with isolated MR, has confirmed that, at 4 months, there is down-regulation of a number of non-collagen genes important in ECM structure, down-regulation of pro-fibrotic connective tissue growth factor and plasminogen activator, and down-regulation of numerous genes in the TGF-β pathway.[115] However, MMP-1 and MMP-9 gene expression was still markedly increased in these dogs with compensated MR compared with controls.[115] As the LV starts to dilate in dogs with chronic myxomatous mitral valve disease, MMP-9 levels decrease.[131]

Over time there are characteristic changes in the MMP/TIMP ratio enabling the ventricle to initially increase compliance in the acute and compensated phases of MR. However, at some point (the "transition" point) there is excessive degradation of the ECM leading to the decompensated and dilated LV.[28,132] What controls the steady deterioration in the

myocardium in response to volume overload is not clear and appears to be complex. In the early stages of volume overload there are decreases in ECM deposition (compared with pressure overload)[115] but late in the progression of the dilating volume-loaded heart an increase in perivascular collagen deposition has been noted,[27,128] which may reduce ventricular compliance and promote systolic dysfunction.[28]

1.2.6. CPMR activates the neurohormonal system: implications for beta-blocker therapy

Patients with CPMR demonstrate LV systolic dysfunction even before a reduction in LVEF occurs.[133,134] As with heart failure due to any other cause, CPMR results in activation of the neurohormonal system and inflammatory cascade at both systemic and local levels.[135-137] With neurohormonal activation, myocardial angiotensin II plays an important role in the regulation of cell proliferation, apoptosis, inflammation and production of mediators of remodelling such as platelet-derived growth factor and MMPs.[138] Persistent angiotensin receptor-1 activation by angiotensin II not only results in the generation of ROS but also alterations in protein synthesis via tyrosine kinase receptor activation and MAPK signalling.[139] Furthermore, angiotensin II-activated ROS act as second messengers that also have effects on inflammation and cell growth.[140] Angiotensin II also acts on the sympathetic nerve endings in the myocardium to facilitate catecholamine release.[141,142]

Long-term increases in myocardial angiotensin II increase local TGF-β with resultant increases in activation of genes involved in ECM production via nuclear translocation of NFκB.[112,143] Unlike the pressure overloaded heart where there is progressive fibrosis,[144] the increase in myocardial angiotensin II in volume overload results in an increase in ECM

turnover with loss of interstitial ECM.[145] Despite the clear link between angiotensin and remodelling in heart failure, to date there has been little clinical evidence to support the role of medical therapy directed against angiotensin in subjects with chronic organic MR.[16,146-148] This may be explained by the fact that ACEIs reduce the breakdown of bradykinin, which has been implicated in the initial increase in MMP activity and collagen breakdown seen in volume overload.[145]

Three types of β-adrenergic receptors (β-ARs) are known to exist in the myocardium: β_1, β_2 and β_3 with an approximate ratio of 80:17:3.[149] β_1 and β_2 are important in the regulation of myocyte excitation-contraction coupling.[82] β_1-AR is the predominant receptor subtype expressed in the heart and, like other β-ARs, its stimulation results in G protein-coupled activation of the adenyl cyclase-cAMP-protein kinase A (PKA) signalling cascade. This leads to activation of a number of subcellular pathways important in cardiomyocyte contractile function including calcium channel activation and troponin I phosphorylation. In contrast, β_2-AR signalling has negative effects on adenyl cyclase activation and the subsequent G-protein-activated ionotropic response.[82] β_3-AR appears to be important in protection from hypertrophic and fibrotic remodelling by preserving NO/cGMP signalling during cardiac stress.[150]

The β-adrenergic receptor system plays an important role in the pathogenesis of myocardial remodelling and heart failure.[86] The exact mechanisms are unclear but it has been known for decades that chronically increased plasma catecholamines can lead to heart failure,[151,152] possibly through myocyte apoptosis (Figure 1.4).[26]

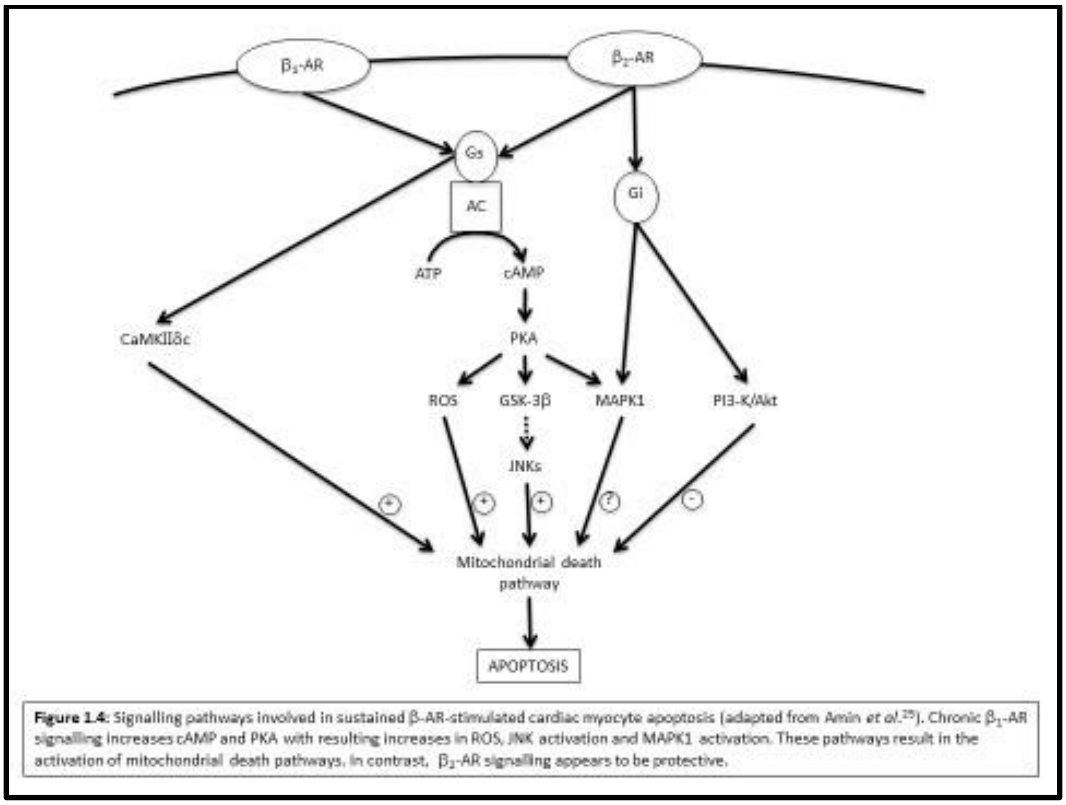

Figure 1.4: Signalling pathways involved in sustained β-AR-stimulated cardiac myocyte apoptosis (adapted from Amin *et al.*[25]). Chronic β_1-AR signalling increases cAMP and PKA with resulting increases in ROS, JNK activation and MAPK1 activation. These pathways result in the activation of mitochondrial death pathways. In contrast, β_2-AR signalling appears to be protective.

In dogs with CPMR there is activation of the adrenergic system[91,110] and recent gene array data in CPMR patients with preserved LVEF demonstrate increased expression of genes involved in β-adrenergic signalling.[58] This indicates that the adrenergic system is activated during the compensatory phase of CPMR and supports the concept that blocking these pathways may reduce their adverse consequences. However, with transition to decompensation there is a reduction in adrenergic responsiveness. In patients with systolic heart failure (HF) several studies in the last four decades show that the β_1-receptor density[153] and its mRNA[154,155] are reduced while β_2-receptor density remains unchanged.[156] Similarly, in animals with HF due to chronic volume-overload, β_1-AR responsiveness is reduced due to neurohormonal activation (Figure 1.3).[48,157] These changes in β_1-AR expression are caused by sustained adrenergic activity causing an increase in the expression and activity of GRK-2 (G protein-coupled receptor kinase; formerly called β-ARK or β-adrenergic receptor kinase) resulting in the β_1-AR being phosphorylated and labelled for

desensitization, internalization and recycling.[158] The result is a reduction in the density of β_1-ARs and a reduced propensity for myocyte activation by chronic β_1-receptor activation, which may protect the myocyte from long-term catecholamine toxicity.[82]

1.3. Beta-blocker therapy improves β_1-AR signalling and clinical outcomes in HF

Chronic β_1-AR activation causes a number of detrimental effects ultimately resulting in changes in the ECM and cell loss from necrosis and apoptosis,[26] which in turn leads to cardiac dilatation and failure.[159] However, the intracellular pathways responsible for these final acts are unclear.[26] What is clear is that β_1-AR antagonists improve clinical outcomes in patients with systolic heart failure and improve cardiac function and myocardial remodelling.[160]

Most β-adrenergic blockers are antagonistic to β-ARs (whether β-1, β-2 or β-3) by occupying the receptor and preventing signal transduction via G-protein activation. Importantly, there is an up-regulation of β_1-AR expression and improvements in receptor sensitivity resulting in reversal of cardiac remodelling.[149] However, the pharmacological and clinical effects of these agents vary quite considerably. Cardioselective beta-blockers (metoprolol, bisoprolol and atenolol, for example) have a greater affinity for β_1-ARs than β_2-ARs, whereas carvedilol binds β_1-ARs more than β_2-ARs and has vasodilatory effects, via nitric oxide and α_1 receptor blockade (Figure 1.5). There are other important differences between carvedilol and other beta-blockers. For example, metoprolol up-regulates cardioprotective-β_3-AR expression, whereas carvedilol does not.[161,162] Carvedilol has antioxidant and antiproliferative properties[163-165] and differs from metoprolol in its effects on hemodynamics, LV function and β_1-AR expression.[166,167] Carvedilol[168] and

bisoprolol[169] have also been shown to improve right ventricular (RV) ejection fraction, attenuate RV dilatation and reduce pulmonary artery hypertension in patients with ischemic and non-ischemic dilated cardiomyopathy. Although there are no recent confirmatory studies, these improvements in RV function may be related to reductions in RV afterload and/or improvements in RV contractility.[168,169] In contrast, short-term (2 week) metoprolol did not improve RV function in patients with moderate-to-severe degenerative MR.[170]

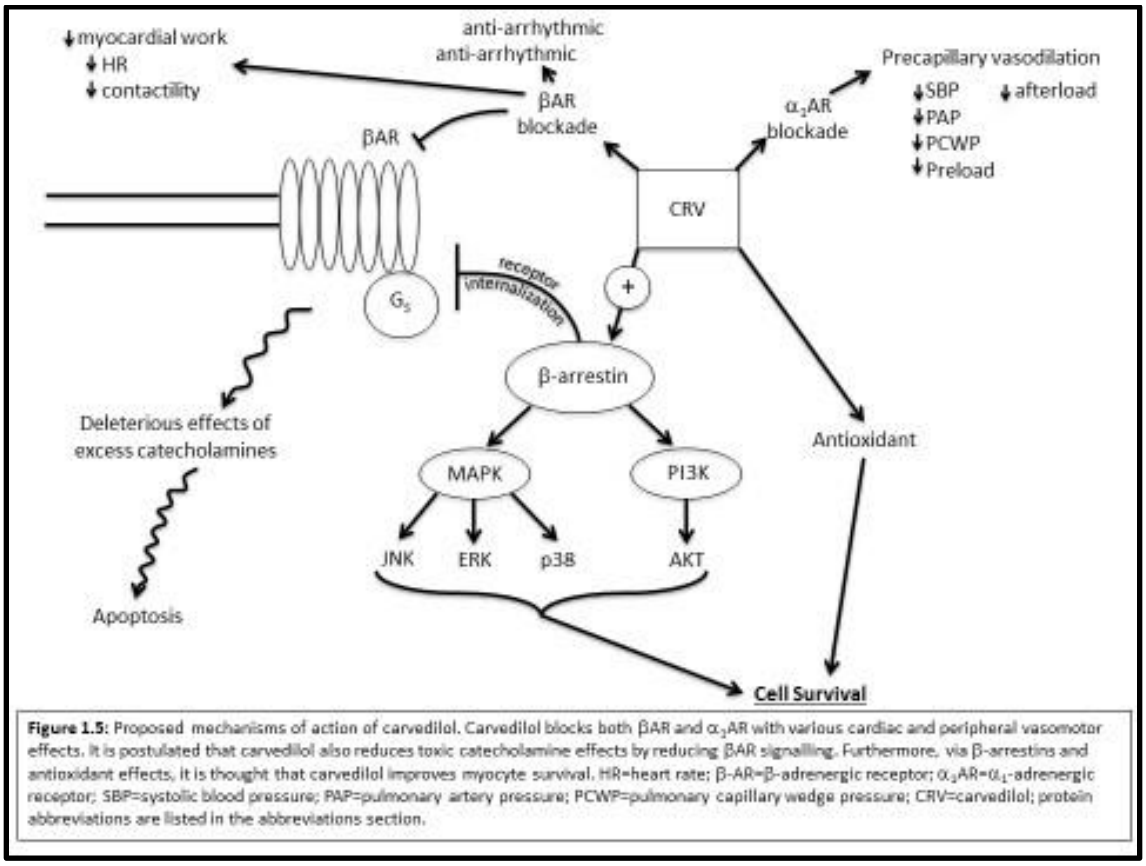

Figure 1.5: Proposed mechanisms of action of carvedilol. Carvedilol blocks both βAR and α_1AR with various cardiac and peripheral vasomotor effects. It is postulated that carvedilol also reduces toxic catecholamine effects by reducing βAR signalling. Furthermore, via β-arrestins and antioxidant effects, it is thought that carvedilol improves myocyte survival. HR=heart rate; β-AR=β-adrenergic receptor; α_1AR=α_1-adrenergic receptor; SBP=systolic blood pressure; PAP=pulmonary artery pressure; PCWP=pulmonary capillary wedge pressure; CRV=carvedilol; protein abbreviations are listed in the abbreviations section.

Clinical support for β-adrenergic receptor blocker therapy in patients with heart failure is well known,[160,171,172] with some data suggesting that patient outcomes are better with carvedilol than the immediate-release form of metoprolol.[173]

Several mechanisms for the improvement in outcomes with β_1-receptor blockade have been proposed[86] including anti-arrhythmic properties;[174] improved β-adrenergic signalling by

cardiac β-AR upregulation;[82] free radical scavenging;[163] improvements in calcium cycling by the sarcoplasmic reticulum;[85,175] bradycardia reducing myocardial work, mechanical stress,[176] and prolonging diastolic calcium uptake and cycling by the sarcoplasmic reticulum; inhibition of the renin-angiotensin-aldosterone system; and there is growing evidence that β-antagonists, in particular carvedilol,[164,165] directly reduce apoptosis[80,177-179] and collagen loss by MMP activation.[180]

1.4. β-AR blockade in MR counters adverse adrenergic effects

Since MR leads to a reduction in forward stroke volume, it is hypothesized that the adrenergic system is activated to maintain systemic blood pressure and perfusion and blockade of the adrenergic system should limit adverse left ventricular remodelling. There is evidence that CPMR results in excessive activation of the sympathetic nervous system with increases in myocardial catecholamine levels,[91,120,136] similar to heart failure from other causes.[181]

Tallaj *et al.*[120] demonstrated that β-AR blockade with extended-release metoprolol succinate attenuated angiotensin II-mediated norepinephrine and epinephrine release in the myocardium of dogs with 'subacute' (2-4 weeks' duration) isolated MR. Similarly, Hankes *et al.*[91] demonstrated that norepinephrine release into the cardiac interstitium was significantly higher in dogs with 'subacute' MR, which was reduced by β_1-AR blockade. In an earlier study by Tsutsui *et al.*[92] in 'chronic' (3 months) canine MR, the β_1-AR blocker atenolol improved left ventricular function, which was associated with improvement in contractile function of isolated cardiomyocytes and an increase in the number of contractile elements. This was supported by a similar study by Nemoto *et al.*[147], which showed that

only when a β_1-AR blocker was added to an ACEI did forward stroke volume and cardiac contractility return to normal. Recently, Trappanese *et al*.[182] demonstrated an improvement in β_3-AR expression and β_3-NO-cGMP coupling with chronic therapy with metoprolol in dogs with primary MR. Since β_3-AR is cardioprotective, this may partially explain the potential beneficial effects of β_1-AR blockade in primary MR.[161]

1.5. β-AR blockade therapy for CPMR

At present there is no proven medical therapy for CPMR. Surgery is the mainstay of treatment for severe MR but carries perioperative risk and patients are potentially subjected to the lifetime risk of anticoagulation if they undergo mitral valve replacement. Although tissue valves are commonly used in the degenerative mitral valve disease in older patients, these are less durable in younger patients. Many patients in the developing world are from poor and rural backgrounds where access to regular medication and regular anti-coagulation assessment is difficult. A medication that could limit or even reverse the LV dysfunction associated with the volume-loaded state of CPMR would be extremely beneficial to these patients even if only to delay the need for surgical intervention. This would especially be true in women of child-bearing age. Warfarin is teratogenic and many women with prosthetic valves have complicated pregnancies related to the teratogenic effects of warfarin or the risks related to bleeding during pregnancy.

Persistent, and often worsened, postoperative LV dysfunction is a major cause of morbidity and mortality in these patients,[135] although this is not a universal finding especially when patients are referred for early surgery.[183-185] Nevertheless, a means to improve LV function

in the perioperative period might improve the postoperative morbidity and mortality associated with left ventricular dysfunction.

Current guidelines recommend surgery for patients with severe pulmonary hypertension on presentation or a progressively dilating LV, even if they are asymptomatic.[1,2] However, timing of surgery is uncertain[186,187] and there is no clear guideline as to the urgency of the surgery in asymptomatic patients without overt LV systolic dysfunction (LVEF <60%). Several studies support early surgery for CPMR.[188-190] Enriquez-Sarano *et al*.[13] showed that patients with an effective regurgitant orifice area of at least 40 mm^2 as assessed by echocardiography should promptly be considered for cardiac surgery. Barbieri *et al*.[191] found that asymptomatic patients with evidence of pulmonary hypertension (>50mmHg at rest) should undergo prompt surgery. However, there is also evidence that asymptomatic patients with severe MR can be followed until they become symptomatic or demonstrate echocardiographic signs of LV dysfunction.[134,192] How these patients should be managed in the interim is unclear but it is important that patients are not left untreated until irreversible LV remodelling has taken place. In resource-limited hospitals, patients who do not need emergency surgery often wait several months before they undergo surgery by which time there has been progressive advancement of ventricular remodelling leading to permanent impairment of function. Medical therapy that could reverse or at least attenuate LV remodelling may improve outcomes in these patients.

To date, there is little evidence to support medical therapy in the treatment of patients with organic valve disease or in the reversal or attenuation of LV remodelling which may delay the need for surgery in asymptomatic patients.[193] Vasodilator therapy which reduces

peripheral vascular resistance and LV afterload,[121] have generally not improved outcomes in patients with MR or in experimental MR canine models.[16,124,147,194] Although several very small studies from the 1970s to the 1990s showed benefit of vasodilator therapy in acute MR,[146] small human studies from the same period failed to show long-term benefit.[195] One retrospective study, however, demonstrated an improvement in echocardiographic LVEF in patients treated with afterload-reducing agents.[148] However, there are no large randomized studies assessing long-term vasodilator therapy, including ACEIs, in humans.

There is some clinical evidence to support the concept that β-AR blockade may attenuate remodelling in patients with primary MR (Table 1.1). Stewart *et al.*[196] recruited 25 patients with moderate or severe degenerative MR and randomly assigned the participants to the β_1-AR blocker metoprolol or placebo for approximately two weeks. Left ventricular function was assessed at baseline and on study completion by cardiac magnetic resonance imaging. They found that the β_1-AR blocker resulted in a decrease in LV work and an increase in forward stroke volume.[196] Mitral annular dimensions also appeared to improve over the 2 week period in the same cohort of patients.[197] A retrospective observational study involving 895 patients in California showed that participants on β_1-AR blocker therapy with severe MR and normal left ventricular function had a significantly lowered mortality hazard regardless of the presence of hypertension or coronary artery disease.[198] Ahmed *et al.*[199] published the results of the first randomized controlled Phase IIb trial of beta-blockade in patients with chronic degenerative MR. Thirty eight asymptomatic patients with moderate-to-severe isolated MR were randomized to either placebo or long-acting metoprolol for 2 years. Cardiac magnetic resonance analysis showed that patients randomized to the β-AR blocker had significantly better LVEFs after 2 years of therapy.

In contrast, there are several pre-clinical and clinical studies demonstrating that beta-blocker therapy actually worsens LV dimensions and function in chronic primary MR (Table 1.1).[110,148,197,200,201] A recent, longer-term (23 to 35 weeks) study in rats found that echocardiographic measures of LV remodelling were not improved by carvedilol.[201] In fact, LV dimensions, ejection fraction and survival were significantly lower with long-term carvedilol use. Similarly, in a 4-month dog model, extended-release metoprolol succinate failed to attenuate the adverse global LV remodelling and ECM loss, but did preserve cardiomyocyte function.[200] Interestingly, all dogs treated with β_1-AR blocker (n=6) survived to 4 months whereas only 5 out of 9 of the untreated dogs survived to 4 months. Similarly, Sabri *et al.*[110] found that, despite reductions in interstitial collagen degradation and reductions in adverse-remodelling-related intracellular signalling, extended-release metoprolol succinate failed to attenuate LV dilatation or decline in LV function. A retrospective echocardiographic study in 134 human subjects with moderate-to-severe MR (67% degenerative and 20% 'non-specific thickening') found that patients exposed to β-AR blockade developed worsening of their ejection fraction over a mean of 20 months follow up.[148] Finally, despite improvements in LV work and annular dimensions[197] in patients treated over a short period with metoprolol, there were significant increases in LVESV and LVEDV with no significant change in LVEF or regurgitant volume.[196]

At the present time, there are no recommendations regarding medical therapy in CPMR. Afterload reduction has not consistently been shown to improve long-term outcomes.[16,124,147,148,195] Data from heart failure trials[160,171,172] as well as from animal models[92] and human trials[199] suggest a role for beta-blockade in MR. However, other

studies do not support a role for beta-blockade in MR.[110,148,197,200,201] The discrepancies of these findings are unclear but some explanations can be proposed.

Firstly, studies have been performed in different experimental models and at different stages in the evolution of MR-related LV remodelling. Many of the experiments performed thus far have been in animal models with controlled formation of volume overload showing that early introduction of beta-blocker therapy[91,92,120] may be beneficial and this is supported to some extent by the work of Ahmed *et al*.[199] in humans. However, there appears to be a time-dependent pattern during the remodelling of the LV in chronic primary MR. Early after the development of MR there is a marked increase in the inflammatory and neurohormonal response to the acute volume overload.[27,115] A period of compensation and a relatively normal inflammatory response appears to follow until the late decompensated stage is reached when adverse pathway activation seems to increase.[27] Depending on when, in this evolution of LV remodelling, studies to date have been performed, there may be discrepant findings with respect to the impact of beta-blockade on LV remodelling. Beta-blockade may have more impressive effects if used early in the evolution of volume overload-related LV remodelling but may be less effective later on.

Secondly, various beta-adrenergic agents have been tested under different circumstances. Compared to the impressive beneficial results in heart failure patients with the mixed adrenergic blocker, carvedilol,[160,202] Pu *et al*.[201] demonstrated that this drug caused worsening LV dimensions and function in animal subjects with primary MR. In contrast, treatment of dogs with the selective beta-blocker atenolol improved LV remodelling[92]

whereas treatment with metoprolol in animals and humans have had mixed results.[110,182,196,197,199,200]

Thirdly, an important question is whether patients presenting in more advanced stages of LV remodelling will respond to anti-remodelling therapy or whether the wall stresses determined by the LaPlace Law will outweigh any potential beta-blocker effect. In this regard the findings of Pat *et al*. [200] are interesting because although there were improvements in cardiomyocyte contractility and beta-receptor responsiveness, LV remodelling was not attenuated by metoprolol. It was postulated that β-AR blockade failed to preserve interstitial collagen loss and therefore failed to prevent on-going myocyte slippage. There appears to be a strong early adrenergic response to CPMR[58] and beta-blocker therapy before onset of LV dilatation may have more benefit.

Lastly, in patients with rheumatic mitral valve disease, there is a possibility that rheumatic fever causing rheumatic carditis may have long-lasting effects on the myocardium attenuating reverse remodelling by beta-blockers.

Table 1.1. Studies of beta-blocker therapy & LV function in primary MR.

Abbreviations: BB = beta-blocker; MVP = mitral valve prolapse; RCT = randomised controlled trial; MR = mitral regurgitation; NE = norepinephrine; + indicates that the study favoured BB therapy in primary MR; - indicates that the study did not favour BB therapy in primary MR; LV = left ventricle; LVEF = left ventricular ejection fraction; LVEDV = left ventricular end diastolic volume; LVESV = left ventricular end systolic volume; CO = cardiac output; RAAS = renin-angiotensin aldosterone system; echo = echocardiogram; MRI = magnetic resonance imaging; PPM = parts per million.

Authors	Year	Subject	Cause of MR	Number treated with BB	Type of study	Control	Type of BB	Duration of BB	Outcome measures	Favours BB
Tsutsui *et al*.[91]	1994	Dog	Experimental chordal rupture	N = 6	Case controlled	N= 6	Atenolol 50mg daily	3 months	Cardiocyte contractility, myofibrillar density	+
Nemoto *et al*.[146]	2002	Dog	Experimental chordal rupture	N = 11	Longitudinal	NA	Atenolol 100mg daily	3 months	Hemodynamics, LV function	+
Tallaj *et al*.[119]	2003	Dog	Experimental chordal rupture	2 weeks MR+BB: n=6 4 weeks MR+BB: n=8	Case controlled	Normal: n=8 2 weeks MR: n=8 4 weeks MR: n=6	Metoprolol succinate 100mg daily	4 weeks	RAAS activation	+
Hankes *et al*. [90]	2006	Dog	Experimental chordal rupture	4 weeks of MR+BB = 8	Case controlled	Normal = 6 Untreated MR = 6	Metoprolol succinate 100mg daily	4 weeks	NE release into cardiac interstitium	+
Oh *et al*. [147]	2007	Human	71% degenerative	N = 134	Retrospective cohort	NA	Not ascertained	1-88 months	Echo LVEF	-
Pat *et al*. [201]	2008	Dog	Experimental chordal rupture	N = 11	Case controlled	N=10	Metoprolol succinate 100mg twice daily	4 months	LV remodelling by MRI & Echo; cardiomyocyte function	Improved cardiomyocyte function & BB receptiveness but failure to attenuate remodelling

Authors	Year	Subject	Cause of MR	Number treated with BB	Type of study	Control	Type of BB	Duration of BB	Outcome measures	Favours BB
Sabri *et al*.[109]	2008	Dog	Experimental chordal rupture	N = 6	Case controlled	Normal = 6 Untreated MR = 6	Metoprolol succinate 100mg daily	4 weeks	LV remodelling by Echo; interstitial collagen quantification; FAK signalling (integrin signalling)	BB reduced FAK tyrosine phosphorylation but no change in remodelling parameters; BB reduced epicardial collagen loss but not endocardial collagen loss
Varadarajan *et al*.[199]	2008	Human	LVEF >55% + 'severe MR'	N = 218	Retrospective observational cohort study	N = 614	Not stated	8 years	Mortality	+
Stewart *et al*. [197]	2008	Human	MVP	N = 25	Double blind cross-over study	NA	Metoprolol to a maximum 190mg/d	14 days	MRI EF LVEDV LVESV LV 'work' (CO)	 - - - +
Ahmed *et al*. [200]	2012	Human	MVP	N = 19	RCT	N = 19	Toprol XL 25-100mg daily		MRI LVEF MRI LVESV LV longitudinal strain rate	+ - -
Pu *et al*. [202]	2013	Rat	Experimental leaflet disruption	N = 43 'Long-term' BB in 19	RCT	N = 44	Carvedilol (1200 PPM)	36 weeks	Echo only LV dimensions LVESV and mass index FS and EF Survival probability	-
Trappanese *et al*.[181]	2015	Dog	Experimental chordal rupture	N = 8 (MR + BB)	Case controlled	Normal = 10 Untreated MR = 8	Metoprolol succinate 100mg daily	4 weeks	Activation of βAR/NO-cGMP signalling βAR expression	+ +

1.6. Conclusion

Left ventricular remodelling in response to the volume load created by CPMR is a complex process that stems from excessive diastolic stretch of myocytes. Excessive stretch triggers activation of numerous signal transduction pathways resulting in an initial adaptive remodelling process in the form of eccentric hypertrophy. However, chronic activation of these pathways results in abnormal increases in reactive oxygen species, catecholamines, angiotensin II and inflammatory cytokines. This is followed by a transition to adverse remodelling involving cardiomyocyte apoptosis and interstitial collagen loss, common to all forms of heart failure.

Limited data does not support the routine long-term use of afterload-reducing agents for the treatment of CPMR. In contrast, there is pre-clinical data demonstrating that β-AR blockade reverses remodelling caused by the volume overload of CPMR and there is some recent clinical data to support this hypothesis. However, there are studies demonstrating worsening LV remodelling with beta-blocker therapy. Whether these contrasting outcomes are related to differences in beta-blockers, varying experimental models or differences in timing of therapy will need clarification. Ultimately, further studies are still required to elucidate the exact mechanisms involved and large randomized clinical trials are needed to clarify the role of these agents for patients with CPMR.

1.7. References

1. Baumgartner H, Falk V, Bax JJ, et al. 2017 ESC/EACTS Guidelines for the management of valvular heart disease. *European heart journal* 2017; **38**(36): 2739-91.
2. Nishimura RA, Otto CM, Bonow RO, et al. 2017 AHA/ACC Focused Update of the 2014 AHA/ACC Guideline for the Management of Patients With Valvular Heart Disease: A Report of the American College of Cardiology/American Heart Association Task Force on Clinical Practice Guidelines. *Circulation* 2017; **135**(25): e1159-e95.
3. Ciarka A, Van de Veire N. Secondary mitral regurgitation: pathophysiology, diagnosis, and treatment. *Heart* 2011; **97**(12): 1012-23.
4. Foster E. Clinical practice. Mitral regurgitation due to degenerative mitral-valve disease. *N Engl J Med* 2010; **363**(2): 156-65.
5. Sliwa K, Mocumbi AO. Forgotten cardiovascular diseases in Africa. *Clin Res Cardiol* 2010; **99**(2): 65-74.
6. McMurray JJ, Adamopoulos S, Anker SD, et al. ESC Guidelines for the diagnosis and treatment of acute and chronic heart failure 2012: The Task Force for the Diagnosis and Treatment of Acute and Chronic Heart Failure 2012 of the European Society of Cardiology. Developed in collaboration with the Heart Failure Association (HFA) of the ESC. *European heart journal* 2012; **33**(14): 1787-847.
7. Burchfield JS, Xie M, Hill JA. Pathological ventricular remodeling: mechanisms: part 1 of 2. *Circulation* 2013; **128**(4): 388-400.
8. Kong P, Christia P, Frangogiannis NG. The pathogenesis of cardiac fibrosis. *Cell Mol Life Sci* 2014; **71**(4): 549-74.
9. Otto CM, Prendergast B. Aortic-valve stenosis--from patients at risk to severe valve obstruction. *N Engl J Med* 2014; **371**(8): 744-56.
10. Carabello BA, Crawford FA. Valvular Heart Disease. *New England Journal of Medicine* 1997; **337**(1): 32-41.
11. Enriquez-Sarano M, Akins CW, Vahanian A. Mitral regurgitation. *The Lancet*; **373**(9672): 1382-94.
12. Avierinos JF, Gersh BJ, Melton LJ, 3rd, et al. Natural history of asymptomatic mitral valve prolapse in the community. *Circulation* 2002; **106**(11): 1355-61.
13. Enriquez-Sarano M, Avierinos JF, Messika-Zeitoun D, et al. Quantitative determinants of the outcome of asymptomatic mitral regurgitation. *N Engl J Med* 2005; **352**(9): 875-83.
14. Ross J, Jr., Sonnenblick EH, Taylor RR, Spotnitz HM, Covell JW. Diastolic geometry and sarcomere lengths in the chronically dilated canine left ventricle. *Circ Res* 1971; **28**(1): 49-61.
15. Grossman W, Jones D, McLaurin LP. Wall stress and patterns of hypertrophy in the human left ventricle. *J Clin Invest* 1975; **56**(1): 56-64.
16. Dell'italia LJ, Balcells E, Meng QC, et al. Volume-overload cardiac hypertrophy is unaffected by ACE inhibitor treatment in dogs. *Am J Physiol* 1997; **273**(2 Pt 2): H961-70.
17. Matsuo T, Carabello BA, Nagatomo Y, et al. Mechanisms of cardiac hypertrophy in canine volume overload. *Am J Physiol* 1998; **275**(1 Pt 2): H65-74.
18. Kerckhoffs RC, Omens J, McCulloch AD. A single strain-based growth law predicts concentric and eccentric cardiac growth during pressure and volume overload. *Mech Res Commun* 2012; **42**: 40-50.

19. Spinale FG, Ishihra K, Zile M, DeFryte G, Crawford FA, Carabello BA. Structural basis for changes in left ventricular function and geometry because of chronic mitral regurgitation and after correction of volume overload. *J Thorac Cardiovasc Surg* 1993; **106**(6): 1147-57.
20. Wisenbaugh T, Spann JF, Carabello BA. Differences in myocardial performance and load between patients with similar amounts of chronic aortic versus chronic mitral regurgitation. *Journal of the American College of Cardiology* 1984; **3**(4): 916-23.
21. Imamura T, McDermott PJ, Kent RL, Nagatsu M, Cooper Gt, Carabello BA. Acute changes in myosin heavy chain synthesis rate in pressure versus volume overload. *Circ Res* 1994; **75**(3): 418-25.
22. Urabe Y, Mann DL, Kent RL, et al. Cellular and ventricular contractile dysfunction in experimental canine mitral regurgitation. *Circ Res* 1992; **70**(1): 131-47.
23. Tsutsui H, Ishihara K, Cooper Gt. Cytoskeletal role in the contractile dysfunction of hypertrophied myocardium. *Science (New York, NY)* 1993; **260**(5108): 682-7.
24. Carabello BA. Progress in mitral and aortic regurgitation. *Progress in Cardiovascular Diseases* 1988; **43**(6): 457-75.
25. O'Gara P, Sugeng L, Lang R, et al. The role of imaging in chronic degenerative mitral regurgitation. *JACC Cardiovasc Imaging* 2008; **1**(2): 221-37.
26. Amin P, Singh M, Singh K. beta-Adrenergic Receptor-Stimulated Cardiac Myocyte Apoptosis: Role of beta1 Integrins. *J Signal Transduct* 2011; **2011**: 179057.
27. Chen YW, Pat B, Gladden JD, et al. Dynamic molecular and histopathological changes in the extracellular matrix and inflammation in the transition to heart failure in isolated volume overload. *Am J Physiol Heart Circ Physiol* 2011; **300**(6): H2251-60.
28. Hutchinson KR, Stewart JA, Jr., Lucchesi PA. Extracellular matrix remodeling during the progression of volume overload-induced heart failure. *J Mol Cell Cardiol* 2010; **48**(3): 564-9.
29. Knoll R, Marston S. On mechanosensation, acto/myosin interaction, and hypertrophy. *Trends Cardiovasc Med* 2012; **22**(1): 17-22.
30. Buyandelger B, Mansfield C, Knoll R. Mechano-signaling in heart failure. *Pflugers Arch* 2014; **466**(6): 1093-9.
31. Lyon RC, Zanella F, Omens JH, Sheikh F. Mechanotransduction in cardiac hypertrophy and failure. *Circ Res* 2015; **116**(8): 1462-76.
32. Israeli-Rosenberg S, Manso AM, Okada H, Ross RS. Integrins and integrin-associated proteins in the cardiac myocyte. *Circ Res* 2014; **114**(3): 572-86.
33. Opie LH BD. Mechanisms of cardiac contraction and relaxation. 10 ed. Philadelphia: Saunders Elsevier; 2015.
34. Miller MK, Granzier H, Ehler E, Gregorio CC. The sensitive giant: the role of titin-based stretch sensing complexes in the heart. *Trends Cell Biol* 2004; **14**(3): 119-26.
35. Zou P, Pinotsis N, Lange S, et al. Palindromic assembly of the giant muscle protein titin in the sarcomeric Z-disk. *Nature* 2006; **439**(7073): 229-33.
36. Knoll R, Hoshijima M, Hoffman HM, et al. The cardiac mechanical stretch sensor machinery involves a Z disc complex that is defective in a subset of human dilated cardiomyopathy. *Cell* 2002; **111**(7): 943-55.
37. Hishiya A, Kitazawa T, Takayama S. BAG3 and Hsc70 interact with actin capping protein CapZ to maintain myofibrillar integrity under mechanical stress. *Circ Res* 2010; **107**(10): 1220-31.
38. Kuwahara K, Kinoshita H, Kuwabara Y, et al. Myocardin-related transcription factor A is a common mediator of mechanical stress- and neurohumoral stimulation-induced cardiac

hypertrophic signaling leading to activation of brain natriuretic peptide gene expression. *Mol Cell Biol* 2010; **30**(17): 4134-48.
39. Lange S, Xiang F, Yakovenko A, et al. The kinase domain of titin controls muscle gene expression and protein turnover. *Science (New York, NY)* 2005; **308**(5728): 1599-603.
40. Wagner MA, Siddiqui MA. The JAK-STAT pathway in hypertrophic stress signaling and genomic stress response. *Jakstat* 2012; **1**(2): 131-41.
41. Puchner EM, Alexandrovich A, Kho AL, et al. Mechanoenzymatics of titin kinase. *Proceedings of the National Academy of Sciences of the United States of America* 2008; **105**(36): 13385-90.
42. Arber S, Hunter JJ, Ross J, Jr., et al. MLP-deficient mice exhibit a disruption of cardiac cytoarchitectural organization, dilated cardiomyopathy, and heart failure. *Cell* 1997; **88**(3): 393-403.
43. Knoll R, Kostin S, Klede S, et al. A common MLP (muscle LIM protein) variant is associated with cardiomyopathy. *Circ Res* 2010; **106**(4): 695-704.
44. Boateng SY, Senyo SE, Qi L, Goldspink PH, Russell B. Myocyte remodeling in response to hypertrophic stimuli requires nucleocytoplasmic shuttling of muscle LIM protein. *J Mol Cell Cardiol* 2009; **47**(4): 426-35.
45. Wang BW, Hung HF, Chang H, Kuan P, Shyu KG. Mechanical stretch enhances the expression of resistin gene in cultured cardiomyocytes via tumor necrosis factor-alpha. *Am J Physiol Heart Circ Physiol* 2007; **293**(4): H2305-12.
46. Chen Y, Pat B, Zheng J, et al. Tumor necrosis factor-alpha produced in cardiomyocytes mediates a predominant myocardial inflammatory response to stretch in early volume overload. *J Mol Cell Cardiol* 2010; **49**(1): 70-8.
47. Wang TL, Yang YH, Chang H, Hung CR. Angiotensin II signals mechanical stretch-induced cardiac matrix metalloproteinase expression via JAK-STAT pathway. *J Mol Cell Cardiol* 2004; **37**(3): 785-94.
48. Gealekman O, Abassi Z, Rubinstein I, Winaver J, Binah O. Role of myocardial inducible nitric oxide synthase in contractile dysfunction and beta-adrenergic hyporesponsiveness in rats with experimental volume-overload heart failure. *Circulation* 2002; **105**(2): 236-43.
49. Baud V, Karin M. Signal transduction by tumor necrosis factor and its relatives. *Trends Cell Biol* 2001; **11**(9): 372-7.
50. Lebrec H, Ponce R, Preston BD, Iles J, Born TL, Hooper M. Tumor necrosis factor, tumor necrosis factor inhibition, and cancer risk. *Curr Med Res Opin* 2015; **31**(3): 557-74.
51. Griendling KK, Sorescu D, Lassegue B, Ushio-Fukai M. Modulation of protein kinase activity and gene expression by reactive oxygen species and their role in vascular physiology and pathophysiology. *Arterioscler Thromb Vasc Biol* 2000; **20**(10): 2175-83.
52. Grote K, Flach I, Luchtefeld M, et al. Mechanical stretch enhances mRNA expression and proenzyme release of matrix metalloproteinase-2 (MMP-2) via NAD(P)H oxidase-derived reactive oxygen species. *Circ Res* 2003; **92**(11): e80-6.
53. Siwik DA, Pagano PJ, Colucci WS. Oxidative stress regulates collagen synthesis and matrix metalloproteinase activity in cardiac fibroblasts. *Am J Physiol Cell Physiol* 2001; **280**(1): C53-60.
54. Birukov KG. Cyclic stretch, reactive oxygen species, and vascular remodeling. *Antioxid Redox Signal* 2009; **11**(7): 1651-67.
55. Keith M, Geranmayegan A, Sole MJ, et al. Increased oxidative stress in patients with congestive heart failure. *Journal of the American College of Cardiology* 1998; **31**(6): 1352-6.

56. Ahmed MI, Gladden JD, Litovsky SH, et al. Increased oxidative stress and cardiomyocyte myofibrillar degeneration in patients with chronic isolated mitral regurgitation and ejection fraction >60%. *Journal of the American College of Cardiology* 2010; **55**(7): 671-9.
57. Yancey DM, Guichard JL, Ahmed MI, et al. Cardiomyocyte mitochondrial oxidative stress and cytoskeletal breakdown in the heart with a primary volume overload. *American journal of physiology Heart and circulatory physiology* 2015; **308**(6): H651-63.
58. Zheng J, Yancey DM, Ahmed MI, et al. Increased Sarcolipin Expression and Adrenergic Drive in Humans With Preserved Left Ventricular Ejection Fraction and Chronic Isolated Mitral Regurgitation. *Circulation: Heart Failure* 2014; **7**(1): 194-202.
59. Mann DL. Innate immunity and the failing heart: the cytokine hypothesis revisited. *Circ Res* 2015; **116**(7): 1254-68.
60. Nakano M, Knowlton AA, Dibbs Z, Mann DL. Tumor necrosis factor-alpha confers resistance to hypoxic injury in the adult mammalian cardiac myocyte. *Circulation* 1998; **97**(14): 1392-400.
61. Hamid T, Gu Y, Ortines RV, et al. Divergent tumor necrosis factor receptor-related remodeling responses in heart failure: role of nuclear factor-kappaB and inflammatory activation. *Circulation* 2009; **119**(10): 1386-97.
62. Pagani FD, Baker LS, Hsi C, Knox M, Fink MP, Visner MS. Left ventricular systolic and diastolic dysfunction after infusion of tumor necrosis factor-alpha in conscious dogs. *J Clin Invest* 1992; **90**(2): 389-98.
63. Franco F, Thomas GD, Giroir B, et al. Magnetic resonance imaging and invasive evaluation of development of heart failure in transgenic mice with myocardial expression of tumor necrosis factor-alpha. *Circulation* 1999; **99**(3): 448-54.
64. Krown KA, Page MT, Nguyen C, et al. Tumor necrosis factor alpha-induced apoptosis in cardiac myocytes. Involvement of the sphingolipid signaling cascade in cardiac cell death. *J Clin Invest* 1996; **98**(12): 2854-65.
65. Haudek SB, Taffet GE, Schneider MD, Mann DL. TNF provokes cardiomyocyte apoptosis and cardiac remodeling through activation of multiple cell death pathways. *J Clin Invest* 2007; **117**(9): 2692-701.
66. Dhingra S, Bagchi AK, Ludke AL, Sharma AK, Singal PK. Akt regulates IL-10 mediated suppression of TNFalpha-induced cardiomyocyte apoptosis by upregulating Stat3 phosphorylation. *PLoS One* 2011; **6**(9): e25009.
67. Engel D, Peshock R, Armstong RC, Sivasubramanian N, Mann DL. Cardiac myocyte apoptosis provokes adverse cardiac remodeling in transgenic mice with targeted TNF overexpression. *Am J Physiol Heart Circ Physiol* 2004; **287**(3): H1303-11.
68. Dhingra S, Sharma AK, Arora RC, Slezak J, Singal PK. IL-10 attenuates TNF-alpha-induced NF kappaB pathway activation and cardiomyocyte apoptosis. *Cardiovasc Res* 2009; **82**(1): 59-66.
69. Sivasubramanian N, Coker ML, Kurrelmeyer KM, et al. Left ventricular remodeling in transgenic mice with cardiac restricted overexpression of tumor necrosis factor. *Circulation* 2001; **104**(7): 826-31.
70. Diwan A, Dibbs Z, Nemoto S, et al. Targeted overexpression of noncleavable and secreted forms of tumor necrosis factor provokes disparate cardiac phenotypes. *Circulation* 2004; **109**(2): 262-8.
71. Levick SP, Gardner JD, Holland M, Hauer-Jensen M, Janicki JS, Brower GL. Protection from adverse myocardial remodeling secondary to chronic volume overload in mast cell deficient rats. *J Mol Cell Cardiol* 2008; **45**(1): 56-61.

72. Levine B, Kalman J, Mayer L, Fillit HM, Packer M. Elevated circulating levels of tumor necrosis factor in severe chronic heart failure. *N Engl J Med* 1990; **323**(4): 236-41.
73. Kapadia SR, Yakoob K, Nader S, Thomas JD, Mann DL, Griffin BP. Elevated circulating levels of serum tumor necrosis factor-alpha in patients with hemodynamically significant pressure and volume overload. *Journal of the American College of Cardiology* 2000; **36**(1): 208-12.
74. Sliwa K, Skudicky D, Bergemann A, Candy G, Puren A, Sareli P. Peripartum cardiomyopathy: analysis of clinical outcome, left ventricular function, plasma levels of cytokines and Fas/APO-1. *Journal of the American College of Cardiology* 2000; **35**(3): 701-5.
75. Bujak M, Frangogiannis NG. The role of IL-1 in the pathogenesis of heart disease. *Arch Immunol Ther Exp (Warsz)* 2009; **57**(3): 165-76.
76. Palmieri EA, Benincasa G, Di Rella F, et al. Differential expression of TNF-alpha, IL-6, and IGF-1 by graded mechanical stress in normal rat myocardium. *Am J Physiol Heart Circ Physiol* 2002; **282**(3): H926-34.
77. Oral H, Sivasubramanian N, Dyke DB, et al. Myocardial proinflammatory cytokine expression and left ventricular remodeling in patients with chronic mitral regurgitation. *Circulation* 2003; **107**(6): 831-7.
78. Spina GS, Tarasoutchi F, Sampaio RO, et al. Neurohormonal profile of rheumatic patients with significant chronic aortic regurgitation. *Arq Bras Cardiol* 2009; **92**(2): 143-56.
79. Cheng W, Li B, Kajstura J, et al. Stretch-induced programmed myocyte cell death. *J Clin Invest* 1995; **96**(5): 2247-59.
80. Communal C, Singh K, Pimentel DR, Colucci WS. Norepinephrine stimulates apoptosis in adult rat ventricular myocytes by activation of the beta-adrenergic pathway. *Circulation* 1998; **98**(13): 1329-34.
81. Geng YJ, Ishikawa Y, Vatner DE, et al. Apoptosis of cardiac myocytes in Gsalpha transgenic mice. *Circ Res* 1999; **84**(1): 34-42.
82. Lymperopoulos A, Rengo G, Koch WJ. Adrenergic nervous system in heart failure: pathophysiology and therapy. *Circ Res* 2013; **113**(6): 739-53.
83. Orrenius S, McConkey DJ, Bellomo G, Nicotera P. Role of Ca2+ in toxic cell killing. *Trends Pharmacol Sci* 1989; **10**(7): 281-5.
84. Mulieri LA, Tischler MD, Martin BJ, et al. Regional differences in the force-frequency relation of human left ventricular myocardium in mitral regurgitation: implications for ventricular shape. *Am J Physiol Heart Circ Physiol* 2005; **288**(5): H2185-91.
85. Gupta RC, Mishra S, Mishima T, Goldstein S, Sabbah HN. Reduced sarcoplasmic reticulum Ca(2+)-uptake and expression of phospholamban in left ventricular myocardium of dogs with heart failure. *J Mol Cell Cardiol* 1999; **31**(7): 1381-9.
86. Sabbah HN. Biologic rationale for the use of beta-blockers in the treatment of heart failure. *Heart Fail Rev* 2004; **9**(2): 91-7.
87. Leszek P, Korewicki J, Klisiewicz A, et al. Reduced myocardial expression of calcium handling protein in patients with severe chronic mitral regurgitation. *Eur J Cardiothorac Surg* 2006; **30**(5): 737-43.
88. Dorn GW, 2nd. Apoptotic and non-apoptotic programmed cardiomyocyte death in ventricular remodelling. *Cardiovasc Res* 2009; **81**(3): 465-73.
89. Foo RS, Mani K, Kitsis RN. Death begets failure in the heart. *J Clin Invest* 2005; **115**(3): 565-71.

90. Remondino A, Kwon SH, Communal C, et al. Beta-adrenergic receptor-stimulated apoptosis in cardiac myocytes is mediated by reactive oxygen species/c-Jun NH2-terminal kinase-dependent activation of the mitochondrial pathway. *Circ Res* 2003; **92**(2): 136-8.
91. Hankes GH, Ardell JL, Tallaj J, et al. Beta1-adrenoceptor blockade mitigates excessive norepinephrine release into cardiac interstitium in mitral regurgitation in dog. *Am J Physiol Heart Circ Physiol* 2006; **291**(1): H147-51.
92. Tsutsui H, Spinale FG, Nagatsu M, et al. Effects of chronic beta-adrenergic blockade on the left ventricular and cardiocyte abnormalities of chronic canine mitral regurgitation. *J Clin Invest* 1994; **93**(6): 2639-48.
93. Janicki JS, Brower GL. The role of myocardial fibrillar collagen in ventricular remodeling and function. *J Card Fail* 2002; **8**(6 Suppl): S319-25.
94. Spinale FG. Myocardial matrix remodeling and the matrix metalloproteinases: influence on cardiac form and function. *Physiol Rev* 2007; **87**(4): 1285-342.
95. Spinale FG, Coker ML, Heung LJ, et al. A matrix metalloproteinase induction/activation system exists in the human left ventricular myocardium and is upregulated in heart failure. *Circulation* 2000; **102**(16): 1944-9.
96. King MK, Coker ML, Goldberg A, et al. Selective matrix metalloproteinase inhibition with developing heart failure: effects on left ventricular function and structure. *Circ Res* 2003; **92**(2): 177-85.
97. Ahmed SH, Clark LL, Pennington WR, et al. Matrix metalloproteinases/tissue inhibitors of metalloproteinases: relationship between changes in proteolytic determinants of matrix composition and structural, functional, and clinical manifestations of hypertensive heart disease. *Circulation* 2006; **113**(17): 2089-96.
98. George J, Patal S, Wexler D, Roth A, Sheps D, Keren G. Circulating matrix metalloproteinase-2 but not matrix metalloproteinase-3, matrix metalloproteinase-9, or tissue inhibitor of metalloproteinase-1 predicts outcome in patients with congestive heart failure. *Am Heart J* 2005; **150**(3): 484-7.
99. Buralli S, Dini FL, Ballo P, et al. Circulating matrix metalloproteinase-3 and metalloproteinase-9 and tissue Doppler measures of diastolic dysfunction to risk stratify patients with systolic heart failure. *Am J Cardiol* 2010; **105**(6): 853-6.
100. Lovelock JD, Baker AH, Gao F, et al. Heterogeneous effects of tissue inhibitors of matrix metalloproteinases on cardiac fibroblasts. *Am J Physiol Heart Circ Physiol* 2005; **288**(2): H461-8.
101. Chakraborti S, Mandal M, Das S, Mandal A, Chakraborti T. Regulation of matrix metalloproteinases: an overview. *Mol Cell Biochem* 2003; **253**(1-2): 269-85.
102. Vincenti MP, Brinckerhoff CE. Signal transduction and cell-type specific regulation of matrix metalloproteinase gene expression: can MMPs be good for you? *J Cell Physiol* 2007; **213**(2): 355-64.
103. Klein T, Bischoff R. Physiology and pathophysiology of matrix metalloproteases. *Amino Acids* 2011; **41**(2): 271-90.
104. Siwik DA, Chang DL, Colucci WS. Interleukin-1beta and tumor necrosis factor-alpha decrease collagen synthesis and increase matrix metalloproteinase activity in cardiac fibroblasts in vitro. *Circ Res* 2000; **86**(12): 1259-65.
105. MacKenna DA, Dolfi F, Vuori K, Ruoslahti E. Extracellular signal-regulated kinase and c-Jun NH2-terminal kinase activation by mechanical stretch is integrin-dependent and matrix-specific in rat cardiac fibroblasts. *J Clin Invest* 1998; **101**(2): 301-10.

106. MacKenna D, Summerour SR, Villarreal FJ. Role of mechanical factors in modulating cardiac fibroblast function and extracellular matrix synthesis. *Cardiovasc Res* 2000; **46**(2): 257-63.
107. Manso AM, Elsherif L, Kang SM, Ross RS. Integrins, membrane-type matrix metalloproteinases and ADAMs: potential implications for cardiac remodeling. *Cardiovasc Res* 2006; **69**(3): 574-84.
108. Ross RS. The extracellular connections: the role of integrins in myocardial remodeling. *J Card Fail* 2002; **8**(6 Suppl): S326-31.
109. Coker ML, Jolly JR, Joffs C, et al. Matrix metalloproteinase expression and activity in isolated myocytes after neurohormonal stimulation. *Am J Physiol Heart Circ Physiol* 2001; **281**(2): H543-51.
110. Sabri A, Rafiq K, Seqqat R, Kolpakov MA, Dillon R, Dell'italia LJ. Sympathetic activation causes focal adhesion signaling alteration in early compensated volume overload attributable to isolated mitral regurgitation in the dog. *Circ Res* 2008; **102**(9): 1127-36.
111. Ogawa K, Chen F, Kuang C, Chen Y. Suppression of matrix metalloproteinase-9 transcription by transforming growth factor-beta is mediated by a nuclear factor-kappaB site. *Biochem J* 2004; **381**(Pt 2): 413-22.
112. Rouet-Benzineb P, Gontero B, Dreyfus P, Lafuma C. Angiotensin II induces nuclear factor- kappa B activation in cultured neonatal rat cardiomyocytes through protein kinase C signaling pathway. *J Mol Cell Cardiol* 2000; **32**(10): 1767-78.
113. Seeland U, Haeuseler C, Hinrichs R, et al. Myocardial fibrosis in transforming growth factor-beta(1) (TGF-beta(1)) transgenic mice is associated with inhibition of interstitial collagenase. *Eur J Clin Invest* 2002; **32**(5): 295-303.
114. Bujak M, Frangogiannis NG. The role of TGF-beta signaling in myocardial infarction and cardiac remodeling. *Cardiovasc Res* 2007; **74**(2): 184-95.
115. Zheng J, Chen Y, Pat B, et al. Microarray identifies extensive downregulation of noncollagen extracellular matrix and profibrotic growth factor genes in chronic isolated mitral regurgitation in the dog. *Circulation* 2009; **119**(15): 2086-95.
116. Zhang YM, Bo J, Taffet GE, et al. Targeted deletion of ROCK1 protects the heart against pressure overload by inhibiting reactive fibrosis. *Faseb j* 2006; **20**(7): 916-25.
117. Jellis C, Martin J, Narula J, Marwick TH. Assessment of nonischemic myocardial fibrosis. *Journal of the American College of Cardiology* 2010; **56**(2): 89-97.
118. Dell'Italia LJ, Meng QC, Balcells E, et al. Increased ACE and chymase-like activity in cardiac tissue of dogs with chronic mitral regurgitation. *Am J Physiol* 1995; **269**(6 Pt 2): H2065-73.
119. Stewart JA, Jr., Wei CC, Brower GL, et al. Cardiac mast cell- and chymase-mediated matrix metalloproteinase activity and left ventricular remodeling in mitral regurgitation in the dog. *J Mol Cell Cardiol* 2003; **35**(3): 311-9.
120. Tallaj J, Wei CC, Hankes GH, et al. Beta1-adrenergic receptor blockade attenuates angiotensin II-mediated catecholamine release into the cardiac interstitium in mitral regurgitation. *Circulation* 2003; **108**(2): 225-30.
121. Lin A, Stewart R. Medical treatment of asymptomatic chronic aortic regurgitation. *Expert Rev Cardiovasc Ther* 2011; **9**(9): 1249-54.
122. Weidemann F, Herrmann S, Stork S, et al. Impact of myocardial fibrosis in patients with symptomatic severe aortic stenosis. *Circulation* 2009; **120**(7): 577-84.

123. Weinberg EO, Schoen FJ, George D, et al. Angiotensin-converting enzyme inhibition prolongs survival and modifies the transition to heart failure in rats with pressure overload hypertrophy due to ascending aortic stenosis. *Circulation* 1994; **90**(3): 1410-22.
124. Perry GJ, Wei CC, Hankes GH, et al. Angiotensin II receptor blockade does not improve left ventricular function and remodeling in subacute mitral regurgitation in the dog. *Journal of the American College of Cardiology* 2002; **39**(8): 1374-9.
125. Babbitt CJ, Shai SY, Harpf AE, Pham CG, Ross RS. Modulation of integrins and integrin signaling molecules in the pressure-loaded murine ventricle. *Histochem Cell Biol* 2002; **118**(6): 431-9.
126. Bloor CM, Nimmo L, McKirnan MD, Zhang Y, White FC. Increased gene expression of plasminogen activators and inhibitors in left ventricular hypertrophy. *Mol Cell Biochem* 1997; **176**(1-2): 265-71.
127. Brower GL, Chancey AL, Thanigaraj S, Matsubara BB, Janicki JS. Cause and effect relationship between myocardial mast cell number and matrix metalloproteinase activity. *Am J Physiol Heart Circ Physiol* 2002; **283**(2): H518-25.
128. Janicki JS, Brower GL, Gardner JD, et al. Cardiac mast cell regulation of matrix metalloproteinase-related ventricular remodeling in chronic pressure or volume overload. *Cardiovasc Res* 2006; **69**(3): 657-65.
129. Nagatomo Y, Carabello BA, Coker ML, et al. Differential effects of pressure or volume overload on myocardial MMP levels and inhibitory control. *Am J Physiol Heart Circ Physiol* 2000; **278**(1): H151-61.
130. Chancey AL, Brower GL, Peterson JT, Janicki JS. Effects of matrix metalloproteinase inhibition on ventricular remodeling due to volume overload. *Circulation* 2002; **105**(16): 1983-8.
131. Ljungvall I, Rajamaki MM, Crosara S, et al. Evaluation of plasma activity of matrix metalloproteinase-2 and -9 in dogs with myxomatous mitral valve disease. *Am J Vet Res* 2011; **72**(8): 1022-8.
132. Iwanaga Y, Aoyama T, Kihara Y, Onozawa Y, Yoneda T, Sasayama S. Excessive activation of matrix metalloproteinases coincides with left ventricular remodeling during transition from hypertrophy to heart failure in hypertensive rats. *Journal of the American College of Cardiology* 2002; **39**(8): 1384-91.
133. Moustafa SE, Kansal M, Alharthi M, Deng Y, Chandrasekaran K, Mookadam F. Prediction of incipient left ventricular dysfunction in patients with chronic primary mitral regurgitation: a velocity vector imaging study. *Eur J Echocardiogr* 2011; **12**(4): 291-8.
134. Magne J, Mahjoub H, Dulgheru R, Pibarot P, Pierard LA, Lancellotti P. Left ventricular contractile reserve in asymptomatic primary mitral regurgitation. *European heart journal* 2014; **35**(24): 1608-16.
135. Le Tourneau T, de Groote P, Millaire A, et al. Effect of mitral valve surgery on exercise capacity, ventricular ejection fraction and neurohormonal activation in patients with severe mitral regurgitation. *Journal of the American College of Cardiology* 2000; **36**(7): 2263-9.
136. Mehta RH, Supiano MA, Oral H, et al. Compared with control subjects, the systemic sympathetic nervous system is activated in patients with mitral regurgitation. *Am Heart J* 2003; **145**(6): 1078-85.
137. Nagatsu M, Zile MR, Tsutsui H, et al. Native beta-adrenergic support for left ventricular dysfunction in experimental mitral regurgitation normalizes indexes of pump and contractile function. *Circulation* 1994; **89**(2): 818-26.

138. Touyz RM, Schiffrin EL. Signal transduction mechanisms mediating the physiological and pathophysiological actions of angiotensin II in vascular smooth muscle cells. *Pharmacol Rev* 2000; **52**(4): 639-72.
139. Schieffer B, Bernstein KE, Marrero MB. The role of tyrosine phosphorylation in angiotensin II mediated intracellular signaling and cell growth. *J Mol Med (Berl)* 1996; **74**(2): 85-91.
140. Abe J, Berk BC. Reactive oxygen species as mediators of signal transduction in cardiovascular disease. *Trends Cardiovasc Med* 1998; **8**(2): 59-64.
141. Brasch H, Sieroslawski L, Dominiak P. Angiotensin II increases norepinephrine release from atria by acting on angiotensin subtype 1 receptors. *Hypertension* 1993; **22**(5): 699-704.
142. Farrell DM, Wei CC, Tallaj J, et al. Angiotensin II modulates catecholamine release into interstitial fluid of canine myocardium in vivo. *Am J Physiol Heart Circ Physiol* 2001; **281**(2): H813-22.
143. Kagami S, Border WA, Miller DE, Noble NA. Angiotensin II stimulates extracellular matrix protein synthesis through induction of transforming growth factor-beta expression in rat glomerular mesangial cells. *J Clin Invest* 1994; **93**(6): 2431-7.
144. Goldsmith EC, Bradshaw AD, Spinale FG. Cellular mechanisms of tissue fibrosis. 2. Contributory pathways leading to myocardial fibrosis: moving beyond collagen expression. *Am J Physiol Cell Physiol* 2013; **304**(5): C393-402.
145. Ryan TD, Rothstein EC, Aban I, et al. Left ventricular eccentric remodeling and matrix loss are mediated by bradykinin and precede cardiomyocyte elongation in rats with volume overload. *Journal of the American College of Cardiology* 2007; **49**(7): 811-21.
146. Levine HJ, Gaasch WH. Vasoactive drugs in chronic regurgitant lesions of the mitral and aortic valves. *Journal of the American College of Cardiology* 1996; **28**(5): 1083-91.
147. Nemoto S, Hamawaki M, De Freitas G, Carabello BA. Differential effects of the angiotensin-converting enzyme inhibitor lisinopril versus the beta-adrenergic receptor blocker atenolol on hemodynamics and left ventricular contractile function in experimental mitral regurgitation. *Journal of the American College of Cardiology* 2002; **40**(1): 149-54.
148. Oh SH, Meyers DG. Afterload reduction may halt and beta-adrenergic blockade may worsen progression of left ventricular dysfunction in patients with chronic compensated mitral regurgitation: a retrospective cohort study. *Angiology* 2007; **58**(2): 196-202.
149. Woo AY, Xiao RP. beta-Adrenergic receptor subtype signaling in heart: from bench to bedside. *Acta Pharmacol Sin* 2012; **33**(3): 335-41.
150. Belge C, Hammond J, Dubois-Deruy E, et al. Enhanced Expression of β3-Adrenoceptors in Cardiac Myocytes Attenuates Neurohormone-Induced Hypertrophic Remodeling Through Nitric Oxide Synthase. *Circulation* 2014; **129**(4): 451-62.
151. Chidsey CA, Braunwald E, Morrow AG, Mason DT. Myocardial norepinephrine concentration in man. Effects of reserpine and of congestive heart failure. *N Engl J Med* 1963; **269**: 653-8.
152. Fowler MB, Bristow MR. Rationale for beta-adrenergic blocking drugs in cardiomyopathy. *Am J Cardiol* 1985; **55**(10): 120d-4d.
153. Bristow MR, Ginsburg R, Minobe W, et al. Decreased catecholamine sensitivity and beta-adrenergic-receptor density in failing human hearts. *N Engl J Med* 1982; **307**(4): 205-11.
154. Lowes BD, Minobe W, Abraham WT, et al. Changes in gene expression in the intact human heart. Downregulation of alpha-myosin heavy chain in hypertrophied, failing ventricular myocardium. *J Clin Invest* 1997; **100**(9): 2315-24.

155. Lowes BD, Gilbert EM, Abraham WT, et al. Myocardial gene expression in dilated cardiomyopathy treated with beta-blocking agents. *N Engl J Med* 2002; **346**(18): 1357-65.
156. Engelhardt S, Bohm M, Erdmann E, Lohse MJ. Analysis of beta-adrenergic receptor mRNA levels in human ventricular biopsy specimens by quantitative polymerase chain reactions: progressive reduction of beta 1-adrenergic receptor mRNA in heart failure. *Journal of the American College of Cardiology* 1996; **27**(1): 146-54.
157. Hammond HK, Roth DA, Insel PA, et al. Myocardial beta-adrenergic receptor expression and signal transduction after chronic volume-overload hypertrophy and circulatory congestion. *Circulation* 1992; **85**(1): 269-80.
158. Choi DJ, Koch WJ, Hunter JJ, Rockman HA. Mechanism of beta-adrenergic receptor desensitization in cardiac hypertrophy is increased beta-adrenergic receptor kinase. *J Biol Chem* 1997; **272**(27): 17223-9.
159. Osadchii OE, Norton GR, McKechnie R, Deftereos D, Woodiwiss AJ. Cardiac dilatation and pump dysfunction without intrinsic myocardial systolic failure following chronic beta-adrenoreceptor activation. *Am J Physiol Heart Circ Physiol* 2007; **292**(4): H1898-905.
160. Packer M, Fowler MB, Roecker EB, et al. Effect of carvedilol on the morbidity of patients with severe chronic heart failure: results of the carvedilol prospective randomized cumulative survival (COPERNICUS) study. *Circulation* 2002; **106**(17): 2194-9.
161. Kohout TA, Takaoka H, McDonald PH, et al. Augmentation of cardiac contractility mediated by the human beta(3)-adrenergic receptor overexpressed in the hearts of transgenic mice. *Circulation* 2001; **104**(20): 2485-91.
162. Zhao Q, Wu TG, Jiang ZF, Chen GW, Lin Y, Wang LX. Effect of beta-blockers on beta3-adrenoceptor expression in chronic heart failure. *Cardiovasc Drugs Ther* 2007; **21**(2): 85-90.
163. Yue TL, Cheng HY, Lysko PG, et al. Carvedilol, a new vasodilator and beta adrenoceptor antagonist, is an antioxidant and free radical scavenger. *J Pharmacol Exp Ther* 1992; **263**(1): 92-8.
164. Ohlstein EH, Douglas SA, Sung CP, et al. Carvedilol, a cardiovascular drug, prevents vascular smooth muscle cell proliferation, migration, and neointimal formation following vascular injury. *Proceedings of the National Academy of Sciences of the United States of America* 1993; **90**(13): 6189-93.
165. Wisler JW, DeWire SM, Whalen EJ, et al. A unique mechanism of beta-blocker action: carvedilol stimulates beta-arrestin signaling. *Proceedings of the National Academy of Sciences of the United States of America* 2007; **104**(42): 16657-62.
166. Gilbert EM, Abraham WT, Olsen S, et al. Comparative hemodynamic, left ventricular functional, and antiadrenergic effects of chronic treatment with metoprolol versus carvedilol in the failing heart. *Circulation* 1996; **94**(11): 2817-25.
167. Stoschitzky K, Koshucharova G, Zweiker R, et al. Differing beta-blocking effects of carvedilol and metoprolol. *Eur J Heart Fail* 2001; **3**(3): 343-9.
168. Quaife RA, Christian PE, Gilbert EM, Datz FL, Volkman K, Bristow MR. Effects of carvedilol on right ventricular function in chronic heart failure. *Am J Cardiol* 1998; **81**(2): 247-50.
169. Beck-da-Silva L, de Bold A, Davies R, et al. Effect of bisoprolol on right ventricular function and brain natriuretic peptide in patients with heart failure. *Congest Heart Fail* 2004; **10**(3): 127-32.
170. Hongning Y, Stewart RA, Whalley GA. The impact of beta-blockade on right ventricular function in mitral regurgitation. *Heart Lung Circ* 2014; **23**(4): 378-80.

171. The Cardiac Insufficiency Bisoprolol Study II (CIBIS-II): a randomised trial. *Lancet* 1999; **353**(9146): 9-13.
172. Effect of metoprolol CR/XL in chronic heart failure: Metoprolol CR/XL Randomised Intervention Trial in Congestive Heart Failure (MERIT-HF). *Lancet* 1999; **353**(9169): 2001-7.
173. Poole-Wilson PA, Swedberg K, Cleland JG, et al. Comparison of carvedilol and metoprolol on clinical outcomes in patients with chronic heart failure in the Carvedilol Or Metoprolol European Trial (COMET): randomised controlled trial. *Lancet* 2003; **362**(9377): 7-13.
174. Naccarelli GV, Lukas MA. Carvedilol's antiarrhythmic properties: therapeutic implications in patients with left ventricular dysfunction. *Clin Cardiol* 2005; **28**(4): 165-73.
175. Bristow MR. beta-adrenergic receptor blockade in chronic heart failure. *Circulation* 2000; **101**(5): 558-69.
176. Nagatsu M, Spinale FG, Koide M, et al. Bradycardia and the role of beta-blockade in the amelioration of left ventricular dysfunction. *Circulation* 2000; **101**(6): 653-9.
177. Communal C, Singh K, Sawyer DB, Colucci WS. Opposing effects of beta(1)- and beta(2)-adrenergic receptors on cardiac myocyte apoptosis : role of a pertussis toxin-sensitive G protein. *Circulation* 1999; **100**(22): 2210-2.
178. Mason RP, Giles TD, Sowers JR. Evolving mechanisms of action of beta blockers: focus on nebivolol. *J Cardiovasc Pharmacol* 2009; **54**(2): 123-8.
179. Saini-Chohan HK, Hatch GM. Biological actions and metabolism of currently used pharmacological agents for the treatment of congestive heart failure. *Curr Drug Metab* 2009; **10**(3): 206-19.
180. Wu TC, Chen YH, Leu HB, et al. Carvedilol, a pharmacological antioxidant, inhibits neointimal matrix metalloproteinase-2 and -9 in experimental atherosclerosis. *Free Radic Biol Med* 2007; **43**(11): 1508-22.
181. Lohse MJ, Engelhardt S, Eschenhagen T. What is the role of beta-adrenergic signaling in heart failure? *Circ Res* 2003; **93**(10): 896-906.
182. Trappanese DM, Liu Y, McCormick RC, et al. Chronic beta1-adrenergic blockade enhances myocardial beta3-adrenergic coupling with nitric oxide-cGMP signaling in a canine model of chronic volume overload: new insight into mechanisms of cardiac benefit with selective beta1-blocker therapy. *Basic Res Cardiol* 2015; **110**(1): 456.
183. Starling MR. Effects of valve surgery on left ventricular contractile function in patients with long-term mitral regurgitation. *Circulation* 1995; **92**(4): 811-8.
184. Witkowski TG, Thomas JD, Delgado V, et al. Changes in left ventricular function after mitral valve repair for severe organic mitral regurgitation. *Ann Thorac Surg* 2012; **93**(3): 754-60.
185. Kainuma S, Taniguchi K, Toda K, et al. B-type natriuretic peptide response and reverse left ventricular remodeling after surgical correction of functional mitral regurgitation in patients with advanced cardiomyopathy. *J Cardiol* 2015; **66**(4):279-85.
186. Hetzer R, Dandel M. Early detection of left ventricular dysfunction in patients with mitral regurgitation due to flail leaflet is still a challenge. *European heart journal* 2011; **32**(6): 665-7.
187. Carabello BA. Beta-blockade for mitral regurgitation: could the management of valvular heart disease actually be moving into the 21st century? *Journal of the American College of Cardiology* 2012; **60**(9): 839-40.

188. Samad Z, Kaul P, Shaw LK, et al. Impact of early surgery on survival of patients with severe mitral regurgitation. *Heart* 2011; **97**(3): 221-4.
189. Kang DH, Park SJ, Sun BJ, et al. Early surgery versus conventional treatment for asymptomatic severe mitral regurgitation: a propensity analysis. *Journal of the American College of Cardiology* 2014; **63**(22): 2398-407.
190. Yazdchi F, Koch CG, Mihaljevic T, et al. Increasing Disadvantage of "Watchful Waiting" for Repairing Degenerative Mitral Valve Disease. *Ann Thorac Surg* 2015; **99**(6): 1992-2000.
191. Barbieri A, Bursi F, Grigioni F, et al. Prognostic and therapeutic implications of pulmonary hypertension complicating degenerative mitral regurgitation due to flail leaflet: a multicenter long-term international study. *European heart journal* 2011; **32**(6): 751-9.
192. Rosenhek R, Rader F, Klaar U, et al. Outcome of watchful waiting in asymptomatic severe mitral regurgitation. *Circulation* 2006; **113**(18): 2238-44.
193. Carabello BA. The current therapy for mitral regurgitation. *Journal of the American College of Cardiology* 2008; **52**(5): 319-26.
194. Wisenbaugh T. Vasoactive medications in the treatment of severe mitral regurgitation. *Coron Artery Dis* 2000; **11**(1): 19-22.
195. Wisenbaugh T, Sinovich V, Dullabh A, Sareli P. Six month pilot study of captopril for mildly symptomatic, severe isolated mitral and isolated aortic regurgitation. *J Heart Valve Dis* 1994; **3**(2): 197-204.
196. Stewart RA, Raffel OC, Kerr AJ, et al. Pilot study to assess the influence of beta-blockade on mitral regurgitant volume and left ventricular work in degenerative mitral valve disease. *Circulation* 2008; **118**(10): 1041-6.
197. Ennis DB, Rudd-Barnard GR, Li B, et al. Changes in mitral annular geometry and dynamics with ss-blockade in patients with degenerative mitral valve disease. *Circ Cardiovasc Imaging* 2010; **3**(6): 687-93.
198. Varadarajan P, Joshi N, Appel D, Duvvuri L, Pai RG. Effect of Beta-blocker therapy on survival in patients with severe mitral regurgitation and normal left ventricular ejection fraction. *Am J Cardiol* 2008; **102**(5): 611-5.
199. Ahmed MI, Aban I, Lloyd SG, et al. A Randomized Controlled Phase IIb Trial of Beta1-Receptor Blockade for Chronic Degenerative Mitral Regurgitation. *Journal of the American College of Cardiology* 2012; **60**(9): 833-8.
200. Pat B, Killingsworth C, Denney T, et al. Dissociation between cardiomyocyte function and remodeling with beta-adrenergic receptor blockade in isolated canine mitral regurgitation. *Am J Physiol Heart Circ Physiol* 2008; **295**(6): H2321-7.
201. Pu M, Gao Z, Pu DK, Davidson WR, Jr. Effects of early, late, and long-term nonselective beta-blockade on left ventricular remodeling, function, and survival in chronic organic mitral regurgitation. *Circ Heart Fail* 2013; **6**(4): 756-62.
202. Capomolla S, Febo O, Gnemmi M, et al. Beta-blockade therapy in chronic heart failure: diastolic function and mitral regurgitation improvement by carvedilol. *Am Heart J* 2000; **139**(4): 596-608.

Chapter 2

Overall study rationale, aims, materials and methods.

2.1. Study rationale

In order to address the main question (can a β-adrenergic receptor blocker reverse or at least attenuate left ventricular remodelling due to chronic non-ischaemic mitral regurgitation?), the rationale for this study centred on determining changes in left ventricular remodelling in patients with chronic primary mitral regurgitation (CPMR) over time in relation to treatment with the beta-blocker carvedilol. The first chapter described the rationale for using beta-blocker therapy in primary chronic mitral regurgitation but a detailed examination of the effects of the beta-blocker carvedilol, which has been proven to improve outcomes in patients with heart failure from a variety of other diseases, has never been described in patients with CPMR. Assessment of attenuation of adverse remodelling (worsening of left ventricular dimensions and function) and/or reverse-remodelling (improvements in left ventricular dimensions and function) in response to β-adrenergic receptor blockade can be done using non-invasive investigations (clinical, echocardiographic and serum markers) and invasive investigations (gene expression at the tissue level). In order to determine whether carvedilol improves left ventricular remodelling in patients with CPMR it is critical to be able to follow these patients over months to years since beta-blocker therapy needs time to effect changes in myocyte biology. In an ideal situation patients with this disorder undergo surgical repair or replacement of the defective mitral valve very soon after the diagnosis of their condition. However, in our setting at Charlotte Maxeke Johannesburg Academic Hospital (CMJAH), a large academic public hospital in Johannesburg, South Africa, patients frequently wait several months from the time of diagnosis to time of mitral valve surgery mainly due to limited resources. This gave a unique opportunity to temporally examine left ventricular remodelling due to CPMR in response to carvedilol therapy.

2.2. Aim

To determine the effects of the β_1-adrenergic receptor blocker carvedilol on left ventricular structure and function in patients with chronic primary mitral regurgitation.

2.3. Inclusion criteria

Patients were included if they met ESC[1] and AHA/ACC[2] criteria for mitral valve surgery:

1. Patients with isolated severe chronic primary mitral regurgitation who are symptomatic;
2. Asymptomatic patients with isolated CPMR as defined by:
   a. An end systolic dimension of >40mm or an ejection fraction of <60% on echocardiography; and/or
   b. Pulmonary hypertension (pulmonary artery pressure > 50mmHg) that cannot be attributed to another cause.

2.4. Exclusion criteria

1. Secondary ('functional') mitral regurgitation.
2. Acute mitral regurgitation.
3. Patients with CPMR but an ejection fraction <30% and considered to be unfit for surgery.
4. In cases of rheumatic mitral regurgitation, a mitral valve area of $<2cm^2$ (to exclude patients with mixed mitral valve disease).
5. Any other hemodynamically significant comorbid valvular disease.
6. Active rheumatic carditis.
7. Active infective endocarditis.

8. Patients who require urgent surgery.
9. Patients with coronary artery disease.
10. Other chronic debilitating illnesses such as AIDS and chronic renal disease.
11. Patients with contraindications to the use of β_1-receptor blocker therapy.
12. Patients who refused to take part in the study.

2.5. Study methods

2.5.1. Enrolment

Twenty consecutive patients with isolated CPMR, who fulfilled the inclusion and exclusion criteria and gave informed consent to a protocol approved by the Human Research Ethics Committee of the University of the Witwatersrand, were recruited and underwent all baseline investigations (Appendix 1).

2.5.2. Study protocol

Patients from both groups underwent baseline investigations, before initiation of treatment, as detailed below. All patients were admitted to the coronary care unit at CMJAH for observation on the day of initial investigations. Patients underwent standard preparation for cardiac catheterization and coronary angiography in the cardiac catheterization laboratory including being kept nil per mouth overnight prior to cardiac catheterization and ensuring that the patients had normal full blood counts, renal function and no bleeding tendency. After ruling out any complications from the initial investigations patients were discharged after an overnight stay. Immediately after baseline investigations, including cardiac catheterization and endomyocardial biopsy (EMB), patients were randomized (using a random number generator from the online website www.random.org) to receive carvedilol or no anti-

remodelling therapy. Anti-remodelling therapy included beta-adrenergic receptor antagonists, angiotensin-converting enzyme inhibitors, angiotensin receptor blockers and mineralocorticoid receptor antagonists. In the study group carvedilol was initiated at a dose of 3.125mg twice daily and up-titrated to 25mg twice daily over a period of one month. This resulted in two groups of patients, one of which acted as the study control group. Patients allocated to carvedilol were initiated and then up titrated on their medication at home for the first week and returned for follow up at 2 and 4 weeks after enrolment and then monthly until surgery. Patients were presented for surgery immediately after their baseline cardiac catheterization and their contact details were given to the cardiothoracic unit at CMJAH. The timing of the patients' surgery was determined by the cardiothoracic unit, according to their surgical list. At the time of admission for surgery final investigations (see below) were undertaken and a final EMB specimen was obtained during surgery by the cardiothoracic surgeon (Figure 2.1).

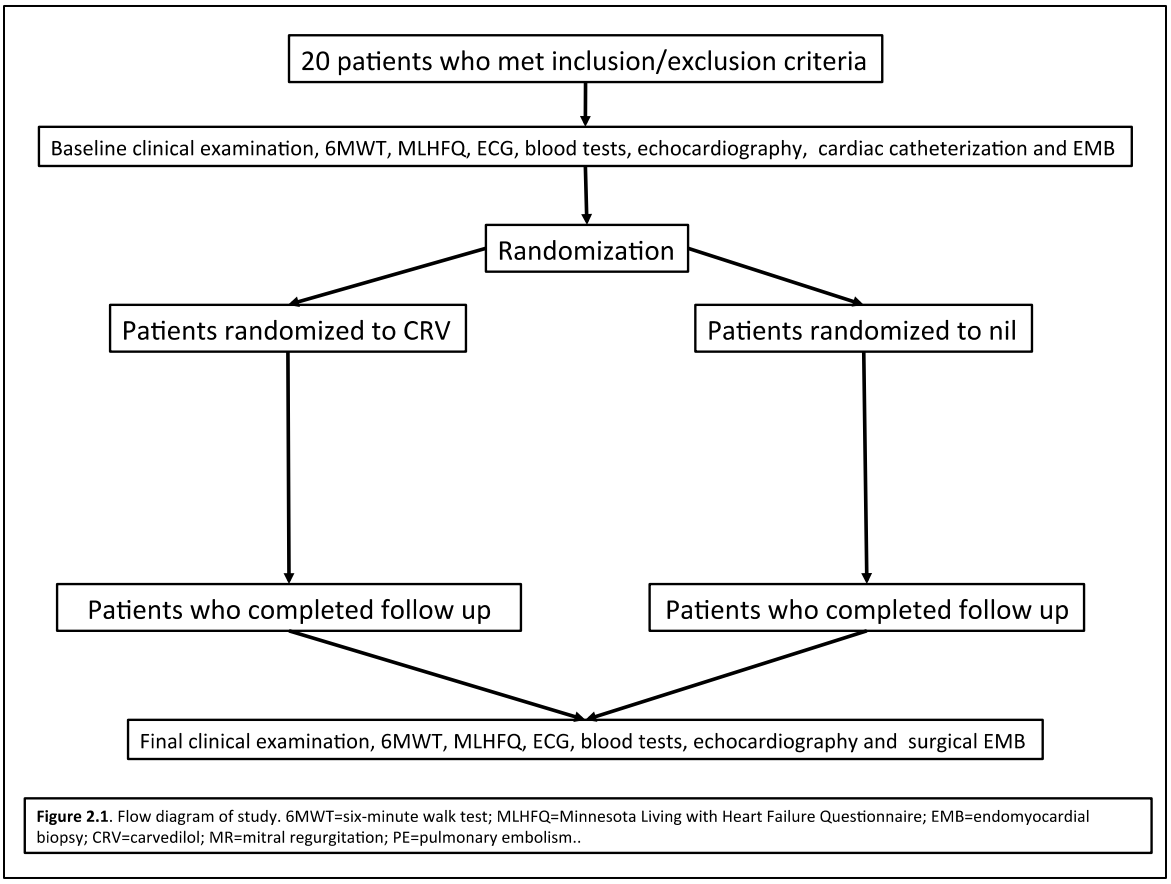

Figure 2.1. Flow diagram of study. 6MWT=six-minute walk test; MLHFQ=Minnesota Living with Heart Failure Questionnaire; EMB=endomyocardial biopsy; CRV=carvedilol; MR=mitral regurgitation; PE=pulmonary embolism..

For comparison of gene expression in the CPMR patients recruited in this study with gene expression in normal hearts, total heart RNA (from cadavers with no history of cardiac disease) was purchased from commercial suppliers. Appendix 2A-C shows the details of the three donor RNA samples from five donor hearts.

2.6. Data collection

2.6.1. Six-minute walk test (6MWT)

The 6MWT is a simple, safe and inexpensive test used to estimate functional capacity in cardiac patients. Although measurement of oxygen consumption during cardiopulmonary testing is the gold standard for determining functional capacity, the 6MWT can be used to assess changes in functional capacity in patients over time.[3] The 6MWT has been found to

be a reliable method of assessing functional ability in cardiac rehabilitation patients[4] and a meta-analysis determined that the 6MWT was responsive to changes in patients' clinic status.[3] In this regard, the 6MWT can be used to assess changes in functional capacity in patients on heart failure medication such as carvedilol. Study patients undertook a 6MWT at the time of recruitment to the study and immediately prior to surgery (Figure 2.1). This entailed walking at a comfortable pace on a flat surface for six minutes. All recruits walked the same 'course'. The distance walked during this period was then determined.

2.6.2. Heart Failure Questionnaire

The Minnesota Living with Heart Failure Questionnaire (MLHFQ) is one of the most widely used quality of life (QOL) questionnaires in heart failure trials.[5] The MLHFQ was selected since it is representative of the ways heart failure and treatments can affect the key physical, emotional, social and mental components of QOL. The MLHFQ asks each patient to indicate, using a zero to five scale, how much each of 21 facets (Appendix 3) prevented them from living as they desired. This subjectively quantifies the effects that symptoms, functional limitations and psychological distress have on an individual's QOL. The questionnaire enables assessment of how patients feel in response to heart failure therapy by stimulating the patient to consider various aspects of daily living that may have been affected by heart failure. The MLHFQ has been validated in several randomised heart failure trials and is a useful tool to monitor response to therapy.[6]

2.6.3. Echocardiographic assessment of left ventricular function

Baseline and pre-operative echocardiography [by a single (blinded) echocardiographic technologist] was performed on all recruited patients. Echocardiographic examinations were

performed with an iE-33® imaging device (Koninklijke Philips, NV, USA). All Doppler echocardiographic data were obtained in digital format and stored on an Xcelera® workstation (Koninklijke Philips, NV, USA) for off-line analysis. Echocardiographic data was collected according to current guidelines.[7-10] MMode and 2D measurements of chamber dimensions, tissue Doppler measurements of left and right ventricular function and speckle imaging for strain assessment were recorded. These measurements permitted the determination of left ventricular ejection fraction (LVEF), LV end diastolic (LVEDD) and end systolic dimensions (LVESD), left atrial dimensions, right ventricular dimensions and systolic tricuspid annular motion, quantification of tricuspid regurgitation and measurement of right ventricular systolic pressure and inferior vena cava dimensions (for determination of pulmonary artery pressure) and quantification of mitral regurgitant volume, LV systolic and diastolic wall motion, strain and strain rate. Mitral regurgitation severity was determined by a combination of enlargement of the left atrium and ventricle, visual judgement of the regurgitant jet into the left atrium, vena contracta measurement, effective regurgitant orifice measurement by the proximal isovelocity surface area method and regurgitant volume measurement.

2.6.3.1. Determining the severity of MR

Severe MR is diagnosed by a combination of clinical and echocardiographic parameters. For example, from a clinical point of view, the presence of heart failure due to MR would constitute severe MR. Other clinical findings include: evidence of pulmonary hypertension, a displaced and volume-loaded apex beat and a loud pansystolic murmur. However, echocardiography is the most validated method of evaluation of LV function and the severity of MR in clinical practice. Severity of MR is diagnosed on echo using colour Doppler jet

area, vena contracta width, proximal isovelocity surface area (PISA), regurgitant volume (RV) and evidence of LA and LV dilatation.[11] A vena contracta width (VCW) of ≥ 0.7cm, an effective regurgitant orifice area (EROA) ≥0.4cm^2 or a RV of ≥60ml by PISA method is diagnostic of severe MR according to the European Association of Echocardiography.[12] However, when the EROA or VCW are not measurable then the size of the colour flow jet can be used. A very large central jet or an eccentric jet that adheres to the LA wall and reaches the posterior wall of the LA constitutes severe MR. Also, the continuous wave (CW) signal of a severe MR jet is very dense and triangular. Finally, semi-quantitative measures such as pulmonary vein systolic flow reversal and an E velocity in the mitral inflow of ≥1.5cm/s are indicative of severe MR.[12]

PISA is a method that relies on the ability to determine the velocity of regurgitant blood as it approaches the valve orifice. In more severe cases of regurgitation the acceleration of blood flow occurs more proximal to the orifice (i.e. deeper in the LV cavity) and this convergence of flow forms a hemisphere which is identified by CW Doppler. The radius of this hemisphere is measured and a flow rate (cm/s) is calculated using the product of the surface area of the hemisphere ($2\Pi r^2$) and the aliasing velocity (Va) at the hemisphere. The EROA is calculated using these measures (where EROA = ($6.28r^2$ x Va)/peak velocity of the MR jet by CW). The RV is then calculated by multiplying the EROA by the MR jet CW velocity time integral (VTI). Although PISA is the most validated measure of MR severity, in many cases of primary MR, in particular rheumatic MR where the leaflets are often asymmetrically tethered, the jet is not central. In these cases semi-quantitative and qualitative measures of MR severity are required. The RV can also be determined using volumetric methods if the LVOT and mitral annulus can be reliably measured.[11] RV = [TSV

– FSV] where TSV (total stroke volume) is determined through the mitral valve in diastole and FSV (forward stroke volume) is determined through the aortic valve during systole. This method is difficult because if the diameter of the LV outflow tract (LVOT) or the mitral annulus are measured incorrectly, that error is squared (since CSA = Πr^2). However, this method has been validated against other methods including cardiac magnetic resonance imaging and found to be highly reproducible.[13]

2.6.3.2. Assessment of LV function by echocardiography

LV function is determined by myocardial contractility, which is the ability of the myocardium to generate force independent of loading conditions.[14] With gradual development of MR, the LV end diastolic volume (LVEDV) increases slowly over a period of months to years (Figure 1.1). As discussed in Chapter 1, this leads to the development of eccentric hypertrophy and chronic, so-called 'compensated' MR. LVEF is the difference between the LVEDV and LV end systolic volume (LVESV) and is a validated and easily measured parameter by echocardiography. LVEF can be measured by MMode, Simpson's method or by 3D volumetric analysis. However, LVEF is load-dependent and therefore markedly affected by preload and afterload. MR increases preload by virtue of a regurgitant volume into the LA. Therefore, patients with MR have an increased LVEDV and LVEF automatically increases simply on the basis of an increase in diastolic volume. Initially, there is an increase in the LVEF as a result of the increase in LVEDV and the ejection of a portion of the TSV into the low pressure LA. This is a false assessment of LV function and does not truly assess the ability of the myocardium to contact.[15] An increase in preload and/or a decrease in afterload elevate LVEF despite a lack in the change in the myocardial contractile state. As discussed in Chapter 1, myocyte dysfunction occurs well before the LVEF starts to

deteriorate in cases of primary MR.[16] Therefore, guidelines for surgery for patients with MR often quote a LVEF <60% as indicative of LV dysfunction and an indication for mitral valve surgery.[1,2]

Evidence of LV dilatation is indicative of LV dysfunction. Therefore, increases in LVEDV and LVESV can be used as surrogate indicators of LV dysfunction and surgery is indicated when the ESD (end-systolic dimension, which is a surrogate measure of ESV) is more than 40mm.[1,2] LV contractile reserve can be assessed by measuring the LVEF response to exercise.[17] However, this is not a frequent clinical test in pre-operative workup of the patient with primary MR. LV dp/dt has also been used as a measure of LV contractile function.[18] This parameter is determined by measuring the rate at which the LV produces the MR jet in the first second of systole and is easily reproducible and measurable.

Myocardial strain imaging is a load-independent method of assessing LV function, which is potentially important in patients with primary MR.[15] Strain is a mechanical characteristic that describes the deformation (lengthening and shortening) of myocardial segments and is described by the equation $\varepsilon = \Delta L/L_0$.[19] L_0 is the original length of a segment of myocardium and ΔL is the length change noted in that segment during contraction or relaxation. The strain value is dimensionless and is expressed as a percent or fraction. Strain rate is the rate of deformation (i.e. how quickly the segment changes length). Both strain and strain rate have been shown to correlate well with measures of LV function.[20] Speckle tracking, which is based on grayscale B-mode images with the production of 'speckles' created by the constructive and destructive interference of ultrasound beams in the myocardium,[19] enables assessment of strain independent of the Doppler angle. This technology permits assessment

of LV function using 4 types of strain: longitudinal, circumferential, radial and rotational. Although myocardial segments deform in a 3-dimensional manner, most studies have been performed using individual strain measures, for example longitudinal strain.

Speckle tracking technology has been used to identify early LV dysfunction in patients with primary MR.[21,22] Kim *et al*.[23] studied 59 patients with primary severe MR and LVEF of ≥50% and compared them with healthy controls. They showed that LV longitudinal dysfunction occurred earlier than short axis dysfunction in patients with primary MR compared with controls. This is supported by data demonstrating latent LV systolic dysfunction in patients with severe primary MR.[24] In addition, in 122 patients undergoing mitral valve repair with normal LV systolic function (LVEF >60% and LVESD < 40mm), pre-operative echocardiography with longitudinal strain assessment demonstrated myocardial contractile dysfunction, which improved with long-term (1-3 years) follow-up.[25] Furthermore, longitudinal strain has been shown to be an independent determinant of event-free survival and independently correlates with increases in brain natriuretic peptide (BNP) in moderate-to-severe degenerative MR patients with normal LV volumes and LVEF.[26]

2.6.4. Serum

Venesection was performed on all study patients at baseline and immediately prior to mitral valve surgery. Blood was collected in BD Vacutainer® EST II Advance tubes (BD Plymouth, UK) and allowed to clot over 30 minutes at room temperature and then centrifuged for 15 minutes at 3200 G. The serum was aspirated and aliquoted into pre-labelled 1.5 ml Eppendorf® tubes (Hamburg, Germany). These tubes were stored at -80º until the day of assaying.

2.6.4.1. BNP. Brain natriuretic peptide (BNP) and its inactive amino terminal portion (NT-proBNP) are neurohormones released by myocytes in response to volume expansion and pressure overload.[27] Both BNP and NT-pro-BNP are released by the myocardium in response to changes in atrial and ventricular size due to alterations in volume load.[28] In patients with chronic primary mitral regurgitation, increased levels of BNP are associated with poorer prognosis.[29] Serum for BNP was submitted to the National Health Laboratory Services (NHLS, Johannesburg, RSA) at study baseline and immediately prior to surgery.

2.6.4.2. CRP. Inflammation has been well-documented to be associated with the pathogenesis of heart failure. C-reactive protein (CRP) is an acute phase reactant produced by the liver in response to increases in IL-6 secretion by macrophages and T cells.[30] Elevation of serum levels of CRP have also been shown to be a risk for the development of heart failure[31] and higher levels of CRP have been found to be associated with more severe heart failure and with poor outcomes.[32] Furthermore, there is evidence that CRP together with other biomarkers, such as BNP and ST2, better identifies patients at higher risk of adverse outcomes.[33] Serum for CRP was submitted to the National Health Laboratory Services (NHLS, Johannesburg, RSA) at study baseline and immediately prior to surgery.

2.6.4.3. TNF-α, IL-1β, IL-6, IL-33, ST2, Fas-Ligand, Fas, MMP-1, -2, and -9 & TIMP-1 and -4 quantification. As detailed in Chapter 1, inflammation, apoptosis and ECM turnover are important processes in LV remodelling in patients with chronic primary MR. Important biomarkers of inflammation include TNF-α and the interleukins. Fas and Fas Ligand are serum markers of apoptosis while several MMPs and TIMPs are responsible for ECM turnover. Baseline and pre-operative serum was collected for the following tests: soluble Fas/APO-1 receptor (sFas), an inhibitor of apoptosis, and soluble Fas ligand (sFas-L), an inducer of apoptosis;[34,35] sST2 and Il-33 levels;[33,36,37] inflammatory cytokines (TNF-α, Il-1, Il-6);[38-40] and MMP-1, -2 and -9, and TIMP-1 and -4.[41-45]

2.6.4.3.1. TNF-α, IL-1β, IL-6, IL-33, ST2, Fas-Ligand and Fas serum quantification. Quantification of the serum concentration of these analytes was performed after thawing frozen serum. Magnetic Luminex® Screening Assays (RnD Systems, Inc., MN, USA) were used according to the manufacturer's guidelines (Appendix 4A). Briefly, a 96-well plate was used with 7 diluted standard cocktails to generate a standard concentration curve. Standards were provided in the kit. For IL-33, ST2, Fas and Fas-L the Kit Lot number was 1423662. For TNF-α, IL-1β and IL-6 the Kit Lot number was 1423659. Concentrations for standard analytes are given in the Certificate of Analysis for the analytes (Appendix 4B and 4C). Standard cocktails were reconstituted with 0.2ml of the Kit 'Calibrator Diluent RD6-52'. After allowing the standard cocktails to stand for 15 minutes, a 3-fold dilution series was prepared in order to generate the standard curve for the analytes. The Microparticle Cocktail, Biotin Antibody Cocktail and Streptavidin-PE solution were prepared according to the protocol. 50µL of the Microparticle Cocktail was added to each of the 96 microplate wells. Following this, 50µL of standard or sample was added to each well. Samples were run in

duplicate 1:2 dilutions and single 1:10 dilutions with 2 blanks well making up the 96 wells. The standards and samples were initially incubated with the microparticles. This was followed by washing the standards and samples and then incubating with the Biotin Antibody Cocktail. Following further wash steps the standards and samples were then incubated with Streptavidin-PE. After a final wash the standards and samples were re-suspended in Wash Buffer before being analysed in the Bio-Plex System (Bio-Rad Laboratories, PA, USA).

2.6.4.3.2. MMP-1, -2, and -9 & TIMP-1 and -4 quantification. Quantification of the serum concentrations of these analytes was performed after thawing frozen serum. Milliplex® MMP panels (EMD Millipore Corporation, MA, USA) were used according to the manufacturer's guidelines (Appendix 5A and 5B). For MMP-1, -2 and -9 the HMMP2MAG-55K Kit was used (Kit Lot number 2753476) (Appendix 5A). For TIMP-1 and -4 the HTMP2MAG-54K Kit was used (Kit Lot number 2753477) (Appendix 5B). Standards and Quality Controls were prepared according to the Kit protocol. For the MMP Kit, the standard and the Quality controls (QCs) were reconstituted (separately) with 250µL of deionized water and seven 1:3 serial dilutions were prepared. The microplate wells were then washed with Wash Buffer and 25 µL aliquots of standards, quality controls and samples were added to the wells. A 96-well plate was used with the 7 diluted standard cocktails to generate a standard concentration curve. MMP samples were run in duplicate 1:20 dilutions and single 1:50 dilutions with 2 blank wells making up the 96 wells. Mixed beads, Detection Antibody and Streptavidin-PE were sequentially added after washing in between each step. Finally 100µL of Sheath Fluid (Bio-Rad Laboratories, PA, USA) was used to re-suspend the beads before analysing the standards, QCs and samples in the Bio-Plex System (Bio-Rad

Laboratories, PA, USA). The same process was followed for the TIMPs according to the manufacturers protocol. TIMP-1 was run in duplicate 1:20 dilutions and TIMP-4 was run neat as per the distributor's recommendation.

All multiplex panels were analysed on a Bio-Plex 200 System (Bio-Rad Laboratories, PA, USA) and results were copied into an Excel® spreadsheet (Microsoft Corporation, WA, USA) for analysis.

2.6.5. Cardiac catheterization & Endomyocardial Biopsy

Patients underwent cardiac catheterization and endomyocardial biopsy (EMB) at baseline. Patients were prepared according to the standard protocol for preparation of patients for coronary angiogram and cardiac catheterization at CMJAH as described above. Coronary angiography was necessary to rule out coronary artery disease and cardiac catheterization and left ventricular cineventriculography were used to assess pulmonary pressures, left ventricular contractility and confirm the severity of mitral regurgitation.[46]

Coronary angiography and left and right heart catheterization were performed according to standard protocols. Patients were given a small dose of sedation by the attending anaesthetist. The patient was then draped and the groin was cleaned with a sterile solution. After infusion of local anaesthetic in the right groin, the right femoral artery and vein were punctured. A 7F sheath was inserted into the artery and a 6F sheath was inserted into the vein. Coronary angiography was performed using standard right and left 6F Judkins catheters. A 6F pigtail catheter was used to determine LV and aortic pressures and to perform an LV ventriculogram. A right heart study was subsequently performed using a 6F multipurpose catheter. Pressures and oxygen saturations were obtained from the right atrium, right ventricle, pulmonary artery and, where possible, the pulmonary capillary wedge. LV EMB was subsequently performed via the right femoral artery as described below.

At the time of cardiac catheterization and coronary angiography the following data were obtained: coronary anatomy, LV end diastolic pressure and ejection fraction, regional wall motion assessment, quantification of mitral regurgitation by contrast angiography, pulmonary artery pressures, pulmonary capillary wedge pressure, forward stroke volume,

cardiac output and indexed cardiac output (by Fick method) and regurgitant volume (LV output [EDV-ESV] – FSV).[46]

2.6.5.1. Endomyocardial biopsy

The use of EMB is gaining increased relevance in clinical practice because of new therapies for cardiomyopathies. EMB is an important tool to understand the cellular and molecular pathophysiology of cardiovascular disease. *In vivo* myocyte biology can only be studied from tissue specimens and although there are non-invasive and serum markers of inflammation and fibrosis, the value of these markers remains experimental.

Both LV and right ventricular EMB are safe procedures when performed by experienced interventionalists.[47] Two studies have found low rates of EMB-related complications for both right ventricular[48] and left ventricular EMB[47]. In the study by Yilmaz *et al*.,[47] in 755 patients, the rate of major complications for LV-EMB and RV-EMB was 0.64% and 0.82%, respectively. A lower rate of minor complication was reported for LV-EMB (2.89%) than for RV-EMB (5.1%).

In the present study, EMB was performed according to the technique of Yilmaz *et al*.[47] Left femoral artery access was used to introduce a 7F guiding catheter (JR4.0, AL1.0 or JL4.0) (Medtronic, MN, USA) after intravenous infusion of 5000u of unfractionated heparin. Biopsy specimens were taken using disposable 2.2mm x 105cm Jawz® Endomyocardial Biopsy Forceps (Argon Medical, Tx, USA). The EMB procedure started with a 7F JR4 coronary guiding catheter, which was passed retrograde through the aortic valve into the LV using a standard J tip guide wire. If we failed to achieve a suitable position in the LV with

the JR4.0 guide then we tried an AL 1.0 or a JL 4.0 (Medtronic, MN, USA). The bioptome was then advanced through the guiding catheter into the LV under fluoroscopic guidance. Care was taken that the jaws of the bioptome were opened within the LV cavity before close wall contact was reached. Upon wall contact with the opened jaws as much pressure as needed to produce a smooth curve at the end of the guiding catheter and the bioptome was used. Several (3-5) biopsy specimens were taken from random sites within the middle one third of the LV. The biopsy specimens measured approximately $1mm^2$ each. After each biopsy, aspiration of blood from the guiding catheter and rinsing with heparinised sodium chloride solution was performed to prevent clotting. Echocardiography was used to assist in positioning of the bioptome and to detect complications related to the procedure.[49] Following biopsy, patients were admitted to the coronary care unit for overnight observation.

At the time of mitral valve surgery, the cardiothoracic surgeon obtained myocardial biopsy specimens under direct visualization of the left ventricle. These specimens measured approximately $2mm^2$ each. These specimens were also taken from random positions within the LV.

At the time of percutaneous or surgical EMB the biopsy specimens were either flash frozen in liquid nitrogen for gene expression analysis (see below) or collected in formalin for histopathology (see below). The frozen specimens were then stored at -80º until all specimens had been collected.

Tissue acquired at the time of EMB and at the time of surgery was prepared for light microscopy and electron microscopy examination for potential quantification of interstitial

collagen, myocardial inflammation, fibrosis and apoptosis.[50,51] Microscopy specimens were examined by Professor Martin Hale from the Department of Anatomical Pathology, University of the Witwatersrand to confirm that the endomyocardium was adequately represented in the biopsy specimens. For light microscopy, specimens were fixed in 10% buffered formalin and processed for paraffin embedding according to the method of Tsutsui *et al*.[50]. 4µm slices were cut from the specimen blocks, which were then mounted on glass slides and stained with hematoxylin and eosin for morphometric analysis.

2.6.6. Gene expression analysis

2.6.6.1. RNA extraction and quantification

All tissue specimens were processed at the same time on completion of specimen collection. Lysis and homogenization of tissue was performed using miRNeasy Mini Kit® and TissueRuptor® (Qiagen Sciences, MD, USA) according to the manufacturer's protocol (Appendix 6). In the case where more than one tissue fragment was available for individual patients (samples) at baseline biopsy, these frozen biopsy specimens were combined in order to increase the total RNA (only baseline specimens for a patient were combined with specimens taken at the same time since the fragments were very small). The specimens were first thawed at room temperature before lysis and homogenization of the tissue was performed. Briefly, the tissue samples were placed in 700 µL QIAzol Lysis Reagent. The tissue was homogenized using disposable TissueRuptor® (Qiagen Sciences, MD, USA) probes until the tissue lysate was uniformly homogeneous. 140µL of chloroform was added followed by centrifugation at 12000g for 15 minutes in order to separate the solution into an aqueous and an organic phase. The organic phase was discarded and 100% ethanol was used to precipitate the RNA. The samples were pipetted into spin columns in order to trap RNA.

After cleaning with the supplied buffer several times the RNA was finally eluted in RNase-free water. The RNA was re-suspended in 30μL RNase-free water and stored at -80º.

The RNA extracted from the samples was quantified using spectrophotometric analysis on a NanoDrop ND-2000 Spectrophotometer (NanoDrop Technologies Inc., Wilmington, Del.). The concentration of the RNA was calculated by using the standard that 1 OD260 = 40ng RNA/μL. The quality of the samples was assessed by calculating the OD260/OD280 ratio. Quality of samples was considered to be good when the OD260/OD280 ratio was close to 2.0 (Appendix 7).

The integrity of the RNA was evaluated using the Agilent RNA 6000 Nano Kit (Agilent Technologies, CA, USA) (Appendix 8A). 1μL of each sample (RNA in RNase-free water) was added to Agilent Gel-Dye mix (Agilent Technologies, CA, USA) in the supplied 16-well chips which were then inserted into an Agilent 2100 Bioanalyzer (Agilent Technologies, CA, USA) for analysis.

2.6.6.2. Gene expression (GX)

Unfortunately there was a problem with the first Agilent cassette. This resulted in poor clarity to the gel for samples 1 to 12, including the ladder (Appendix 8B) whereas the cassette for samples 13-24 were much clearer. This resulted in variable RNA Integrity Numbers (RIN) (Appendix 8C), which meant that comparing expression between samples would potentially be difficult using microarray. Because of this, we decided to submit the RNA to Nanostring (Nanostring, Seattle, USA) for gene expression (GX) determination.

Twenty-nine total RNA samples (13 baseline, 13 final and three normal heart RNA samples) were sent to Nanostring (in Seattle, USA) for analysis with their Gene Expression Assay® (Appendix 9). This system is based on the polymerase chain reaction (PCR) but uses a novel digital colour-coded barcode technology that enables determination of gene expression in very small quantities of tissue since no amplification steps are required. A list of genes of interest, including Genbank® (National Institutes of Health, NIH, USA) accession numbers, were sent to Nanostring for gene expression analysis.

Multiplex gene expression analysis, using 100ng total RNA per sample, was performed commercially by NanoString (Seattle, USA) using an nCounter® Custom (based on the genes selected) Codeset. Results were analysed using the NanoString nSolver Analysis Software Package 3.0®. A background subtraction using the geometric mean of the negative controls was included and gene expression levels were normalised to both the geometric mean of the positive controls and the geometric mean of three reference genes (*GAPDH*, *PGK1* and *HPRT1*). The additional reference genes were excluded from the analysis because of high variation in expression levels between samples (*SDHA* and *STR*) and expression levels at or

below background levels (*RPLPO*). Eight candidate genes (*ADRB3, FasLG, IL1B, IL10, MMP-1, MMP-13, PDCD1* and *SAG*) were expressed at levels at or below that of the negative controls and thus were also excluded from the analysis. Normalised counts were used to generate ratio data, 95% confidence intervals (CIs) and false discovery rates (FDRs) for all genes comparing CPMR patients at baseline to the normal heart controls, and "CRV" patients to "Nil" patients at baseline and at follow-up.

2.6.6.3. Selection of genes for analysis

Due to budget constraints only 109 candidate genes and 6 housekeeping genes could be selected for analysis. The 109 candidate genes were selected based on previous gene expression studies in animals and humans with heart failure, volume overload and CPMR.[39,52-57] Genes were selected if they were known to be directly involved in β-receptor signalling, cardiac bioenergetics, ECM remodelling, cell survival, apoptosis, inflammatory and fibrosis pathways.

Appendix 10 gives a full list of the genes that were selected for analysis. The gene, Genbank® (National Institutes of Health) accession number, gene name and alternative gene name, brief description of role of the gene product and a more detailed description of the gene products are given in Appendix 10.

Most of the genes were selected based on those genes previously found to be up/down-regulated in animal or human subjects with chronic primary MR or models of volume overload. For example, 24 genes that had previously been found to be significantly up/down-regulated in patients with primary MR (compared with normal hearts) were selected from

data published by Zheng *et al*.[56] Zheng *et al*.[54] used microarray to identify genes significantly up/downregulated in four dogs with experimental primary MR. From this study 31 genes were selected for analysis (Appendix 11). Chen *et al*.[39] identified a number of genes involved in ECM and inflammatory pathways that were up/down-regulated in a mouse model of volume overload. Thirty-eight of the genes from this study were selected. Several genes were found to have significantly altered expression in more than one of these studies. For example, CTGF (Connective tissue growth factor) was found to have significantly altered gene expression in all three of the studies mentioned above. Lezsek *et al*.[58] and Zheng *et al*.[54] demonstrated that *SERCA2* was down-regulated in patients and dogs (respectively) with primary MR and therefore this gene was selected for analysis (Appendix 10). For some genes there is no specified original reference in the table but these genes were selected based on their known role in important pathways. For example, *β_1-AR* and *β_2-AR* were selected because of their importance in β-AR signalling (see Chapter 1). *ADRBK1* and *ADRBK2* (BARK-1 and BARK-2, respectively) were selected because of their importance in G-protein receptor coupled signalling and β-AR down-regulation (see Chapter 1). *AGTR1* (angiotensin receptor-1) was selected because of its fundamental importance in angiotensin II signalling (see Chapter 1). *FAS*, *FASL*, *FADD* (Fas-associated via death domain), *Caspase-1* and *Caspase-10* were selected because of their known importance in apoptotic pathways (see Chapter 1) (Figure 2.2). The TGF-β receptors were selected because of their importance in ECM remodelling and signalling. *IL-10, NFKβ, TNFα* and the TNF receptor superfamily members 1A and 1B were selected because of their known importance in inflammatory pathways and TNF-related apoptotic and inflammatory pathways (see Chapter 1) (Figure 2.2). The natriuretic peptides and *ST2* (and *IL-33*) were selected because of their known role as markers of myocardial volume overload.[28,33]

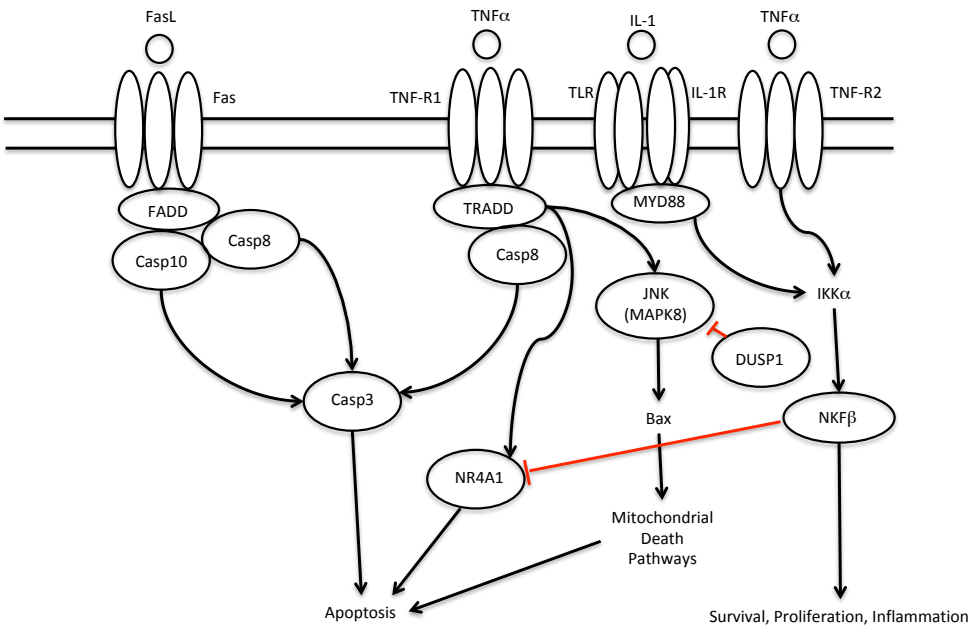

Figure 2.2: Important protein components of TNF and FAS apoptotic pathways.

Adapted from Wajant *et al.*[59] & Foo *et al.*[60]

2.7. Data Entry

Data was collected on a hard copy sheet and each patient was allocated a patient identification number to maintain confidentiality and to maintain blinding during echocardiography. Data from the datasheets and the serum and molecular work was combined into a single Excel® spreadsheet prior to statistical analysis.

2.8. Statistics

Clinical, echocardiographic and serum parameters were compared using non-parametric analyses using medians and inter-quartile ranges. The changes between baseline and follow-up readings were calculated for each individual separately and the medians of these differences calculated and compared between the two groups using a 2-sample Wilcoxon Mann-Whitney test. A p-value <0.05 was considered to be statistically significant and a p-value of <0.1 to show a trend.

The gene expression pattern of the panel of 109 genes in the CPMR patients at baseline was compared with that from normal heart tissue. The changes between baseline and follow-up readings were calculated for each individual separately and the medians of these differences calculated and compared between the two groups using a 2-sample Wilcoxon Mann-Whitney test. Two methods were used to validate that the changes that were found were indeed true and not by chance. Firstly, the fold-changes in gene expression in the patients with CPMR (compared with normal controls) were compared with previous findings.[56] Secondly, online bioinformatics tools were used. Differentially expressed genes were assigned to significantly enriched processes using the online bioinformatics tool WebGestalt (WEB-based Gene SeT AnaLysis Toolket) (http://www.webgestalt.org).[61] WebGestalt is designed for functional genomic, proteomic and large-scale genetic studies and incorporates information from different public resources including Gene Ontology (GO) (http://www.geneontology.org). Using WebGestalt, it was possible to associate genes with individual disease and drug terms using GLAD4U.[62] The results obtained by WebGestalt were confirmed by DAVID 6.8 (https://david.ncifcrf.gov) and STRING 10.5 (https://string-db.org) both consulted in January 2018. DAVID provides a functional annotation environment to systematically extract

biological themes behind large gene lists. It is based on established medical literature (for example, data from articles available on PubMed).[63] The P values provide an estimate of the probability that a given enrichment is present by chance alone and are derived using corrections for multiple comparisons (Benjamini and Hochberg false discovery rates). This is a validated method of determining whether changes in the expression of multiple genes are by chance or have likely occurred due to a true change in a biological/cellular/molecular processes – i.e. that the changes in the expression of the genes are truly pathological.

Subsequently, the effect of carvedilol upon gene expression was investigated using each individual subject as their own control, in order to minimize biological variation, to identify those genes whose expression was most altered in relation to carvedilol therapy. Bioinformatics and hierarchic clustering was used to investigate patterns, which improved the statistical relevance by combining data on several genes. nCounter® data were converted to 2 log values and the delta (difference of gene expression between baseline and final) for each gene was calculated in the individual patients. The mean expression values were then computed for the CRV and for the Nil group for the different genes. Using hierarchical clustering, genes that were most determining for the effect of carvedilol were identified. The most upregulated and most down-regulated genes for CRV treatment vs Nil treatment were identified from those genes with a delta fold change $\geq +1.75$ or ≤ -1.75. One gene (*NPPB*) was omitted because of large inter-individual variation. The changes between baseline and follow-up readings were calculated for each individual separately and the medians of these differences calculated and compared between the two groups using a 2-sample Wilcoxon Mann-Whitney test. A p-value <0.05 was considered to be statistically significant and a p-value of <0.1 to show a trend.

2.9. References

1. Baumgartner H, Falk V, Bax JJ, et al. 2017 ESC/EACTS Guidelines for the management of valvular heart disease. *European heart journal* 2017; **38**(36): 2739-91.
2. Nishimura RA, Otto CM, Bonow RO, et al. 2017 AHA/ACC Focused Update of the 2014 AHA/ACC Guideline for the Management of Patients With Valvular Heart Disease: A Report of the American College of Cardiology/American Heart Association Task Force on Clinical Practice Guidelines. *Circulation* 2017; **135**(25): e1159-e95.
3. Bellet RN, Adams L, Morris NR. The 6-minute walk test in outpatient cardiac rehabilitation: validity, reliability and responsiveness—a systematic review. *Physiotherapy*; **98**(4): 277-87.
4. Hamilton DM, Haennel RG. Validity and reliability of the 6-minute walk test in a cardiac rehabilitation population. *J Cardiopulm Rehabil* 2000; **20**(3): 156-64.
5. Naveiro-Rilo JC, Diez-Juarez DM, Romero Blanco A, Rebollo-Gutierrez F, Rodriguez-Martinez A, Rodriguez-Garcia MA. Validation of the Minnesota living with heart failure questionnaire in primary care. *Rev Esp Cardiol* 2010; **63**(12): 1419-27.
6. Rector TS, Cohn JN. Assessment of patient outcome with the Minnesota Living with Heart Failure questionnaire: reliability and validity during a randomized, double-blind, placebo-controlled trial of pimobendan. Pimobendan Multicenter Research Group. *Am Heart J* 1992; **124**(4): 1017-25.
7. Lancellotti P, Tribouilloy C, Hagendorff A, et al. Recommendations for the echocardiographic assessment of native valvular regurgitation: an executive summary from the European Association of Cardiovascular Imaging. *Eur Heart J Cardiovasc Imaging* 2013; **14**(7): 611-44.
8. Lang RM, Badano LP, Mor-Avi V, et al. Recommendations for cardiac chamber quantification by echocardiography in adults: an update from the American Society of Echocardiography and the European Association of Cardiovascular Imaging. *Eur Heart J Cardiovasc Imaging* 2015; **16**(3): 233-70.
9. Rudski LG, Lai WW, Afilalo J, et al. Guidelines for the echocardiographic assessment of the right heart in adults: a report from the American Society of Echocardiography endorsed by the European Association of Echocardiography, a registered branch of the European Society of Cardiology, and the Canadian Society of Echocardiography. *Journal of the American Society of Echocardiography : official publication of the American Society of Echocardiography* 2010; **23**(7): 685-713; quiz 86-8.
10. Remenyi B, Wilson N, Steer A, et al. World Heart Federation criteria for echocardiographic diagnosis of rheumatic heart disease--an evidence-based guideline. *Nature reviews Cardiology* 2012; **9**(5): 297-309.
11. Grayburn PA, Weissman NJ, Zamorano JL. Quantitation of mitral regurgitation. *Circulation* 2012; **126**(16): 2005-17.
12. Lancellotti P, Moura L, Pierard LA, et al. European Association of Echocardiography recommendations for the assessment of valvular regurgitation. Part 2: mitral and tricuspid regurgitation (native valve disease). *Eur J Echocardiogr* 2010; **11**(4): 307-32.
13. Dele-Michael AO, Fujikura K, Devereux RB, et al. Left ventricular stroke volume quantification by contrast echocardiography - comparison of linear and flow-based methods to cardiac magnetic resonance. *Echocardiography* 2013; **30**(8): 880-8.

14. Nakano K, Swindle MM, Spinale F, et al. Depressed contractile function due to canine mitral regurgitation improves after correction of the volume overload. *J Clin Invest* 1991; **87**(6): 2077-86.
15. O'Gara P, Sugeng L, Lang R, et al. The role of imaging in chronic degenerative mitral regurgitation. *JACC Cardiovasc Imaging* 2008; **1**(2): 221-37.
16. Urabe Y, Mann DL, Kent RL, et al. Cellular and ventricular contractile dysfunction in experimental canine mitral regurgitation. *Circulation research* 1992; **70**(1): 131-47.
17. Leung DY, Griffin BP, Stewart WJ, Cosgrove DM, 3rd, Thomas JD, Marwick TH. Left ventricular function after valve repair for chronic mitral regurgitation: predictive value of preoperative assessment of contractile reserve by exercise echocardiography. *Journal of the American College of Cardiology* 1996; **28**(5): 1198-205.
18. Esterly JS, Darin KM, Gerzenshtein L, Othman F, Postelnick MJ, Scarsi KK. Clinical implications of antiretroviral drug interactions with warfarin: a case-control study. *J Antimicrob Chemother* 2013; **68**(6): 1360-3.
19. Gorcsan J, 3rd, Tanaka H. Echocardiographic assessment of myocardial strain. *Journal of the American College of Cardiology* 2011; **58**(14): 1401-13.
20. Greenberg NL, Firstenberg MS, Castro PL, et al. Doppler-derived myocardial systolic strain rate is a strong index of left ventricular contractility. *Circulation* 2002; **105**(1): 99-105.
21. Lancellotti P, Cosyns B, Zacharakis D, et al. Importance of left ventricular longitudinal function and functional reserve in patients with degenerative mitral regurgitation: assessment by two-dimensional speckle tracking. *J Am Soc Echocardiogr* 2008; **21**(12): 1331-6.
22. Mascle S, Schnell F, Thebault C, et al. Predictive value of global longitudinal strain in a surgical population of organic mitral regurgitation. *J Am Soc Echocardiogr* 2012; **25**(7): 766-72.
23. Kim MS, Kim YJ, Kim HK, et al. Evaluation of left ventricular short- and long-axis function in severe mitral regurgitation using 2-dimensional strain echocardiography. *Am Heart J* 2009; **157**(2): 345-51.
24. Moustafa SE, Kansal M, Alharthi M, Deng Y, Chandrasekaran K, Mookadam F. Prediction of incipient left ventricular dysfunction in patients with chronic primary mitral regurgitation: a velocity vector imaging study. *Eur J Echocardiogr* 2011; **12**(4): 291-8.
25. Witkowski TG, Thomas JD, Delgado V, et al. Changes in left ventricular function after mitral valve repair for severe organic mitral regurgitation. *Ann Thorac Surg* 2012; **93**(3): 754-60.
26. Magne J, Mahjoub H, Pierard LA, et al. Prognostic importance of brain natriuretic peptide and left ventricular longitudinal function in asymptomatic degenerative mitral regurgitation. *Heart* 2012; **98**(7): 584-91.
27. Maisel A. B-Type Natriuretic Peptide Levels: Diagnostic and Prognostic in Congestive Heart Failure: What's Next? *Circulation* 2002; **105**(20): 2328-31.
28. Januzzi JL, Troughton R. Are Serial BNP Measurements Useful in Heart Failure Management?: Serial Natriuretic Peptide Measurements Are Useful in Heart Failure Management. *Circulation* 2013; **127**(4): 500-8.
29. Clavel MA, Tribouilloy C, Vanoverschelde JL, et al. Association of B-Type Natriuretic Peptide With Survival in Patients With Degenerative Mitral Regurgitation. *Journal of the American College of Cardiology* 2016; **68**(12): 1297-307.
30. Pepys MB, Hirschfield GM. C-reactive protein: a critical update. *J Clin Invest* 2003; **111**(12): 1805-12.

31. Kardys I, Knetsch AM, Bleumink GS, et al. C-reactive protein and risk of heart failure. The Rotterdam Study. *Am Heart J* 2006; **152**(3): 514-20.
32. Anand IS, Latini R, Florea VG, et al. C-Reactive Protein in Heart Failure: Prognostic Value and the Effect of Valsartan. *Circulation* 2005; **112**(10): 1428-34.
33. Mebazaa A, Di Somma S, Maisel AS, Bayes-Genis A. ST2 and multimarker testing in acute decompensated heart failure. *Am J Cardiol* 2015; **115**(7 Suppl): 38b-43b.
34. Nishigaki K, Minatoguchi S, Seishima M, et al. Plasma Fas ligand, an inducer of apoptosis, and plasma soluble Fas, an inhibitor of apoptosis, in patients with chronic congestive heart failure. *Journal of the American College of Cardiology* 1997; **29**(6): 1214-20.
35. Sliwa K, Skudicky D, Bergemann A, Candy G, Puren A, Sareli P. Peripartum cardiomyopathy: analysis of clinical outcome, left ventricular function, plasma levels of cytokines and Fas/APO-1. *Journal of the American College of Cardiology* 2000; **35**(3): 701-5.
36. Shah RV, Januzzi JL, Jr. ST2: a novel remodeling biomarker in acute and chronic heart failure. *Curr Heart Fail Rep* 2010; **7**(1): 9-14.
37. Seki K, Sanada S, Kudinova AY, et al. Interleukin-33 prevents apoptosis and improves survival after experimental myocardial infarction through ST2 signaling. *Circ Heart Fail* 2009; **2**(6): 684-91.
38. Mann DL. Innate immunity and the failing heart: the cytokine hypothesis revisited. *Circulation research* 2015; **116**(7): 1254-68.
39. Chen YW, Pat B, Gladden JD, et al. Dynamic molecular and histopathological changes in the extracellular matrix and inflammation in the transition to heart failure in isolated volume overload. *Am J Physiol Heart Circ Physiol* 2011; **300**(6): H2251-60.
40. Kapadia SR, Yakoob K, Nader S, Thomas JD, Mann DL, Griffin BP. Elevated circulating levels of serum tumor necrosis factor-alpha in patients with hemodynamically significant pressure and volume overload. *Journal of the American College of Cardiology* 2000; **36**(1): 208-12.
41. Wilson EM, Gunasinghe HR, Coker ML, et al. Plasma matrix metalloproteinase and inhibitor profiles in patients with heart failure. *J Card Fail* 2002; **8**(6): 390-8.
42. Jordan A, Roldan V, Garcia M, et al. Matrix metalloproteinase-1 and its inhibitor, TIMP-1, in systolic heart failure: relation to functional data and prognosis. *J Intern Med* 2007; **262**(3): 385-92.
43. Nagatomo Y, Carabello BA, Coker ML, et al. Differential effects of pressure or volume overload on myocardial MMP levels and inhibitory control. *Am J Physiol Heart Circ Physiol* 2000; **278**(1): H151-61.
44. Spinale FG. Myocardial matrix remodeling and the matrix metalloproteinases: influence on cardiac form and function. *Physiol Rev* 2007; **87**(4): 1285-342.
45. George J, Patal S, Wexler D, Roth A, Sheps D, Keren G. Circulating matrix metalloproteinase-2 but not matrix metalloproteinase-3, matrix metalloproteinase-9, or tissue inhibitor of metalloproteinase-1 predicts outcome in patients with congestive heart failure. *Am Heart J* 2005; **150**(3): 484-7.
46. Oral H, Sivasubramanian N, Dyke DB, et al. Myocardial proinflammatory cytokine expression and left ventricular remodeling in patients with chronic mitral regurgitation. *Circulation* 2003; **107**(6): 831-7.

47. Yilmaz A, Kindermann I, Kindermann M, et al. Comparative evaluation of left and right ventricular endomyocardial biopsy: differences in complication rate and diagnostic performance. *Circulation* 2010; **122**(9): 900-9.
48. Holzmann M, Nicko A, Kuhl U, et al. Complication rate of right ventricular endomyocardial biopsy via the femoral approach: a retrospective and prospective study analyzing 3048 diagnostic procedures over an 11-year period. *Circulation* 2008; **118**(17): 1722-8.
49. Platts D, Brown M, Javorsky G, West C, Kelly N, Burstow D. Comparison of fluoroscopic versus real-time three-dimensional transthoracic echocardiographic guidance of endomyocardial biopsies. *Eur J Echocardiogr* 2010; **11**(7): 637-43.
50. Tsutsui H, Spinale FG, Nagatsu M, et al. Effects of chronic beta-adrenergic blockade on the left ventricular and cardiocyte abnormalities of chronic canine mitral regurgitation. *J Clin Invest* 1994; **93**(6): 2639-48.
51. Dell'italia LJ, Balcells E, Meng QC, et al. Volume-overload cardiac hypertrophy is unaffected by ACE inhibitor treatment in dogs. *The American journal of physiology* 1997; **273**(2 Pt 2): H961-70.
52. Lowes BD, Minobe W, Abraham WT, et al. Changes in gene expression in the intact human heart. Downregulation of alpha-myosin heavy chain in hypertrophied, failing ventricular myocardium. *J Clin Invest* 1997; **100**(9): 2315-24.
53. Lowes BD, Gilbert EM, Abraham WT, et al. Myocardial gene expression in dilated cardiomyopathy treated with beta-blocking agents. *The New England journal of medicine* 2002; **346**(18): 1357-65.
54. Zheng J, Chen Y, Pat B, et al. Microarray identifies extensive downregulation of noncollagen extracellular matrix and profibrotic growth factor genes in chronic isolated mitral regurgitation in the dog. *Circulation* 2009; **119**(15): 2086-95.
55. Zhang YM, Bo J, Taffet GE, et al. Targeted deletion of ROCK1 protects the heart against pressure overload by inhibiting reactive fibrosis. *Faseb j* 2006; **20**(7): 916-25.
56. Zheng J, Yancey DM, Ahmed MI, et al. Increased Sarcolipin Expression and Adrenergic Drive in Humans With Preserved Left Ventricular Ejection Fraction and Chronic Isolated Mitral Regurgitation. *Circulation: Heart Failure* 2014; **7**(1): 194-202.
57. Zhang W, Qu X, Chen B, et al. Critical Roles of STAT3 in β-Adrenergic Functions in the Heart. *Circulation* 2016; **133**(1): 48-61.
58. Leszek P, Korewicki J, Klisiewicz A, et al. Reduced myocardial expression of calcium handling protein in patients with severe chronic mitral regurgitation. *Eur J Cardiothorac Surg* 2006; **30**(5): 737-43.
59. Wajant H, Pfizenmaier K, Scheurich P. Tumor necrosis factor signaling. *Cell Death Differ* 0000; **10**(1): 45-65.
60. Foo RS, Mani K, Kitsis RN. Death begets failure in the heart. *J Clin Invest* 2005; **115**(3): 565-71.
61. Wang J, Duncan D, Shi Z, Zhang B. WEB-based GEne SeT AnaLysis Toolkit (WebGestalt): update 2013. *Nucleic acids research* 2013; **41**(Web Server issue): W77-83.
62. Jourquin J, Duncan D, Shi Z, Zhang B. GLAD4U: deriving and prioritizing gene lists from PubMed literature. *BMC genomics* 2012; **13 Suppl 8**: S20.
63. Dennis G, Jr., Sherman BT, Hosack DA, et al. DAVID: Database for Annotation, Visualization, and Integrated Discovery. *Genome biology* 2003; **4**(5): P3.

Chapter 3

Clinical, echocardiographic and serum markers of left ventricular remodelling in response to treatment with carvedilol in patients with chronic primary mitral regurgitation.

3.1. Introduction

Chronic primary mitral regurgitation (CPMR) develops in patients over months to years due to a progressive abnormality of the mitral valve apparatus predominantly related to degenerative disease in developed countries and rheumatic heart disease in developing countries, where it remains the most common form of acquired cardiovascular disease in children and adults.[1]

Patients are asymptomatic for long periods while the left ventricle (LV) progressively dilates in response to abnormal preload.[2] The eccentric hypertrophy that develops normalizes afterload leading to a period of so-called 'compensation'. However, due to inadequate protein synthesis and progressive deterioration in myocardial function, the hypertrophy that develops is insufficient to fully compensate for the wall stress.[3] This leads to an increase in inflammatory cytokine expression, neurohormonal activation and reactive oxygen species generation. These chronic stressors activate a number of complex inflammatory and apoptotic pathways in a similar manner to heart failure from other causes. Early in the LV remodelling process there is loss of interstitial collagen and cell slippage due to degradation of the myocardial extracellular matrix (ECM). Later changes include myocyte apoptosis and pathological ECM fibrosis.[4] As a result, chronic decompensated MR ensues, and the LV resembles end-stage dilated cardiomyopathy. Subsequent LV dysfunction translates into increases in end-diastolic pressure, increased left atrial pressure and pulmonary hypertension, which leads to right ventricular dilatation and dysfunction. These changes are easily measurable using invasive and non-invasive imaging techniques such as echocardiography[5]

and result in the activation of a number of molecular pathways within the myocardium, which can be measured using serum markers.[4,6,7]

Adrenergic drive is increased in animals and humans with chronic volume overload and is thought to result in increased adverse effects within the myocardium including inflammation, cell loss and breakdown of extracellular matrix proteins.[8] Therefore, β-adrenergic blockade has been explored in a number of animal and human studies with variable effect (Table 1.1). Carvedilol is a particularly interesting agent in this regard but has only been studied in rats with experimental mitral regurgitation.[9] It blocks both β_1 and β_2 adrenergic receptors and also peripheral α receptors, which should reduce LV afterload reducing the degree of mitral regurgitation, consequently, volume overload.

To date, no human study has detailed the left ventricular response to treatment of patients with CPMR with carvedilol. It was the hypothesis of this study that carvedilol would attenuate LV remodelling in patients with CPMR while they awaited definitive mitral valve surgery.

3.2. Methods

Details of the materials and methods are provided in chapter 2.

3.2.1. Study subjects

The investigation conforms to the principles outlined in the Declaration of Helsinki. Informed consent was obtained from all patients according to a protocol approved by the Human Research Ethics Committee of the University of the Witwatersrand (M101036). Patients were included in the study if they had CPMR and met guideline criteria for elective mitral valve surgery.[10] Patients were excluded if they had aortic valve disease, mitral stenosis, active infective endocarditis, co-morbid coronary artery disease, chronic kidney disease, contraindications to β-blocker therapy, were pregnant, or had a history of anti-remodelling therapy use (β-blockers, angiotensin converting enzyme (ACE) inhibitors, angiotensin receptor blockers or mineralocorticoid receptor antagonists).

Patients underwent baseline clinical examination, transthoracic echocardiography, blood analysis and cardiac catheterization. Immediately after baseline investigations patients were randomized to receive standard of care (diuretics, potassium supplementation) plus carvedilol ("CRV" group) or standard of care only ("Nil" group). In the CRV group, the dose of carvedilol was up-titrated to 25mg twice daily over a period of one month. Patients were presented for surgery to the cardiothoracic unit immediately after their baseline cardiac catheterization. The timing of the patients' surgery, which was largely dependent on the surgical waiting list, was determined by the cardiothoracic unit.

3.2.2. Echocardiography

Baseline and pre-operative echocardiography was performed with an iE-33® ultrasound device (Koninklijke Philips, NV, USA) by a single sonographer blinded to study medication protocol on all recruited patients according to established guidelines.[11-13]

3.2.3. Serum

Baseline and pre-operative serum was collected for CRP, NT-pro BNP, soluble Fas/APO-1 receptor (sFas) and soluble Fas ligand (sFas-L),[14] sST2,[15] TNF-α, Il-1, Il-6,[6,16] MMP-1, MMP-2, MMP-9, and TIMP-1 and TIMP-4.[17,18] Quantification was performed using Magnetic Luminex® Screening Assays (R&D Systems, Inc., MN, USA) (for TNF-α, IL-1β, IL-6, ST2, Fas-Ligand and Fas) or Milliplex® MAP panels (EMD Millipore Corporation, MA, USA) (for MMP-1, -2, and -9 & TIMP-1 and -4) according to manufacturers' guidelines. Assays were run using the Bio-PlexTM 200 system (Bio-Rad, Texas, USA), and concentrations generated automatically using the Bio-Plex manager software, version 5.0 (Bio-Rad Laboratories Inc, Hercules, USA).

3.2.3.1. Selection of serum tests

Due to financial constraints only a limited number of serum tests could be selected. NT-proBNP, ST2 and IL-33 were selected because of their known use as markers of myocardial volume overload.[15,19] The MMPs and TIMPs were selected based on prior studies showing that an important aspect of myocardial remodelling in volume overload is loss of normal ECM due to MMP activation and an increase in the MMP/TIMP ratio.[20-22] Major serum markers of

inflammation were selected based on prior work.[6,23-25] Finally, since cell loss is an important part of the pathophysiology of remodelling in models of volume overload, Fas ligand and serum Fas receptor were selected as serum markers of apoptosis in these patients. Increased plasma levels of soluble Fas receptors have been found in patients with heart failure and peripartum cardiomyopathy.[14,26]

3.3. Results

3.3.1. Study population

The first patient was recruited in November 2011 and last patient underwent her final surgery in December 2015. Twenty consecutive patients with CPMR, who gave informed consent, underwent baseline investigation including clinical examination, ECG, echocardiography, 6MWT, blood tests, cardiac catheterization and LV EMB according to the study protocol. Unfortunately the LV wall was perforated at the apex in the first EMB patient. She was taken for emergent surgery and underwent a successful mitral valve replacement without further complication. Patient number 8 developed a deep vein thrombosis and ultimately fatal pulmonary embolism while waiting at home for surgery. Four patients were lost to follow up despite many attempts to make contact and locate them. In one patient, screening failed to identify intermittent hypertension. Therefore, seven patients were excluded from the final analysis. Thirteen patients underwent full baseline and final investigations as per study protocol and were included in the final analysis (Figure 3.1).

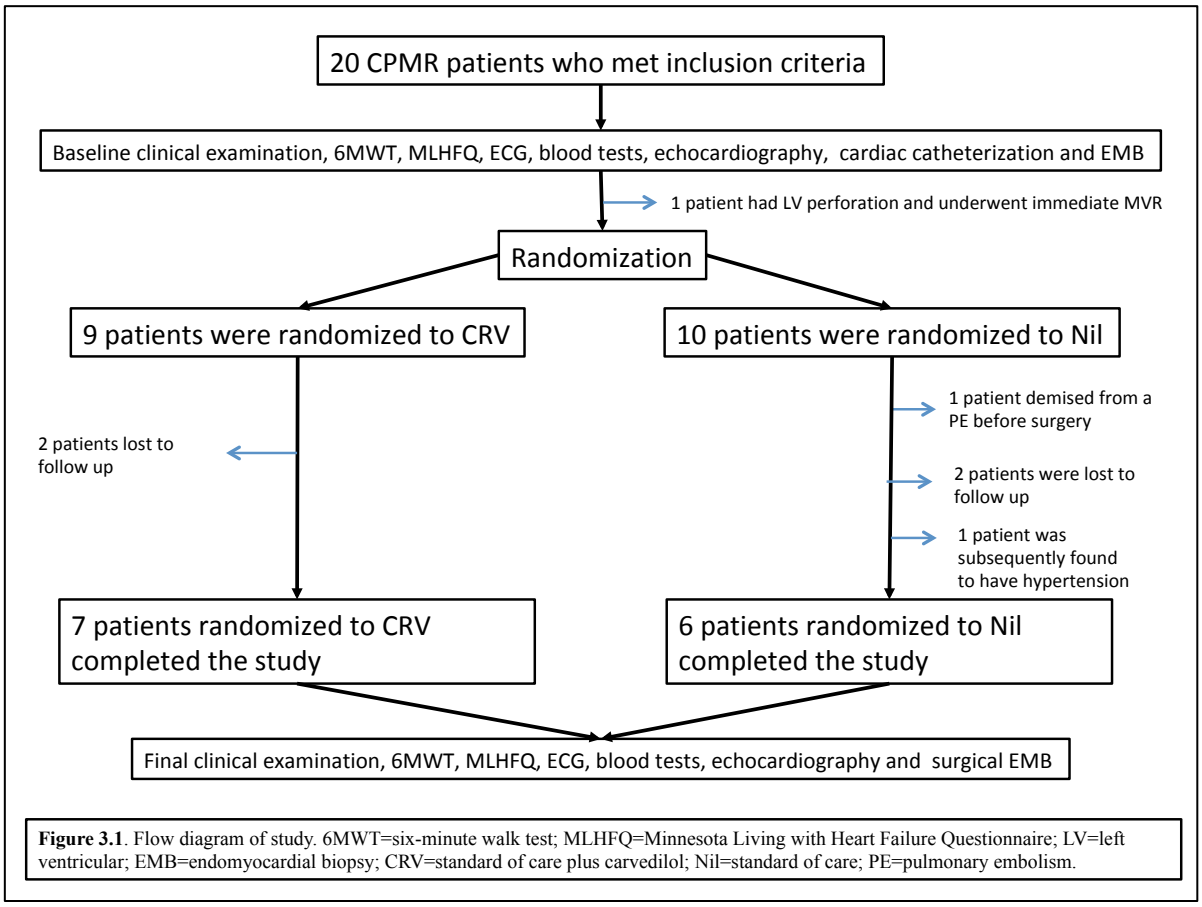

Figure 3.1. Flow diagram of study. 6MWT=six-minute walk test; MLHFQ=Minnesota Living with Heart Failure Questionnaire; LV=left ventricular; EMB=endomyocardial biopsy; CRV=standard of care plus carvedilol; Nil=standard of care; PE=pulmonary embolism.

3.3.2. Baseline characteristics

3.3.2.1. Baseline demographic and general characteristics

There were no significant differences between the two groups of patients with respect to clinical characteristics (Table 3.1). In 12 (92%) patients the cause of CPMR was rheumatic heart disease. The median duration of follow up from the time of therapeutic carvedilol dosing (the time at which the CRV patients were on 50mg daily) or baseline investigations (in the case of the Nil group) to the time of surgery was 10 months and 7 months, respectively (p=0.4738). All patients had evidence of severe CPMR with 11 of 13 patients being in NYHA functional class ≥2. Baseline parameters for the entire group included median resting

pulmonary artery pressure of 57mmHg, median LV end systolic diameter of 40mm (indexed 25.5mm/m^2), median ejection fraction of 61% with an effective regurgitant orifice of 0.68cm^2, and a median serum NT-proBNP of 822 ng/L.

Table 3.1. Baseline clinical characteristics.

	Carvedilol	Nil	P value
Number	7	6	
Age (years)	34	42	NS
Female	4	5	NS
Black race	6	6	NS
Atrial fibrillation*	2	1	NS
Body surface area (m^2)	1.69	1.82	NS
Cause of MR			
Rheumatic	6	6	NS
Mitral valve prolapse	1	0	NS
Clinical			
Duration of follow up (months)	10	7	NS
NYHA I	1	1	NS
NYHA II	3	5	NS
NYHA III	2	0	NS
NYHA IV	1	0	NS
ECG heart rate (bpm)	78	81	NS
Systolic blood pressure (mmHg)	110	116	0,0981
Six minute walk test (m)	450	450	NS
MLHFQ	56	56.5	NS
Drugs			
Furosemide (mg/day)	40	40	NS
Digoxin (mg/day)	0	0	NS

NYHA=New York Heart Association, MLHFQ=Minnesota Living with Heart Failure Questionnaire; NS=not significant.
*Patients with atrial fibrillation were treated with warfarin according to their INR.

3.3.2.2. Baseline echocardiographic parameters

At baseline the median LV dimensions were significantly greater in those patients allocated to carvedilol therapy (Table 3.2). The median LVEDDI was 41mm/m^2 in the CRV group compared with 31.13mm/m^2 in the control group (p=0.0152). The median LVESDI was 29.03mm/m^2 compared with 19.48mm/m^2 in the two groups, respectively (p=0.0066). The median LVEDVI was 125.33ml/m^2 in the CRV group at baseline but only 89.99ml/m^2 in the control group (p=0.0223). Similarly, the LVESVI in the CRV group at baseline was 68.98ml/m^2 compared with 37,63ml/m^2 in the control group at baseline (p=0.0152) (Figure 3.2A-D).

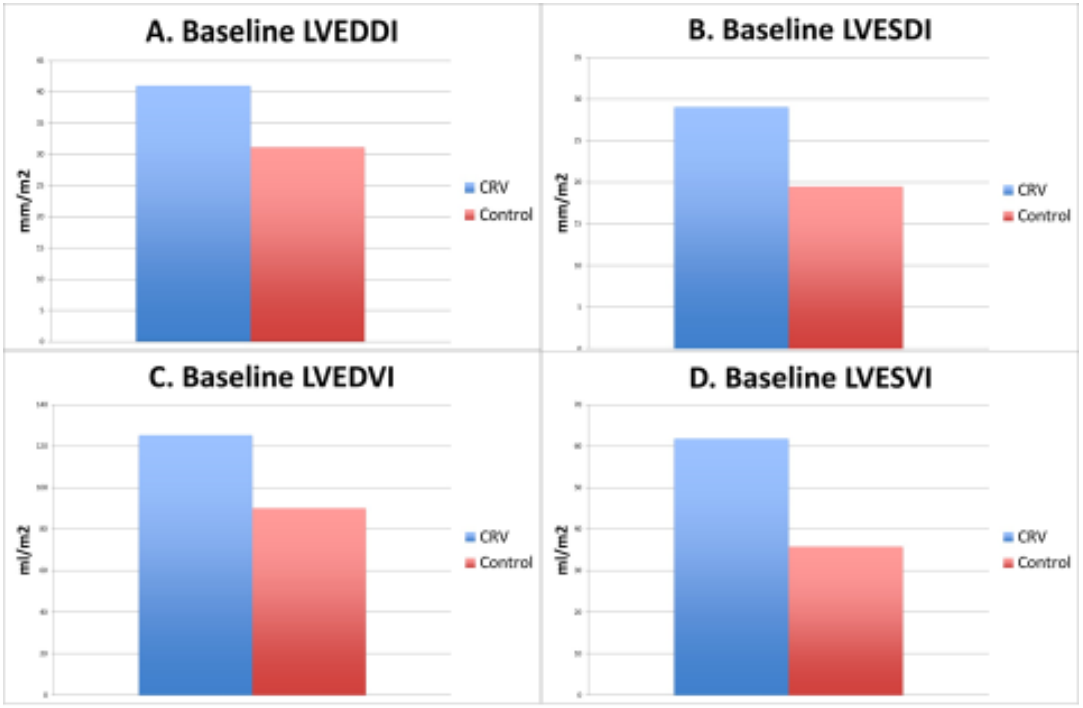

Figure 3.2. Baseline left ventricular dimensions and volumes in the two study groups.

There were no significant differences between the two groups with respect to the remaining baseline echocardiographic parameters, cardiac catheterization findings or serum markers of LV remodelling (Table 3.2). The baseline median LVEF was 57% in the CRV group and 64% in the control group (p=0.1331). The median LVdp/dt was 1518mmHg/s in the CRV group and 1375.5mmHg/s in the control group (p=0.7714). The indexed cardiac output (C.I.) was 1866.1ml/min/m^2 in the CRV group and 2073.05ml/min/m^2 in the control group (p=0.4751). The baseline median GLS (global longitudinal strain) was -16% in the CRV group and -16% in the control group (p=0.6723). Indexed LA volume was 142.51ml/m^2 in the CRV group and 97.88ml/m^2 in the control group at baseline (p=0.1531). Baseline median vena contracta was 10mm in the CRV group and 8.5mm in the control group (p=0.1682). Median effective regurgitant orifice in the CRV group was 0.8mm^2 and 0.38mm^2 in the control group (p=0.224). Baseline median mitral regurgitant volume was 119ml in the CRV group and 81.5ml in the control group (p=0.4314). Median right ventricular base was 40mm at baseline in both groups (p=0.6141). Tricuspid annular plane systolic excursion as a measure of right ventricular function was 17mm in the CRV group and 18.5mm in the control group at baseline (p=0.3146). The pulmonary artery pressure estimate (based on maximum velocity of the tricuspid regurgitant jet) was 43.5mmHg in the CRV group and 34mmHg in the control group (p=0.5218).

3.3.2.3. Baseline cardiac catheterization findings

Baseline median pulmonary artery systolic pressure was 57mmHg in the CRV group and 49mmHg in the control group (p=0.8862). Median mean pulmonary artery pressure was

37mmHg and 37.5mmHg in the two groups, respectively (p=0.943). LV end diastolic pressure was 17mmHg in the CRV group and 13mmHg in the control group (p=0.4314). Indexed cardiac output was 1960ml/min/m^2 in the CRV group and 2200ml/min/m^2 in the control group (p=0.3914).

Table 3.2. Baseline echocardiographic and invasive hemodynamic data.

	Carvedilol	**Nil**	P value
Echocardiography			
LVEDD Indexed (mm/m^2)	41	31,13	0,0152
LVESD indexed (mm/m^2)	29,03	19,48	0,0066
LVEDV indexed (ml/m^2)	125,33	89,99	0,0223
LVESV indexed (ml/m^2)	61,83	35,75	0,0152
Ejection fraction (%)	57	64	NS
Left ventricular dp/dt (mmHg/s)	1518	1375,5	NS
Cardiac output indexed (ml/min/m^2)	1866,1	2073,05	NS
Global longitudinal strain (%)	-16	-16	NS
LA volume indexed (ml/m^2)	142,51	97,88	NS
Vena contracta (mm)	10	8,5	NS
Effective regurgitant orifice (cm^2)	0,8	0,38	NS
Regurgitant volume (ml)	119	81,5	NS
Right ventricular base (mm)	40	40	NS
Tricuspid annular plane systolic excursion (mm)	17	18,5	NS
Right ventricular lateral S' (cm/s)	12,3	12,3	NS
PASP (estimate based on TR Vmax)(mmHg)	43,5	34	NS
Cardiac catheterization			
PASP (mmHg)	57	49	NS
PA mean (mmHg)	37	37,5	NS
LV EDP (mmHg)	17	13	NS
Cardiac output indexed (ml/min/m^2)	1960	2200	NS

LV=left ventricular; EDD=end diastolic diameter; ESD=end systolic diameter; EDV=end diastolic volume; ESV=end systolic volume; LA=left atrium; PASP=pulmonary artery systolic pressure; PA=pulmonary artery; EDP=end diastolic pressure; NS=not significant.

Table 3.3. Baseline serum data.

	Carvedilol	Nil	P value
NT-proBNP (ng/L)	839	367,5	NS
CRP (mg/L)	0	7	NS
MMP-1 (pg/ml)	13654,99	13571,66	NS
MMP-2 (pg/ml)	182525,05	202869,62	NS
MMP-9 (pg/ml)	67245,59	91953,76	NS
TIMP-1 (pg/ml)	115526,67	126303,75	NS
TIMP-4 (pg/ml)	157,475	220,075	NS
MMP1:TIMP1	0,1147	0,0948	NS
MMP1:TIMP4	143,142	70,127	NS
MMP2:TIMP1	1,435	1,898	NS
MMP2:TIMP4	1317,979	1030,88	NS
MMP9:TIMP1	0,4232	0,692	NS
MMP9:TIMP4	281,023	417,664	NS
TNFα (pg/ml)	3,59	3,355	NS
IL1β (pg/ml)	0	0	NS
IL6 (pg/ml)	2,6	2,91	NS
Fas (pg/ml)	5494,98	4581,79	NS
FasL (pg/ml)	37,85	27,985	NS
ST2 (pg/ml)	9434,18	8649,1	NS

NS=not significant.

3.3.2.4. Baseline serum results (Table 3.3)

NT-pro BNP levels were 839ng/L in the CRV group and 367.5ng/L in the control group (p=0.5677). CRP levels were not significantly different in the two groups (p=0.2899). Baseline MMP-1 levels were not significantly different between the CRV group and the control group (p=0.7751). Similarly there were no significant baseline differences between the two groups with respect to MMP-2 (p=0.5677), MMP-9 (p=0.2531), TIMP-1 (0.7751) or TIMP-4 (p=0.5218) levels. There were no significant differences between baseline MMP/TIMP ratios between the CRV and control groups.

3.3.2.5. Comparison of the two groups after removal of EM

One patient (EM) in the study group had a LV EF of 38% at the time of recruitment. After removing this patient from the analysis, the baseline characteristics of the two groups were unchanged (there was still a statistically significant difference in the LV dimensions at baseline with greater dimensions in the study group).

3.3.2.6. Comparison of the two groups after including only those with EF >60%

Several studies have presented data on patients with patients `preserved´ LV function (EF >60%).[27,28] The data was analysed after removing patients with an LV EF <60%. In this analysis there were no statistically significant differences in the baseline characteristics between the study group and the control group. However, after removing patients with low LV EF, there were only 3 patients in each group.

3.3.3. Changes in clinical, echocardiographic and serum parameters from baseline to final (in response to treatment with carvedilol) (Table 3.4)

Median absolute change and median percentage change for each variable from baseline to final measurement was compared between the two groups.

3.3.3.1. Change in heart rate (measured by resting ECG) over time

In the CRV group the median heart rate (HR) fell by a median of 16 beats per minute while there was no absolute change in the HR in the control group. This did not translate into a statistically significant change between the two groups over time (p=0.2505) (Figure 3.3). There was also no significant difference in the percentage change of the ECG-determined HR between the two groups over time. When the analysis was conducted after excluding patient EM or including only patients with an LV EF >60%, no significant changes between the two groups were found over time.

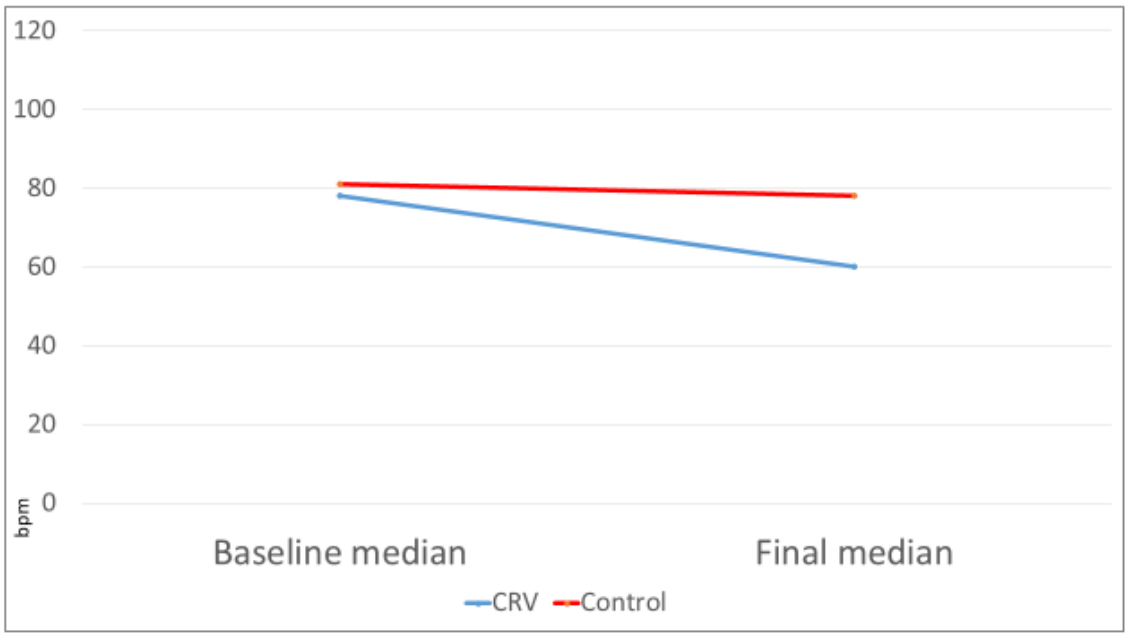

Figure 3.3. Absolute change in median ECG HR. bpm = beats per minute.

Table 3.4. Changes in clinical, echocardiographic and serum parameters in response to carvedilol treatment.

	Carvedilol		Nil		
	Absolute Change	% change	Absolute change	% change	P value
Parameters					
ECG heart rate (beats/min)	-16	-21,43	0	-1,15	NS
Systolic BP (mmHg)	-3	-2,5	3,5	3,22	NS
6MWT (meters)	0	0	-12,5	-2,38	NS
Echocardiography					
LVEDD Indexed (mm/m^2)	-1,075	-2,899	-0,3145	-0,877	NS
LVESD indexed (mm/m^2)	-0,592	-1,818	-0,603	-2,705	NS
LVEDV indexed (ml/m^2)	-7,101	-6,74	-3,558	-2,66	NS
LVESV indexed (ml/m^2)	-0,538	-0,8696	1,818	7,998	NS
Ejection fraction (%)	-4	-6,25	-2,5	-3,846	NS
LV dp/dt (mmHg/s)	-216	-18,54	246	16,81	NS
CI (ml/min/m^2)	-306,83	-16,44	-209,831	-8,13	NS
Global longitudinal strain	-1	4,76	-4	22,22	NS
LA volume indexed (ml/m^2)	-28,743	-20,17	13,17	17,36	NS
Vena contracta (mm)	-1	-10	1	13,89	0,0590
Effective regurgitant orifice (cm^2)	-0,33	-34,78	0,025	2,38	0,0150
MR volume (ml)	-53	-41,21	6	3,96	0,0321
Right ventricular base (mm)	1	2,7	5	12,05	NS
TAPSE (mm)	-3	-15,79	2	9,81	0,0307
Right ventricular lateral S' (cm/s)	-3,04	-24,72	-0,9	-7,32	0,0865
PASP (mmHg)	1	2,22	4	10,39	NS
Bloods					
BNP (ng/L)	789	96,47	-11	0,597	0,0865
CRP (mg/L)	0	-2,899	11,5	-0,877	NS
Serum analytes (pg/ml)					
MMP-1	-2243,69	-14,31	-253,94	2,91	NS
MMP-2	4075,75	2,23	-60249,91	-35,62	0,0455
MMP-9	13335,56	19,2	-10428,35	-5,51	NS
TIMP-1	-28614,02	-20,77	-8741,78	-8,69	NS
TIMP-4	-23,77	-12,01	-39,225	-24,57	NS
MMP1:TIMP1	0,00244	2,84	0,00476	9,16	NS
MMP1:TIMP4	15,4767	19,73	14,2805	29,54	NS
MMP2:TIMP1	0,46089	32,43	-0,372899	-25,79	0,0223
MMP2:TIMP4	206,0855	27,07	-178,8797	-25,95	NS
MMP9:TIMP1	0,45197	72,33	-0,0679	-2,88	NS
MMP9:TIMP4	172,5031	44,02	14,34744	4,22	NS
TNF-α	-0,46	-11,36	-0,365	-14,17	NS
IL1-β	0	-	0	-	NS
IL6	-0,84	-29,5	0,1	3,53	NS
Fas	556,34	8,5	-492,02	-10,84	0,0633
FasL	-3,14	-8,3	5,505	24,95	NS
ST2	-2010,78	-23,36	-1952,99	-17,81	NS

6MWT=six minute walk test; LV=left ventricular; EDD=end diastolic diameter; ESD=end systolic diameter; EDV=end diastolic volume; ESV=end systolic volume; LA=left atrium; PASP=pulmonary artery systolic pressure; CI=cardiac output indexed; TAPSE=tricuspid annular plane systolic excursion; NS=not significant.

3.3.3.2. Change in systolic blood pressure (at rest) over time

The median change in resting systolic blood pressure in the CRV was -3mmHg. In the control group the blood pressure increased by 3.5mmHg. There was no statistically significant difference when the two groups were compared (p=0.3524) even after removing patient EM from the analysis (p=0.3776) or when the analysis was performed using patients with LV EF >60% (p=0.2967).

3.3.3.3. Change in distance walked in 6 minutes from baseline to final

There was no change in the distance walked between baseline and final in the CRV group. There was a median reduction in distance walked between baseline and final among the control group of 12.5 meters. There was no significant difference in the absolute (p=0.7184) or percentage (p=0.8292) change between the two groups over time (Figure 3.4), whether patient EM was excluded (p=0.7471) or only patients with preserved LV EF were included (p=0.7642).

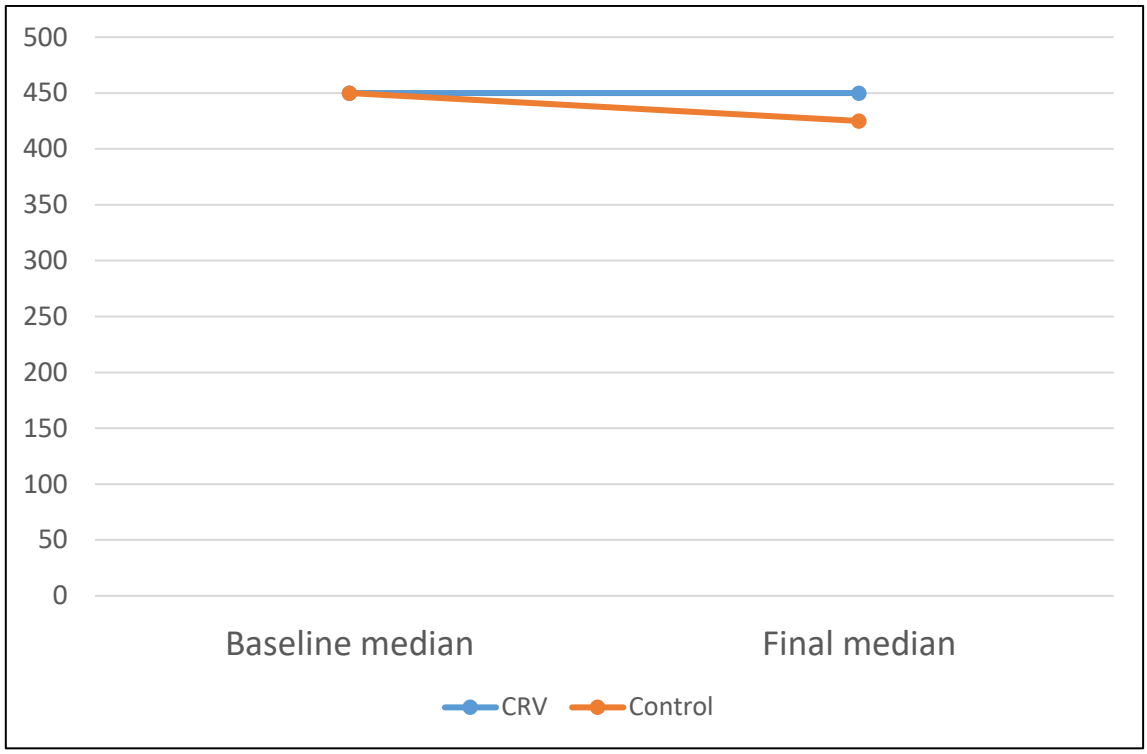

Figure 3.4. Change in distance (in meters) walked by patients during six minute walk test (p=0.7184).

3.3.3.4. Change in Minnesota Living with Heart Failure Questionnaire Score

The MLHFQ score increased by a median of 7 points in the CRV group over time and decreased by a median of 12.5 points in the control group with no statistically significant difference in the absolute (p=0.6682) or percentage (p=0.4751) or when patient EM was removed from the analysis (p=0.5218) or when only patients with preserved LVEF were included (p=0.6547).

3.3.3.5. Changes in dosing of furosemide and digoxin over time

There were no statistically significant differences in the dosing of furosemide or digoxin over time between the CRV group and the control group (p=1.000 for furosemide & p=0.3545 for digoxin). This did not change when patient EM was excluded or only patients with preserved LVEF were included.

3.3.3.6 Changes in echocardiographic and serum markers in response to carvedilol therapy.

3.3.3.6.1 Ejection fraction

The median reduction in EF in the CRV and control groups was 4% and 2.5%, respectively, with no significant difference in the change between the two groups (p=0.7206) (Figure 3.5). No statistical difference between the two groups was noted when EM was removed from the analysis or when only those with preserved LVEF were included in the analysis.

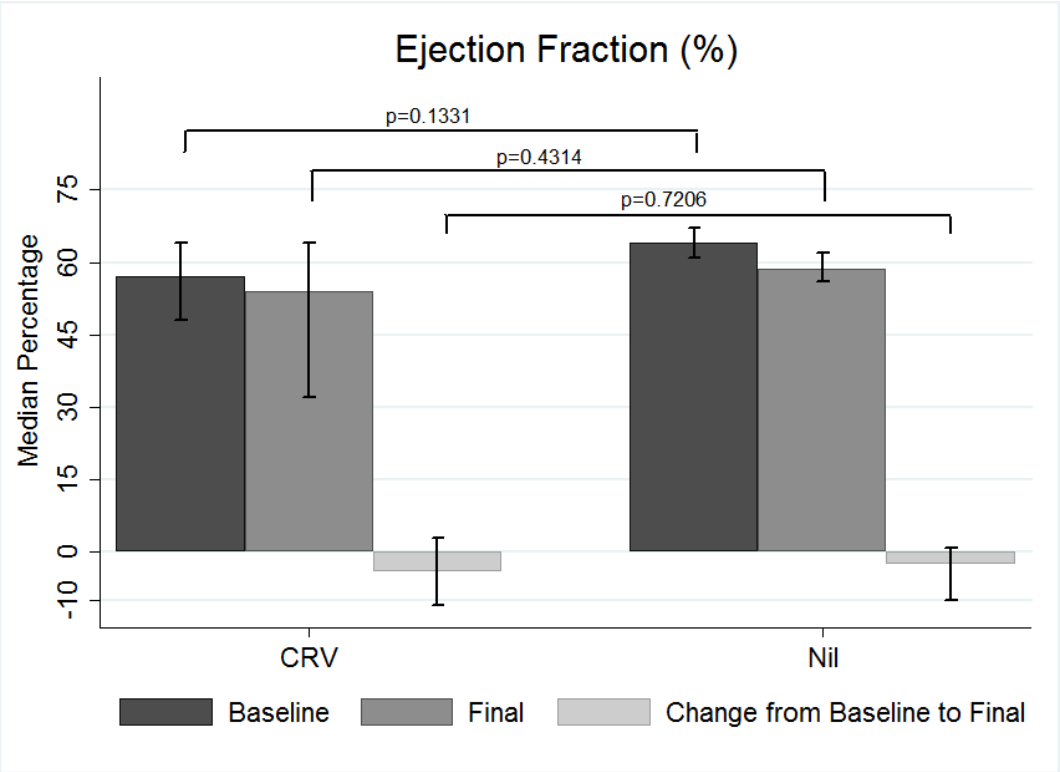

Figure 3.5. Change in ejection fraction in patients treated with carvedilol (CRV) versus standard of care (NIL). Error bars indicate interquartile range.

3.3.3.6.2 LVEDDI (LV end diastolic dimension indexed to BSA)

There was a median reduction in LVEDDI in the CRV group by 1.075mm/m^2 and 0.3145mm/^{2} in the control group with no statistical significant difference in the absolute (p=0.6166) or percentage (p=0.6166) change over time. No statistical difference between the two groups was noted when EM was removed from the analysis or when only those with preserved LVEF were included in the analysis.

3.3.3.6.3 LVESDI (LV end systolic dimension indexed to BSA)

There was a median reduction in LVESDI in the CRV group by 0.592mm/m^2 and 0.603 mm/m^2 in the control group with no statistical significant difference in the absolute (p=0.721) or percentage (p=0.6682) change over time. No statistical difference between the two groups was noted when EM was removed from the analysis or when only those with preserved LVEF were included in the analysis.

3.3.3.6.4 LVEDVI (LV end diastolic volume indexed to BSA)

There was a median reduction in the LVEDVI of 7.101 ml/m^2 in the CRV and 3.558 ml/m^2 in the control group over time. There was no statistical difference between the two groups with respect to these changes (p=0.7751 for the absolute and percentage change). No statistical difference between the two groups was noted when EM was removed from the analysis or when only those with preserved LVEF were included in the analysis.

3.3.3.6.5 LVESVI (LV end systolic volume indexed to BSA)

There was a median reduction in the LVESVI in the CRV group by 0.538 ml/m^2 and a minor increase of 1.818 ml/m^2 in the control group. This was no statistically significant difference between the two groups (p=0.8864) (Figure 3.6). No statistical difference between the two groups was noted when EM was removed from the analysis or when only those with preserved LVEF were included in the analysis.

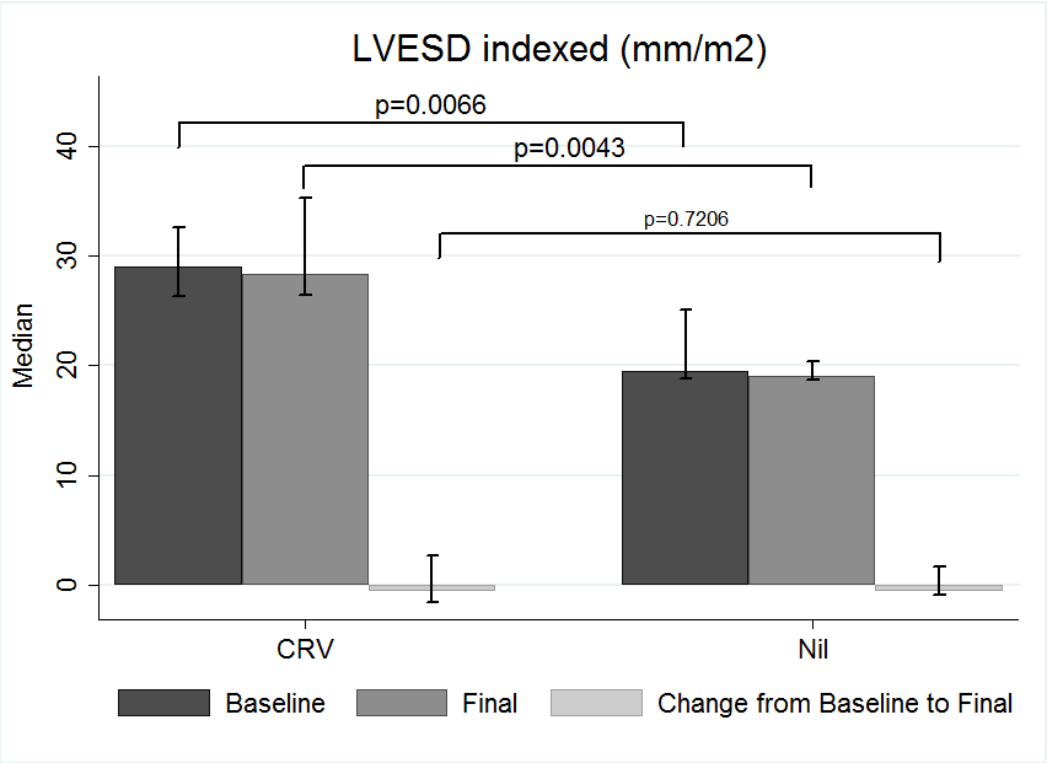

Figure 3.6. Change in left ventricular end systolic dimension (indexed to body surface area) in patients treated with carvedilol (CRV) versus standard of care (NIL). Error bars indicate interquartile range.

3.3.3.6.6 LV dp/dt

The LV dp/dt decreased by a median of 216 mmHg/s in the CRV group and increased by 246 mmHg/s in the control group, which was not significantly different (p=0.224). No statistical difference between the two groups was noted when EM was removed from the analysis or when only those with preserved LVEF were included in the analysis.

3.3.3.6.7 Cardiac output indexed to body surface area

There was a reduction in the echocardiographic-estimated CI in both groups. The median decrease in CI in the CRV group was 306.83 ml/min/m^2 and 209.83 ml/min/m^2 in the control group with no statistical significant difference between the two groups (p= 0.7751). No statistical difference between the two groups was noted when EM was removed from the analysis or when only those with preserved LVEF were included in the analysis.

3.3.3.6.8 Global longitudinal strain (GLS)

There was a median reduction in GLS in the CRV group by 1% and by 4% in the control group over the duration of the study. This was not statistically different (p=0.1127). No statistical difference between the two groups was noted when EM was removed from the analysis or when only those with preserved LVEF were included in the analysis.

3.3.3.6.9 Left atrial volume indexed to BSA

The LA volume (indexed) decreased by a median of 28.74 ml/m^2 in the CRV group but increased by a median of 13.17 ml/m^2 in the control group. However, this was not statistically different (p=0.3914). No statistical difference between the two groups was noted when EM was removed from the analysis or when only those with preserved LVEF were included in the analysis.

3.3.3.6.10 Vena contracta

The vena contracta decreased by a median of 1mm in the CRV group but increased by a median of 1mm in the control group. This was not statistically different between the two groups (p=0.059) and there was no effect of removing EM from the analysis or including only those with EF >60%.

3.3.3.6.11 Effective regurgitant orifice

There was a statistically significant difference in the median change in ERO between the CRV and the control groups over time (absolute change: p=0.015; percentage change: p=0.01). In the CRV group there was a median reduction in the ERO of 0.33cm^2 but in the control group there was a median increase of 0.38cm^2. When EM was removed from the analysis, there remained a statistically significant difference between the two group (p=0.0161) but if the analysis was only performed with those patients with an LV EF >60% then there was no statistically significant difference in the change of ERO over time between the two groups (p=0.1771). Changes in ERO over time are represented in Figure 3.7.

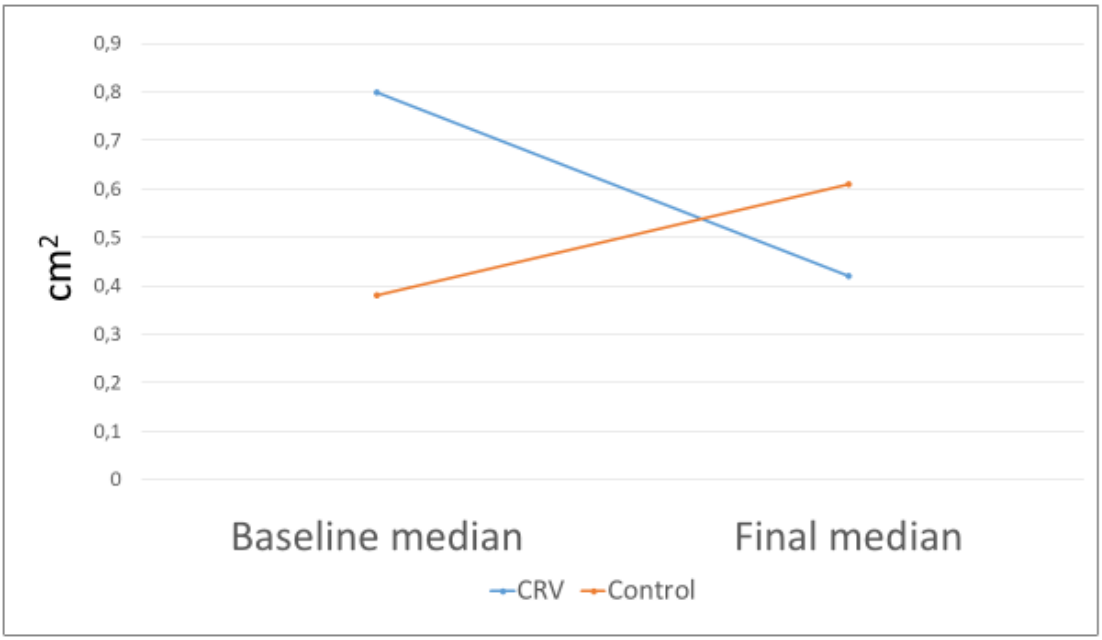

Figure 3.7. Change in median effective regurgitant orifice (p=0.015).

3.3.3.6.12 MR volume

There was a median reduction in MR volume of 53ml in the CRV in comparison to a 6ml median increase in the MR volume in the control group. This was statistically significant (p=0.0321) even when EM was removed (p=0.0161) but not when analysis was only performed with patients with preserved LV EF (p=0.1771). Changes in MR volume over time are represented in Figure 3.8.

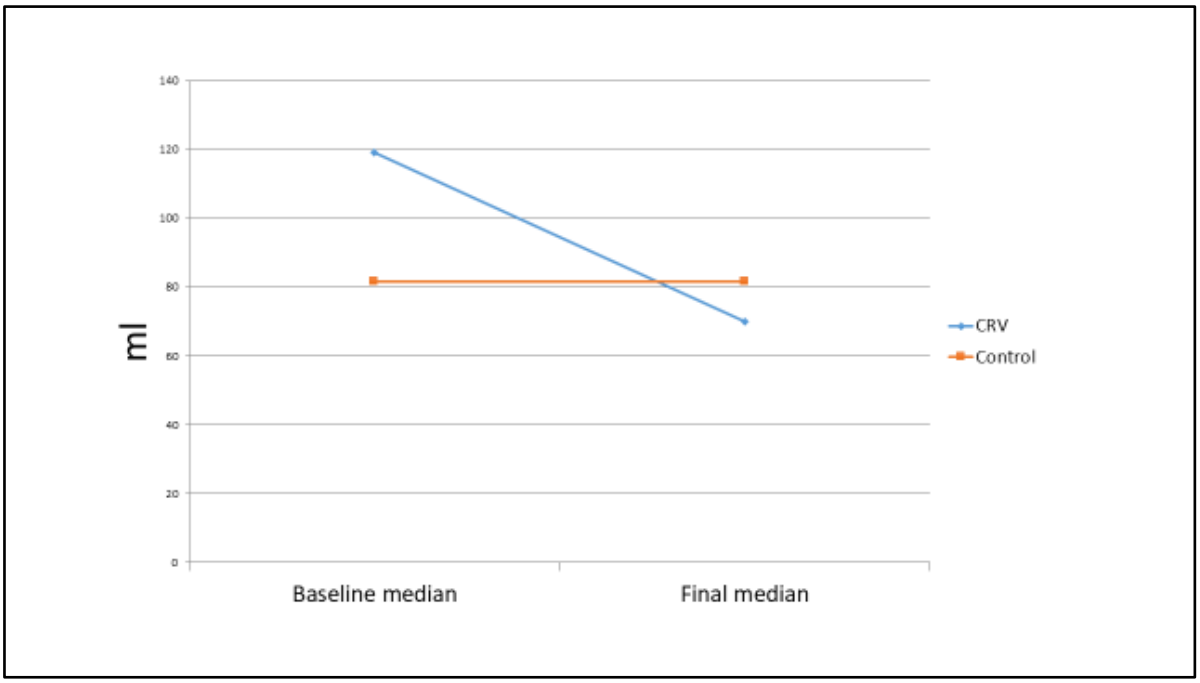

Figure 3.8. Change in median mitral regurgitant volume (p=0.0321).

3.3.3.6.13 Right ventricular base diameter

There was a median increase in the RV base in the CRV group of 1mm and 5mm in the control group. This was not statistically different between the two groups (p=0.4308) and there was no effect of removing EM from the analysis or including only those with EF >60%.

3.3.3.6.14 Tricuspid annular plane systolic excursion (TAPSE)

There was a decrease in the TAPSE in the CRV group by a median of 3mm while this increased by a median of 2mm in the control group. This was found to be a statistically significant change between the two groups (p=0.0307) but not when EM or patients with LVEF <60% were removed from the analysis (Figure 3.9).

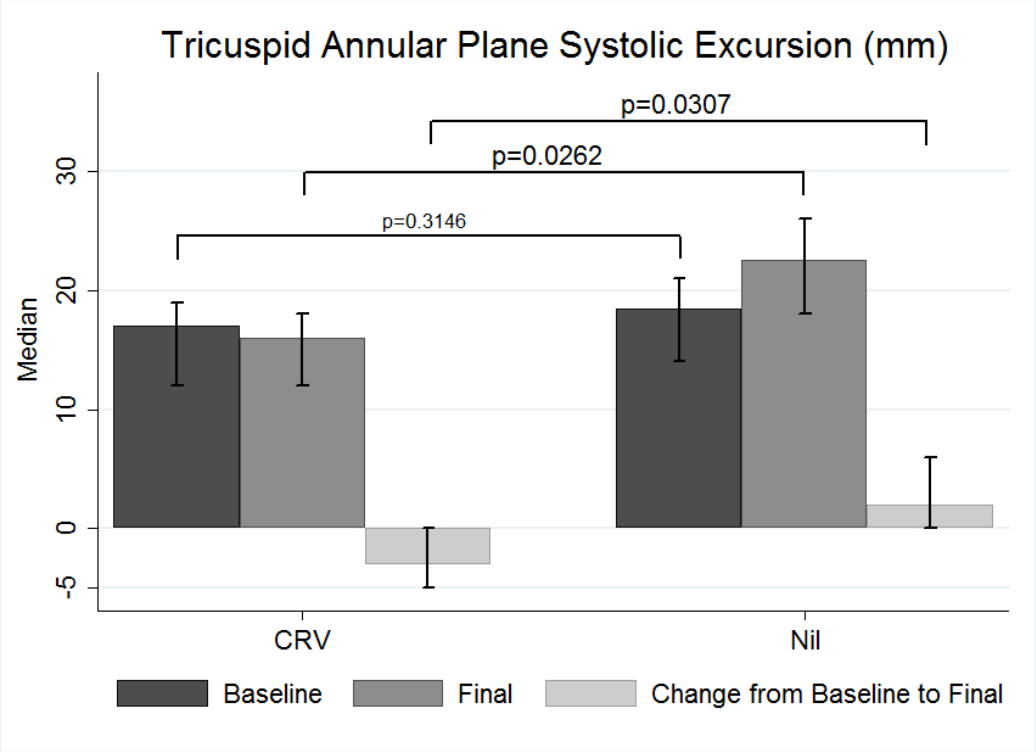

Figure 3.9. Change in tricuspid annular plane systolic excursion in patients treated with carvedilol (CRV) versus standard of care (NIL). Error bars indicate interquartile range.

3.3.3.6.15 Right ventricular tissue Doppler velocity (S') (cm/s)

This decreased more in patients treated with carvedilol with a trend towards significance (p=0.0865) (Figure 3.10).

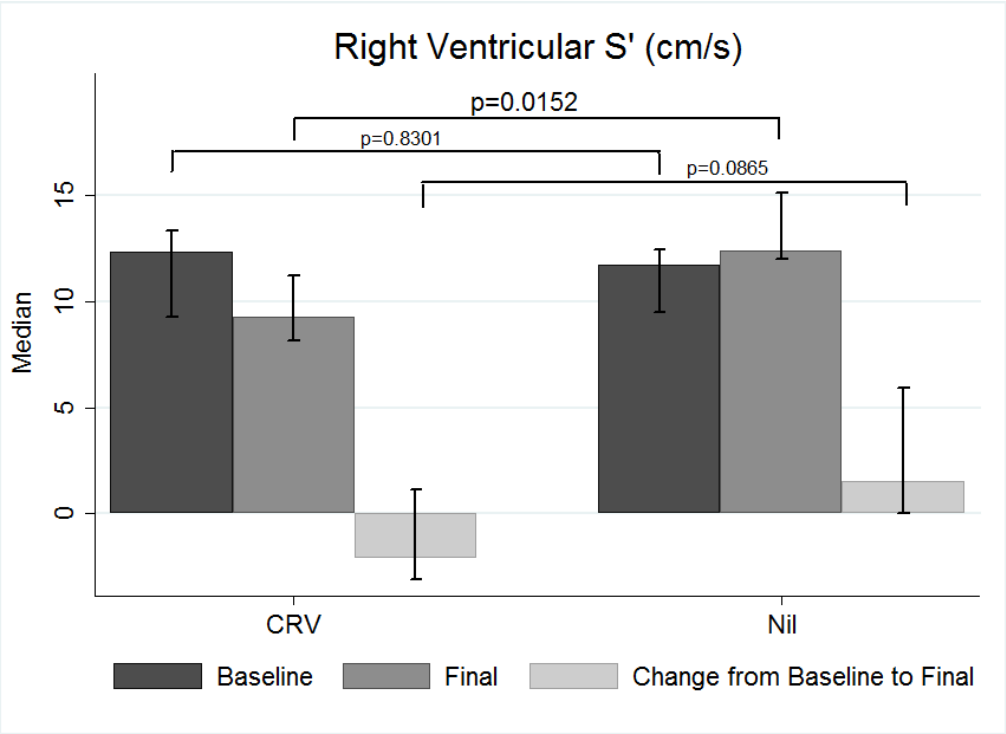

Figure 3.10. Change in right ventricular S' in patients treated with carvedilol (CRV) versus standard of care (NIL). Error bars indicate interquartile range.

3.3.3.6.16 TR Vmax (maximum velocity of the TR Doppler jet; in mmHg)

The TR Vmax increased by 1mmHg and by 4mmHg in the CRV and control groups, respectively. There was not statistically significant change between the two groups irrespective of patient exclusions. This suggests that pulmonary artery pressure was not affected by treatment with carvedilol.

3.3.3.6.17 NT-pro-BNP

The BNP increased by a median of 789ng/L in the CRV group during the follow up period. In contrast, the BNP decreased by a median of 11ng/L in the control group. Although the absolute change was not statistically different between the two groups (p=0.0865), there was a statistically significant difference between the two groups when the median changes were analysed as percentage changes (p=0.0455) (Figure 3.11). Even when EM was removed from

the analysis there was a statistically significant increase in BNP in the CRV group compared with the control group during the follow-up period (p=0.0374). However, there was no difference between the two groups when the analysis was only performed on patients with a baseline EF >60% (p=0.4561).

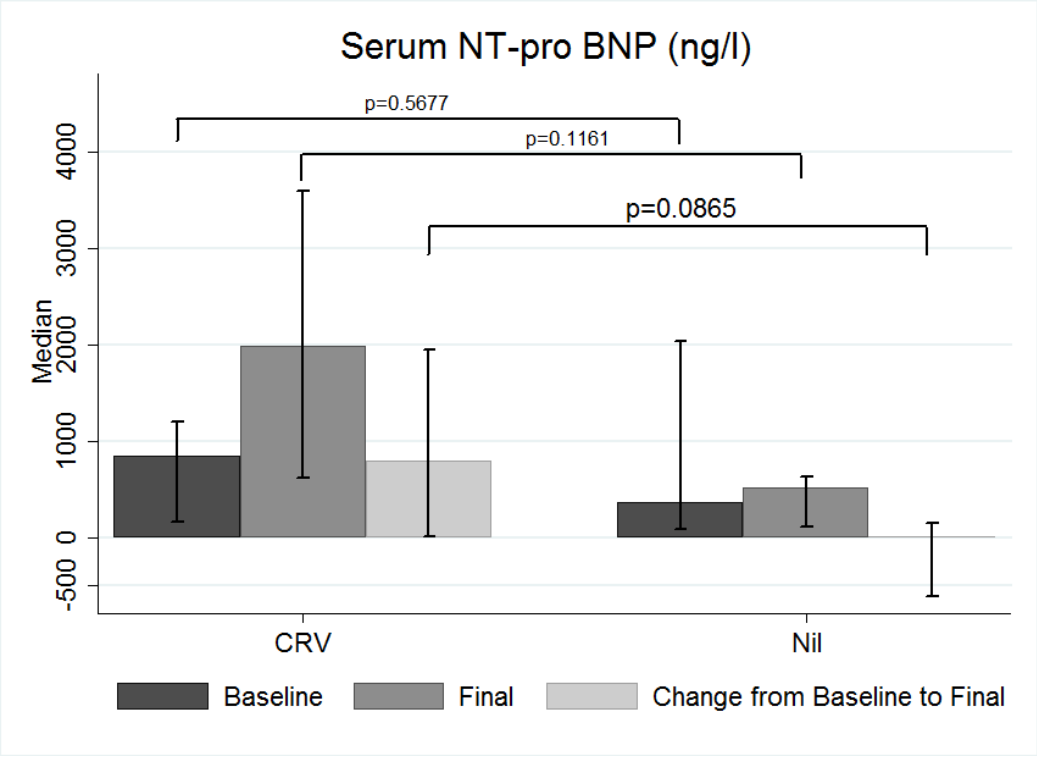

Figure 3.11. Change in serum NT-pro BNP in patients treated with carvedilol (CRV) versus standard of care (NIL). Error bars indicate interquartile range.

3.3.3.6.18 CRP

There was no significant change in CRP between the two groups.

3.3.3.6.19 Changes in TNF-α over time

Serum TNF-α levels decreased in both groups over the duration of the study. In the CRV group there was a decrease from 3.59pg/mL by a median of 0.46pg/mL and in the control

group the decrease was from 3.355pg/mL by a median of 0.365pg/mL with no significant difference between the two groups (p=0.8864). Removing EM from the analysis or performing the analysis with only preserved EF patients did not change the outcome.

3.3.3.6.20 IL-1β

Serum levels of IL-1β could not be quantified in either group because the circulating levels of this cytokine were below the measurable limits.

3.3.3.6.21 IL-6

The median decline in IL-6 in the CRV group was 0.84pg/mL while there was an increase in IL-6 in the control group by a median of 0.1. However this did not translate into a significant difference between the two groups (p=0.3914) even when EM or patients with reduced LV EF were removed.

3.3.3.6.22 Fas

There was a median increase in serum Fas in the CRV group of 556.34pg/mL but a decrease in serum levels of this marker of apoptosis in the control group by a median of 492.02pg/mL. There was a trend to statistical significance when the two groups were compared (p=0.0633) (Figure 3.12). This difference was not statistically significant when patients with reduced LV EF were removed from the analysis.

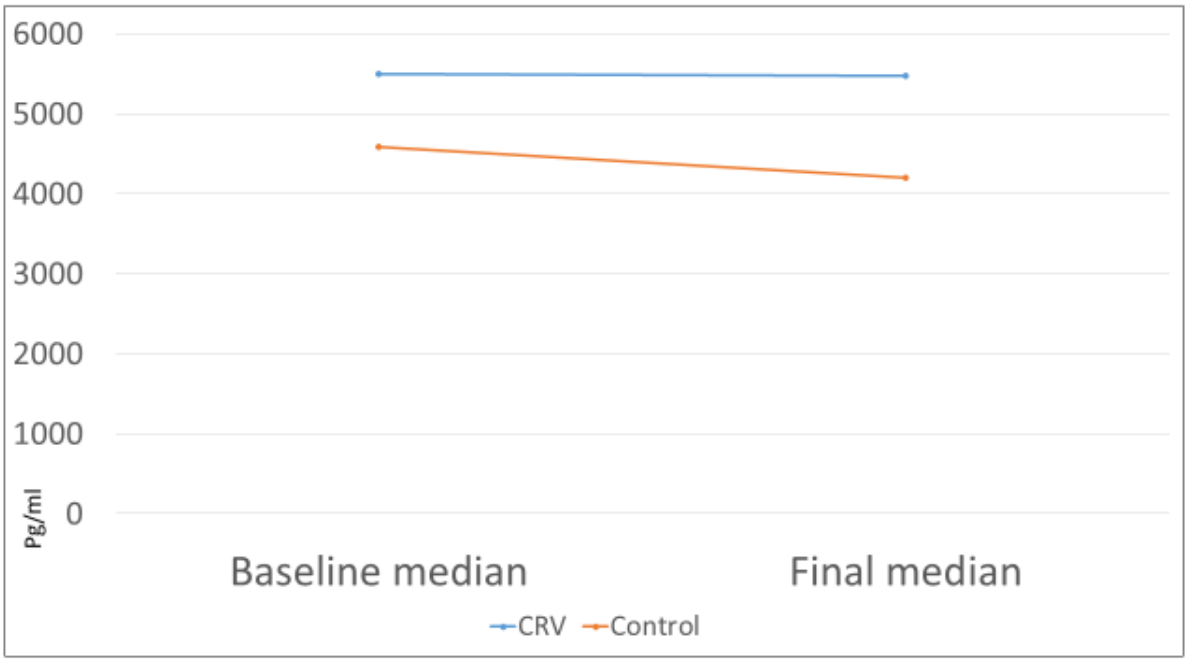

Figure 3.12. Absolute change in median serum Fas (p=0.0633).

3.3.3.6.23 Fas Ligand

There was a median decrease in serum FasL in the CRV group by 3.14pg/mL and a median decrease in the control group by 5.505pg/mL, which was not significantly different between the two groups (p=0.6682) even when the analysis was performed without patients with low LVEF.

3.3.3.6.24 ST2

ST2 levels decreased in both groups over time. In the CRV group there was a median decrease of 2010.78pg/mL and in the control group this decrease was a median of 1952.969pg/mL, which was not significantly different (p=0.6682). There was no change in the analysis when patients with low LV EF were excluded.

3.3.3.6.25 IL-33

Serum levels of IL-33 could not be quantified in either group because the circulating levels of this cytokine were below the measurable limits.

3.3.3.6.26 MMP-1

MMP-1 decreased from 13654.99pg/mL by a median of 2243.69pg/mL in the CRV group and from 13571.66pg/mL by a median of 253.94pg/mL in the control group with no significant difference between the two groups with respect to changes in MMP-1 over time (p=0.1985).

3.3.3.6.27 MMP-2

MMP-2 increased by a median of 4075.75pg/mL from 182525.05pg/mL in the CRV group but decreased by a median of 60249.91pg/mL from 202869.62pg in the control group. There was a statistically significant difference in the changes in MMP-2 levels between the two groups over time (p=0.0455) (Figure 3.13).

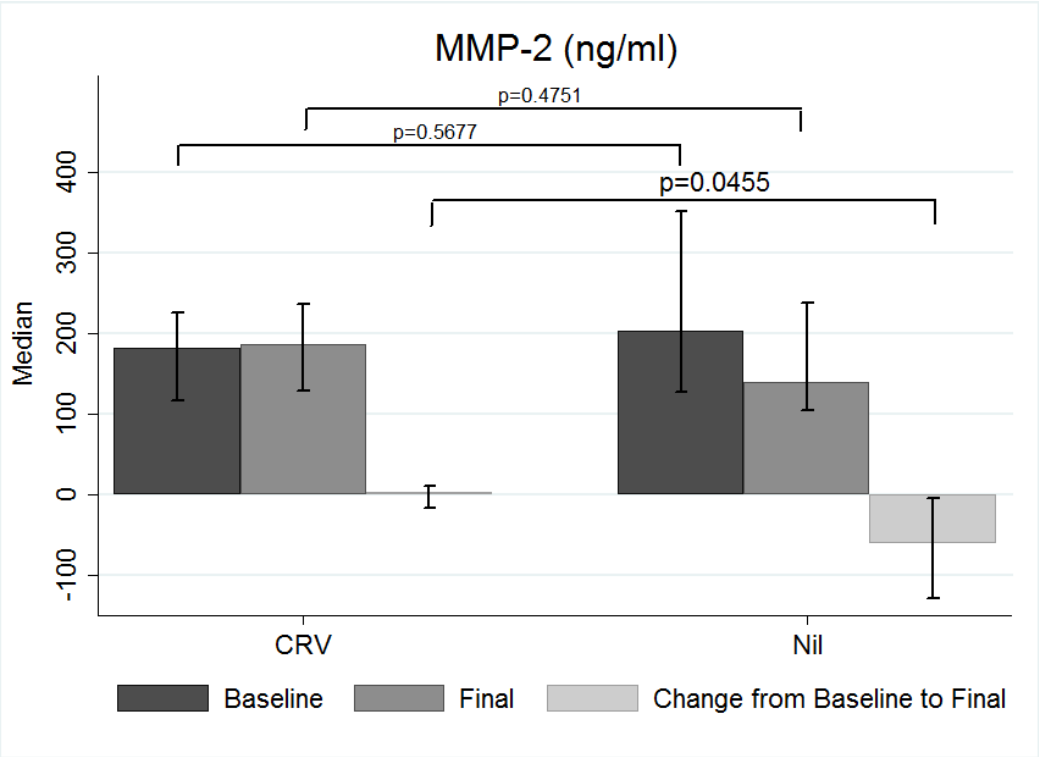

Figure 3.13. Change in serum MMP-2 in patients treated with carvedilol (CRV) versus standard of care (NIL). Error bars indicate interquartile range.

3.3.3.6.28 MMP-9

The MMP-9 levels increased by a median of 13335.56pg/mL in the CRV group and decreased by a median of 10428.35 pg/mL in the control group.

3.3.3.6.29 TIMP-1

TIMP-1 levels decreased by a median of 28614.02pg/mL in the CRV group and by a median of 8741.78pg/mL in the control group.

3.3.3.6.30 TIMP-4

Serum levels of TIMP-4 were extremely low in both groups of patients with no statistically significant changes over time (p=0.1093).

3.3.3.6.31 Changes in the MMP/TIMP ratios over time

Since the TIMPs inhibit the MMPs an important measure of MMP activity is the ratio of MMP to TIMP.[21]

3.3.3.6.31.1 MMP-1/TIMP-1 ratio

This ratio increased by a median of 0.00244 compared with a median increase of 0.00476 in the control group (p=0.8864).

3.3.3.6.31.2 MMP-1/TIMP-4 ratio

There was no statistically significant difference in the median change of this ratio over time between the two groups (p=1.000).

3.3.3.6.31.3 MMP-2/TIMP-1 ratio

The ratio of MMP-2 to TIMP-1 increased by a median of 0.46089 over time in the CRV group, whereas it decreased by 0.372899 in the control group. This was statistically significant (p=0.0223).

3.3.3.6.31.4 MMP-2/TIMP-4 ratio

Because the serum levels of TIMP-4 were so low compared with the high serum levels of MMP-2, the MMP-2/TIMP-4 ratios were extremely high. There was a median increase in the MMP-2/TIMP-4 ratio of 206.0855 and a median decrease in the ratio of 178.8797 in the control group. However this was not statistically significant (p=0.1003).

3.3.3.6.31.5 MMP-9/TIMP-1 ratio

This ratio increased by a median of 0.45197 in the CRV group and decreased by a median of 0.0679 in the control group, which was not significantly different (p=0.6682).

3.3.3.6.31.6 MMP-9/TIMP-4 ratio

Again, because of the low serum levels of TIMP-4, these ratios were particularly high. Despite this no statistically significant difference in the changes over time was detected between the CRV and the control groups (p=0.4652).

3.4. Discussion

This small, randomised, controlled study is the first to examine the effects of carvedilol on left ventricular remodelling in humans with CPMR. Complete data was available for 13 out of an initial 20 patients. The duration of follow up (a median of 10 months in the study group and 7 months in the control group) should have been sufficiently long enough to see changes in left ventricular dimensions in response to carvedilol.[27,29] Overall, this was a cohort of patients with severe decompensated CPMR as evidenced by NYHA clinical status that was ≥2 in the majority, Heart Failure questionnaire with high scores,[30] elevated LV dimensions in both groups at baseline with evidence of LV dysfunction (GLS reduced to a median of -16 in both groups), and pulmonary hypertension.

At baseline, patients randomised to carvedilol were well matched with respect to the control patients except for the LV dimensions and volumes on transthoracic echocardiography. This suggests that the patients randomised to carvedilol were possibly at a more advanced stage of LV remodelling than the controls. Even when one patient, who had a poor baseline LVEF, was removed from the comparison there was still a significant difference between the baseline LV dimensions and volumes compared with the controls. One might expect that should an intervention have a positive effect, it would most likely demonstrate this in patients with more severe disease. Therefore, by treating the patients with more severe LV remodelling (by chance) it would be expected that, should carvedilol truly attenuate or reverse adverse remodelling in patients with CPMR, it would manifest in this study. However, this was not the case. Even when the comparison was restricted only to patients with EF <60% at baseline (four patients allocated to treatment and one allocated to control), changes in clinical and

echocardiographic parameters followed those for the whole group described here (data not shown).

One possible argument for failure of an attenuation effect with carvedilol seen in this study is that these patients had significantly dilated hearts and were thus possibly beyond the point of deriving benefit from carvedilol. Wall stress probably outweighs any potential beta-blocker effect and patients with already marked dilatation and dysfunction at baseline are probably most sensitive to the effect of the La Place Law, hence the failure of carvedilol to show benefit in the group with more LV dysfunction.

Overall, there was no evidence that carvedilol improved or worsened the clinical condition of patients during their wait for surgery. There was no significant effect of carvedilol on LV dimensions or function compared with controls, which is consistent with lack of improvement in LV dimensions after metoprolol treatment.[29] The effective regurgitant orifice and regurgitant volume decreased significantly in the group treated with carvedilol corroborating previous findings in patients treated with other beta-blockers.[31] This may be a result of the negative ionotropic and chronotropic effects of beta-blockade and possibly due to afterload-reducing effects of alpha-receptor vasodilatory effect of the drug.

Right ventricular function is an important measure of LV function since RV function is directly influenced by LV function. Firstly, the LV and RV share the interventricular septum and, due to septal contractile dysfunction, dysfunction in the LV directly affects RV function.[32] Secondly, the ventricles share one pericardial compartment leading to dependent restrictions.[33] This is particularly important in the case of the eccentrically hypertrophied and

dilated LV in patients with mitral regurgitation. With further LV adverse remodelling there is further LV dilatation and compromise of RV function within the confines of a single pericardial chamber. There was no statistical difference in tricuspid regurgitation between the two groups over time and the right ventricle size did not change markedly over the duration of the study. However, RV function worsened significantly in the CRV group compared with the control group, which is consistent with metoprolol treatment in patients with degenerative mitral regurgitation.[34]

Since RV dysfunction in patients with CPMR is associated with impaired cardiovascular outcomes,[35] it is concerning that patients treated with carvedilol had significant worsening of RV function during the course of the study without an obvious increase in echocardiographic-estimated pulmonary artery pressure. Although RV function was only assessed using tricuspid annular plane systolic excursion (TAPSE) and tissue Doppler S', these relatively simple measures have been validated and been shown to be useful in predicting mortality in patients undergoing valve surgery.[36]

In terms of the serum tests, the serum marker of apoptosis was increased in patients treated with carvedilol compared with controls. Previous studies in peripartum cardiomyopathy and dilated cardiomyopathy have demonstrated that serum Fas levels correlate with LV dysfunction.[26,37] There were no other significant differences between the two groups with respect to the markers of inflammation (TNF-α, IL-1 and IL-6) or ST2 and its ligand IL-33. Although circulating levels of cytokines are increased in patients with heart failure, cardiomyopathies and volume overload,[6,26,38] use of carvedilol in the current study to treat

CPMR did not significantly reduce serum markers of inflammation. This may be due to the lack of effect of carvedilol on the myocardial and systemic inflammatory state in these patients, implying a lack of drug effect, or that these tests are not sensitive enough to quantify a significant drug effect.

Serum ST2 levels were measured because previous studies have found it to be a useful marker in patients with heart failure.[15] Since the IL-33/ST2 system may be important in the pathophysiology of myocardial fibrosis,[39] these two proteins were included in the serum panel in this study. However, measurable levels of IL-33 were not detected in the serum of these patients and sST2 levels decreased in both groups with no treatment effect noted. In contrast, an increase in serum BNP was noted in patients treated with carvedilol, which suggests that there is an increase in myocardial loading in patients taking carvedilol. Recent data shows that patients with CPMR, who have elevated NT-proBNP, have markedly poor prognosis.[40-42] The fact that serum levels of BNP increased in patients treated with carvedilol suggests that patients treated with this drug may possibly have worse long-term prognosis.

The extra-cellular matrix is a highly dynamic part of the myocardium that changes depending on the degree and type of mechanical stress, neurohormonal activation, inflammation and oxidative stress. These stressors result in changes in the regulatory pathways responsible for alterations in collagen deposition and degradation. MMPs and TIMPs are expressed and secreted into the extracellular space by a variety of cells including cardiac myocytes, cardiac fibroblasts and macrophages.[21] In response to different hemodynamic overloads (pressure versus volume), the ECM undergoes different patterns of remodelling.[4] For example, volume

overload results in loss of interstitial collagen,[43] whereas pressure overload increases fibrogenic factors and collagen deposition.[44,45]

Overall there are time-dependent increases and decreases in MMP activity during the evolution of LV remodelling in response to CPMR (Figure 1.3).[46,47] In animal models there is an early rise in myocardial MMP levels after the volume-loaded state is created but this seems to normalize after the acute phase.[18,48] Microarray studies in dogs with isolated MR, has shown that, at 4 months, there is down-regulation of a number of genes important in ECM structure and function with on-going activation of MMPs.[43] However, as the LV starts to dilate in dogs with chronic myxomatous mitral valve disease, MMP-9 levels decrease.[49] In time MMP activity is reduced and late in the progression of adverse LV remodelling there is an increase in perivascular collagen deposition,[47,50] which may reduce ventricular compliance and promote systolic dysfunction.[4]

In this study there was a significant increase in serum MMP-2 and the ratio of serum MMP-2/TIMP-1 in patients who were treated with carvedilol compared with patients who received no anti-remodelling therapy. However, there were no significant changes in MMP-1, MMP-9 or the remaining MMP/TIMP ratios. This is the first study to demonstrate an increase in MMP-2 in response to drug therapy in patients with CPMR and is consistent with myocardial MMP studies in some patients with heart failure[51-54] but not others.[17] Supporting the current study, Yamazaki *et al*.[55] demonstrated increased serum MMP-2 levels in patients with heart failure and George *et al*.[20] demonstrated that serum levels of MMP-2, but not MMP-9, were correlated with poor outcomes in patients with congestive heart failure. Studies in patients with ischemic heart disease[56] and aortic or aortic valve disease[57] suggest that changes in serum

MMP levels may depend on the underlying pathology. Increased levels of MMP-2 would be associated with increased ECM degradation[4] and imply that carvedilol treatment is associated with on-going ECM degradation. Although there is evidence to suggest that the myocardium is an important source of MMPs it is not possible to exclude other sources.[58,59] Activation of MMP pathways in other organs may explain the increased circulating levels of MMP-s in these patients. Supporting this hypothesis are the gene expression findings, which are detailed later. There were no significant changes in the expression of MMP genes in the carvedilol group compared with the control group. In fact, there was a non-significant down-regulation of MMP-2 in the hearts of patients treated with carvedilol. The discrepancy between the serum and tissue expression data in this study also suggest that the cause of the increased serum MMP-2 in patients treated with carvedilol is not the heart and cautions against relying on circulating MMP levels to determine drug effects in patients with CPMR.

3.5. Conclusion

This small, randomized, controlled study is the first to examine the effects of carvedilol on left ventricular remodelling in patients with severe CPMR. At baseline, patients randomized to carvedilol had slightly larger LV dimensions and volumes compared with the patients who were not treated. This suggests that the patients randomized to carvedilol were possibly at a more advanced stage of LV remodelling than the controls. However, to address the baseline differences, patients were used as their own controls to determine treatment effect. After a median follow up of 10 months, patients treated with carvedilol did not show improvements in clinical, echocardiographic or serum markers of LV remodelling. Of concern was a decrease in right ventricular function with an associated increase in serum Fas and NT-proBNP suggesting that, if anything, there was a detrimental effect of carvedilol in these patients.

Carvedilol treatment was associated with a significant increase in serum levels of MMP-2 and MMP-2/TIMP-1. Based on prior studies in patients with heart failure this finding suggests that patients in the treatment arm were disadvantaged by carvedilol therapy since levels of MMP-2 are associated with ECM degradation.

The results of the current study do not support the hypothesis that carvedilol reverses adverse remodelling in patients with CPMR. Combined with the findings described in subsequent chapters, these results suggest that patients treated with carvedilol may in fact contribute to adverse LV remodelling. Furthermore, these results support the findings of Pu *et al*.,[9] who demonstrated adverse remodelling and a reduction in survival when rats with experimental primary MR were treated with carvedilol.

3.6. References

1. Sliwa K, Mocumbi AO. Forgotten cardiovascular diseases in Africa. *Clin Res Cardiol* 2010; **99**(2): 65-74.
2. Carabello BA, Crawford FA. Valvular Heart Disease. *New England Journal of Medicine* 1997; **337**(1): 32-41.
3. Urabe Y, Mann DL, Kent RL, et al. Cellular and ventricular contractile dysfunction in experimental canine mitral regurgitation. *Circulation research* 1992; **70**(1): 131-47.
4. Hutchinson KR, Stewart JA, Jr., Lucchesi PA. Extracellular matrix remodeling during the progression of volume overload-induced heart failure. *J Mol Cell Cardiol* 2010; **48**(3): 564-9.
5. Magne J, Mahjoub H, Dulgheru R, Pibarot P, Pierard LA, Lancellotti P. Left ventricular contractile reserve in asymptomatic primary mitral regurgitation. *European heart journal* 2014; **35**(24): 1608-16.
6. Kapadia SR, Yakoob K, Nader S, Thomas JD, Mann DL, Griffin BP. Elevated circulating levels of serum tumor necrosis factor-alpha in patients with hemodynamically significant pressure and volume overload. *Journal of the American College of Cardiology* 2000; **36**(1): 208-12.
7. Jellis C, Martin J, Narula J, Marwick TH. Assessment of nonischemic myocardial fibrosis. *Journal of the American College of Cardiology* 2010; **56**(2): 89-97.
8. Barnes J, Dell'Italia LJ. The multiple mechanistic faces of a pure volume overload: implications for therapy. *Am J Med Sci* 2014; **348**(4): 337-46.
9. Pu M, Gao Z, Pu DK, Davidson WR, Jr. Effects of early, late, and long-term nonselective beta-blockade on left ventricular remodeling, function, and survival in chronic organic mitral regurgitation. *Circ Heart Fail* 2013; **6**(4): 756-62.
10. Baumgartner H, Falk V, Bax JJ, et al. 2017 ESC/EACTS Guidelines for the management of valvular heart disease. *European heart journal* 2017; **38**(36): 2739-91.
11. Lang RM, Badano LP, Mor-Avi V, et al. Recommendations for cardiac chamber quantification by echocardiography in adults: an update from the American Society of Echocardiography and the European Association of Cardiovascular Imaging. *European heart journal cardiovascular Imaging* 2015; **16**(3): 233-70.
12. Remenyi B, Wilson N, Steer A, et al. World Heart Federation criteria for echocardiographic diagnosis of rheumatic heart disease--an evidence-based guideline. *Nature reviews Cardiology* 2012; **9**(5): 297-309.
13. Rudski LG, Lai WW, Afilalo J, et al. Guidelines for the echocardiographic assessment of the right heart in adults: a report from the American Society of Echocardiography endorsed by the European Association of Echocardiography, a registered branch of the European Society of Cardiology, and the Canadian Society of Echocardiography. *Journal of the American Society of Echocardiography : official publication of the American Society of Echocardiography* 2010; **23**(7): 685-713; quiz 86-8.
14. Nishigaki K, Minatoguchi S, Seishima M, et al. Plasma Fas ligand, an inducer of apoptosis, and plasma soluble Fas, an inhibitor of apoptosis, in patients with chronic congestive heart failure. *Journal of the American College of Cardiology* 1997; **29**(6): 1214-20.
15. Mebazaa A, Di Somma S, Maisel AS, Bayes-Genis A. ST2 and multimarker testing in acute decompensated heart failure. *Am J Cardiol* 2015; **115**(7 Suppl): 38b-43b.

16. Oral H, Sivasubramanian N, Dyke DB, et al. Myocardial proinflammatory cytokine expression and left ventricular remodeling in patients with chronic mitral regurgitation. *Circulation* 2003; **107**(6): 831-7.
17. Wilson EM, Gunasinghe HR, Coker ML, et al. Plasma matrix metalloproteinase and inhibitor profiles in patients with heart failure. *J Card Fail* 2002; **8**(6): 390-8.
18. Nagatomo Y, Carabello BA, Coker ML, et al. Differential effects of pressure or volume overload on myocardial MMP levels and inhibitory control. *Am J Physiol Heart Circ Physiol* 2000; **278**(1): H151-61.
19. Januzzi JL, Troughton R. Are Serial BNP Measurements Useful in Heart Failure Management?: Serial Natriuretic Peptide Measurements Are Useful in Heart Failure Management. *Circulation* 2013; **127**(4): 500-8.
20. George J, Patal S, Wexler D, Roth A, Sheps D, Keren G. Circulating matrix metalloproteinase-2 but not matrix metalloproteinase-3, matrix metalloproteinase-9, or tissue inhibitor of metalloproteinase-1 predicts outcome in patients with congestive heart failure. *Am Heart J* 2005; **150**(3): 484-7.
21. Spinale FG. Myocardial matrix remodeling and the matrix metalloproteinases: influence on cardiac form and function. *Physiol Rev* 2007; **87**(4): 1285-342.
22. Buralli S, Dini FL, Ballo P, et al. Circulating matrix metalloproteinase-3 and metalloproteinase-9 and tissue Doppler measures of diastolic dysfunction to risk stratify patients with systolic heart failure. *Am J Cardiol* 2010; **105**(6): 853-6.
23. Anand IS, Latini R, Florea VG, et al. C-Reactive Protein in Heart Failure: Prognostic Value and the Effect of Valsartan. *Circulation* 2005; **112**(10): 1428-34.
24. Wang BW, Hung HF, Chang H, Kuan P, Shyu KG. Mechanical stretch enhances the expression of resistin gene in cultured cardiomyocytes via tumor necrosis factor-alpha. *Am J Physiol Heart Circ Physiol* 2007; **293**(4): H2305-12.
25. Chen Y, Pat B, Zheng J, et al. Tumor necrosis factor-alpha produced in cardiomyocytes mediates a predominant myocardial inflammatory response to stretch in early volume overload. *J Mol Cell Cardiol* 2010; **49**(1): 70-8.
26. Sliwa K, Skudicky D, Bergemann A, Candy G, Puren A, Sareli P. Peripartum cardiomyopathy: analysis of clinical outcome, left ventricular function, plasma levels of cytokines and Fas/APO-1. *Journal of the American College of Cardiology* 2000; **35**(3): 701-5.
27. Ahmed MI, Aban I, Lloyd SG, et al. A Randomized Controlled Phase IIb Trial of Beta1-Receptor Blockade for Chronic Degenerative Mitral Regurgitation. *Journal of the American College of Cardiology* 2012; **60**(9): 833-8.
28. Zheng J, Yancey DM, Ahmed MI, et al. Increased Sarcolipin Expression and Adrenergic Drive in Humans With Preserved Left Ventricular Ejection Fraction and Chronic Isolated Mitral Regurgitation. *Circulation: Heart Failure* 2014; **7**(1): 194-202.
29. Stewart RA, Raffel OC, Kerr AJ, et al. Pilot study to assess the influence of beta-blockade on mitral regurgitant volume and left ventricular work in degenerative mitral valve disease. *Circulation* 2008; **118**(10): 1041-6.
30. Naveiro-Rilo JC, Diez-Juarez DM, Romero Blanco A, Rebollo-Gutierrez F, Rodriguez-Martinez A, Rodriguez-Garcia MA. Validation of the Minnesota living with heart failure questionnaire in primary care. *Rev Esp Cardiol* 2010; **63**(12): 1419-27.
31. Ennis DB, Rudd-Barnard GR, Li B, et al. Changes in mitral annular geometry and dynamics with ss-blockade in patients with degenerative mitral valve disease. *Circ Cardiovasc Imaging* 2010; **3**(6): 687-93.

32. Klima U, Guerrero JL, Vlahakes GJ. Contribution of the interventricular septum to maximal right ventricular function. *Eur J Cardiothorac Surg* 1998; **14**(3): 250-5.
33. Hess OM, Bhargava V, Ross J, Jr., Shabetai R. The role of the pericardium in interactions between the cardiac chambers. *Am Heart J* 1983; **106**(6): 1377-83.
34. Hongning Y, Stewart RA, Whalley GA. The impact of beta-blockade on right ventricular function in mitral regurgitation. *Heart Lung Circ* 2014; **23**(4): 378-80.
35. Le Tourneau T, Deswarte G, Lamblin N, et al. Right ventricular systolic function in organic mitral regurgitation: impact of biventricular impairment. *Circulation* 2013; **127**(15): 1597-608.
36. Sun X, Zhang H, Aike B, et al. Tricuspid annular plane systolic excursion (TAPSE) can predict the outcome of isolated tricuspid valve surgery in patients with previous cardiac surgery? *J Thorac Dis* 2016; **8**(3): 369-74.
37. Skudicky D, Sliwa K, Bergemann A, Candy G, Sareli P. Reduction in Fas/APO-1 plasma concentrations correlates with improvement in left ventricular function in patients with idiopathic dilated cardiomyopathy treated with pentoxifylline. *Heart* 2000; **84**(4): 438-9.
38. Levine B, Kalman J, Mayer L, Fillit HM, Packer M. Elevated circulating levels of tumor necrosis factor in severe chronic heart failure. *N Engl J Med* 1990; **323**(4): 236-41.
39. Kakkar R, Lee RT. The IL-33/ST2 pathway: therapeutic target and novel biomarker. *Nat Rev Drug Discov* 2008; **7**(10): 827-40.
40. Clavel MA, Tribouilloy C, Vanoverschelde JL, et al. Association of B-Type Natriuretic Peptide With Survival in Patients With Degenerative Mitral Regurgitation. *Journal of the American College of Cardiology* 2016; **68**(12): 1297-307.
41. Sinha SK, Garg S, Thakur R, et al. Prognostic Importance of Exercise Brain Natriuretic Peptide in Asymptomatic Chronic Organic Severe Mitral Regurgitation: An Observational Study. *J Clin Med Res* 2016; **8**(11): 797-804.
42. Park SJ, Cho EJ, Ahn J, et al. Additive prognostic values of NT-proBNP and exercise stress echocardiography in asymptomatic patients with degenerative mitral regurgitation and preserved left ventricular ejection fraction. *Int J Cardiol* 2017; **236**: 387-92.
43. Zheng J, Chen Y, Pat B, et al. Microarray identifies extensive downregulation of noncollagen extracellular matrix and profibrotic growth factor genes in chronic isolated mitral regurgitation in the dog. *Circulation* 2009; **119**(15): 2086-95.
44. Zhang YM, Bo J, Taffet GE, et al. Targeted deletion of ROCK1 protects the heart against pressure overload by inhibiting reactive fibrosis. *Faseb j* 2006; **20**(7): 916-25.
45. Bloor CM, Nimmo L, McKirnan MD, Zhang Y, White FC. Increased gene expression of plasminogen activators and inhibitors in left ventricular hypertrophy. *Mol Cell Biochem* 1997; **176**(1-2): 265-71.
46. Stewart JA, Jr., Wei CC, Brower GL, et al. Cardiac mast cell- and chymase-mediated matrix metalloproteinase activity and left ventricular remodeling in mitral regurgitation in the dog. *J Mol Cell Cardiol* 2003; **35**(3): 311-9.
47. Chen YW, Pat B, Gladden JD, et al. Dynamic molecular and histopathological changes in the extracellular matrix and inflammation in the transition to heart failure in isolated volume overload. *Am J Physiol Heart Circ Physiol* 2011; **300**(6): H2251-60.
48. Chancey AL, Brower GL, Peterson JT, Janicki JS. Effects of matrix metalloproteinase inhibition on ventricular remodeling due to volume overload. *Circulation* 2002; **105**(16): 1983-8.

49. Ljungvall I, Rajamaki MM, Crosara S, et al. Evaluation of plasma activity of matrix metalloproteinase-2 and -9 in dogs with myxomatous mitral valve disease. *Am J Vet Res* 2011; **72**(8): 1022-8.
50. Janicki JS, Brower GL, Gardner JD, et al. Cardiac mast cell regulation of matrix metalloproteinase-related ventricular remodeling in chronic pressure or volume overload. *Cardiovasc Res* 2006; **69**(3): 657-65.
51. Coker ML, Jolly JR, Joffs C, et al. Matrix metalloproteinase expression and activity in isolated myocytes after neurohormonal stimulation. *Am J Physiol Heart Circ Physiol* 2001; **281**(2): H543-51.
52. Spinale FG, Coker ML, Heung LJ, et al. A matrix metalloproteinase induction/activation system exists in the human left ventricular myocardium and is upregulated in heart failure. *Circulation* 2000; **102**(16): 1944-9.
53. Thomas CV, Coker ML, Zellner JL, Handy JR, Crumbley AJ, 3rd, Spinale FG. Increased matrix metalloproteinase activity and selective upregulation in LV myocardium from patients with end-stage dilated cardiomyopathy. *Circulation* 1998; **97**(17): 1708-15.
54. Li YY, Feldman AM, Sun Y, McTiernan CF. Differential expression of tissue inhibitors of metalloproteinases in the failing human heart. *Circulation* 1998; **98**(17): 1728-34.
55. Yamazaki T, Lee JD, Shimizu H, Uzui H, Ueda T. Circulating matrix metalloproteinase-2 is elevated in patients with congestive heart failure. *European journal of heart failure* 2004; **6**(1): 41-5.
56. Hojo Y, Ikeda U, Ueno S, Arakawa H, Shimada K. Expression of matrix metalloproteinases in patients with acute myocardial infarction. *Japanese circulation journal* 2001; **65**(2): 71-5.
57. Wilton E, Bland M, Thompson M, Jahangiri M. Matrix metalloproteinase expression in the ascending aorta and aortic valve. *Interactive cardiovascular and thoracic surgery* 2008; **7**(1): 37-40.
58. Joffs C, Gunasinghe HR, Multani MM, et al. Cardiopulmonary bypass induces the synthesis and release of matrix metalloproteinases. *The Annals of thoracic surgery* 2001; **71**(5): 1518-23.
59. Vorovich EE, Chuai S, Li M, et al. Comparison of matrix metalloproteinase 9 and brain natriuretic peptide as clinical biomarkers in chronic heart failure. *Am Heart J* 2008; **155**(6): 992-7.

Chapter 4

Gene expression changes in patients with chronic primary mitral regurgitation compared with normal hearts.

4.1. Introduction

Chronic primary mitral regurgitation (CPMR) is caused by a progressive abnormality of the mitral valve apparatus predominantly related to degenerative disease in developed countries and rheumatic heart disease in developing countries, where it remains the most common form of acquired cardiovascular disease in children and adults.[1,2] At present, there is no medical therapy that effectively improves adverse left ventricular remodelling or outcomes in patients with CPMR.[3,4]

Patients with CPMR are often asymptomatic for many years while the left ventricle (LV) progressively dilates in response to abnormal preload. The eccentric hypertrophy that develops normalizes afterload leading to a period of so-called 'compensation'. However, due to inadequate protein synthesis and progressive deterioration in myocardial function, the hypertrophy that develops is insufficient to fully compensate for the wall stress.[5] This leads to persistent neurohormonal activation and reactive oxygen species generation. These chronic stressors activate a number of complex inflammatory and apoptotic pathways in a similar manner to heart failure from other causes. Early in the LV remodelling process there is loss of interstitial collagen and cell slippage caused by disruption of the myocardial extracellular matrix (ECM). Later changes include myocyte apoptosis and pathological ECM fibrosis.[6] As a result, chronic decompensated MR ensues, and the LV resembles end-stage dilated cardiomyopathy.

Recent microarray gene expression data has identified changes in a number of cellular and ECM pathways in response to volume overload in animals and humans.[7] Adrenergic drive, in particular, is increased both early and late in the evolution of volume overload supporting β-

adrenergic receptor blockade for CPMR.[8-13] Only one previous study has determined changes in molecular remodelling pathways in patients with CPMR. Zheng *et al*.[13] performed microarrays from LV tissue of 35 patients taken at the time of mitral valve surgery compared with 13 normal cadaver controls. Sixteen of the 35 CPMR patients in their cohort had a history of hypertension and 17 patients had a history of anti-remodelling therapy use. They identified significant up-regulation of pathways involved in β-adrenergic and β-adrenergic second messenger signalling and down-regulation in a number of inflammation pathways. This work has not since been repeated and it would be interesting to confirm these findings in predominantly black African patients and, in particular, in patients with advanced LV remodelling. Furthermore, considering that patients with hypertension were included in the previous study,[13] assessment of the expression of multiple genes in a cohort of patients with pure volume overload due to CPMR has not yet been reported. Therefore, a comparison of gene expression in several pathways previously found to be important in LV remodelling in response to volume overload was carried out in the patients recruited to this study. These were compared with gene expression in tissue from commercially available normal cadaver hearts and this comparison forms the basis for this chapter.

4.2. Methods

Details of the methods and materials are described in Chapter 2.

4.2.1. Study subjects

The investigation conforms to the principles outlined in the Declaration of Helsinki. Informed consent was obtained from all patients according to a protocol approved by the Human Research Ethics Committee of the University of the Witwatersrand (M101036). Patients were included in the study if they had CPMR and met guideline criteria for elective mitral valve surgery.[3,4] Patients were excluded if they had aortic valve disease, mitral stenosis, active infective endocarditis, co-morbid coronary artery disease, chronic kidney disease, contraindications to β-blocker therapy, were pregnant, or had a history of anti-remodelling therapy use (β-blockers, angiotensin converting enzyme (ACE) inhibitors, angiotensin receptor blockers or mineralocorticoid receptor antagonists).

Patients underwent baseline clinical examination, transthoracic echocardiography, blood analysis and cardiac catheterization, during which LV endomyocardial biopsies (EMB) were obtained using disposable 2.2mm x 105cm Jawz® Endomyocardial Biopsy Forceps (Argon Medical, Tx, USA). Several (3-5) biopsy specimens were taken from the middle third of the LV. EMB specimens were frozen in liquid nitrogen for gene expression analysis and collected in 10% buffered formalin for histopathology. The frozen specimens were then stored at -80º. Endomyocardial sampling was confirmed by light microscopy.

4.2.2. RNA isolation

Patient RNA was extracted using the miRNeasy Mini Kit® (Qiagen Sciences, MD, USA). RNA was quantified using spectrophotometric analysis on a NanoDrop ND-2000 Spectrophotometer (NanoDrop Technologies Inc., Wilmington, Del.) and RNA integrity determined using an Agilent 2100 Bioanalyzer (Agilent Technologies, CA, USA). For comparison of gene expression levels in heart tissue from CPMR patients (n=13) with gene expression levels in normal heart tissue, total heart RNA (from five cadavers with no history of cardiac disease) was purchased commercially (one 23-year old female and 4 males between the ages of 24 and 39).

4.2.3. Gene selection

The nCounter® Custom Codeset included 109 candidate genes and 6 reference genes as well as 6 positive and 8 negative controls. Candidate genes were selected based on previous gene expression studies in animals and humans with heart failure, volume overload and CPMR.[13-16] Most of the genes had previously been found to be significantly up/down-regulated in animal or human subjects with CPMR or models of volume overload. Additional genes known to be directly involved in β-receptor signalling, ECM remodelling, cell survival, apoptosis, inflammatory and fibrosis pathways were also selected.[17] The six reference genes were previously shown to be stably expressed with a large dynamic range of expression levels in cardiac tissue. The selection process for these genes is detailed in section 2.6.6.3 (Appendix 10).

4.2.4. Gene expression analysis

Multiplex gene expression analysis, using 100ng total RNA per sample, was performed commercially by NanoString (Seattle, USA) using an nCounter® Custom Codeset. Results were analysed using the NanoString nSolver Analysis Software Package 3.0®. A background subtraction using the geometric mean of the negative controls was included and gene expression levels were normalised to both the geometric mean of the positive controls and the geometric mean of three reference genes (*GAPDH, PGK1* and *HPRT1*). The additional reference genes were excluded from the analysis because of high variation in expression levels between samples (*SDHA* and *STR*) and expression levels at or below background levels (*RPLPO*). Eight candidate genes (*ADRB3, FasLG, IL1B, IL10, MMP-1, MMP-13, PDCD1* and *SAG*) were expressed at levels at or below that of the negative controls and thus were also excluded from the analysis. Normalised counts were used to generate ratio data, 95% confidence intervals (CIs) and false discovery rates (FDRs) for all genes comparing CPMR patients at baseline to the normal heart controls.

4.2.5. Statistical analysis

The gene expression pattern of the panel of 109 genes in the CPMR patients at baseline was compared with that from normal heart tissue. Two methods were used to validate that the changes that were found were indeed true and not by chance. Firstly, the fold-changes in gene expression in the patients with CPMR (compared with normal controls) were compared with previous findings.[13] Secondly, online bioinformatics tools were used. Differentially expressed genes were assigned to significantly enriched Gene Ontology (GO) processes using the online bioinformatics tool WebGestalt (WEB-based Gene SeT AnaLysis Toolket) (http://www.webgestalt.org).[18] Using WebGestalt, it was possible to associate genes with

individual disease and drug terms using GLAD4U.[19] The results obtained by WebGestalt were confirmed by DAVID 6.8 (https://david.ncifcrf.gov)[20] and STRING 10.5 (https://string-db.org) both consulted in January 2018. The P value provides an estimate of the probability that a given enrichment is present by chance alone and are derived using corrections for multiple comparisons (Benjamini and Hochberg false discovery rates).

4.3. Results

Appendix 12 lists the fold changes in expression of genes in the CPMR patients versus the normal patients, while the heat map in Figure 4.1 and the schematic in Figure 4.2 highlights significant gene expression level changes between CPMR and normal hearts. The β_1-adrenergic receptor (*ADRB1*) was significantly down-regulated with significant activation of *ADRBK2/GRK3*. There was also down-regulation of genes involved in cell survival (*ATF3/CREB, ARRB2, FOS, JUN, MAPK1, NR4A1* and *PIM1*) and activation of pro-apoptotic *CASP10* in the CPMR patients. Significant down-regulation of *AGTR1, SERCA2 (ATP2A2), DUSP1, HSPA1A, IL-6* and *TGFBR2* genes were noted in patients with CPMR. Overall there was up-regulation of a number of genes involved in ECM structure and regulation (*LTBP2, LTBP4, LUM* and *MMP23*) with a trend towards significant up-regulation of *CTGF, MTN* and *POSTN*. In addition, there was significant down-regulation of *EMILIN2* and *PAI-1*.

Of the abnormally regulated genes, GO analysis using DAVID revealed an enrichment of genes coding for several important molecular functions including receptor binding (GO:0005102; 15 genes; adjusted $p = 9.20 \times 10^{-7}$), G-protein coupled receptor binding genes (6 genes; adjusted $p = 9.59 \times 10^{-5}$) and cytokine receptor binding (8 genes; adjusted $p = 9.20 \times 10^{-7}$) (Appendix 13 Figure 1A). This suggests that the changes in gene expression found between normal hearts and CPMR patients was not by chance, but that there were indeed pathological changes in several molecular processes due to changes in the genes listed in Appendix 13 Figure 1A. Only the genes related to "receptor binding" are listed as an illustration.

Further GO analysis revealed an enrichment of genes important in a number of biological processes such as "response to hormone stimulus" (GO:0009725; 15 genes; $p = 9.21 \times 10^{-9}$) (Appendix 13 Figure 1B). Finally, GO analysis revealed an enrichment of genes coding for collagen and non-collagen ECM proteins (GO:0044421; 18 genes; adjusted $p = 1.87 \times 10^{-11}$) (Appendix 13 1C). Furthermore, differentially expressed genes were highly significantly linked to vascular and heart diseases (Appendix 13 Figure 1D), which further suggests that the changes in the expression of the individual genes is related to cardiovascular pathology rather than another pathology or chance. For example, in Appendix 13 Figure 1D, the simultaneous abnormal regulation of *MMP9*¸*AGTR1*, *ATP2A2 CCL2*, *IL6, SLN*, *ADRB1*, *TIMP4*, *NPPB* and *NPPC*, is strongly linked to "Heart Disease" ($p = 3.02 \times 10^{-11}$).

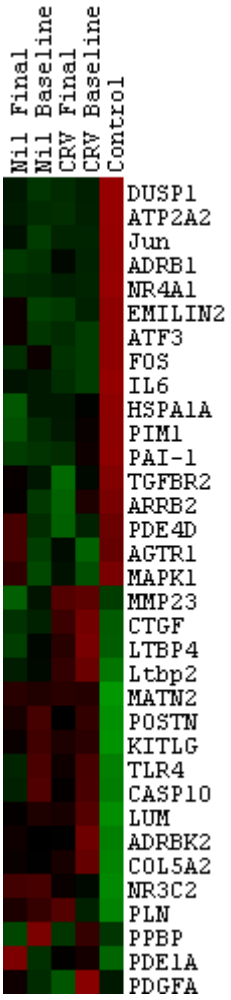

Figure 4.1. Heat map highlighting significant changes in expression levels of several genes important in left ventricular remodelling in normal heart tissue (Control), patients with CPMR at Baseline and Final (after treatment with carvedilol). Note, for this chapter, only the "Baseline" results are relevant. The "Final" results pertain to Chapter 5. Red indicates significant upregulation; green indicates significant down-regulation in relation to housekeeping genes. Colour brightness corresponds with degree of deviation from normal gene expression. For example, *DUSP1* expression levels are elevated in normal hearts, whereas levels are decreased in CPMR hearts (and this remains so regardless of treatment allocation or subsequent treatment with carvedilol). In comparison, *POSTN* expression is higher in CPMR patients than in normal hearts. Comparing "Final" to "Baseline" gene expression levels in response to treatment allocation, there were no significant changes in the expression of these genes in response to carvedilol therapy except in the case of *PDE4D, PDE1A,PDGFA, ARRB2* and *PLN*. Changes in response to carvedilol therapy are discussed in Chapter 5.

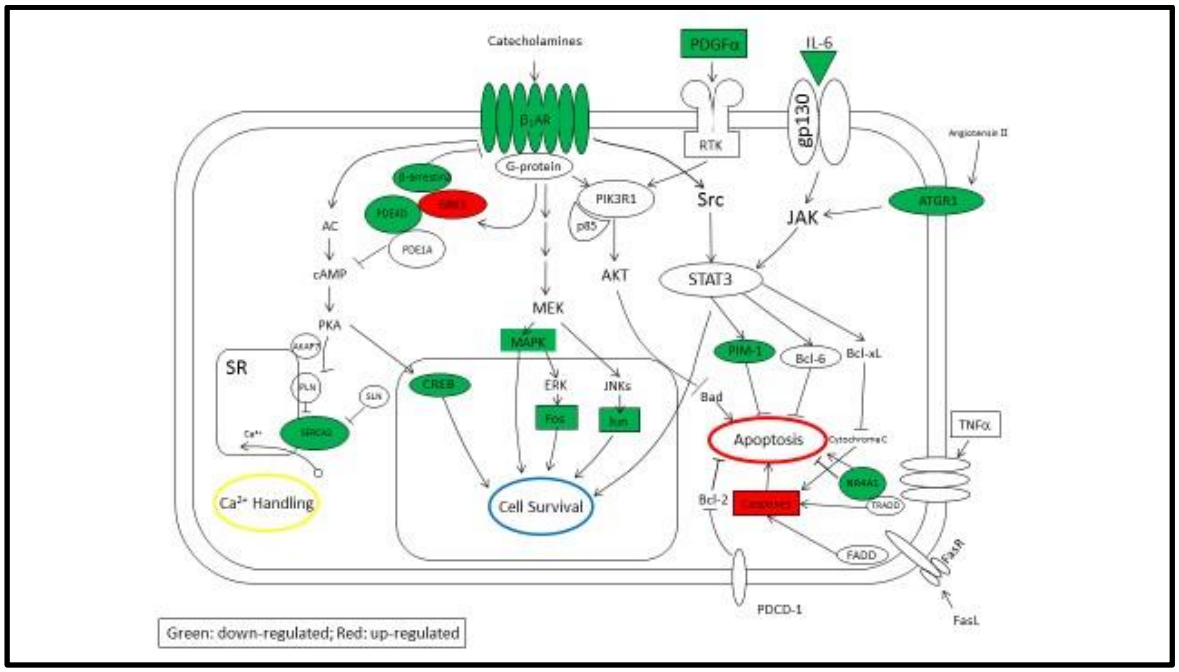

Figure 4.2. Schematic highlighting significant changes in gene expression levels in patients with severe CPMR compared with normal hearts in the current study. Green=down-regulated; Red=upregulated. The β-adrenergic receptor-1 (β_1-AR) was significantly down-regulated associated with compensatory up-regulation of β-adrenergic receptor kinase-2 (GRK3). Significant down-regulation of gene products important in calcium handling, cell survival and apoptosis are highlighted. Gene products included in the study but with no significant expression change are also included in the figure (no colour). CPMR=chronic primary mitral regurgitation; RTK=receptor tyrosine kinase; SR=sarcoplasmic reticulum; p85=PIK3R1. Adapted from Amanfu & Saucerman.[21]

Further supporting the validity of the changes in gene expression in the CPMR patients is found in the data of Zheng *et al*.[13] (Appendix 14). The results in the current study were in overall agreement with their observations; gene expression levels changes followed a similar pattern in both studies. However, the exact level of differential expression between our study and the published results might be explained by slight differences in disease status in the patients recruited in the two studies. Exceptions included a lack of significant change in expression levels of *AKAP7, PRDX3*, *CORIN* and *PDE1A*. Nevertheless, these similar findings are important from two perspectives. Firstly, it supports the findings of Zheng *et al*.[13] and, secondly, indicates that the fold changes found for the current study patients are unlikely due to chance (i.e. acts as validation for the gene expression results in the current

study) and implies that the fold changes in the other genes (not selected from Zheng *et al*.[13]) are likely to be valid.

4.4. Discussion

4.4.1. Animal models of mitral regurgitation versus human CPMR

A number of genes were selected from animal studies.[14,15] However, there is clearly a lack of consistency in the direction of regulation (up/down) of the genes in the different experimental subjects. Table 4.1 compares the fold changes in genes expression between the dog experiments of Zheng *et al*.[14] and the human data performed by the same group (Louis J Dell'Italia laboratory).[13] Although common genes and pathways were significantly up/down-regulated due to MR, there are several examples where the direction of the fold change was opposite in the animal experiment versus the human analysis. For example, *ATF3* (or CREB protein), an important signal transduction protein involved in cell survival and growth pathways (Figure 4.2), was up-regulated 2.58 fold in 4 dogs after 4 months of MR[14] whereas in 35 patients with primary MR at the time of surgery *ATF3* was down-regulated 3.27 fold.[13] Similarly *PDE4D* was up-regulated in the dogs but down-regulated in the humans. In contrast, *CTGF*, an important protein in ECM regulation and cell adhesion, was down-regulated 1.56 fold in dogs but found to be up-regulated in humans by 2.28 fold.

Of the 47 genes selected for this study that had previously been examined in both the human and animal studies[13-15] there was only a correlation (same direction of regulation) in 17 of these genes (Appendix 15). This is in stark contrast to the correlation between the two human studies (this study and the study of Zheng *et al*.[13]), where there is a strong correlation between the results of the two human studies in terms of direction and magnitude of gene expression fold changes versus normal controls, except for the lack of change in expression levels of *AKAP7, PRDX3, CORIN* and *PDE1A*.

In addition, there was also a lack of correlation between the two animal studies.[14,15] For example, *CTGF* was significantly up-regulated in the two human studies and up-regulated in rats with aorto-caval (ACF)-induced volume overload at 15 weeks,[15] but this gene was significantly down-regulated in the dog model of CPMR.[14]

Table 4.1 Comparison of results from dogs and humans with MR from Dell'Italia research group.

Gene	Fold change in dogs[14]	Fold changes in humans[13]	Correlation between studies?
ANF	3,74	21,87	Yes
ATF3	2,58	-3,27	No
ATP2A2	down (no value given)	No result given	
C1QA	-1,89	No result given	
COL5A2	-1,6	No result given	
CSF1R	-3,76	No result given	
CTGF	-1,56	2,28	No
CXCR4	1,75	No result given	
DCN	-1,8	No result given	
FBLN1	-1,78	No result given	
FBN1	-1,79	No result given	
ICAM1	-2,65	No result given	
ITGAV	-1,6	No result given	
KITLG	1,93	No result given	
LUM	-1,63	No result given	
Ltbp2	-1,87	No result given	
MMP1	5,14	No result given	
MMP9	10,13	No result given	
MMRN1	-6,14	No result given	
NPPB	3,68	5,13	Yes
PAI-1	-2,99	No result given	
PDE4D	2	-2,64	No
PPBP	13,03	No result given	
SELL	6,1	No result given	
SELP	3,96	No result given	
TGFB2	-1,68	No result given	
TGFB3	-1,52	No result given	
THBS1	-2,41	-2,18	Yes
TLR4	-1,77	No result given	
VCAN	-1,67	No result given	
VTN	-2,19	No result given	

Therefore, whether the animal models are completely representable of CPMR in humans needs further clarification.[22] Firstly, there are innate differences between humans and animals. Secondly, the volume overload in rats was due to ACF formation and not MR. Thirdly, the volume overload created in the animal models occurred suddenly (at the time of study initiation) whereas CPMR takes many years to develop in human. Lastly, there are probably time-dependent changes in the expression of various genes in the myocardium during the evolution of LV remodelling in response to volume overload. It is impossible to directly correlate 15 weeks of ACF volume overload in the rat (referred to as "chronic" volume overload) with an undetermined duration of CPMR in humans.

This suggests that it is difficult to make direct comparisons with the fold results obtained in the current human study subjects with those of the animal experiments. There are likely to be significant differences in the expression of these genes in humans compared with animals, which may be related to the type of overload (ACF versus MR) and the duration of overload (months in dogs versus years in humans). However, the genes were selected because they have been found to be markedly up/down-regulated in volume overload and MR subjects and because they are known to be involved in important signalling pathways related to β-AR signalling, apoptosis, inflammation and ECM remodelling. Therefore, changes in the expression of these genes in humans treated with a medication may lead to important conclusions.

It is important, however, to highlight that the two human studies correlated. This strengthens the findings in these patients in response to carvedilol, which is described in a later chapter.

4.4.2. Gene expression in patients with CPMR compared with normal hearts

This is the first study to compare gene expression in a cohort of patients with pure volume overload due to CPMR on no prior anti-remodelling therapy with normal hearts. One previous study has performed a similar comparison with normal hearts but included CPMR patients with a history of hypertension and anti-remodelling therapy.[13] The results of the current study were in overall agreement with their observations, genes expression levels changes followed a similar pattern in both studies (Appendix 14). However, the exact level of differential expression between our study and the published results might be explained by slight differences in disease status in the patients recruited in the two the studies.

CPMR is characterized by LV volume overload and dilatation, left atrial volume overload and dilatation, pulmonary hypertension and right ventricular pressure overload and dysfunction. It is not surprising, therefore, that an increase in the expression of atrial natriuretic factor (*ANF*) and brain natriuretic peptide (*BNP*) were found in the patients with CPMR compared with normal hearts. These results also validate the trustworthiness of the gene expression data. There was no significant change in *CORIN*, a gene that encodes the peptidase that converts pro-ANF to biologically active ANF, or in the levels of natriuretic peptide C. *ST2* ligand expression was also increased in the study patients compared with normal hearts, whereas *ST2* was down-regulated. This may indicate a regulatory response to chronic volume overload, which needs further investigation.

Expression of the β_1-adrenergic receptor (β_1-AR) (*ADRB1*) was significantly down-regulated in CPMR hearts compared with normal hearts, which compares well with previous

studies in patients with heart failure.[23,24] β_2-adrenergic receptor (*ADRB2*) expression was not found to be different between the CPMR hearts and normal hearts, also consistent with failing hearts.[23] This is the first known report of down-regulation of β_1-AR gene expression in humans with CPMR supporting previous animal data[25,26] and suggests that the patients in the current study were at a more advanced stage of decompensation than those in the Zheng *et al*. study.[13] In response to increased metabolic stress the sympathetic nervous system, via catecholamines, stimulates cardiac function via beta-adrenergic and alpha-adrenergic receptors. Recent data suggests that the predominant myocyte adrenergic receptors are the β-1 and the α-1-B, and that β-2 and β-3 adrenergic receptors are mostly absent from myocytes but are abundant on non-myocytes.[27] β_1-AR activation results in increased ionotropy, lusitropy and chronotropy via Gs/cAMP-dependent PKA activation. At the same time, there is activation of self-regulatory β-arrestin/GRK, which, if chronically activated, mediates the β-AR for internalisation and desensitization. Chronic stimulation of β_1-AR produces myocyte hypertrophy and apoptosis[28] and therefore, in order to protect against these negative effects of chronic sympathetic activation, a reduction in β_1-AR promotes survival in the face of excessive catecholamine levels. However, this leads to decreased responsiveness to β_1-AR agonists and contributes to impaired cardiac contractility.[29]

Consistent with prior findings,[30] SERCA2 (*ATP2A2*) was down-regulated in CPMR hearts, suggestive of advanced myocyte calcium dysregulation and cellular dysfunction.[31] Further evidence of abnormal beta-adrenergic signalling, and confirming previous findings,[13] was the significant down-regulation of *PDE4D* in patients with CPMR. PDE4D is responsible for activation of PKA-mediated β-AR desensitization and deficiency results in a reduction in β_1-AR signalling, increasing the risk for heart failure and cardiac arrhythmias.[32] The

phosphodiesterases (PDEs) comprise a large group of genes divided into eleven families and are thought to control cAMP levels resulting in localized cAMP gradients within the cytoplasm, which control the activity of, among other proteins, protein kinase A (PKA).[33,34] In the heart, PDE4D has been identified as possibly the most important regulator of cAMP in cardiac myocytes and is responsible for signalling complexes involving β-AR, β-arrestin, PKA and A-kinase anchoring proteins (AKAPs).[32,35] Complexing of PDE4D with AKAP and PKA results in the activation of calcium release from the sarcoplasmic reticulum for excitation-contraction coupling by the ryanodine receptor. PDE4D is also responsible for activation of PKA-mediated β-AR desensitization.

Activation of different β-adrenergic receptors (β_1 versus β_2 for example) by β-AR agonists results in recruitment of different PDE signalling complexes. In particular, β_1-AR activation initiates PDE4D variant 8, whereas binding of β_2-AR by a β-AR agonist triggers PDE4D variant 5.[36] At rest (without β-AR agonist binding) PDE4D binds directly to β_1-AR preventing a local increase in cAMP levels under basal conditions (Figure 4.3), which protects the β_1-AR from PKA-mediated phosphorylation and desensitisation.[36] However, with β-AR -agonist binding, PDE4D no longer binds β_1-AR permitting a local increase in cAMP levels and PKA-mediated increased desensitization of β_1-AR resulting in a reduction in expression of β_1-AR. Importantly, a deficiency of PDE4D results in an increase in β_1-AR desensitization and a subsequent reduction in β_1-AR signalling and PDE4D deficiency has been identified as an important risk factor for heart failure and cardiac arrhythmias.[32]

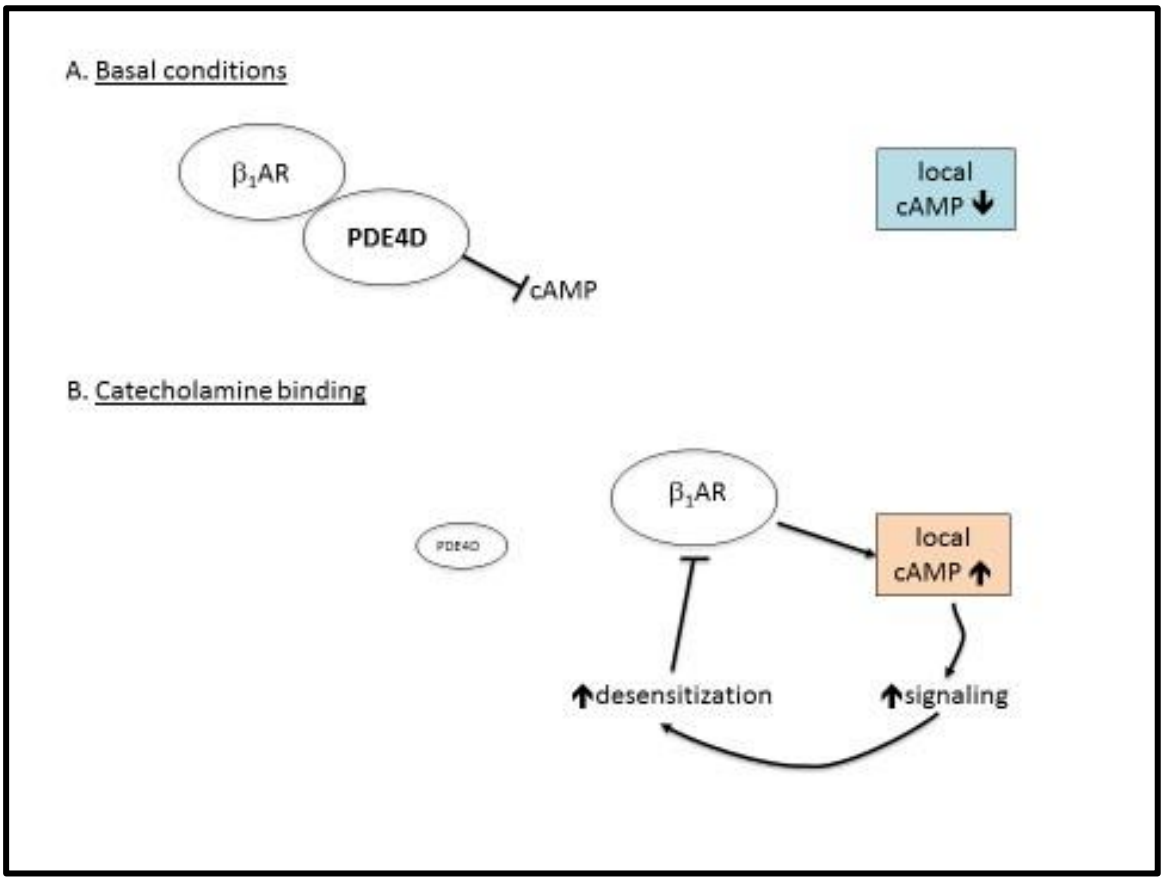

Figure 4.3. PDE4D is important in β_1-adrenergic receptor regulation and signaling. During basal conditions PDE4D binds the β_1AR inhibits cAMP resulting in low local levels of cAMP and reduced β_1AR signaling (A). However, when the β_1AR is activated by catecholamine binding then PDE4D is released permitting β_1AR activation of adenylcyclase resulting in increases in local cAMP. This permits β_1AR signaling and regulation through desensitization (B).

PDE4D down-regulation in patients with CPMR has previously been documented[13] and was confirmed in the current study. There was a 2.4 negative fold change (p=0.0146) in *PDE4D*, a negative feedback regulator of critical β-adrenergic-signalling protein PKA. These results (down-regulation of *ADRB1* and *PDE4D*) highlight that patients with CPMR are at higher risk for heart failure and arrhythmia[32] and explain, to some extent, the molecular basis of decompensation in these patients.

Overall there was a predominant down-regulation of cell survival pathway genes (*ATF3/CREB, ARRB2, FOS, JUN, MAPK1, NR4A1* and *PIM1*) and an up-regulation of apoptotic *CASP10* in patients with advanced CPMR. Significant changes in gene expression levels were also found in several other genes important in cellular signalling (*NR4A1* and *DUSP1*) for which no clear role in LV remodelling has yet been established.[37,38]

Chronic adrenergic activation in response to reduced forward stroke volume and long-standing myocyte stress activates a number of death signals resulting in cardiomyocyte apoptosis (Figure 1.4).[5,39-41] The cellular pathways involved in cell death and survival are extremely complex but several important gene products at key positions in these pathways were analysed in the current study (Figure 4.2). Consistent with previous findings in humans,[13] the pro-survival protein *ATF3* (or CREB) was significantly down-regulated in humans with CPMR. Further significant down-regulation was noted for *DUSP-1, JUN* and *FOS*. There was also significant down-regulation of *PIM-1* in the current study supporting the findings of the previous study in humans.[13] *PIM-1* is an important downstream component of AKT-induced cardioprotection.[42] *PIM-1* down-regulation increases apoptosis,[43] which supports that hypothesis that, in patients with advanced CPMR there is an increase in myocardial cell death.

Some discussion is included here on STAT3 since further study on this important second messenger is justified. STAT 1 and STAT3 are members of the signal transducer and activator of transcription (STAT) protein family. These are transcription factors predominantly activated by membrane receptor-associated Janus Kinases (JAKs). The JAK-STAT pathway plays an important role in a number of hypertrophy and cardioprotective

signals.[44] For example, mechanical cardiomyocyte stretch activates the JAK-STAT pathway via the angiotensin II receptor type 1,[45] matrix-metalloproteinase activation in response to stretch is mediated by the angiotensin II-JAK-STAT pathway[46] and stretched myocardial fibroblasts activate cardiomyocyte JAK-STAT signalling through paracrine IL-6 communication.[47]

STAT3, in particular, appears to be important in the activation of cardioprotective and anti-apoptotic genes.[48] As discussed earlier, sustained β_1-adrenergic receptor activation potentiates cardiomyocyte apoptosis and fibrosis but how this is controlled at a sub-cellular level is still unclear. Several studies demonstrate that β-ARs activate several pathways in addition to the traditional second-messenger (PKA-dependent) mechanism.[49-51] Recently, Zhang *et al*. [52] demonstrated that STAT3 is a pivotal non-second messenger transcription regulator of β_1-AR signalling and that activation of STAT3 is cardioprotective. In knockout mice the researchers were able to demonstrate increased cell death and cardiac fibrosis in response to chronic β-AR stimulation.[52] Therefore, the function of STAT3 is essential for normal β_1-AR-mediated suppression of adverse remodelling and hence STAT3, or lack thereof, is critical to the pathogenesis of heart failure (Figure 4.4).

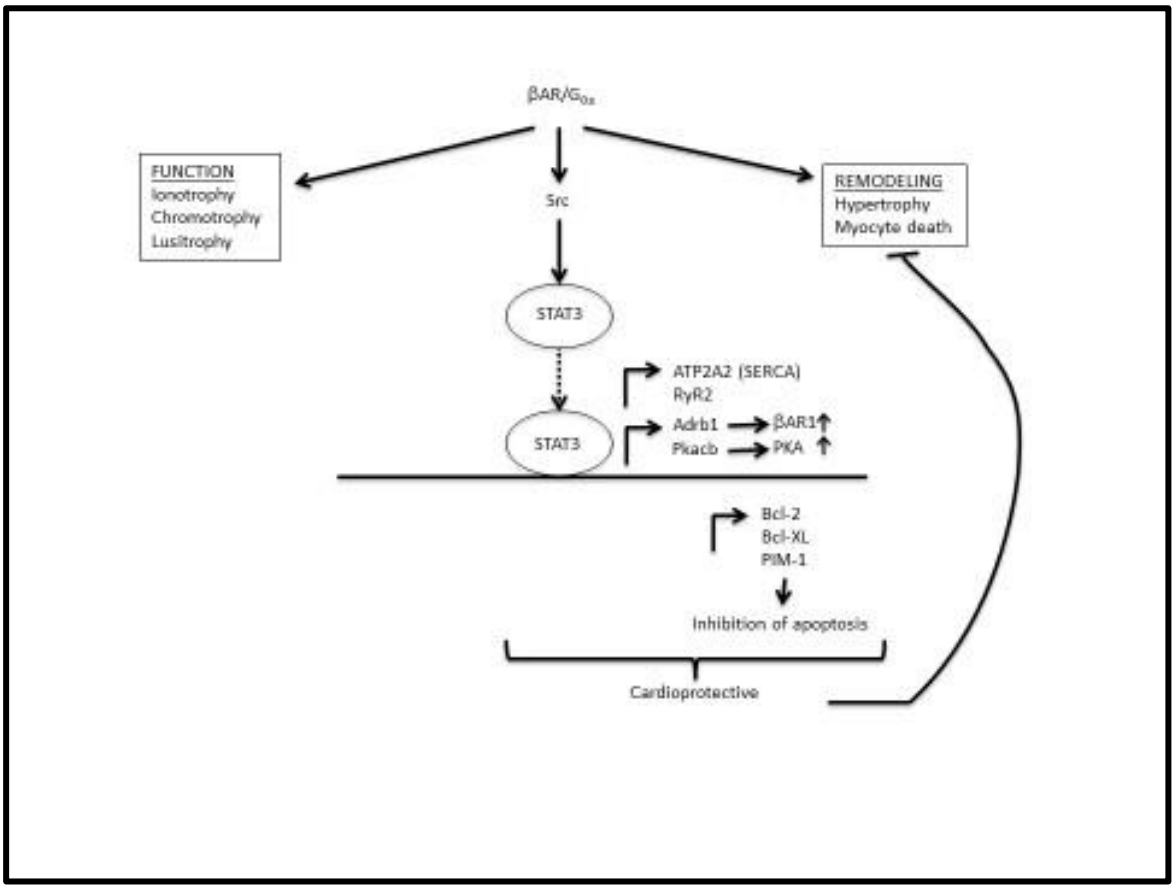

Figure 4.4. *STAT3* is activated by β_1-AR signalling resulting in the transcription of both excitation-contraction (EC) gene products such as the ryanodine receptor (*RyR2*) and *SERCA2* and non-EC genes such as the β_1-AR gene itself (*Adrb1*). Furthermore, there is an increase in a number of pro-survival genes such as *Bcl-2, Bcl-XL* and *PIM-1* promoting cell proliferation and survival. Adapted from Zhang *et al*.[52]

STAT3 has also been shown to protect hearts from the adverse effects of chronic β-AR activation[53] and low cardiac STAT3 has been described in patients with poor prognosis peri-partum cardiomyopathy.[54] In the current study, in patients with CPMR, there was also a non-significant 2.22-fold down-regulation of *STAT3*. Based on the data available, a reduction in the activation of STAT3 would imply a lack of the cardio-protective effect of this transcription factor in these patients with volume overload-induced heart failure. It could be hypothesized that down-regulation of *STAT3* would potentiate further adverse remodelling in the myocardium due to further cell loss and fibrosis. Although this result was not significant, the down-regulation by 2.22-fold of *STAT3* in the CPMR patients and the recent

data suggesting that low levels of expressed *STAT3* potentiate cell death and adverse myocardial remodelling certainly indicate that further reductions in the activation of *STAT3* would be detrimental in these patients and justify future research focused on the JAK-STAT pathway in patients with CPMR.

The negative regulator of phosphoinositide-3 kinase (PI3K), *PIK3R1* (p85) was increased by 4.07 fold in the MR patients (consistent with the 2.2 fold increase found by Zheng *et al*.[13]). The PI3K pathway controls important cellular processes such as protein synthesis, cell growth and proliferation, angiogenesis, cell cycle and survival.[55] Following activation, PI3K activates AKT via several intermediaries. AKT then regulates activation of a number of effectors involved in survival and cell growth. PIK3 is an important non-cAMP-dependent mediator of β-adrenergic receptor signalling and has been found to promote cardiomyocyte survival via AKT activation.[56] An increase in the negative regulator of PI3K, i.e. PI3KR1 (p85),[57] would reduce AKT production and subsequently reduce pro-survival signals.

Overall there is a predominant down-regulation of cell survival pathway genes and an up-regulation of apoptotic pathway genes in these patients with advanced CPMR. This supports the hypothesis that with progression of disease in patients with CPMR there is predominant cell loss and adverse left ventricular remodelling. Without intervention these patients will progress to irreversible LV dilatation and end-stage heart failure.

In the patients with CPMR there was both up- and down-regulation of genes known to be involved in inflammation (Appendix 12). Noticeably, there was a significant increase in

PPBP and *TLR4*, and a marked decreased in *IL-6*. Significant activation of *C6* and down-regulation of *IL-6* was also found by Zheng *et al*.[13] Though not statistically significant, there appeared to be an overall picture of inflammatory activation (activation of *C6, CSF1R, JAK2* and *SELP*) consistent with persistent inflammatory stress in these patients. Down-regulation of *CCL2*, which is normally cardioprotective,[58] is also consistent with on-going adverse remodelling in the myocardium of these patients. However, the cellular effects of cytokine production by cardiomyocytes are extremely complex, unpredictable and non-linear. For example, the cardio-protective or -destructive effects of TNF-α depend upon whether TNFR1 or TNFR2 activation predominates.[59] Therefore, the level of cytokine gene expression in patients with CPMR may be extremely variable depending on where the individual patient lies in the spectrum of left ventricular remodelling. This is supported by a lack of consistent benefit from TNF-α neutralization in rats with volume overload[60] or in humans with heart failure.[61]

It is difficult to completely explain the inconsistent changes identified in this study. Zheng *et al*.[13] reported extensive down-regulation of humoral immune response and cytokine signalling but an increase in complement in patients with CPMR. In the study of Chen *et al*.,[15] there was a more striking and consistent activation of inflammatory pathways with chronic volume overload. These findings support the idea that expression of inflammatory pathway proteins may be dependent on the stage of heart failure in subjects with volume overload.

Compared with normal hearts, there was a significant down-regulation of the angiotensin II receptor 1 gene (*AGTR1*). This protein is the major receptor mediating the cardiovascular effects of angiotensin II and has a number of pleiotropic effects including activation of PAI-1 (Figure 4.5) and the pro-survival *JAK-STAT* pathway in cardiomyocytes.[45,62] Previous studies have failed to show benefit with ACE-inhibitor therapy in animal models or in patients with CPMR.[63-65] The fact that *AGTR1* is down-regulated in CPMR may, to some extent, explain the lack of effect of ACE-inhibitors on LV remodelling in these patients.

The mineralocorticoid receptor *NR3C2* was up-regulated 1.59 fold (p=0.0008) consistent with the findings of Zheng *et al*.[13] How this impacts LV remodelling in CPMR is unclear but this receptor is known to be important in ECM regulation (Figure 4.5).[66]

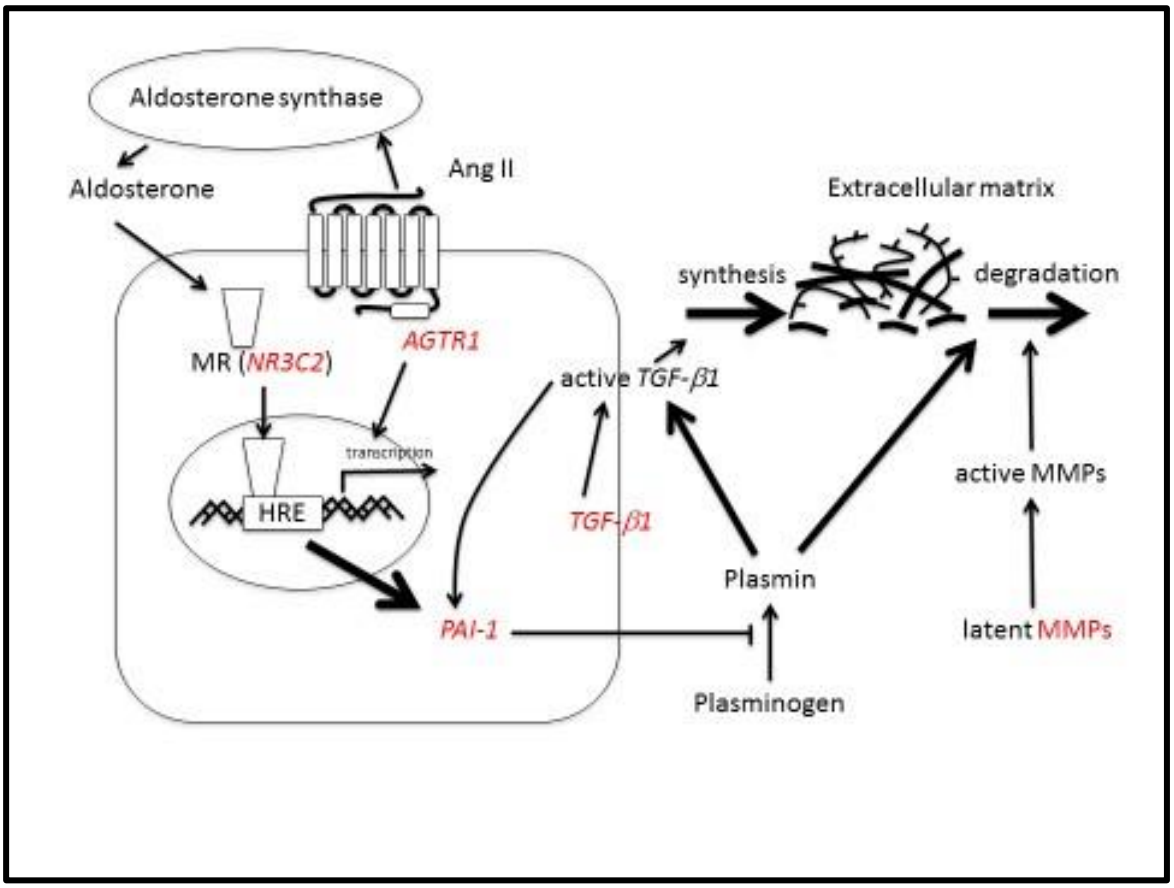

Figure 4.5. Basic relationship between renin-angiotensin-aldosterone system and extra-cellular matrix remodeling. Gene products analyzed in current study are highlighted in red. AngII= angiotensin II; MR=mineralocorticoid receptor; HRE=hormone response element; MMP=matrix metalloproteinase. Adapted from Marney & Brown.[66]

The results in the current study support the idea that these patients were at a very advanced stage of adverse LV remodelling. Many pro-fibrotic genes were activated in CPMR patients at baseline compared with normal hearts. *CTGF*, which enhances TGF-β-mediated fibrosis (Figure 4.6),[67] was 2.3-fold higher, corroborating previous studies with chronic volume overload.[13,15] Similarly, there was significant up-regulation of the latent transforming growth factors binding proteins-2 and -4, which are required for the secretion and correct folding of TGF-β and permit appropriate TGF-β interactions with the ECM.[68] Although not significant, there was also up-regulation of TGF-β itself and the TGF-β receptor-1. Increased expression of a number of ECM structural protein genes such *LUM*, *MATN2* and *POSTN* were also

noted with non-significant 2.43-fold increased expression of type 1 collagen. Increased collagen expression late in the evolution of LV remodelling is consistent with the findings of Chen *et al*.[15] who demonstrated a clear biphasic increase in collagens in rats with volume overload. Late increases in collagen expression are probably responsible for the development of pathological fibrosis in these patients. Increased ECM protein expression may reflect pathological fibrosis late in the evolution of LV remodelling.[15] Additionally, we noted down-regulation of the ECM protein *EMILIN2* and a 5.7-fold down-regulation of *PAI-1*, supporting previous findings.[13] Down-regulation of *PAI-1* in these patients suggests a predisposition towards pathological cardiac fibrosis.[69,70] Increased expression of *MMP-23* was found with no significant changes in the expression of *MMP-2* or *MMP-9*. The lack of up-regulation of *MMP-2* and *MMP-9* supports a pro-fibrotic ECM environment with little breakdown by MMPs and is consistent with prior findings in dogs with dilated hearts due to CPMR.[71]

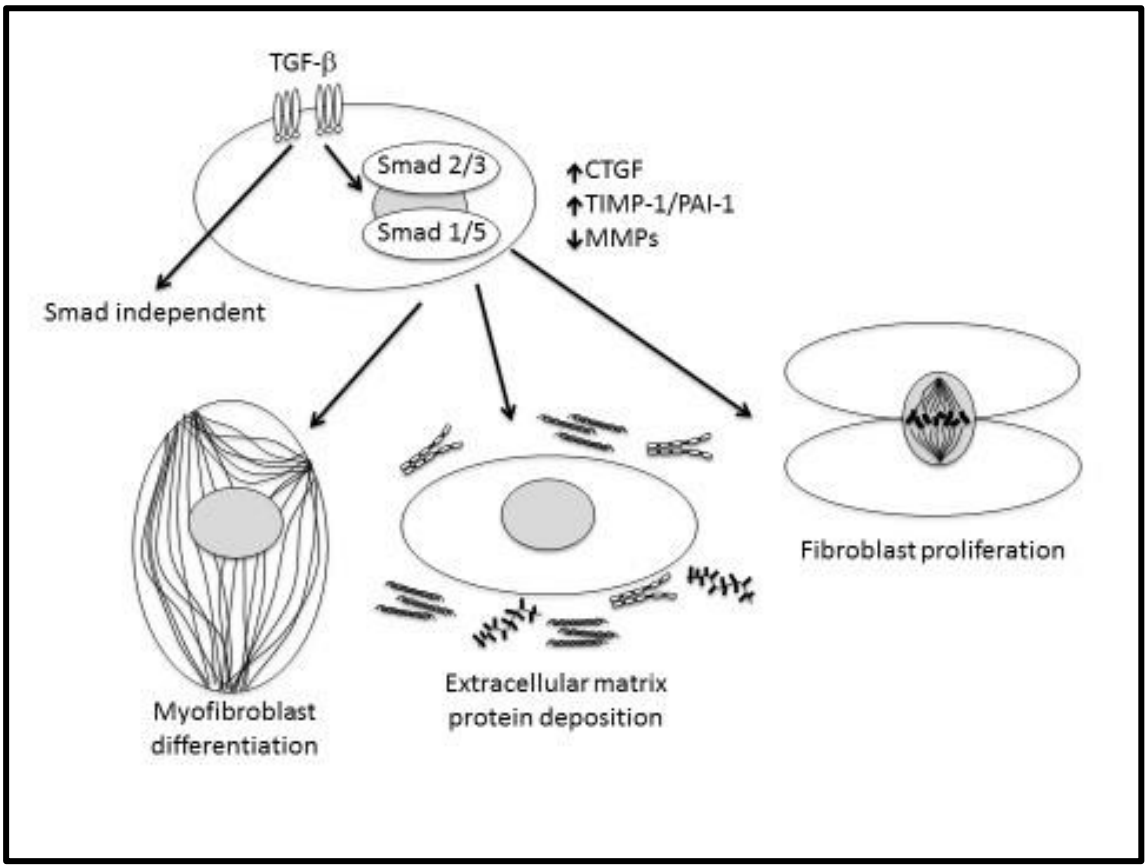

Figure 4.6. Effects of TGF-β on fibroblast phenotype and function. Adapted from Biernacka *et al*. (2011).[72]

Overall, the findings described in this chapter are consistent with a progression towards increased pathological fibrosis, abnormal ECM remodelling and decompensated cardiomyopathy in these patients with CPMR.[6]

4.5. Conclusion

Chronic primary mitral regurgitation is characterized by volume overload resulting in increased left ventricular wall stress, loss of normal interstitial fibrosis and myocyte loss. Although animal models have been particularly important in identifying molecular pathways important in the remodelling process, this study and the previous study in humans[13] highlight the differences between animal models and human patients. The current study findings correlated with the previous findings by Zheng *et al*.[13] with respect to several important genes involved in LV remodelling in patients with CPMR. However, a number of differences were noted between the two human studies and the gene expression results found in previous animal model studies. These differences may be explained by several points. Firstly, that there are innate differences between humans and animals. Secondly, different models of volume overload were used in animal experiments (for example, experimental mitral regurgitation in dogs versus creation of aorto-caval fistulae in rates). Thirdly, that volume overload in animals is created acutely compared with the slowly developing volume overload in human CPMR. Finally, that there are time-dependent changes in the expression of various genes in the myocardium during the evolution of LV remodelling in response to volume overload, which may be consistent in animals but which may be idiosyncratic in humans. These results caution against generalising animal model results to humans. The validity of the results in this study are strengthened by the correlation with the results of Zheng *et al*.[13] and the expected finding of markedly raised expression of natriuretic peptide genes in these patients.

This is the first study to clearly demonstrate a significant down-regulation in β_1-adrenergic receptor in humans with CPMR. This result is consistent with studies in patients with advanced heart failure and supports a strategy of beta-blocker therapy in patients with CPMR but this needs further investigation. There was also a significant down-regulation of the *PDE4D*, an important PKA-dependent regulatory protein. Low levels of this *PDE4D* are associated with increased risk of heart failure and cardiac arrhythmias. Furthermore, in support of previous work,[13,30] there was a significant down-regulation of *SERCA2*, which is associated with abnormal calcium handling and heart failure. This is also the first study to clearly demonstrate a significant down-regulation of the angiotensin II receptor-1 gene in patients with CPMR, which may partly explain the failure of ACE-inhibitors in the medical treatment of chronic mitral regurgitation.

Consistent with advanced adverse LV remodelling in these patients was the overall down-regulation of important pro-survival genes such as *CREB, DUSP-1, FOS, JUN, MAPK1, NR4A1* and *PIM-1* and the activation of important pro-apoptotic genes such as *Caspase-10, FAS* and *PIK3R1*. Furthermore, there was activation of several pro-inflammatory genes and various pro-fibrotic genes indicating on-going myocardial inflammatory stress and abnormal fibrosis.

These results suggest that the patients recruited to this study were at an advanced stage of adverse LV remodelling due to their chronic volume overload. The findings here are consistent with decompensated end-stage cardiomyopathic hearts. This study adds to the current understanding of the evolution of adverse LV remodelling in patients with CPMR

and, in particular, highlights several important signalling pathways that could form the basis for future research into the alterations in molecular pathways in the volume-overloaded heart.

4.6. References

1. Foster E. Clinical practice. Mitral regurgitation due to degenerative mitral-valve disease. *The New England journal of medicine* 2010; **363**(2): 156-65.
2. Sliwa K, Mocumbi AO. Forgotten cardiovascular diseases in Africa. *Clin Res Cardiol* 2010; **99**(2): 65-74.
3. Baumgartner H, Falk V, Bax JJ, et al. 2017 ESC/EACTS Guidelines for the management of valvular heart disease. *European heart journal* 2017; **38**(36): 2739-91.
4. Nishimura RA, Otto CM, Bonow RO, et al. 2017 AHA/ACC Focused Update of the 2014 AHA/ACC Guideline for the Management of Patients With Valvular Heart Disease: A Report of the American College of Cardiology/American Heart Association Task Force on Clinical Practice Guidelines. *Circulation* 2017; **135**(25): e1159-e95.
5. Urabe Y, Mann DL, Kent RL, et al. Cellular and ventricular contractile dysfunction in experimental canine mitral regurgitation. *Circulation research* 1992; **70**(1): 131-47.
6. Hutchinson KR, Stewart JA, Jr., Lucchesi PA. Extracellular matrix remodeling during the progression of volume overload-induced heart failure. *J Mol Cell Cardiol* 2010; **48**(3): 564-9.
7. Barnes J, Dell'Italia LJ. The multiple mechanistic faces of a pure volume overload: implications for therapy. *Am J Med Sci* 2014; **348**(4): 337-46.
8. Le Tourneau T, de Groote P, Millaire A, et al. Effect of mitral valve surgery on exercise capacity, ventricular ejection fraction and neurohormonal activation in patients with severe mitral regurgitation. *Journal of the American College of Cardiology* 2000; **36**(7): 2263-9.
9. Tallaj J, Wei CC, Hankes GH, et al. Beta1-adrenergic receptor blockade attenuates angiotensin II-mediated catecholamine release into the cardiac interstitium in mitral regurgitation. *Circulation* 2003; **108**(2): 225-30.
10. Hankes GH, Ardell JL, Tallaj J, et al. Beta1-adrenoceptor blockade mitigates excessive norepinephrine release into cardiac interstitium in mitral regurgitation in dog. *Am J Physiol Heart Circ Physiol* 2006; **291**(1): H147-51.
11. Nagatsu M, Zile MR, Tsutsui H, et al. Native beta-adrenergic support for left ventricular dysfunction in experimental mitral regurgitation normalizes indexes of pump and contractile function. *Circulation* 1994; **89**(2): 818-26.
12. Mehta RH, Supiano MA, Oral H, et al. Compared with control subjects, the systemic sympathetic nervous system is activated in patients with mitral regurgitation. *Am Heart J* 2003; **145**(6): 1078-85.
13. Zheng J, Yancey DM, Ahmed MI, et al. Increased Sarcolipin Expression and Adrenergic Drive in Humans With Preserved Left Ventricular Ejection Fraction and Chronic Isolated Mitral Regurgitation. *Circulation: Heart Failure* 2014; **7**(1): 194-202.
14. Zheng J, Chen Y, Pat B, et al. Microarray identifies extensive downregulation of noncollagen extracellular matrix and profibrotic growth factor genes in chronic isolated mitral regurgitation in the dog. *Circulation* 2009; **119**(15): 2086-95.
15. Chen YW, Pat B, Gladden JD, et al. Dynamic molecular and histopathological changes in the extracellular matrix and inflammation in the transition to heart failure in isolated volume overload. *Am J Physiol Heart Circ Physiol* 2011; **300**(6): H2251-60.
16. Lowes BD, Gilbert EM, Abraham WT, et al. Myocardial gene expression in dilated cardiomyopathy treated with beta-blocking agents. *The New England journal of medicine* 2002; **346**(18): 1357-65.

17. Zhang W, Qu X, Chen B, et al. Critical Roles of STAT3 in β-Adrenergic Functions in the Heart. *Circulation* 2016; **133**(1): 48-61.
18. Wang J, Duncan D, Shi Z, Zhang B. WEB-based GEne SeT AnaLysis Toolkit (WebGestalt): update 2013. *Nucleic acids research* 2013; **41**(Web Server issue): W77-83.
19. Jourquin J, Duncan D, Shi Z, Zhang B. GLAD4U: deriving and prioritizing gene lists from PubMed literature. *BMC genomics* 2012; **13 Suppl 8**: S20.
20. Dennis G, Jr., Sherman BT, Hosack DA, et al. DAVID: Database for Annotation, Visualization, and Integrated Discovery. *Genome biology* 2003; **4**(5): P3.
21. Amanfu RK, Saucerman JJ. Modeling the effects of beta1-adrenergic receptor blockers and polymorphisms on cardiac myocyte Ca2+ handling. *Mol Pharmacol* 2014; **86**(2): 222-30.
22. Houser SR, Margulies KB, Murphy AM, et al. Animal models of heart failure: a scientific statement from the American Heart Association. *Circulation research* 2012; **111**(1): 131-50.
23. Engelhardt S, Bohm M, Erdmann E, Lohse MJ. Analysis of beta-adrenergic receptor mRNA levels in human ventricular biopsy specimens by quantitative polymerase chain reactions: progressive reduction of beta 1-adrenergic receptor mRNA in heart failure. *Journal of the American College of Cardiology* 1996; **27**(1): 146-54.
24. Bristow MR, Minobe WA, Raynolds MV, et al. Reduced beta 1 receptor messenger RNA abundance in the failing human heart. *J Clin Invest* 1993; **92**(6): 2737-45.
25. Hammond HK, Roth DA, Insel PA, et al. Myocardial beta-adrenergic receptor expression and signal transduction after chronic volume-overload hypertrophy and circulatory congestion. *Circulation* 1992; **85**(1): 269-80.
26. Gealekman O, Abassi Z, Rubinstein I, Winaver J, Binah O. Role of myocardial inducible nitric oxide synthase in contractile dysfunction and beta-adrenergic hyporesponsiveness in rats with experimental volume-overload heart failure. *Circulation* 2002; **105**(2): 236-43.
27. Myagmar BE, Flynn JM, Cowley PM, et al. Adrenergic Receptors in Individual Ventricular Myocytes: The Beta-1 and Alpha-1B Are in All Cells, the Alpha-1A Is in a Subpopulation, and the Beta-2 and Beta-3 Are Mostly Absent. *Circulation research* 2017; **120**(7): 1103-15.
28. Zhu WZ, Wang SQ, Chakir K, et al. Linkage of beta1-adrenergic stimulation to apoptotic heart cell death through protein kinase A-independent activation of Ca2+/calmodulin kinase II. *J Clin Invest* 2003; **111**(5): 617-25.
29. Bristow MR, Ginsburg R, Minobe W, et al. Decreased catecholamine sensitivity and beta-adrenergic-receptor density in failing human hearts. *The New England journal of medicine* 1982; **307**(4): 205-11.
30. Leszek P, Korewicki J, Klisiewicz A, et al. Reduced myocardial expression of calcium handling protein in patients with severe chronic mitral regurgitation. *Eur J Cardiothorac Surg* 2006; **30**(5): 737-43.
31. MacLeod KT. Recent advances in understanding cardiac contractility in health and disease. *F1000Res* 2016; **5**.
32. Lehnart SE, Wehrens XH, Reiken S, et al. Phosphodiesterase 4D deficiency in the ryanodine-receptor complex promotes heart failure and arrhythmias. *Cell* 2005; **123**(1): 25-35.
33. Conti M, Richter W, Mehats C, Livera G, Park JY, Jin C. Cyclic AMP-specific PDE4 phosphodiesterases as critical components of cyclic AMP signaling. *J Biol Chem* 2003; **278**(8): 5493-6.
34. Conti M, Beavo J. Biochemistry and physiology of cyclic nucleotide phosphodiesterases: essential components in cyclic nucleotide signaling. *Annu Rev Biochem* 2007; **76**: 481-511.

35. Dodge KL, Khouangsathiene S, Kapiloff MS, et al. mAKAP assembles a protein kinase A/PDE4 phosphodiesterase cAMP signaling module. *Embo j* 2001; **20**(8): 1921-30.
36. Richter W, Day P, Agrawal R, et al. Signaling from beta1- and beta2-adrenergic receptors is defined by differential interactions with PDE4. *Embo j* 2008; **27**(2): 384-93.
37. Shen J, Zhang Y, Yu H, et al. Role of DUSP1/MKP1 in tumorigenesis, tumor progression and therapy. *Cancer Med* 2016; **5**(8): 2061-8.
38. Delgado E, Boisen MM, Laskey R, et al. High expression of orphan nuclear receptor NR4A1 in a subset of ovarian tumors with worse outcome. *Gynecologic oncology* 2016; **141**(2): 348-56.
39. Mulieri LA, Tischler MD, Martin BJ, et al. Regional differences in the force-frequency relation of human left ventricular myocardium in mitral regurgitation: implications for ventricular shape. *Am J Physiol Heart Circ Physiol* 2005; **288**(5): H2185-91.
40. Tsutsui H, Spinale FG, Nagatsu M, et al. Effects of chronic beta-adrenergic blockade on the left ventricular and cardiocyte abnormalities of chronic canine mitral regurgitation. *J Clin Invest* 1994; **93**(6): 2639-48.
41. Amin P, Singh M, Singh K. beta-Adrenergic Receptor-Stimulated Cardiac Myocyte Apoptosis: Role of beta1 Integrins. *J Signal Transduct* 2011; **2011**: 179057.
42. Muraski JA, Rota M, Misao Y, et al. Pim-1 regulates cardiomyocyte survival downstream of Akt. *Nat Med* 2007; **13**(12): 1467-75.
43. Miyamoto S, Rubio M, Sussman MA. Nuclear and mitochondrial signalling Akts in cardiomyocytes. *Cardiovasc Res* 2009; **82**(2): 272-85.
44. Wagner MA, Siddiqui MA. The JAK-STAT pathway in hypertrophic stress signaling and genomic stress response. *Jakstat* 2012; **1**(2): 131-41.
45. Pan J, Fukuda K, Saito M, et al. Mechanical stretch activates the JAK/STAT pathway in rat cardiomyocytes. *Circulation research* 1999; **84**(10): 1127-36.
46. Wang TL, Yang YH, Chang H, Hung CR. Angiotensin II signals mechanical stretch-induced cardiac matrix metalloproteinase expression via JAK-STAT pathway. *J Mol Cell Cardiol* 2004; **37**(3): 785-94.
47. Sano M, Fukuda K, Kodama H, et al. Interleukin-6 family of cytokines mediate angiotensin II-induced cardiac hypertrophy in rodent cardiomyocytes. *J Biol Chem* 2000; **275**(38): 29717-23.
48. Bolli R, Stein AB, Guo Y, et al. A murine model of inducible, cardiac-specific deletion of STAT3: its use to determine the role of STAT3 in the upregulation of cardioprotective proteins by ischemic preconditioning. *J Mol Cell Cardiol* 2011; **50**(4): 589-97.
49. Noma T, Lemaire A, Naga Prasad SV, et al. Beta-arrestin-mediated beta1-adrenergic receptor transactivation of the EGFR confers cardioprotection. *J Clin Invest* 2007; **117**(9): 2445-58.
50. Luttrell LM, Ferguson SS, Daaka Y, et al. Beta-arrestin-dependent formation of beta2 adrenergic receptor-Src protein kinase complexes. *Science* 1999; **283**(5402): 655-61.
51. Lavoie C, Mercier JF, Salahpour A, et al. Beta 1/beta 2-adrenergic receptor heterodimerization regulates beta 2-adrenergic receptor internalization and ERK signaling efficacy. *J Biol Chem* 2002; **277**(38): 35402-10.
52. Zhang W, Qu X, Chen B, et al. Critical Roles of STAT3 in beta-Adrenergic Functions in the Heart. *Circulation* 2016; **133**(1): 48-61.
53. Stapel B, Kohlhaas M, Ricke-Hoch M, et al. Low STAT3 expression sensitizes to toxic effects of β-adrenergic receptor stimulation in peripartum cardiomyopathy. *European heart journal* 2017; **38**(5): 349-61.

54. Hilfiker-Kleiner D, Kaminski K, Podewski E, et al. A cathepsin D-cleaved 16 kDa form of prolactin mediates postpartum cardiomyopathy. *Cell* 2007; **128**(3): 589-600.
55. Cantley LC. The phosphoinositide 3-kinase pathway. *Science* 2002; **296**(5573): 1655-7.
56. Shiraishi I, Melendez J, Ahn Y, et al. Nuclear targeting of Akt enhances kinase activity and survival of cardiomyocytes. *Circulation research* 2004; **94**(7): 884-91.
57. Luo J, Cantley LC. The negative regulation of phosphoinositide 3-kinase signaling by p85 and it's implication in cancer. *Cell Cycle* 2005; **4**(10): 1309-12.
58. Tarzami ST, Calderon TM, Deguzman A, Lopez L, Kitsis RN, Berman JW. MCP-1/CCL2 protects cardiac myocytes from hypoxia-induced apoptosis by a G(alphai)-independent pathway. *Biochemical and biophysical research communications* 2005; **335**(4): 1008-16.
59. Hamid T, Gu Y, Ortines RV, et al. Divergent tumor necrosis factor receptor-related remodeling responses in heart failure: role of nuclear factor-kappaB and inflammatory activation. *Circulation* 2009; **119**(10): 1386-97.
60. Chen Y, Pat B, Zheng J, et al. Tumor necrosis factor-alpha produced in cardiomyocytes mediates a predominant myocardial inflammatory response to stretch in early volume overload. *J Mol Cell Cardiol* 2010; **49**(1): 70-8.
61. Mann DL. Innate immunity and the failing heart: the cytokine hypothesis revisited. *Circulation research* 2015; **116**(7): 1254-68.
62. Zou Y, Akazawa H, Qin Y, et al. Mechanical stress activates angiotensin II type 1 receptor without the involvement of angiotensin II. *Nat Cell Biol* 2004; **6**(6): 499-506.
63. Nemoto S, Hamawaki M, De Freitas G, Carabello BA. Differential effects of the angiotensin-converting enzyme inhibitor lisinopril versus the beta-adrenergic receptor blocker atenolol on hemodynamics and left ventricular contractile function in experimental mitral regurgitation. *Journal of the American College of Cardiology* 2002; **40**(1): 149-54.
64. Perry GJ, Wei CC, Hankes GH, et al. Angiotensin II receptor blockade does not improve left ventricular function and remodeling in subacute mitral regurgitation in the dog. *Journal of the American College of Cardiology* 2002; **39**(8): 1374-9.
65. Wisenbaugh T, Sinovich V, Dullabh A, Sareli P. Six month pilot study of captopril for mildly symptomatic, severe isolated mitral and isolated aortic regurgitation. *J Heart Valve Dis* 1994; **3**(2): 197-204.
66. Marney Annis M, Brown Nancy J. Aldosterone and end-organ damage. *Clinical Science* 2007; **113**(6): 267-78.
67. Abreu JG, Ketpura NI, Reversade B, De Robertis EM. Connective-tissue growth factor (CTGF) modulates cell signalling by BMP and TGF-beta. *Nat Cell Biol* 2002; **4**(8): 599-604.
68. Saharinen J, Hyytiainen M, Taipale J, Keski-Oja J. Latent transforming growth factor-beta binding proteins (LTBPs)--structural extracellular matrix proteins for targeting TGF-beta action. *Cytokine & growth factor reviews* 1999; **10**(2): 99-117.
69. Flevaris P, Khan SS, Eren M, et al. Plasminogen Activator Inhibitor Type I Controls Cardiomyocyte Transforming Growth Factor-beta and Cardiac Fibrosis. *Circulation* 2017; **136**(7): 664-79.
70. Ghosh AK, Bradham WS, Gleaves LA, et al. Genetic deficiency of plasminogen activator inhibitor-1 promotes cardiac fibrosis in aged mice: involvement of constitutive transforming growth factor-beta signaling and endothelial-to-mesenchymal transition. *Circulation* 2010; **122**(12): 1200-9.

71. Ljungvall I, Rajamaki MM, Crosara S, et al. Evaluation of plasma activity of matrix metalloproteinase-2 and -9 in dogs with myxomatous mitral valve disease. *Am J Vet Res* 2011; **72**(8): 1022-8.
72. Biernacka A, Dobaczewski M, Frangogiannis NG. TGF-beta signaling in fibrosis. *Growth Factors* 2011; **29**(5): 196-202.

Chapter 5

Effect of long-term carvedilol therapy on molecular markers of left ventricular remodelling in patients with severe chronic primary mitral regurgitation.

5.1. Introduction

Chronic primary mitral regurgitation (CPMR) is caused by a progressive abnormality of the mitral valve apparatus predominantly related to degenerative disease in developed countries and rheumatic heart disease in developing countries, where it remains the most common form of acquired cardiovascular disease in children and adults.[1,2] At present, there is no medical therapy that effectively improves adverse left ventricular remodelling or outcomes in patients with CPMR.[3,4]

Patients with CPMR are often asymptomatic for many years while the left ventricle (LV) progressively dilates in response to abnormal preload. The eccentric hypertrophy that develops normalizes afterload leading to a period of so-called 'compensation'. However, due to inadequate protein synthesis and progressive deterioration in myocardial function, the hypertrophy that develops is insufficient to fully compensate for the wall stress.[5] This leads to an increase in inflammatory cytokine expression, neurohormonal activation and reactive oxygen species generation. These chronic stressors activate a number of complex inflammatory and apoptotic pathways in a similar manner to heart failure from other causes. Early in the LV remodelling process there is loss of interstitial collagen and cell slippage caused by disruption of the myocardial extracellular matrix (ECM). Later changes include myocyte apoptosis and pathological ECM fibrosis.[6]

Recent microarray gene expression data has identified changes in a number of cellular and extra cellular matrix pathways in response to volume overload in animals and humans.[7-9] Since adrenergic drive is increased in volume overload, β-adrenergic blockade has been explored in a number of animal and human studies with variable effect.[10-17] Carvedilol,

which blocks both β_1-, β_2- and α-adrenergic receptors, is a particularly interesting agent in this regard since it potentially reduces afterload through α-adrenergic blockade, blocks the β-adrenergic system and has been found to significantly improve outcomes in patients with heart failure.[18]

To date, carvedilol has only been studied in rats with experimental mitral regurgitation.[17] Based on the remarkable benefit of carvedilol in human patients with heart failure with reduced ejection fraction[18] we hypothesized that carvedilol would attenuate LV remodelling in patients with CPMR. In order to address this question, we examined changes in expression of genes important in β-adrenergic signalling, ECM remodelling, cell survival and energy metabolism pathways in hearts of patients with CPMR treated with carvedilol.

5.2. Methods

5.2.1. Study subjects

The investigation conforms to the principles outlined in the Declaration of Helsinki. Informed consent was obtained from all patients according to a protocol approved by the Human Research Ethics Committee of the University of the Witwatersrand (M101036). Patients were included in the study if they had CPMR and met guideline criteria for elective mitral valve surgery.[3,4] Patients were excluded if they had aortic valve disease, mitral stenosis, active infective endocarditis, co-morbid coronary artery disease, chronic kidney disease, contraindications to β-blocker therapy, were pregnant, or had a history of anti-remodelling therapy use (β-blockers, angiotensin converting enzyme (ACE) inhibitors, angiotensin receptor blockers or mineralocorticoid receptor antagonists).

Patients underwent baseline clinical examination, transthoracic echocardiography, blood analysis and cardiac catheterization, during which LV endomyocardial biopsies (EMB) were obtained using disposable 2.2mm x 105cm Jawz® Endomyocardial Biopsy Forceps (Argon Medical, Tx, USA). Several (3-5) biopsy specimens were taken from the middle third of the LV. Immediately after baseline investigations patients were randomized to receive standard of care (diuretics, potassium supplementation) plus carvedilol ("CRV" group) or standard of care only ("Nil" group). In the CRV group, the dose of carvedilol was up-titrated to 25mg twice daily over a period of one month. Patients were presented for surgery to the cardiothoracic unit immediately after their baseline cardiac catheterization. The timing of the patients' surgery, which is largely dependent on the surgical waiting list, was determined by the cardiothoracic unit. At the time of surgery, a second EMB specimen was obtained. Percutaneous or surgical biopsy specimens were frozen in liquid nitrogen for gene

expression analysis and collected in 10% buffered formalin for histopathology. The frozen specimens were then stored at -80º. Light microscopy was used to confirm endomyocardial sampling.

5.2.2. Echocardiography

Baseline and pre-operative echocardiography was performed with an iE-33® ultrasound device (Koninklijke Philips, NV, USA) by a single sonographer blinded to study medication protocol on all recruited patients according to established guidelines.[19]

5.2.3. RNA isolation

RNA was extracted using the miRNeasy Mini Kit® (Qiagen Sciences, MD, USA). RNA was quantified using spectrophotometric analysis on a NanoDrop ND-2000 Spectrophotometer (NanoDrop Technologies Inc., Wilmington, Del.) and RNA integrity determined using an Agilent 2100 Bioanalyzer (Agilent Technologies, CA, USA). For comparison of gene expression levels in heart tissue from CPMR patients (n=13) at baseline with gene expression levels in normal heart tissue, total heart RNA (from five cadavers with no history of cardiac disease) was purchased commercially (one 23-year old female and 4 males between the ages of 24 and 39).

5.2.4. Gene selection

One hundred and nine candidate genes, 6 reference genes as well as 6 positive and 8 negative control genes were selected. Candidate genes were selected based on previous gene expression studies in animals and humans with heart failure, volume overload and CPMR (Appendix 10).[7-9] Most of the genes had previously been found to be significantly up/down-

regulated in animal or human subjects with CPMR or models of volume overload. Additional genes known to be directly involved in β-receptor signalling, ECM remodelling, cell survival, apoptosis, inflammatory and fibrosis pathways were also selected.[20-23] The six reference genes were previously shown to be stably expressed with a large dynamic range of expression levels in cardiac tissue.

5.2.5. Gene expression analysis

Multiplex gene expression analysis, using 100ng total RNA per sample, was performed commercially by NanoString (Seattle, USA) using an nCounter® Custom Codeset (for the candidate genes). Results were analysed using the NanoString nSolver Analysis Software Package 3.0®. A background subtraction using the geometric mean of the negative controls was included and gene expression levels were normalised to both the geometric mean of the positive controls and the geometric mean of three reference genes (*GAPDH, PGK1* and *HPRT1*). The additional reference genes were excluded from the analysis because of high variation in expression levels between samples (*SDHA* and *STR*) and expression levels at or below background levels (*RPLPO*). Eight candidate genes (*ADRB3, FasLG, IL1B, IL10, MMP-1, MMP-13, PDCD1* and *SAG*) were expressed at levels at or below that of the negative controls and thus were also excluded from the analysis. Normalised counts were used to generate ratio data, 95% confidence intervals (CIs) and false discovery rates (FDRs) for all genes comparing CPMR patients at baseline to the normal heart controls, and "CRV" patients to "Nil" patients at baseline and at follow-up.

5.2.6. Statistical analysis

In the panel of 109 genes, the effect of carvedilol upon gene expression was investigated using each individual subject as their own control (in order to minimize biological variation) to identify those genes whose expression was most altered in relation to carvedilol therapy. The changes between baseline and follow-up readings were calculated for each individual separately and the medians of these differences calculated and compared between the two groups using a 2-sample Wilcoxon Mann-Whitney test. A p-value <0.05 was considered to be statistically significant and a p-value of <0.1 to show a trend. Using hierarchical clustering, genes that were most determining for the effect of carvedilol were identified. The most upregulated and most down-regulated genes for CRV treatment vs Nil treatment were identified from those genes with a delta fold change $\geq +1.75$ or ≤ -1.75. One gene (*NPPB*) was omitted because of large inter-individual variation.

5.3. Results

Twenty consecutive patients with CPMR were recruited according to the study protocol. Seven patients did not undergo final surgery for various reasons as outlined in Figure 3.1. Therefore, thirteen patients underwent full baseline and final investigations as per study protocol and were included in the final analysis. Seven patients were randomly assigned to receive carvedilol and were up-titrated to a dose of 50mg daily ("CRV" group).

5.3.1. Baseline results

There were no significant differences between the two groups of patients with respect to clinical characteristics (Table 3.1). In 12 patients the cause of CPMR was rheumatic heart disease. The median duration of follow up from the time of therapeutic carvedilol dosing (the time at which the CRV patients were on 50mg daily) or baseline investigations (in the case of the Nil group) to the time of surgery was 10 months and 7 months, respectively ($p=0.4738$). All patients had evidence of severe CPMR with 11 of 13 patients being in NYHA functional class ≥ 2. Baseline parameters for the entire group included median resting pulmonary artery pressure of 57mmHg, median LV end systolic diameter of 40mm (indexed 25.5mm/m^2), median ejection fraction of 61% with an effective regurgitant orifice of 0.68cm^2, and a median serum NT-pro-BNP of 822 ng/L. At baseline the median LV dimensions were slightly greater in those patients allocated to carvedilol therapy (Table 3.2). There were no significant differences between the two groups with respect to the remaining baseline echocardiographic parameters, cardiac catheterization findings or serum markers of LV remodelling (Table 3.3).

There were no significant differences between the two groups with respect to baseline levels of expression of the candidate genes except for increased *CTGF*, *LTBP2*, *PDE6A* and *PDGFα* in the patients allocated to carvedilol treatment (Appendix 16). However, since the FDR for all these changes was 1, the likelihood of these differences actually being significant is low.

5.3.2. Gene expression changes in response to carvedilol treatment

Overall carvedilol treatment did not significantly alter the expression levels of most of the genes in this study (Figure 4.1) (Appendix 17). However, in patients treated with carvedilol, down-regulation of genes important in β-adrenergic signalling (*ARRB2*, *PDE1A* and *PDE4D*) as well as *PDGFα* and *COL5A2* and activation of *PLN* was demonstrated (Figures 5.1-5.6).

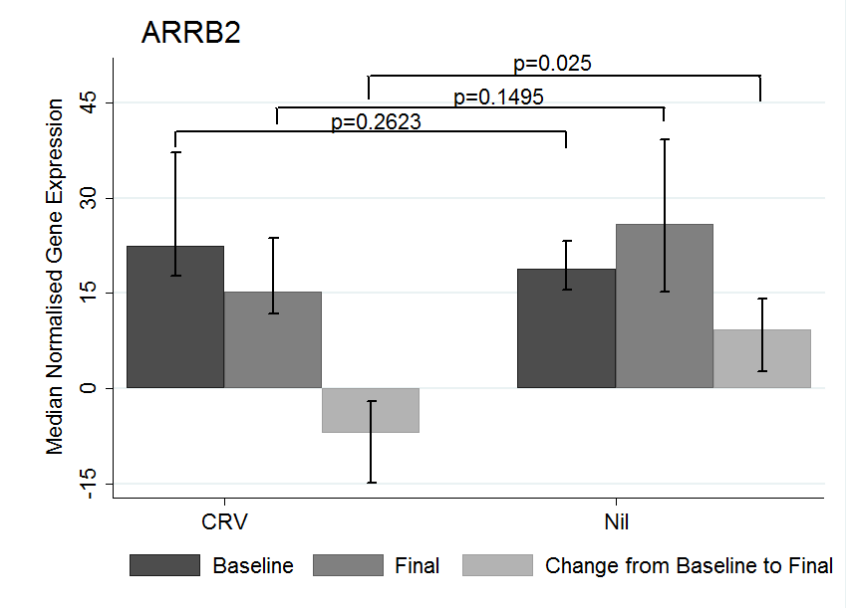

Figure 5.1. Change in levels of *ARRB2* gene expression in CRV and Nil groups.

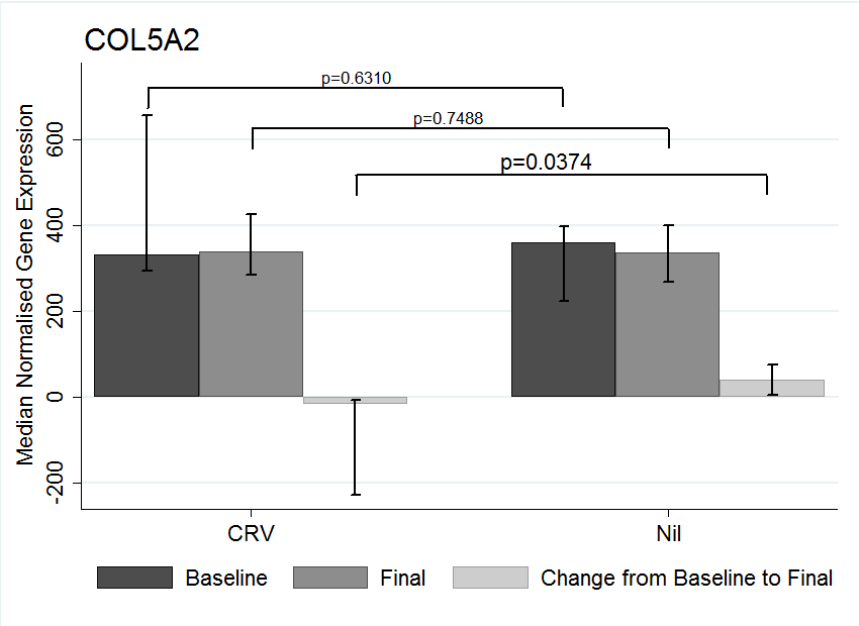

Figure 5.2. Change in levels of *COL5A2* gene expression in CRV and Nil groups.

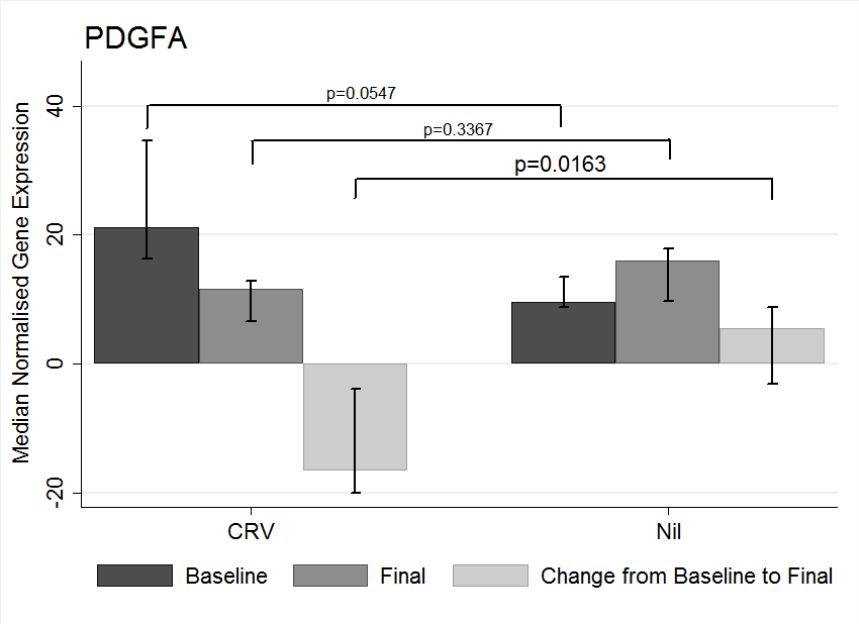

Figure 5.3. Change in levels of *PDGFA* gene expression in CRV and Nil groups.

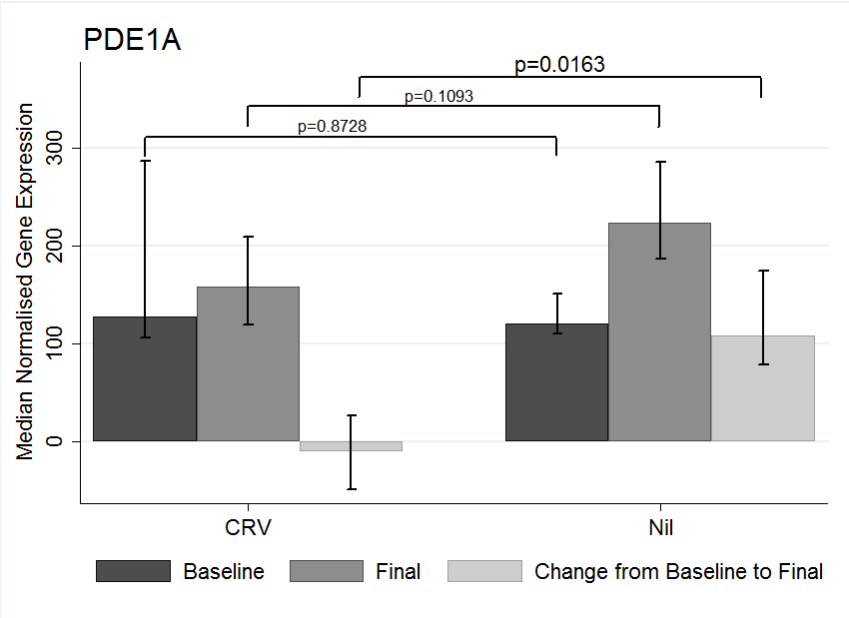

Figure 5.4. Change in levels of *PDE1A* gene expression in CRV and Nil groups.

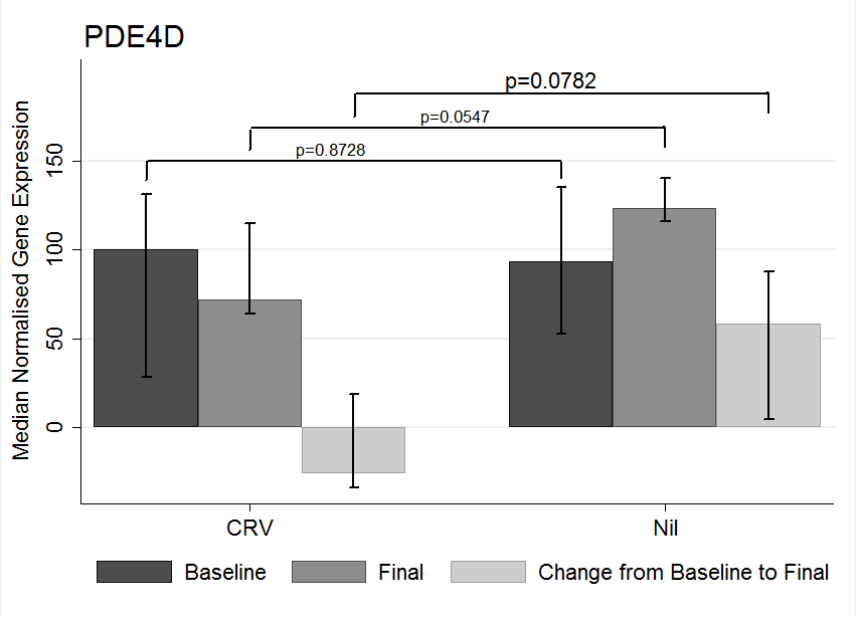

Figure 5.5. Change in levels of *PDE4D* gene expression in CRV and Nil groups.

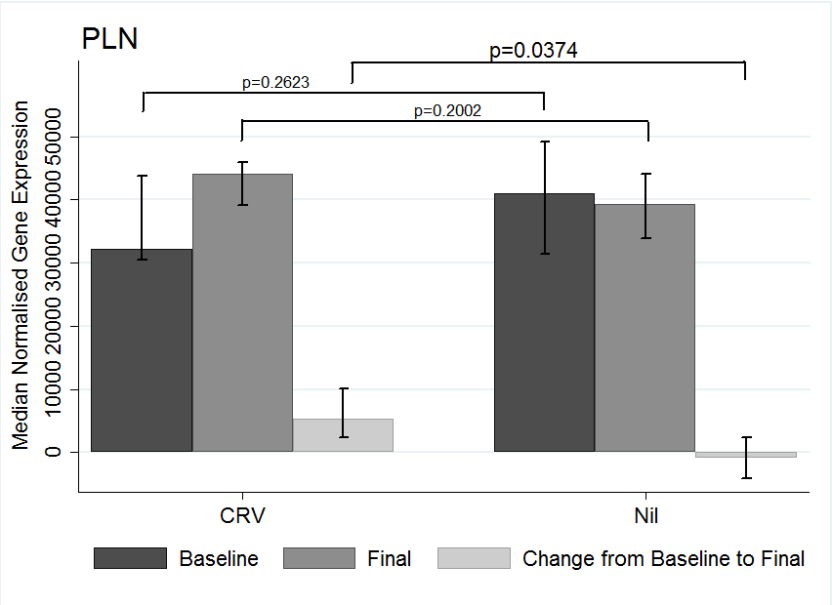

Figure 5.6. Change in levels of *PLN* gene expression in CRV and Nil groups.

When hierarchic clustering and Pearson's correlation statistics was performed on all 12 CPMR patients, we observed a good separation of the patients into two groups with the majority of the treated patients clustering into the CRV group (5 out of 6 patients) and the same for the non-treated patients in the Nil group (Figure 5.7). This analysis confirmed the changes in gene expression levels of *ARRB2, PDE1A, PDE4D* and *PDGFα* but not *COL5A2* or *PLN*. Additionally, significant clustering was noted for *THBS1, ANF, CCL2, PPBP, IL1β, FOS, EMILIN2* and *TIMP4*.

A

Gene	FOLD CHANGE
MMP9	3.06
CCL2	3.03
ANF	2.84
PPBP	2.70
IL1B	2.49
FOS	2.44
NPPB*	2.22
THBS1	1.75
COL3A1	-1.79
PDE1A	-1.92
EMILIN2	-2.00
COL1A1	-2.04
ARRB2	-2.27
TIMP4	-2.44
PDE4D	-2.86
PDGFA	-2.94

B

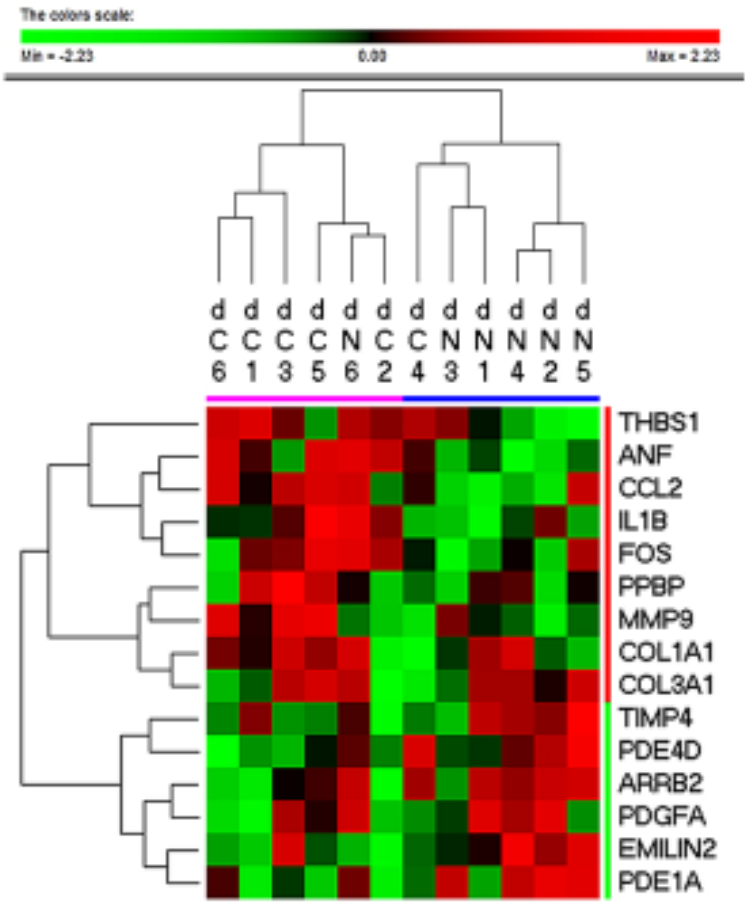

Figure 5.7 Molecular analysis of effect of carvedilol therapy on markers of left ventricular remodelling in patients with severe chronic primary mitral regurgitation. A) The top upregulated and down-regulated genes for CRV treatment vs Nil treatment were selected as those genes with a delta fold change $\geq +1.75$ or ≤ -1.75. One gene (NPPB) was omitted because of the large inter-individual variation. B) Hierarchic clustering of the 12 CPMR patients (6 CRV (dCx), 6 Nil (dNx)). By combining the delta expression values of the 15 top genes (4A) per patient and using Pearson's correlation statistics in hierarchic clustering, variation between the subjects is visualized. The patients separated into two groups with the large majority of the treated patients in the CRV group (pink line; 5/6) and the same for the non-treated patients in the Nil group (blue line). The colour scale on the top indicates upregulation in red and reduced expression in green.

5.4. Discussion

In patients treated with carvedilol there was a significant reduction in the expression of β-arrestin-2 (*ARRB2*), *COL5A2, PDE1A* and *PDGFa* with a trend towards significant down-regulation of *PDE4A* and significant increased expression levels of *PLN*. Figure 5.8 highlights the roles of *ARRB2, PDE1A, PDE4D, PDGFα* and *PLN* in cardiomyocyte signalling. Hierarchical clustering confirmed these findings and identified additional gene expression changes that clustered according to treatment allocation. There was no significant change in the expression of β_1-AR in patients treated with carvedilol compared with the controls over time. Since there was already a significant reduction in the β_1-AR at baseline in these patients, further reduction in the expression of the β_1-AR after treatment with carvedilol may have been less apparent. It has previously been demonstrated that, in patients with heart failure with reduced ejection fraction, metoprolol increases β_1-AR density whereas there is little or no change in cardiac β_1-AR density in the hearts of patients treated with carvedilol, which may explain the findings in the current study.[24]

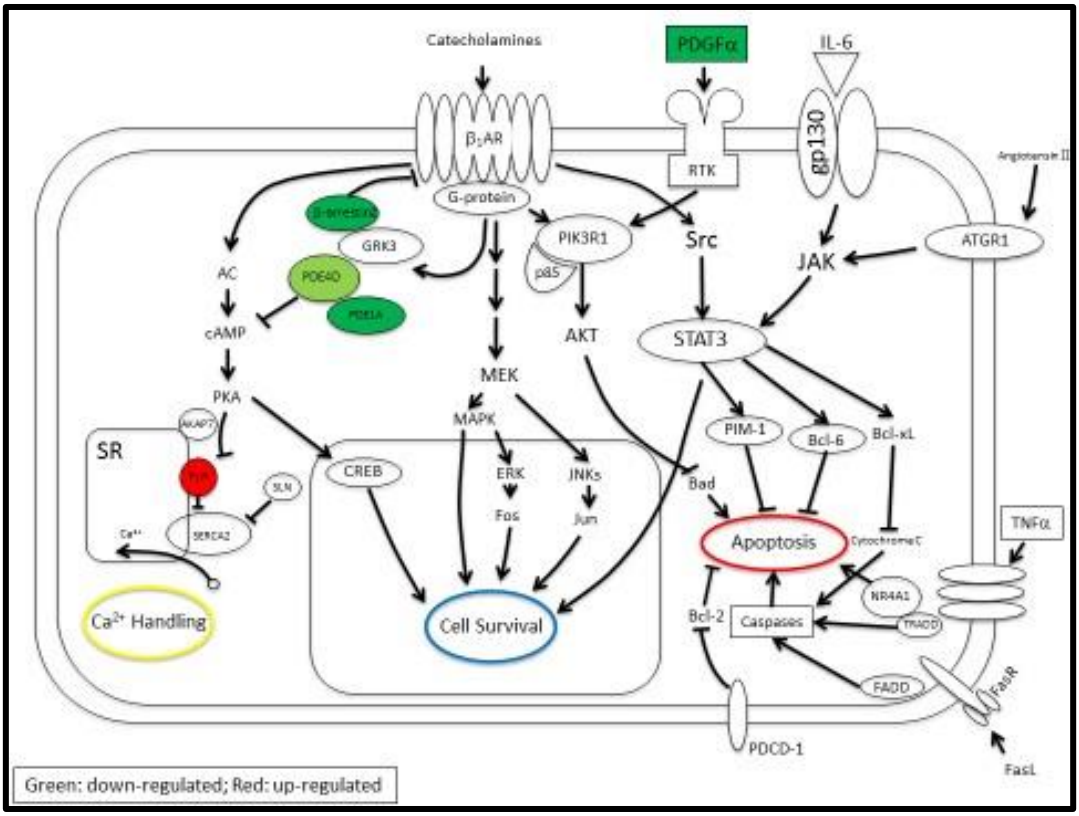

Figure 5.8. Schematic highlighting the significant changes in patients treated with carvedilol versus patients not treated. Green=down-regulated; Red=upregulated; CPMR=chronic primary mitral regurgitation; RTK=receptor tyrosine kinase; SR=sarcoplasmic reticulum. Adapted from Amanfu & Saucerman.[25]

As discussed previously, β-AR are one of thousands of the seven-transmembrane receptors (7TMRs) and, on binding by a β-AR-agonist, undergo conformational changes that allow GTP-binding protein (G protein) activation. These activated G proteins exchange GTP for GDP activating a number of effector enzymes such as adenylate cyclase.[26] Besides G proteins, two other protein families are able to interact with 7TMRs: the G-protein-coupled receptor kinases (GRKs) and β-arrestins.[27] GRK 2 (G protein-coupled receptor kinase; formerly called β-ARK-1 or β-agonist receptor kinase-1) and GRK 3 are ubiquitously expressed in human tissue and are responsible for most agonist-dependent receptor labelling and β-arrestin recruitment.[28] GRKs, together with β-arrestins, are important in the β_1-AR

phosphorylation and labelling for desensitization, internalization and recycling (Figure 5.9).[29,30] β_1-AR desensitization occurs due to a decrease in receptor gene expression (a reduction in β_1-AR mRNA) and/or an increase in receptor uncoupling due to phosphorylation by GRK followed by binding of inhibitor β-arrestin to the phosphorylated receptor. Once bound to β-arrestin the receptor is internalized and undergoes degradation. Therefore, enhancement of GRK2 (β-ARK1) expression, an increase in β-arrestin and/or a reduction in expression of β_1-AR has been associated with heart failure.[30,31]

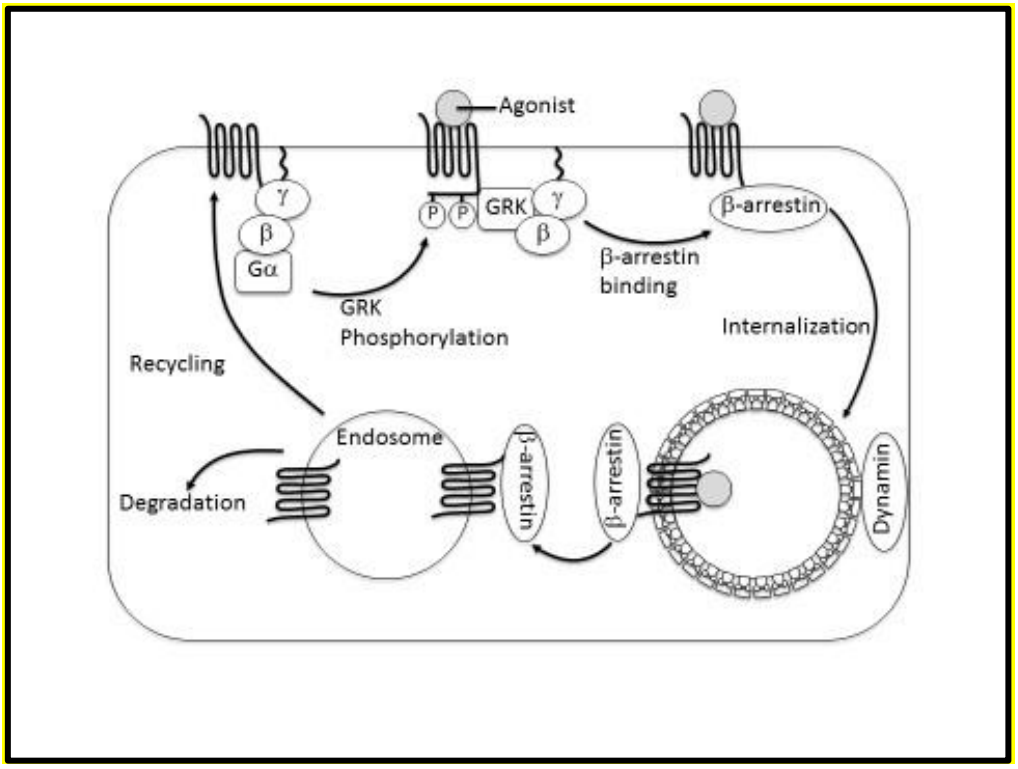

Figure 5.9. β-adrenergic receptor production, phosphorylation, internalization and degradation. See text for details. Gα: G protein α subunit;βγ: beta-gamma subunit of G-protein; GRK: G-protein-coupled receptor kinase. Adapted from Pierce *et al*.[26]

β-arrestins, together with GRKs, are also involved in several G-protein-independent signal transduction pathways (such as proliferation, cell activation and cell death).[32,33] Six arrestins

have been identified, two of which (β-arrestin-1 and β-arrestin-2) are expressed in most tissues, two are found mainly in visual tissue (including S-antigen visual arrestin or SAG) and two remain to be fully characterized.[27] β-arrestin-1 and -2 appear to substitute for each other to some extent since knock-out mice lacking one of the β-arrestins appear to be healthy but double knock-out mice die during embryonic growth.[34] However, they sometimes oppose one another's function in a specific pathway.[35] Their exact role in several important pathways remains to be determined[36] but they have been shown to be important scaffolds in a number of signal transduction pathways including ERK1/2,[37,38] JNK3,[39] MAPK/p38[40] and PI3K.[41] Furthermore, there is evidence to suggest that β-arrestins may have important anti-apoptotic roles in the cell.[41,42] Both β-arrestins desensitize GPCRs but β-arrestin-1 is localised to the cytoplasm and nucleus, suggesting that it may have nuclear transcription factor capabilities, while β-arrestin-2 is localised only to the cytoplasm.[43]

β-arrestin-2 (*ARRB2*), which was already significantly down-regulated in CPMR patients at baseline, was further down-regulated in the patients allocated to carvedilol. The molecular consequences of these changes in patients with CPMR are unclear and may be unimportant especially considering that the major isoform of β-arrestin in the heart is β-arrestin-1 with baseline expression of β-arrestin-2 being very low. Therefore, significant changes in the levels of expression of *ARRB2* may have no translational effect. Nevertheless, further investigation is needed since some beta-blockers are able to induce signal transduction activation through G-protein independent, β-arrestin-dependent mechanisms. Carvedilol has been shown to activate the cardioprotective EGFR pathway through β-arrestin-dependent mechanisms more than other β-blockers.[44] In a rat model, metoprolol increased cardiac

fibrosis through β-arrestin-2 signal transduction[32] whereas loss of β-arrestin-mediated signalling has been shown to increase apoptosis and cardiac deterioration.[45] At present it is difficult to predict what the effects of abnormal β-arrestin-mediated signalling would be in humans with volume overload. Furthermore, it is unclear whether a reduction in β-arrestin-2 gene expression, compared with β-arrestin-1 gene expression, would result in further adverse remodelling or not.

Carvedilol-treated patients demonstrated down-regulation of *PDE1A* and *PDE4D*. As discussed in Chapter 4, these proteins are important in β-adrenergic signalling regulation and deficiency increases the risk of heart failure and cardiac arrhythmias.[46] In addition, significant down-regulation of platelet-derived growth factor (*PDGFA),* an important driver of numerous developmental and pathological processes including cell survival and cardiac fibrosis was noted in patients allocated to carvedilol therapy. Down-regulation of *PDGFA* in carvedilol-treated patients may promote adverse LV remodelling.[47]

Phospholamban (*PLN*) expression was significantly increased in patients treated with carvedilol. Phospholamban regulates cardiac myocyte calcium handling by inhibiting SERCA2a (ATP2A2) and phosphorylation by PKA relieves SERCA2a inhibition permitting calcium influx into the sarcoplasmic reticulum. Mutations in *PLN* and superinhibition of SERCA by mutant *PLN* have been associated with contractile dysfunction, dilated cardiomyopathy and premature cardiac death.[48,49] Abnormal increased expression of *PLN* has already been described in patients with CPMR[9] and we have already demonstrated that SERCA2 expression is reduced in patients with advanced CPMR. Further increased

expression of *PLN*, with potential exacerbation of SERCA2 inhibition, in CPMR patients treated with carvedilol may promote abnormal calcium regulation and amplify contractile dysfunction.

Hierarchical clustering identified increased *ANF* and *NPPB* gene expression, consistent with the increase in serum NT-proBNP, suggest increased and progressive abnormal myocardial loading in patients allocated to carvedilol treatment. Myocardial inflammation in carvedilol-treated patients is reflected by increased expression of *FOS*, *CCL2*, *IL1B* and *IL10*.[8] In patients treated with carvedilol, we found increased expression of *MMP9* and *MMP23* with down-regulation of collagens and *EMILIN2*, which have been associated with adverse LV remodelling.[7,9] Increased expression of *THBS1* and *PPBP* and down-regulation of *PDGFA* have been associated with pathological cardiac fibrosis.[7,47,50,51]

Lack of significant changes in the expression levels of ECM genes may reflect steady-state pathological fibrosis with no further significant changes in relation to drug therapy. *MMP* gene expression was not significantly different between the two groups, which is in contrast to the serum findings: circulating MMP-2 was significantly increased in patients treated with carvedilol. Activation of MMP pathways in other organs may explain the increased circulating levels of MMPs in these patients.

There was a non-significant decrease in the expression of *PAI-1* in patients treated with carvedilol compared with the controls. *PAI-1* protects against cardiac fibrosis (Figure

5.10).[50] Therefore a reduction in expression of *PAI-1* by carvedilol may signal an increased risk of pathological fibrosis in patients treated with carvedilol.

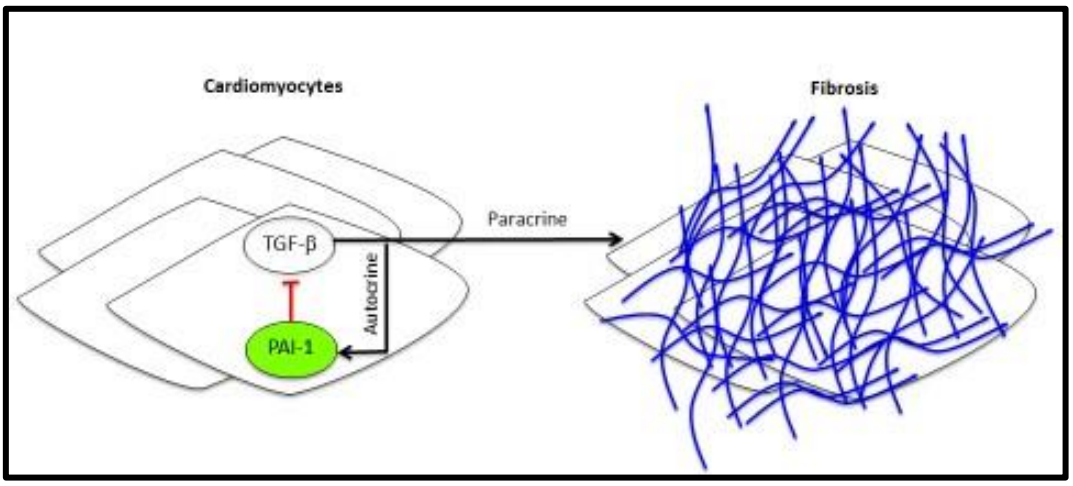

Figure 5.10 Role of cardiomyocyte PAI-1 in TGF-β mediated cardiac fibrosis. Adapted from Flevaris *et al*.[50]

Altered cardiac metabolism, characterized by abnormal substrate utilization, abnormal oxidative phosphorylation and abnormal ATP metabolism, plays and important role in HF.[52] Volume overload is associated with abnormal intramyocyte lipid accumulation, contractile dysfunction and down-regulation of a number of genes important in metabolism.[53,54] The lipid accumulation is caused by an inability of the heart to oxidise excessive circulating free fatty acids. In rats with chronic volume overload there is suppression of a number of lipid-regulating *PPARA*-associated genes possibly due to activation of inflammatory pathways.[8] *PPARA* appears to be important in limiting lipid accumulation and preserving cardiomyocyte metabolic function in CPMR since activation of *PPARA* reduces ventricular dysfunction in experimental CPMR.[54] Apart from a relatively lower expression of *PPARA* in patients treated with carvedilol there were no significant changes in the expression of genes involved

in bioenergetics (*ATP5A1, FASN* and *MCAD*). However, it is tempting to argue that further down-regulation of *PPARA* due to carvedilol treatment (possibly due to inflammatory pathway activation) may exacerbate pathological myocardial energy metabolism and promote contractile dysfunction in patients with CPMR.

Overall, in patients allocated to carvedilol treatment, there were no significant improvements in the expression levels of genes important in LV remodelling. Several reasons for these findings are worth considering. Firstly, the study may have lacked power to show a benefit due to the small sample size. However, if anything, there was a signal of deterioration among those patients treated with carvedilol. Secondly, it is unknown whether patients presenting in more advanced stages of CPMR will respond to anti-remodelling therapy or whether the wall stresses determined by the LaPlace Law will outweigh any potential beta-blocker effect. In fact, beta-blocker depression of the sympathetic nervous system may exacerbate LV dilatation in CPMR.[17] In contrast to patients with heart failure due to reduced ejection fraction, who clearly benefit from the anti-remodelling effects of carvedilol, patients with CPMR have substantial preload due to significant mitral regurgitation. This additional volume load on an already dilated and dysfunctional LV is unlikely to be overcome by just addressing adverse remodelling processes in the LV.

By chance, patients allocated to the carvedilol arm of the study had greater LV dimensions at baseline than patients in the control group. It could be argued that these patients were already at greater risk for further adverse remodeling considering potential increases in wall tension. To address this, individual patients were used as their own controls in this analysis

and consistent changes in the expression of genes were still identified between CRV and Nil patients. Furthermore, if carvedilol was to have a beneficial effect, the effect might have been expected to be more pronounced in hearts with more advanced adverse remodeling, which was not found. In this regard the findings of Pat *et al*.[14] are interesting because despite improvements in cardiomyocyte contractility and beta-receptor responsiveness, LV remodelling was not attenuated by metoprolol. It was postulated that β-AR blockade failed to preserve interstitial collagen loss and therefore failed to prevent ongoing myocyte slippage.[14]

Thirdly, prior studies have been performed in a variety of experimental models and at different stages in the evolution of MR-related LV remodelling. Many of the experiments performed thus far have been in animal models with controlled formation of volume overload showing that early introduction of beta-blocker therapy[10,11] may be beneficial and this is supported by the work of Ahmed *et al*.[16] in humans. Since previous studies have been conducted at various stages in the evolution of LV remodelling, there may be variable findings with respect to the impact of beta-blockade on LV remodelling. Beta-blockade may be beneficial if used early in the evolution of volume overload-related LV remodelling but may be less effective later on. Fourthly, various beta-adrenergic agents have been tested under different circumstances. Compared to the impressive beneficial results in heart failure patients with carvedilol,[18] Pu *et al*.[17] demonstrated that carvedilol worsened LV dimensions and function in rats with primary MR. In contrast, treatment of dogs with the selective beta-blocker atenolol improved LV remodelling[10] whereas treatment with metoprolol in animals and humans have had mixed results.[14,16,55,56] Finally, although evidence has been presented

to suggest that there is down-regulation of cardio-protective pathways, the molecular pathogenesis of LV remodeling in volume overload is complex.[53] Several of the genes studied here are involved in many different pathways with many possible effects that justify further investigation.

5.5. Conclusion

This is the first study to prospectively investigate changes in gene expression levels in the hearts of humans with CPMR in response to treatment with carvedilol. Carvedilol failed to have a significant effect on the expression levels of most of the genes investigated here. Furthermore, significant down-regulation of several cardio-protective genes and significant increased expression of an important calcium regulator, *PLN*, was found in the hearts of CPMR patients after treatment with carvedilol. Consistent with the lack of beneficial effect of carvedilol on echocardiographic and serum markers of cardiac remodelling, and consistent with previous animal model data, there was no signal of benefit in CPMR patients allocated to carvedilol therapy. Further research is still required to better understand the molecular changes during the evolution of LV remodelling in patients with CPMR. Finally, based on these findings, caution is needed before using carvedilol in patients with CPMR.

5.6. References

1. Foster E. Clinical practice. Mitral regurgitation due to degenerative mitral-valve disease. *The New England journal of medicine* 2010; **363**(2): 156-65.
2. Sliwa K, Mocumbi AO. Forgotten cardiovascular diseases in Africa. *Clin Res Cardiol* 2010; **99**(2): 65-74.
3. Baumgartner H, Falk V, Bax JJ, et al. 2017 ESC/EACTS Guidelines for the management of valvular heart disease. *European heart journal* 2017; **38**(36): 2739-91.
4. Nishimura RA, Otto CM, Bonow RO, et al. 2017 AHA/ACC Focused Update of the 2014 AHA/ACC Guideline for the Management of Patients With Valvular Heart Disease: A Report of the American College of Cardiology/American Heart Association Task Force on Clinical Practice Guidelines. *Circulation* 2017; **135**(25): e1159-e95.
5. Urabe Y, Mann DL, Kent RL, et al. Cellular and ventricular contractile dysfunction in experimental canine mitral regurgitation. *Circulation research* 1992; **70**(1): 131-47.
6. Hutchinson KR, Stewart JA, Jr., Lucchesi PA. Extracellular matrix remodeling during the progression of volume overload-induced heart failure. *J Mol Cell Cardiol* 2010; **48**(3): 564-9.
7. Zheng J, Chen Y, Pat B, et al. Microarray identifies extensive downregulation of noncollagen extracellular matrix and profibrotic growth factor genes in chronic isolated mitral regurgitation in the dog. *Circulation* 2009; **119**(15): 2086-95.
8. Chen YW, Pat B, Gladden JD, et al. Dynamic molecular and histopathological changes in the extracellular matrix and inflammation in the transition to heart failure in isolated volume overload. *Am J Physiol Heart Circ Physiol* 2011; **300**(6): H2251-60.
9. Zheng J, Yancey DM, Ahmed MI, et al. Increased Sarcolipin Expression and Adrenergic Drive in Humans With Preserved Left Ventricular Ejection Fraction and Chronic Isolated Mitral Regurgitation. *Circulation: Heart Failure* 2014; **7**(1): 194-202.
10. Tsutsui H, Spinale FG, Nagatsu M, et al. Effects of chronic beta-adrenergic blockade on the left ventricular and cardiocyte abnormalities of chronic canine mitral regurgitation. *J Clin Invest* 1994; **93**(6): 2639-48.
11. Nemoto S, Hamawaki M, De Freitas G, Carabello BA. Differential effects of the angiotensin-converting enzyme inhibitor lisinopril versus the beta-adrenergic receptor blocker atenolol on hemodynamics and left ventricular contractile function in experimental mitral regurgitation. *Journal of the American College of Cardiology* 2002; **40**(1): 149-54.
12. Hankes GH, Ardell JL, Tallaj J, et al. Beta1-adrenoceptor blockade mitigates excessive norepinephrine release into cardiac interstitium in mitral regurgitation in dog. *Am J Physiol Heart Circ Physiol* 2006; **291**(1): H147-51.
13. Oh SH, Meyers DG. Afterload reduction may halt and beta-adrenergic blockade may worsen progression of left ventricular dysfunction in patients with chronic compensated mitral regurgitation: a retrospective cohort study. *Angiology* 2007; **58**(2): 196-202.
14. Pat B, Killingsworth C, Denney T, et al. Dissociation between cardiomyocyte function and remodeling with beta-adrenergic receptor blockade in isolated canine mitral regurgitation. *Am J Physiol Heart Circ Physiol* 2008; **295**(6): H2321-7.
15. Varadarajan P, Joshi N, Appel D, Duvvuri L, Pai RG. Effect of Beta-blocker therapy on survival in patients with severe mitral regurgitation and normal left ventricular ejection fraction. *Am J Cardiol* 2008; **102**(5): 611-5.

16. Ahmed MI, Aban I, Lloyd SG, et al. A Randomized Controlled Phase IIb Trial of Beta1-Receptor Blockade for Chronic Degenerative Mitral Regurgitation. *Journal of the American College of Cardiology* 2012; **60**(9): 833-8.
17. Pu M, Gao Z, Pu DK, Davidson WR, Jr. Effects of early, late, and long-term nonselective beta-blockade on left ventricular remodeling, function, and survival in chronic organic mitral regurgitation. *Circ Heart Fail* 2013; **6**(4): 756-62.
18. Packer M, Fowler MB, Roecker EB, et al. Effect of carvedilol on the morbidity of patients with severe chronic heart failure: results of the carvedilol prospective randomized cumulative survival (COPERNICUS) study. *Circulation* 2002; **106**(17): 2194-9.
19. Lang RM, Badano LP, Mor-Avi V, et al. Recommendations for cardiac chamber quantification by echocardiography in adults: an update from the American Society of Echocardiography and the European Association of Cardiovascular Imaging. *Eur Heart J Cardiovasc Imaging* 2015; **16**(3): 233-70.
20. Lowes BD, Gilbert EM, Abraham WT, et al. Myocardial gene expression in dilated cardiomyopathy treated with beta-blocking agents. *The New England journal of medicine* 2002; **346**(18): 1357-65.
21. Zhang W, Qu X, Chen B, et al. Critical Roles of STAT3 in β-Adrenergic Functions in the Heart. *Circulation* 2016; **133**(1): 48-61.
22. Bristow MR, Minobe WA, Raynolds MV, et al. Reduced beta 1 receptor messenger RNA abundance in the failing human heart. *J Clin Invest* 1993; **92**(6): 2737-45.
23. Engelhardt S, Bohm M, Erdmann E, Lohse MJ. Analysis of beta-adrenergic receptor mRNA levels in human ventricular biopsy specimens by quantitative polymerase chain reactions: progressive reduction of beta 1-adrenergic receptor mRNA in heart failure. *Journal of the American College of Cardiology* 1996; **27**(1): 146-54.
24. Gilbert EM, Abraham WT, Olsen S, et al. Comparative hemodynamic, left ventricular functional, and antiadrenergic effects of chronic treatment with metoprolol versus carvedilol in the failing heart. *Circulation* 1996; **94**(11): 2817-25.
25. Amanfu RK, Saucerman JJ. Modeling the effects of beta1-adrenergic receptor blockers and polymorphisms on cardiac myocyte Ca2+ handling. *Mol Pharmacol* 2014; **86**(2): 222-30.
26. Pierce KL, Premont RT, Lefkowitz RJ. Seven-transmembrane receptors. *Nat Rev Mol Cell Biol* 2002; **3**(9): 639-50.
27. Reiter E, Lefkowitz RJ. GRKs and beta-arrestins: roles in receptor silencing, trafficking and signaling. *Trends Endocrinol Metab* 2006; **17**(4): 159-65.
28. Ren XR, Reiter E, Ahn S, Kim J, Chen W, Lefkowitz RJ. Different G protein-coupled receptor kinases govern G protein and beta-arrestin-mediated signaling of V2 vasopressin receptor. *Proc Natl Acad Sci U S A* 2005; **102**(5): 1448-53.
29. Choi DJ, Koch WJ, Hunter JJ, Rockman HA. Mechanism of beta-adrenergic receptor desensitization in cardiac hypertrophy is increased beta-adrenergic receptor kinase. *J Biol Chem* 1997; **272**(27): 17223-9.
30. Ungerer M, Parruti G, Bohm M, et al. Expression of beta-arrestins and beta-adrenergic receptor kinases in the failing human heart. *Circulation research* 1994; **74**(2): 206-13.
31. Ungerer M, Bohm M, Elce JS, Erdmann E, Lohse MJ. Altered expression of beta-adrenergic receptor kinase and beta 1-adrenergic receptors in the failing human heart. *Circulation* 1993; **87**(2): 454-63.

32. Nakaya M, Chikura S, Watari K, et al. Induction of Cardiac Fibrosis by β-Blocker in G Protein-independent and G Protein-coupled Receptor Kinase 5/β-Arrestin2-dependent Signaling Pathways. *Journal of Biological Chemistry* 2012; **287**(42): 35669-77.
33. Ranjan R, Gupta P, Shukla AK. GPCR Signaling: beta-arrestins Kiss and Remember. *Curr Biol* 2016; **26**(7): R285-8.
34. DeWire SM, Ahn S, Lefkowitz RJ, Shenoy SK. Beta-arrestins and cell signaling. *Annu Rev Physiol* 2007; **69**: 483-510.
35. Ahn S, Wei H, Garrison TR, Lefkowitz RJ. Reciprocal regulation of angiotensin receptor-activated extracellular signal-regulated kinases by beta-arrestins 1 and 2. *J Biol Chem* 2004; **279**(9): 7807-11.
36. Gu Y-j, Sun W-y, Zhang S, Wu J-j, Wei W. The emerging roles of [beta]-arrestins in fibrotic diseases. *Acta Pharmacol Sin* 2015; **36**(11): 1277-87.
37. Eichel K, Jullie D, von Zastrow M. beta-Arrestin drives MAP kinase signalling from clathrin-coated structures after GPCR dissociation. *Nat Cell Biol* 2016; **18**(3): 303-10.
38. Manson ME, Corey DA, Rymut SM, Kelley TJ. beta-arrestin-2 regulation of the cAMP response element binding protein. *Biochemistry* 2011; **50**(27): 6022-9.
39. McDonald PH, Chow CW, Miller WE, et al. Beta-arrestin 2: a receptor-regulated MAPK scaffold for the activation of JNK3. *Science* 2000; **290**(5496): 1574-7.
40. Sun Y, Cheng Z, Ma L, Pei G. Beta-arrestin2 is critically involved in CXCR4-mediated chemotaxis, and this is mediated by its enhancement of p38 MAPK activation. *J Biol Chem* 2002; **277**(51): 49212-9.
41. Beaulieu JM, Sotnikova TD, Marion S, Lefkowitz RJ, Gainetdinov RR, Caron MG. An Akt/beta-arrestin 2/PP2A signaling complex mediates dopaminergic neurotransmission and behavior. *Cell* 2005; **122**(2): 261-73.
42. Wisler JW, DeWire SM, Whalen EJ, et al. A unique mechanism of beta-blocker action: carvedilol stimulates beta-arrestin signaling. *Proc Natl Acad Sci U S A* 2007; **104**(42): 16657-62.
43. Scott MG, Le Rouzic E, Perianin A, et al. Differential nucleocytoplasmic shuttling of beta-arrestins. Characterization of a leucine-rich nuclear export signal in beta-arrestin2. *J Biol Chem* 2002; **277**(40): 37693-701.
44. Kim IM, Tilley DG, Chen J, et al. Beta-blockers alprenolol and carvedilol stimulate beta-arrestin-mediated EGFR transactivation. *Proc Natl Acad Sci U S A* 2008; **105**(38): 14555-60.
45. Noma T, Lemaire A, Naga Prasad SV, et al. Beta-arrestin-mediated beta1-adrenergic receptor transactivation of the EGFR confers cardioprotection. *J Clin Invest* 2007; **117**(9): 2445-58.
46. Lehnart SE, Wehrens XH, Reiken S, et al. Phosphodiesterase 4D deficiency in the ryanodine-receptor complex promotes heart failure and arrhythmias. *Cell* 2005; **123**(1): 25-35.
47. Gallini R, Lindblom P, Bondjers C, Betsholtz C, Andrae J. PDGF-A and PDGF-B induces cardiac fibrosis in transgenic mice. *Experimental cell research* 2016; **349**(2): 282-90.
48. Schmitt JP, Kamisago M, Asahi M, et al. Dilated cardiomyopathy and heart failure caused by a mutation in phospholamban. *Science (New York, NY)* 2003; **299**(5611): 1410-3.
49. Haghighi K, Kolokathis F, Gramolini AO, et al. A mutation in the human phospholamban gene, deleting arginine 14, results in lethal, hereditary cardiomyopathy.

Proceedings of the National Academy of Sciences of the United States of America 2006; **103**(5): 1388-93.
50. Flevaris P, Khan SS, Eren M, et al. Plasminogen Activator Inhibitor Type I Controls Cardiomyocyte Transforming Growth Factor-beta and Cardiac Fibrosis. *Circulation* 2017; **136**(7): 664-79.
51. Frangogiannis NG, Ren G, Dewald O, et al. Critical role of endogenous thrombospondin-1 in preventing expansion of healing myocardial infarcts. *Circulation* 2005; **111**(22): 2935-42.
52. Neubauer S. The Failing Heart — An Engine Out of Fuel. *New England Journal of Medicine* 2007; **356**(11): 1140-51.
53. Barnes J, Pat B, Chen YW, et al. Whole-genome profiling highlights the molecular complexity underlying eccentric cardiac hypertrophy. *Therapeutic advances in cardiovascular disease* 2014; **8**(3): 97-118.
54. Nemoto S, Razeghi P, Ishiyama M, De Freitas G, Taegtmeyer H, Carabello BA. PPAR-gamma agonist rosiglitazone ameliorates ventricular dysfunction in experimental chronic mitral regurgitation. *American journal of physiology Heart and circulatory physiology* 2005; **288**(1): H77-82.
55. Stewart RA, Raffel OC, Kerr AJ, et al. Pilot study to assess the influence of beta-blockade on mitral regurgitant volume and left ventricular work in degenerative mitral valve disease. *Circulation* 2008; **118**(10): 1041-6.
56. Ennis DB, Rudd-Barnard GR, Li B, et al. Changes in mitral annular geometry and dynamics with ss-blockade in patients with degenerative mitral valve disease. *Circ Cardiovasc Imaging* 2010; **3**(6): 687-93.

Chapter 6

Concluding remarks.

6.1. Introduction

Chronic primary mitral regurgitation (CPMR), caused by failure of adequate coaptation of the mitral leaflets, results in an increased left atrial volume load and subsequent abnormal LV preload. Hemodynamically, this causes a decrease in forward stroke volume and cardiac output, increased pulmonary and right ventricular pressures, and a chronically volume-overloaded left ventricle. The most common cause of CPMR in sub-Saharan Africa is rheumatic heart disease, with degenerative mitral valve more commonly found among populations from developed countries.[1]

Current guidelines recommend surgery for patients with severe pulmonary hypertension on presentation or a progressively dilating LV, even if they are asymptomatic.[2,3] However, timing of surgery is uncertain and how these patients should be managed in the interim is unclear.[4] Certainly, it is important that patients are not left untreated until irreversible LV remodelling has taken place. In resource-limited settings, patients who do not need emergency surgery often wait several months before they undergo surgery by which time there has been a progression of adverse LV remodelling leading to permanent impairment of function. Medical therapy that could reverse or at least attenuate LV remodelling may improve outcomes in these patients. However, currently, there is no recommendation for drug therapy in patients with CPMR except in palliative cases.[2,3] This means that for patients with LV systolic dysfunction due to CPMR there is very little evidence that LV deterioration can be attenuated either prior to surgery or after repair/replacement of the mitral valve.[5,6]

Chapter 1 included a detailed description of the structural and molecular evolution of LV remodelling in the volume-overloaded heart based on data reported from *in vitro*, animal and clinical studies. Eccentric hypertrophy, predominantly due to interstitial collagen loss, develops in response to an increase in LV preload leading. This normalizes forward stroke volume and cardiac output but, due to inadequate protein synthesis and progressive deterioration in myocardial function, the eccentric hypertrophy that develops is insufficient to fully compensate for the wall stress.[7] Persistent wall stress promotes cardiac inflammatory cytokine expression,[8-11] neurohormonal activation[12,13] and reactive oxygen species generation,[14] which activate a number of complex molecular pathways.[15] Early in the LV remodelling process there is loss of interstitial collagen and cell slippage caused by disruption of the myocardial extracellular matrix (ECM)-integrin linkages.[16,17] Subsequent changes include myocyte apoptosis and pathological ECM fibrosis.[18,19]

As a result of inadequate tissue perfusion the adrenergic system is activated in patients with CPMR. This has been identified as a potential target in patients with CPMR.[20,21] Therefore, β-adrenergic blockade has been explored in a number of animal and human studies with variable effect.[5,22-29] Carvedilol reduces afterload through α-adrenergic blockade, blocks the β-adrenergic system and has been found to significantly improve outcomes in patients with heart failure with reduced ejection fraction.[30] However, carvedilol has only been studied in rats with experimental mitral regurgitation.[29] Based on the remarkable benefit of carvedilol in human patients with heart failure with reduced ejection fraction[30] it was hypothesized that carvedilol would attenuate LV remodelling in patients with CPMR. In order to address this question, patients with CPMR were recruited prospectively and a number of investigations,

related to LV global and molecular remodelling, were carried out as described in Chapter 2. Patients were then randomized to receive carvedilol therapy or standard of care (diuretics and potassium supplementation if required) while awaiting definitive surgical therapy at which time investigations were repeated in order to determine an effect of carvedilol therapy on LV remodelling.

The findings of this thesis are described in the subsequent chapters. Chapter 3 described the clinical, echocardiographic and serum findings in CPMR patients treated with carvedilol versus those who were treated with the standard of care. Chapter 4 described the baseline expression of 109 genes important in LV remodelling in CPMR patients compared with normal hearts and compared these findings to findings from previous animal and human studies. Finally, Chapter 5 described the changes in expression of these genes in the CPMR patients in response to carvedilol therapy versus standard of care.

6.2. Major highlights of this work

1. This is the first study comparing expression of genes in patients with pure volume overload due to CPMR versus normal hearts.
2. This is the first study in humans with volume overload to measure changes in gene expression over time and in response to medical therapy.
3. This is the first study in humans to show that carvedilol failed to significantly improve clinical, echocardiographic or serum markers of LV remodelling. Furthermore, there was a signal of further adverse LV and right ventricular (RV) remodelling in patients treated

with carvedilol as evidenced by worsening of RV function, an increase in serum BNP and an increase in serum MMP2.

4. In patients with severe CPMR abnormal expression of a number of genes important in extra-cellular matrix remodelling, β-adrenergic signalling, renin-angiotensin aldosterone system regulation, myocardial strain, cell survival and apoptosis, calcium regulation, cellular bioenergetics and stress, and inflammation were found. The changes noted in the patients in the current study were in keeping with prior studies, but with a few notable differences probably related to differences in the severity of adverse LV remodelling in the different study cohorts. Of interest, this is the first study to demonstrate significant down-regulation of the β-adrenergic receptor-1 gene in patients with CPMR. This suggests that the patients recruited in the study were possibly at an advanced stage of adverse LV remodelling. In patients with CPMR significant down-regulation of the angiotensin II receptor 1 gene was also demonstrated, which may have important implications for potential antagonists of the renin-angiotensin aldosterone system in these patients. A number of other cardio-protective genes were found to be down-regulated in the patients with CPMR including genes important in myocyte function, such as *SERCA2/ATP2A2* and *PDE4D*, and genes important in cell survival. Finally, abnormal regulation of several profibrotic genes was also noted.
5. A poor correlation between gene expression data from animal models and human subjects was noted. Because of the difficulties in recruiting large numbers of patients in this field, animal models have often been used. The findings from this study and the previous study of Zheng *et al*.[20] caution against extrapolation of animal gene expression data directly to humans. The differences measured in animals and humans may be due to a number of

reasons including the experimental nature of the volume overload in animal models (including the use of aorto-caval models) and the duration of the volume overload in animal models (it is difficult to determine what "chronic" means in animals).

6. Overall there was little effect of carvedilol on the expression of remodelling genes in patients with CPMR. There appeared to be a signal of further adverse remodelling with down-regulation of cardioprotective *β-arrestin2*, *PDE1A*, and *PDGFα* and a trend towards significant down-regulation of *PDE4D*. Significant up-regulation of *PLN*, which may be associated with abnormal calcium regulation and contractile dysfunction, was noted in patients treated with carvedilol.

The use of beta-blockers in CPMR continues to be controversial. Although selective beta-blocker therapy has attenuated LV remodelling in some animals[22] and human studies,[5] other pre-clinical and clinical studies demonstrate worsening LV function in CPMR after beta-blocker therapy.[21,25,26,29,31] The only previous assessment of the effects of carvedilol on LV function was a long (23 to 35 week) study in rats, with clear exacerbation of echocardiographic measures of LV function.[29] In a 4-month dog model, extended-release metoprolol succinate failed to attenuate the adverse global LV remodelling despite preservation of cardiomyocyte function.[26] Similarly, Sabri *et al.*[21] found that, despite reductions in interstitial collagen degradation and reductions in adverse-remodelling-related intracellular signalling, extended-release metoprolol succinate failed to attenuate LV dilatation or decline in LV function and a retrospective echocardiographic study in 134 human subjects with moderate-to-severe MR (67% degenerative and 20% 'non-specific

thickening') found that patients exposed to beta-adrenergic blockade developed worsening of their ejection fraction over a mean of 20 months follow up.[25]

Overall, carvedilol does not appear to reverse or attenuate adverse remodelling in patients with severe chronic primary mitral regurgitation. Why patients allocated to carvedilol therapy failed to demonstrate improvements in cardiac function is probably multi-factorial and has been discussed in detail at the end of Chapter Five. Despite the small sample size many markers of adverse remodelling consistently worsened in those treated with carvedilol (adverse RV measures, increased BNP, increased serum MMP2, abnormal changes in gene expression levels in several genes important in LV remodelling). It is most likely that the abnormal preload of the LV perpetuates wall stress, which cannot be opposed by medical therapy alone. In fact, these patients are probably completely dependent on the sympathetic response to heart failure and inhibition of the neurohormonal system may exacerbate LV dilatation in CPMR.[29] Ultimately, the only therapy that will counter adverse remodelling is mitral valve surgery.[32]

6.3. Study limitations

The small sample size is the major limitation of this study. The study was underpowered to show a benefit for carvedilol treatment and intra-group heterogeneity may have affected statistical outcomes. To address this, individual patients were used as their own controls in this analysis and consistent changes in the expression of genes were still identified between carvedilol-treated patients and those not treated with carvedilol. The small number of participants in this study should be considered within the context of global research in this

field: the largest gene expression studies have been performed in four dogs before and after experimental induction of MR;[33] in five aorto-caval fistula (ACF) versus five sham rats at 2, 5 and 15 weeks;[15] in 35 patients with CPMR (of whom 16 had a history of hypertension);[20] and in 11 ACF rats versus 11 transverse aortic constriction after 2 weeks of abnormal loading.[34] Finally, prospectively recruiting patients to undergo investigational left ventricular biopsy is challenging and several patients were lost to follow up during the course of the study largely due to poor socio-economic reasons.

The aims included determining, firstly, the changes in the expression of genes in patients with CPMR compared with normal controls, and, secondly, determining changes in echocardiographic and molecular markers of remodelling in response to carvedilol treatment. The reasons for not determining an appropriate sample size are multiple. Firstly, determining a sample size prior to study initiation, was particularly difficult since at the time that the protocol was written and submitted to the ethics committee (in 2010) the only quantitative molecular data available for CPMR was that of Zheng *et al.*[33] in four dogs. No human published data was available to identify a single gene (or a cluster of genes) as a primary endpoint or to permit computation of a sample size. Secondly, the main reason that no sample size calculation was performed was that the protocol called for the performance of left ventricular biopsies in all recruited patients at baseline. Since this is a very invasive and potentially hazardous procedure, we decided to limit the number of patients in order to limit the risk. Thirdly, retrospectively, it was very difficult to recruit patients who met both the inclusion/exclusion criteria *and* were prepared to undergo invasive left ventricular biopsy. Ultimately, it took five years just to recruit the 20 patients (as set out in the protocol).

To get a larger sample size would have meant a much longer study period with limitations arising because of the ever changing practice of medicine (for example, time to surgery was decreasing during the study period), or that the study would have had to have been multicentre.

By chance, patients allocated to the carvedilol arm of the study had greater LV dimensions at baseline than patients in the control group. It could be argued that these patients were already at greater risk for further adverse remodeling considering potential increases in wall tension. However, a beneficial effect of carvedilol might have been expected in patients with the most advanced adverse LV remodeling at baseline, which was not found.

This was an open-label trial. The primary investigator and the patients were aware of drug allocation. However, the technologists involved in the basic clinical examinations (heart rate and blood pressure measurements, for example), echocardiographic and laboratory work were blinded to treatment allocation. It is unlikely that a placebo effect would influence gene expression changes.

6.4. Future studies

Beta-blockers may not be beneficial in patients with advanced decompensation because the volume overload may outweigh any potential benefit that ant-remodelling agents may have.[19] Elimination of the neurohormonal response may therefore be detrimental in subjects with advanced LV remodelling, especially since the volume overload persists.[29] In contrast, in patients with more moderate mitral regurgitation and less evidence of LV remodelling or

dilatation there may still be a role for beta-blockers in preventing further remodelling possibly in combination with other agents known to improve LV function.[6] Future studies should examine the role of beta-blockers in patients and models with milder volume overload. Furthermore, it would be particularly interesting to examine the role of anti-remodelling therapy in patients who have already undergone corrective mitral valve surgery.[32,35]

This study has helped identify a number of important genes to target in more focussed studies in future *in vitro*, animal, pre-clinical and larger clinical trials. For example, further studies on the effects of CPMR and drug therapy on β-adrenergic signalling (in particular β-arrestin and GRK interactions), JAK-STAT signalling, calcium regulation, cell survival, apoptosis and extra-cellular matrix regulation are warranted. It was unfortunate that several other important pathway proteins were not examined in this study. Due to budget constraints it was not possible to perform extensive microarrays. It would be interesting in the future to analyse changes in *PKA* and *AKT* pathways.[36] There were a number of fold changes in the expression of genes when comparing the CPMR and normal hearts and also when comparing the CRV versus Nil treatments groups, which did not reach statistical significance, possibly because of the small numbers, but warrant further investigation. In particular, STAT3 appears to be important in β-adrenergic signalling and cardioprotection.[37-39] In addition, elucidation of the effects of ventricular loading on STAT3 pathway regulation should be the focus of future research.

It would be interesting to repeat a number of these experiments (medical therapy for volume overloaded hearts) with larger numbers of patients or in large-animal models (pigs or sheep). To date, no animal study has measured changes in molecular pathways in CPMR in response to therapy. Large-animal models may be useful to clarify the myocardial response to various anti-remodelling therapies at a molecular level and may avoid the limitations of other animal models.[15] Although animal models are important in terms of hypothesis generation, there is still much work that needs to be carried out in humans. All studies thus far have used surrogate clinical markers (serum, echocardiographic and molecular) as study endpoints. Hard clinical endpoints (such as reductions in hospitalization for heart failure and reductions in cardiovascular death) studies with medical therapies are still required.

6.5. Conclusion

The pathophysiology of remodelling in relation to different loading conditions is a fascinating and growing area in cardiovascular medicine. We still have substantial steps to take in order to better understand the remodelling process in animal models and we are still at a nascent stage with regard to fully defining the pathways that are important in adverse remodelling in humans, whether early in the remodelling process or at more advanced stages of adverse LV remodelling. Even less is known about the right ventricle, which appears to be equally important in long-term outcomes in these patients. Therefore, we still have a great deal of work to do in patients with valvular heart disease to try and understand the adverse remodelling processes, which will hopefully lead to medical breakthroughs in the future. The data presented here do not support the hypothesis that carvedilol reverses or attenuates adverse LV remodelling in patients with severe CPMR and, at present, caution is reommended before considering beta-blockers for patients with severe CPMR. Nevertheless, hopefully these findings contribute to the current knowledge base regarding remodelling in patients with mitral valve disease, potentially leading to further in-depth studies.

6.6. References

1.Sliwa K, Mocumbi AO. Forgotten cardiovascular diseases in Africa. *Clin Res Cardiol* 2010; **99**(2): 65-74.
2.Baumgartner H, Falk V, Bax JJ, et al. 2017 ESC/EACTS Guidelines for the management of valvular heart disease. *European heart journal* 2017; **38**(36): 2739-91.
3.Nishimura RA, Otto CM, Bonow RO, et al. 2017 AHA/ACC Focused Update of the 2014 AHA/ACC Guideline for the Management of Patients With Valvular Heart Disease: A Report of the American College of Cardiology/American Heart Association Task Force on Clinical Practice Guidelines. *Circulation* 2017; **135**(25): e1159-e95.
4.Carabello BA. Beta-blockade for mitral regurgitation: could the management of valvular heart disease actually be moving into the 21st century? *Journal of the American College of Cardiology* 2012; **60**(9): 839-40.
5.Ahmed MI, Aban I, Lloyd SG, et al. A Randomized Controlled Phase IIb Trial of Beta1-Receptor Blockade for Chronic Degenerative Mitral Regurgitation. *Journal of the American College of Cardiology* 2012; **60**(9): 833-8.
6.Meel R, Peters F, Libhaber E, Essop MR. Is there a role for combination anti-remodelling therapy for heart failure secondary to chronic rheumatic mitral regurgitation? *Cardiovasc J Afr* 2017; **28**(5): 280-4.
7.Urabe Y, Mann DL, Kent RL, et al. Cellular and ventricular contractile dysfunction in experimental canine mitral regurgitation. *Circulation research* 1992; **70**(1): 131-47.
8.Oral H, Sivasubramanian N, Dyke DB, et al. Myocardial proinflammatory cytokine expression and left ventricular remodeling in patients with chronic mitral regurgitation. *Circulation* 2003; **107**(6): 831-7.
9.Palmieri EA, Benincasa G, Di Rella F, et al. Differential expression of TNF-alpha, IL-6, and IGF-1 by graded mechanical stress in normal rat myocardium. *Am J Physiol Heart Circ Physiol* 2002; **282**(3): H926-34.
10.Wang BW, Hung HF, Chang H, Kuan P, Shyu KG. Mechanical stretch enhances the expression of resistin gene in cultured cardiomyocytes via tumor necrosis factor-alpha. *Am J Physiol Heart Circ Physiol* 2007; **293**(4): H2305-12.
11.Chen Y, Pat B, Zheng J, et al. Tumor necrosis factor-alpha produced in cardiomyocytes mediates a predominant myocardial inflammatory response to stretch in early volume overload. *J Mol Cell Cardiol* 2010; **49**(1): 70-8.
12.Mehta RH, Supiano MA, Oral H, et al. Compared with control subjects, the systemic sympathetic nervous system is activated in patients with mitral regurgitation. *Am Heart J* 2003; **145**(6): 1078-85.
13.Nagatsu M, Zile MR, Tsutsui H, et al. Native beta-adrenergic support for left ventricular dysfunction in experimental mitral regurgitation normalizes indexes of pump and contractile function. *Circulation* 1994; **89**(2): 818-26.
14.Ahmed MI, Gladden JD, Litovsky SH, et al. Increased oxidative stress and cardiomyocyte myofibrillar degeneration in patients with chronic isolated mitral regurgitation and ejection fraction >60%. *Journal of the American College of Cardiology* 2010; **55**(7): 671-9.
15.Chen YW, Pat B, Gladden JD, et al. Dynamic molecular and histopathological changes in the extracellular matrix and inflammation in the transition to heart failure in isolated volume overload. *Am J Physiol Heart Circ Physiol* 2011; **300**(6): H2251-60.

16.Amin P, Singh M, Singh K. beta-Adrenergic Receptor-Stimulated Cardiac Myocyte Apoptosis: Role of beta1 Integrins. *J Signal Transduct* 2011; **2011**: 179057.
17.Kong P, Christia P, Frangogiannis NG. The pathogenesis of cardiac fibrosis. *Cell Mol Life Sci* 2014; **71**(4): 549-74.
18.Hutchinson KR, Stewart JA, Jr., Lucchesi PA. Extracellular matrix remodeling during the progression of volume overload-induced heart failure. *J Mol Cell Cardiol* 2010; **48**(3): 564-9.
19.Barnes J, Dell'Italia LJ. The multiple mechanistic faces of a pure volume overload: implications for therapy. *Am J Med Sci* 2014; **348**(4): 337-46.
20.Zheng J, Yancey DM, Ahmed MI, et al. Increased Sarcolipin Expression and Adrenergic Drive in Humans With Preserved Left Ventricular Ejection Fraction and Chronic Isolated Mitral Regurgitation. *Circulation: Heart Failure* 2014; **7**(1): 194-202.
21.Sabri A, Rafiq K, Seqqat R, Kolpakov MA, Dillon R, Dell'italia LJ. Sympathetic activation causes focal adhesion signaling alteration in early compensated volume overload attributable to isolated mitral regurgitation in the dog. *Circulation research* 2008; **102**(9): 1127-36.
22.Tsutsui H, Spinale FG, Nagatsu M, et al. Effects of chronic beta-adrenergic blockade on the left ventricular and cardiocyte abnormalities of chronic canine mitral regurgitation. *J Clin Invest* 1994; **93**(6): 2639-48.
23.Nemoto S, Hamawaki M, De Freitas G, Carabello BA. Differential effects of the angiotensin-converting enzyme inhibitor lisinopril versus the beta-adrenergic receptor blocker atenolol on hemodynamics and left ventricular contractile function in experimental mitral regurgitation. *Journal of the American College of Cardiology* 2002; **40**(1): 149-54.
24.Hankes GH, Ardell JL, Tallaj J, et al. Beta1-adrenoceptor blockade mitigates excessive norepinephrine release into cardiac interstitium in mitral regurgitation in dog. *Am J Physiol Heart Circ Physiol* 2006; **291**(1): H147-51.
25.Oh SH, Meyers DG. Afterload reduction may halt and beta-adrenergic blockade may worsen progression of left ventricular dysfunction in patients with chronic compensated mitral regurgitation: a retrospective cohort study. *Angiology* 2007; **58**(2): 196-202.
26.Pat B, Killingsworth C, Denney T, et al. Dissociation between cardiomyocyte function and remodeling with beta-adrenergic receptor blockade in isolated canine mitral regurgitation. *Am J Physiol Heart Circ Physiol* 2008; **295**(6): H2321-7.
27.Varadarajan P, Joshi N, Appel D, Duvvuri L, Pai RG. Effect of Beta-blocker therapy on survival in patients with severe mitral regurgitation and normal left ventricular ejection fraction. *Am J Cardiol* 2008; **102**(5): 611-5.
28.Stewart RA, Raffel OC, Kerr AJ, et al. Pilot study to assess the influence of beta-blockade on mitral regurgitant volume and left ventricular work in degenerative mitral valve disease. *Circulation* 2008; **118**(10): 1041-6.
29.Pu M, Gao Z, Pu DK, Davidson WR, Jr. Effects of early, late, and long-term nonselective beta-blockade on left ventricular remodeling, function, and survival in chronic organic mitral regurgitation. *Circ Heart Fail* 2013; **6**(4): 756-62.
30.Packer M, Fowler MB, Roecker EB, et al. Effect of carvedilol on the morbidity of patients with severe chronic heart failure: results of the carvedilol prospective randomized cumulative survival (COPERNICUS) study. *Circulation* 2002; **106**(17): 2194-9.

31.Ennis DB, Rudd-Barnard GR, Li B, et al. Changes in mitral annular geometry and dynamics with ss-blockade in patients with degenerative mitral valve disease. *Circ Cardiovasc Imaging* 2010; **3**(6): 687-93.
32.Kainuma S, Taniguchi K, Toda K, et al. B-type natriuretic peptide response and reverse left ventricular remodeling after surgical correction of functional mitral regurgitation in patients with advanced cardiomyopathy. *J Cardiol* 2015; **66**(4): 279-85.
33.Zheng J, Chen Y, Pat B, et al. Microarray identifies extensive downregulation of noncollagen extracellular matrix and profibrotic growth factor genes in chronic isolated mitral regurgitation in the dog. *Circulation* 2009; **119**(15): 2086-95.
34.Barnes J, Pat B, Chen YW, et al. Whole-genome profiling highlights the molecular complexity underlying eccentric cardiac hypertrophy. *Therapeutic advances in cardiovascular disease* 2014; **8**(3): 97-118.
35.Le Tourneau T, de Groote P, Millaire A, et al. Effect of mitral valve surgery on exercise capacity, ventricular ejection fraction and neurohormonal activation in patients with severe mitral regurgitation. *Journal of the American College of Cardiology* 2000; **36**(7): 2263-9.
36.Miyamoto S, Rubio M, Sussman MA. Nuclear and mitochondrial signalling Akts in cardiomyocytes. *Cardiovasc Res* 2009; **82**(2): 272-85.
37.Stapel B, Kohlhaas M, Ricke-Hoch M, et al. Low STAT3 expression sensitizes to toxic effects of β-adrenergic receptor stimulation in peripartum cardiomyopathy. *European heart journal* 2017; **38**(5): 349-61.
38.Hilfiker-Kleiner D, Kaminski K, Podewski E, et al. A cathepsin D-cleaved 16 kDa form of prolactin mediates postpartum cardiomyopathy. *Cell* 2007; **128**(3): 589-600.
39.Zhang W, Qu X, Chen B, et al. Critical Roles of STAT3 in beta-Adrenergic Functions in the Heart. *Circulation* 2016; **133**(1): 48-61.

Appendices

Appendix 1: Human Research Ethics Committee (HREC) certificate.

UNIVERSITY OF THE WITWATERSRAND, JOHANNESBURG
Division of the Deputy Registrar (Research)

HUMAN RESEARCH ETHICS COMMITTEE (MEDICAL)
R14/49 Dr Keir McCutcheon

CLEARANCE CERTIFICATE	**M101036**
PROJECT	Can a B-adrenergic receptor blocker reverse or at least attenuate left remodellingdue to chronic non-ischaemic mitral regurgitation?"
INVESTIGATORS	Dr Keir McCutcheon.
DEPARTMENT	Department of Internal Medicine/ Cardiology
DATE CONSIDERED	29/10/2010
DECISION OF THE COMMITTEE*	Approved unconditionally

Unless otherwise specified this ethical clearance is valid for 5 years and may be renewed upon application.

DATE 29/10/2010 **CHAIRPERSON** .....
(Professor PE Cleaton-Jones)

*Guidelines for written 'informed consent' attached where applicable
cc: Supervisor : Prof Pravin Manga

DECLARATION OF INVESTIGATOR(S)

To be completed in duplicate and **ONE COPY** returned to the Secretary at Room 10004, 10th Floor, Senate House, University.
I/We fully understand the conditions under which I am/we are authorized to carry out the abovementioned research and I/we guarantee to ensure compliance with these conditions. Should any departure to be contemplated from the research procedure as approved I/we undertake to resubmit the protocol to the Committee. **I agree to a completion of a yearly progress report.**

PLEASE QUOTE THE PROTOCOL NUMBER IN ALL ENQUIRIES...

Appendix 2A: Certificate for total heart RNA from Donor 1.



Agilent Technologies

Lot	0006273800

Page 1 of 1

Catalog Number	540011
Product Name	MVP Total RNA, Human Heart
Expiration Date	2022-05-30
Quantity	25 µg
Certified By	Dana Faver
Quality Controlled By	Matt Huffman
Shipping Conditions	Shipped on dry ice.
Storage Conditions	Store total RNA at -70°C. Multiple freeze/thaw cycles should be avoided.
Concentration	1.0 µg / µl
RNA Source Information	
Tissue	Single Donor
Sex	Female
Age	23 Years
Pathology	N/A
Strain	N/A
Gestation	N/A

No further RNA source information is available.

Certificate of Analysis

In the interest of conserving resources, we are no longer shipping manuals with products. Please visit **www.clontech.com/manuals** to obtain an electronic version.

PRODUCT: Human Heart Total RNA

CATALOG No. 636532

CONCENTRATION 1 µg/µl

LOT NUMBER 1604239A

FORM
Total RNA provided in RNase-Free water.

STORAGE CONDITIONS
Store at –70°C

SHELF LIFE
1 year from date of receipt under proper storage conditions.

SHIPPING CONDITIONS
Dry ice (–70°C)

DESCRIPTION
Total RNA isolated by a modified guanidinium thiocyanate method (1)

PACKAGE CONTENTS
50 µg Total RNA from the tissues/cells specified below

TOTAL RNA SOURCE
Normal human heart pooled from 3 male Caucasians, ages: 30-39; cause of death: trauma

No further RNA source information is available.

IMPORTANT NOTE
To prevent contamination by RNases, always wear gloves when handling RNA. Avoid multiple freeze/thaw cycles.

FOR RESEARCH USE ONLY

QUALITY CONTROL DATA

This lot of total RNA was analyzed by capillary electrophoresis (CE) using an Agilent 2100 Bioanalyzer. The actual electropherogram trace for this RNA is provided below. RNA concentration and purity were evaluated by UV spectrophotometry.
Both the area ratio of the 28S/18S rRNA peaks, and the proportion (relative percentage) of these two peak areas to the total area under the electropherogram provide reliable quantitative estimates of RNA integrity. For both of these criteria, this sample meets or exceeds Clontech standards for high quality Total RNA.

Peak Areas: 28S: 22.1% 18S: 21.0% Ratio 28S/18S: 1.1 Ratio A_{260}/A_{280}: 2.1

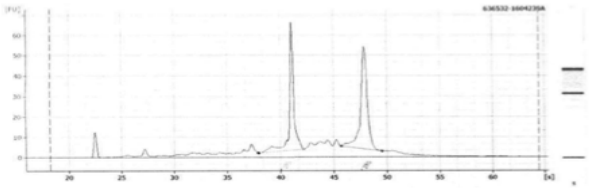

REFERENCES
1. Chomczynski, P. & Sacchi, N. (1987) Single-step method of RNA isolation by acid guanidinium thiocyanate-phenol-chloroform extraction. *Anal. Biochem.* **162**:156-159.

(PA17880)

Clontech

United States/Canada
800.662.2566
Asia Pacific
+1.650.919.7300
Europe
+33.(0)1.3904.6880
Japan
+81.(0)77543.6116

Clontech Laboratories, Inc.
A Takara Bio Company
1290 Terra Bella Ave,
Mountain View, CA 94043
Technical Support (US)
E-mail: tech@clontech.com
www.clontech.com

Notice to Purchaser

Clontech

Human Heart Total RNA

CATALOG NO.

636532

NOTICE TO PURCHASER:

Our products are to be used for research purposes only. They may not be used for any other purpose, including, but not limited to, use in drugs, in vitro diagnostic purposes, therapeutics, or in humans. Our products may not be transferred to third parties, resold, modified for resale, or used to manufacture commercial products or to provide a service to third parties without prior written approval of Clontech Laboratories, Inc.

Your use of this product is also subject to compliance with the licensing requirements listed below and described on the product's web page at http://www.clontech.com. It is your responsibility to review, understand and adhere to any restrictions imposed by these statements.

TRADEMARKS:

Clontech and the Clontech logo are trademarks of Clontech Laboratories, Inc.

All other marks are the property of their respective owners. Certain trademarks may not be registered in all jurisdictions. Clontech is a Takara Bio Company. ©2016 Clontech Laboratories, Inc. This document has been reviewed and approved by the Clontech Quality Assurance Department.

Clontech Laboratories, Inc.
A Takara Bio Company
1290 Terra Bella Avenue, Mountain View, CA 94043, USA
U.S. Technical Support: tech@clontech.com

6/3/2016

United States/Canada	Asia Pacific	Europe	Japan
800.662.2566	+1.650.919.7300	+33.(0)1.3904.6880	+81.(0)77.543.6116

BioChain®

www.biochain.com

Tel: 1-888-762-2568 Fax: 1-510-783-5386 Email: info@biochain.com

Certificate of Analysis

Product Name:

■ **Total RNA**	**Catalog No.: RXXXXXXX**
□ **Human Tumor Total RNA Matched Pair (PP/PM)**	**Catalog No.: R8235XXX-PP/PM**
□ **mRNA**	**Catalog No.: MXXXXXXX**
□ **FFPE Total RNA**	**Catalog No.: RXXXXXXX**
□ **FFPE and Frozen Matched Pair Total RNA**	**Catalog No.: RXXXXXXX-FP**

Storage Condition: -70°C **Shipping Condition:** Dry Ice

Shelf Life: Half a year from the date of receipt under proper storage condition

Description

- **Total RNA** is isolated by modified guanidine thiocyanate techniques and stored in RNA storage buffer.
- **Human tumor matched pair total RNA (PP/PM).** Products include: Primary Pair (PP), or Primary and Metastatic Pair (PM). PP consists of total RNA isolated from primary tumor and its adjacent normal tissue; PM consists of total RNA from primary tumor and corresponding metastatic tumor. Total RNA in each pair is prepared from the same donor. This product line is designed for identifying tumor-specific genes and tumor metastatic genes.
- **mRNA** is purified from high quality of total RNA using a modified Oligo (dT) cellulose method and stored in DEPC treated water. Total RNA is isolated by a modified guanidine thiocyanate method.
- **FFPE Total RNA** FFPE Total RNAs are isolated from Formalin Fixed Paraffin Embedded materials.

Quality Control

- **Total RNA**
  1. The integrity of the RNA is examined by visual inspection for the presence of intact bands of 18s and 28s ribosomal RNA when electrophoreses on a denaturing agarose gel. The quality and purity of total RNA were tested by spectrophotometer. $A_{260/280}$ is between 1.8 and 2.1(detected in 10 mM Tris-HCl, pH 7.5).
  2. The RNA is treated by DNAse I, and is tested as DNA free RNA by PCR.
  3. cDNA synthesis is successfully performed by using this RNA as template.
- **mRNA**:
  1. The quality and purity of mRNA is tested by spectrophotometer. $A_{260/280}$ is between 1.8 and 2.1 (detected in 10mM Tris-HCl, pH 7.5).
  2. The integrity of mRNA is checked by electrophoresis on a denaturing agarose gel with a smear from 0.5 Kb up to more than 9.0 Kb.
- **FFPE Total RNA:**
  The purity of RNA is tested by spectrophotometer. $A_{260/280}$ is between 1.8 and 2.1

Note:

1. Total RNA from some rare tissues and tumor tissues may not be treated by DNAse I
2. To visualize the RNA images on agarose gel, we recommend the same gel system be used as Biochain's (1% agarose gel in 1xMOPS buffer with formaldehyde). Biochain is not responsible for customer's getting degraded RNA images from other gel systems, such as TAE gel, TBE gel, Urea gel, etc.
3. RNA concentration should be measured in 10 mM Tris-HCl, pH 7.5, RNA concentration may vary if it is detected in other solutions, such as DEPC water.

FOR IN VITRO RESEARCH USE ONLY **APPROVED BY** _____

F-753-1COARevB RxxxxxxxCB Active Date: 12312015

BioChain®

www.biochain.com

Tel: 1-888-762-2568 Fax: 1-510-783-5386 Email: info@biochain.com

Data Sheet

Product Name: Total RNA

Catalog No.: ATR1234122-50 **Lot No.: C108093**

Species: ■ Human □ Mouse □ Rat □ Monkey (Rh) □ Guinea Pig □ Porcine □ Bovine □ Hamster □ Dog □ Monkey (Cy) □ Rabbit □ Plant

Tissue Type: ■ Normal ■ Adult □ Fetal □ Tumor □ Disease

Tissue Name: Heart

Donor Information:

Male: 24 year(s) old **Pool of 1 donor(s)**
Female: _____ year(s) old **Pool of _____ donor(s)**

Clinical Diagnosis: Normal

DNase I Treatment: ■ **Yes** □ **No**

Components:

1. 50 μg total RNA per package
2. Certificate of Analysis

Product Image:



Fig. 1 Total RNA was analyzed by electrophoresis on 1% agarose gel

FOR IN VITRO RESEARCH USE ONLY **APPROVED BY:**

Appendix 3: Minnesota Living with Heart Failure Questionnaire.

https://eprovide.mapi-trust.org/instruments/minnesota-living-with-heart-failure-questionnaire

Magnetic Luminex® Screening Assay

Human Premixed Multi-Analyte Kit

Catalog Number LXSAHM

For the simultaneous detection of multiple human biomarkers in cell culture supernates, serum, and plasma.

This package insert must be read in its entirety before using this product.
For research use only. Not for use in diagnostic procedures.

ASSAY PROCEDURE

Bring all reagents and samples to room temperature before use. It is recommended that all samples and standards be assayed in duplicate.

Note: *Protect microparticles and Streptavidin-PE from light at all times.*

1. Prepare all reagents, standards, and samples as directed in the previous sections.
2. Resuspend the diluted microparticle cocktail by inversion or vortexing. Add 50 µL of the microparticle cocktail to each well of the microplate.
3. Add 50 µL of Standard or sample* per well. Securely cover with a foil plate sealer. Incubate for 2 hours at room temperature on a horizontal orbital microplate shaker (0.12" orbit) set at 800 ± 50 rpm. A plate layout is provided to record standards and samples assayed.
4. Using a magnetic device designed to accommodate a microplate, wash by applying the magnet to the bottom of the microplate, removing the liquid, filling each well with Wash Buffer (100 µL) and removing the liquid again. Complete removal of liquid is essential for good performance. Perform the wash procedure three times.

   Note: *Refer to the magnetic device user manual for proper wash technique using a flat bottom microplate.*
5. Add 50 µL of diluted Biotin Antibody Cocktail to each well. Securely cover with a foil plate sealer and incubate for 1 hour at room temperature on the shaker set at 800 ± 50 rpm.
6. Repeat the wash as in step 4.
7. Add 50 µL of diluted Streptavidin-PE to each well. Securely cover with a foil plate sealer and incubate for 30 minutes at room temperature on the shaker set at 800 ± 50 rpm.
8. Repeat the wash as in step 4.
9. Resuspend the microparticles by adding 100 µL of Wash Buffer to each well. Incubate for 2 minutes on the shaker set at 800 ± 50 rpm.
10. Read within 90 minutes using a Luminex or Bio-Rad analyzer.
    Note: *Resuspend microparticles immediately prior to reading.*

*Samples may require dilution. See Sample Preparation section.

Appendix 4B: Certificate of Analysis for IL-33, ST2, Fas and Fas ligand.

Magnetic Luminex® Screening Assays

Premixed Multiplex

Certificate of Analysis

Kit Lot Number	1423662
Kit Catalog Number	LXSAHM- 4
Microparticle Mix Lot Number	1423663
Biotin Antibody Mix Lot Number	1423664

Standard Cocktail Lot Information

	Lot No.	Recon Vol.	
Standard C	1419349	0.25 mL	mL
Standard D	1417618	0.25 mL	mL
Standard E	1387478	0.2 mL	mL
			mL
			mL
			mL
			mL
			mL
			mL
			mL

Analyte	Region	Standard Value pg/mL
IL-33	14	11,360
Fas Ligand	39	4,330

Analyte	Region	Standard Value pg/mL
ST2/IL-1 R4	18	140,860
Fas	73	35,440

This Premixed Multiplex was tested and found to perform within specifications.

Approved by *Diane R. Wotta* *Date* **February 23, 2016**

R D Systems, Inc.
614 NE McKinley Pl.
Minneapolis, MN 55413

PHONE: (612) 379-2956
FAX: (612) 379-6580
752180.3

WATS: (800) 343-7475
E-MAIL: info@rndsystems.com

Appendix 4C: Certificate of Analysis for TNF-α, IL-1β and IL-6.

Magnetic Luminex® Screening Assays

Premixed Multiplex

Certificate of Analysis

Kit Lot Number	1423659
Kit Catalog Number	LXSAHM- 3
Microparticle Mix Lot Number	1423660
Biotin Antibody Mix Lot Number	1423661

Standard Cocktail Lot Information

	Lot No.	Recon Vol.	
Standard A	1402479	0.2 mL	mL
			mL
			mL
			mL
			mL
			mL
			mL
			mL
			mL
			mL

Analyte	Region	Standard Value pg/mL
TNF alpha	12	3,620
IL-1 beta	28	4,320

Analyte	Region	Standard Value pg/mL
IL-6	13	3,420

This Premixed Multiplex was tested and found to perform within specifications.

Approved by *Diane R. Wotta* *Date* **February 23, 2016**

R D Systems, Inc.
614 NE McKinley Pl.
Minneapolis, MN 55413

PHONE: (612) 379-2956
FAX: (612) 379-6580
752180.3

WATS: (800) 343-7475
E-MAIL: info@rndsystems.com

Appendix 5A: Selected pages from MMP Panel instructions.

Human MMP
Magnetic Bead Panel 2

96-Well Plate Assay

Cat # HMMP2MAG-55K

The M logo is a trademark of Merck KGaA, Darmstadt, Germany.
© 2013 EMD Millipore Corporation, Billerica, MA 01821 USA.

IMMUNOASSAY PROCEDURE

- Prior to beginning this assay, it is imperative to read this protocol completely and to thoroughly understand the Technical Guidelines.
- Allow all reagents to warm to room temperature (20-25°C) before use in the assay.
- Diagram the placement of Standards [Std 0 (Background), Standard 1, Standard 2, Standard 3, Standard 4, Standard 5, Standard 6, Standard 7] Controls 1 and 2, and Samples on Well Map Worksheet in a vertical configuration. (Note: Most instruments will only read the 96-well plate vertically by default.) It is recommended to run the assay in duplicate.
- If using a filter plate, set the filter plate on a plate holder at all times during reagent dispensing and incubation steps so that the bottom of the plate does not touch any surface.

1. Add 200 µL of Wash Buffer into each well of the plate. Seal and mix on a plate shaker for 10 minutes at room temperature (20-25°C).
2. Decant Wash Buffer and remove the residual amount from all wells by inverting the plate and tapping it smartly onto absorbent towels several times.
3. Add 25 µL of each Standard or Control into the appropriate wells.
4. Add 25 µL of Assay Buffer to the background and sample wells.
5. Add 25 µL of appropriate matrix to the background, standards, and control wells. When assaying serum, plasma or urine, use the **Assay Buffer** provided in the kit. When assaying tissue culture or other supernatant, use proper control culture medium as the matrix solution.
6. Add 25 µL of Sample (**1:20 diluted serum/plasma or neat urine**) into the appropriate wells.
7. Vortex Mixing Bottle and add 25 µL of the Mixed Beads to each well. (Note: During addition of Beads, shake bead bottle intermittently to avoid settling.)
8. Seal the plate with a plate sealer. Wrap the plate with foil and incubate with agitation on a plate shaker 2h at room temperature (20-25ºC).

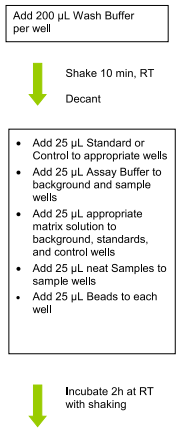

9. Gently remove well contents and wash plate 2 times following instructions listed in the **PLATE WASHING** section.
10. Add 25 µL of Detection Antibodies into each well. (Note: Allow the Detection Antibodies to warm to room temperature prior to addition.)
11. Seal, cover with foil and incubate with agitation on a plate shaker for 1 hour at room temperature (20-25°C). **DO NOT ASPIRATE AFTER INCUBATION.**
12. Add 25 µL Streptavidin-Phycoerythrin to each well containing the 25 µL of Detection Antibodies.
13. Seal, cover with foil and incubate with agitation on a plate shaker for 30 minutes at room temperature (20-25°C).
14. Gently remove well contents and wash plate 2 times following instructions listed in the **PLATE WASHING** section.
15. Add 100 µL of Sheath Fluid (or Drive Fluid if using MAGPIX®) to all wells. Resuspend the beads on a plate shaker for 5 minutes.
16. Run plate on Luminex, 200™, HTS, FLEXMAP 3D™ or MAGPIX® with xPONENT software.
17. Save and analyze the Median Fluorescent Intensity (MFI) data using a 5-parameter logistic or spline curve-fitting method for calculating MMP concentrations in samples. (Note: For diluted samples, multiply the calculated concentration by the dilution factor.)

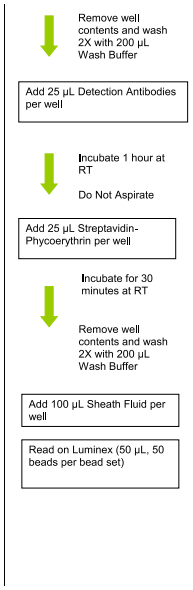

PLATE WASHING

1.) Solid Plate
If using a solid plate, use either a handheld magnet or magnetic plate washer.
A.) Handheld magnet **(EMD Millipore Catalog #40-285)** - Rest plate on magnet for 60 seconds to allow complete settling of magnetic beads. Remove well contents by gently decanting the plate in an appropriate waste receptacle and gently tapping on absorbent pads to remove residual liquid. Wash plate with 200 µL of Wash Buffer by removing plate from magnet, adding Wash Buffer, shaking for 30 seconds, reattaching to magnet, letting beads settle for 60 seconds and removing well contents as previously described after each wash. Repeat wash steps as recommended in Assay Procedure.
B.) Magnetic plate washer **(EMD Millipore Catalog #40-094, #40-095, #40-096 and #40-097)** - Please refer to specific automatic plate washer manual for appropriate equipment settings. Please note that after the final aspiration, there will be approximately 25 µL of residual wash buffer in each well. This is expected when using the BioTek plate washer and this volume does not need to be aspirated from the plate.

If using an automatic plate washer other than BioTek® 405 LS or 405 TS, please refer to the manufacturer's recommendations for programming instructions.

2.) Filter Plate (EMD Millipore Catalog #MX-PLATE)
If using a filter plate, use a vacuum filtration manifold to remove well contents. Wash plate with 200 µL/well of Wash Buffer, removing Wash Buffer by vacuum filtration after each wash. Repeat wash steps as recommended in the Assay Procedure.

EQUIPMENT SETTINGS

Luminex 200™, HTS, FLEXMAP 3D®, and MAGPIX® with xPONENT® software:

These specifications are for the Luminex 200™, Luminex HTS, Luminex FLEXMAP 3D®, and Luminex MAGPIX® with xPONENT® software. Luminex instruments with other software (e.g. MasterPlex®, STarStation, LiquiChip, Bio-Plex Manager™, LABScan™ 100) would need to follow instrument instructions for gate settings and additional specifications from the vendors for reading Luminex magnetic beads.

For magnetic bead assays, the Luminex 200™ and HTS instruments must be calibrated with the xPONENT® 3.1 compatible Calibration Kit (EMD Millipore Catalog #40-275) and performance verified with the Performance Verification Kit (EMD Millipore Catalog #40-276). The Luminex FLEXMAP 3D® instrument must be calibrated with the FLEXMAP 3D® Calibrator Kit (EMD Millipore Catalog #40-028) and performance verified with the FLEXMAP 3D® Performance Verification Kit (EMD Millipore Catalog #40-029). The Luminex MAGPIX® instrument must be calibrated with the MAGPIX® Calibration Kit (EMD Millipore Catalog #40-049) and performance verified with the MAGPIX® Performance Verification Kit (EMD Millipore Catalog #40-050).

NOTE: When setting up a Protocol using the xPONENT® software, you must select MagPlex as the Bead Type in the Acquisition settings.

NOTE: These assays cannot be run on any instruments using Luminex IS 2.3 or Luminex 1.7 software.

Appendix 5B: Selected pages from TIMP-1 and -4 Panel instructions.

Human TIMP Magnetic Bead Panel 2

96-Well Plate Assay

Cat. # HTMP2MAG-54K

The M logo is a trademark of Merck KGaA, Darmstadt, Germany.
© 2013 EMD Millipore Corporation, Billerica, MA 01821 USA.

IMMUNOASSAY PROCEDURE

- Prior to beginning this assay, it is imperative to read this protocol completely and to thoroughly understand the Technical Guidelines.
- Allow all reagents to warm to room temperature (20-25°C) before use in the assay.
- Diagram the placement of Standards [Std 0 pg/mL (Background), Std 1, Std 2, Std 3, Std 4, Std 5, Std 6] Controls 1 and 2, and Samples on Well Map Worksheet in a vertical configuration. (Note: Most instruments will only read the 96-well plate vertically by default.) It is recommended to run the assay in duplicate.
- If using a filter plate, set the filter plate on a plate holder at all times during reagent dispensing and incubation steps so that the bottom of the plate does not touch any surface.

1. Add 200 µL of Wash Buffer into each well of the plate. Seal and mix on a plate shaker for 10 minutes at room temperature (20-25°C).
2. Decant Wash Buffer and remove the residual amount from all wells by inverting the plate and tapping it smartly onto absorbent towels several times.
3. Add 25 µL of each Standard or Control into the appropriate wells. 25 µL Assay Buffer should be used for background and sample wells (0 pg/mL).
4. Add 25 µL of Sample into the appropriate wells.
5. Add 25 µL of appropriate matrix solution to the background, standards, and control wells. When assaying urine, use assay buffer provided in the kit as matrix; when assaying tissue culture or other supernatant, use proper control culture medium as the matrix solution.
6. Vortex Mixing Bottle and add 25 µL of the Mixed Beads to each well. (Note: During addition of Beads, shake bead bottle intermittently to avoid settling.)
7. Seal the plate with a plate sealer. Wrap the plate with foil and incubate with agitation on a plate shaker 2 hours at room temperature (20-25°C) or overnight (16-18 hr) at 4°C.

Add 200 µL Wash Buffer per well

↓ Shake 10 min, RT

↓ Decant

- Add 25 µL Standard or Control to appropriate wells
- Add 25 µL Assay Buffer to background and sample wells
- Add 25 µL of sample to sample wells
- Add 25 µL appropriate matrix solution to background, standards, and control wells
- Add 25 µL Beads to each well

↓ Incubate 2 hours at RT or overnight at 4°C with shaking

8. Gently remove well contents and wash plate 2 times following instructions listed in the **PLATE WASHING** section.
9. Add 25 µL of Detection Antibodies into each well. (Note: Allow the Detection Antibodies to warm to room temperature prior to addition.)
10. Seal, cover with foil and incubate with agitation on a plate shaker for 1 hour at room temperature (20-25°C). **DO NOT ASPIRATE AFTER INCUBATION.**
11. Add 25 µL Streptavidin-Phycoerythrin to each well containing the 25 µL of Detection Antibodies.
12. Seal, cover with foil and incubate with agitation on a plate shaker for 30 minutes at room temperature (20-25°C).
13. Gently remove well contents and wash plate 2 times following instructions listed in the **PLATE WASHING** section.
14. Add 100 µL of Sheath Fluid (or Drive Fluid if using MAGPIX®) to all wells. Resuspend the beads on a plate shaker for 5 minutes.
15. Run plate on Luminex 200™, HTS, FLEXMAP 3D™ or MAGPIX® with xPONENT software.
16. Save and analyze the Median Fluorescent Intensity (MFI) data using a 5-parameter logistic or spline curve-fitting method for calculating analyte concentrations in samples. Note: For diluted samples, multiply the calculated concentration by the dilution factor.

↓ Remove well contents and wash 2X with 200 µL Wash Buffer

Add 25 µL Detection Antibodies per well

↓ Incubate 1 hour at RT

↓ Do Not Aspirate

Add 25 µL Streptavidin-Phycoerythrin per well

↓ Incubate for 30 minutes at RT

↓ Remove well contents and wash 2X with 200 µL Wash Buffer

Add 100 µL Sheath Fluid or Drive Fluid per well

Read on Luminex (50 µL, 50 beads per bead set)

ASSAY CHARACTERISTICS

Cross-Reactivity

There was no or negligible cross-reactivity between the antibodies for an analyte and any of the other analytes in this panel.

Assay Sensitivities (minimum detectable concentrations, pg/mL)

Minimum Detectable Concentration (MinDC) is calculated using MILLIPLEX® Analyst 5.1. It measures the true limits of detection for an assay by mathematically determining what the empirical MinDC would be if an infinite number of standard concentrations were run for the assay under the same conditions.

Analyte	Overnight Protocol (n = 5 Assays)	
	MinDC (pg/mL)	MinDC+2SD (pg/mL)
TIMP-1	7,0	13,6
TIMP-2	17,0	37,4
TIMP-3	46,0	92,3
TIMP-4	4,0	10,1

Analyte	Same Day Protocol (n = 3 Assays)	
	MinDC (pg/mL)	MinDC+2SD (pg/mL)
TIMP-1	4,0	10,1
TIMP-2	9,0	18,4
TIMP-3	52,0	104,2
TIMP-4	4,0	5,6

Precision

Intra-assay precision is generated from the mean of the %CV's from **8** reportable results across two different concentrations of analytes in a single assay. Inter-assay precision is generated from the mean of the %CV's across two different concentrations of analytes across **4** different assays.

Analyte	Overnight Protocol	
	Intra-assay %CV	Inter-assay %CV
TIMP-1	≤ 10%	≤ 10%
TIMP-2	≤ 10%	≤ 10%
TIMP-3	≤ 10%	≤ 10%
TIMP-4	≤ 10%	≤ 10%

Appendix 6: Selected pages from mRNAeasy mini handbook.

December 2014

miRNeasy Mini Handbook

For purification of total RNA, including miRNA, from animal and human cells and tissues



Sample & Assay Technologies

Protocol: Purification of Total RNA, Including Small RNAs, from Animal Tissues

Important points before starting

- If using the miRNeasy Mini Kit for the first time, read "Important Notes" (page 11).
- It is important not to overload the RNeasy Mini spin column, as overloading will significantly reduce RNA yield and quality. Read "Determining the amount of starting material" (page 11).
- If working with RNA for the first time, read Appendix E (page 39).
- For optimal results, stabilize harvested tissues immediately in RNA*later* RNA Stabilization Reagent or AllProtect Stabilization Reagent. Tissues can be stored in the reagent for up to 1 day at 37°C, 7 days at 15–25°C, or 4 weeks at 2–8°C, or archived at –15 to –30°C or –80°C.
- Fresh, frozen, or RNA*later* or AllProtect stabilized tissues can be used. Tissues can be stored for several months at –70°C. Do not allow tissues to thaw during weighing or handling prior to disruption in QIAzol Lysis Reagent. Homogenized tissue lysates (in QIAzol Lysis Reagent, step 3) can also be stored at –70°C for several months. To process frozen homogenized lysates, incubate at 37°C in a water bath until completely thawed and salts are dissolved. Avoid prolonged incubation, which may compromise RNA integrity. Continue with step 4.
- Generally, DNase digestion is not required since the combination of QIAzol and RNeasy technologies efficiently removes most of the DNA without DNase treatment. In addition, miScript Primer Assays and most other assays for mature miRNA are not affected by the presence of small amounts of genomic DNA. However, further DNA removal may be necessary for certain RNA applications that are sensitive to very small amounts of DNA. In these cases, small residual amounts of DNA can be removed by on-column DNase digestion (see Appendix B, page 34) or by DNase digestion after RNA purification (please contact QIAGEN Technical Service for a protocol).
- Buffer RWT may form a precipitate upon storage. If necessary, redissolve by warming and then place at room temperature (15–25°C).
- QIAzol Lysis Reagent and Buffer RWT contain a guanidine salt and are therefore not compatible with disinfecting reagents containing bleach. See page 5 for safety information.
- Except for phase separation (step 7), all protocol and centrifugation steps should be performed at room temperature. During the procedure, work quickly.

Things to do before starting

- Buffers RWT and RPE are supplied as concentrates. Before using for the first time, add the required amounts of ethanol (96–100%), as indicated on the bottle, to obtain a working solution.
- If performing optional on-column DNase digestion, prepare DNase I stock solution as described in Appendix B (page 34).

Procedure

1. **Excise the tissue sample from the animal or remove it from storage. Determine the amount of tissue. Do not use more than 50 mg flash-frozen tissue, 25 mg liver, thymus, spleen, or RNA*later* stabilized tissue, or 100 mg adipose tissue.**

   Unless you are working with RNA*later* or AllProtect stabilized tissue, do not allow the tissue to thaw before placing in QIAzol Lysis Reagent.

2. **If the entire piece of tissue can be used for RNA purification, place it directly into 700 µl QIAzol Lysis Reagent in a suitably sized vessel for disruption and homogenization.**

   If only a portion of the tissue is to be used, determine the weight of the piece to be used and place it into 700 µl QIAzol Lysis Reagent in a suitably sized vessel for disruption and homogenization.

   RNA in tissues is not protected after harvesting until the sample is stabilized in RNA*later* or AllProtect Reagent, flash-frozen, or disrupted and homogenized in step 3. Frozen animal tissue should not be allowed to thaw during handling.

   Note: Use a suitably sized vessel with sufficient headspace to accommodate foaming, which may occur during homogenization.

3. **Homogenize immediately using the TissueLyser II, TissueLyser LT, TissueRuptor, or another method until the sample is uniformly homogeneous (usually 20–40 s).**

   See pages 15–17 for a more detailed description of disruption and homogenization methods.

   Note: Homogenization with the TissueRuptor or the TissueLyser II/TissueLyser LT (see Appendix C, page 37, or the appropriate *TissueLyser Handbook*) generally results in higher total RNA yields than with other homogenization methods.

   Foaming may occur during homogenization, especially of brain tissue. If this occurs, let the homogenate stand at room temperature for 2–3 min until the foam subsides before continuing with the protocol.

   Note: Homogenized tissue lysates can be stored at –70°C for several months.

4. **Place the tube containing the homogenate on the benchtop at room temperature (15–25°C) for 5 min.**

   This step promotes dissociation of nucleoprotein complexes.

5. **Add 140 µl chloroform to the tube containing the homogenate and cap it securely. Shake the tube vigorously for 15 s.**

   Thorough mixing is important for subsequent phase separation.

6. **Place the tube containing the homogenate on the benchtop at room temperature for 2–3 min.**

7. **Centrifuge for 15 min at 12,000 x *g* at 4°C. After centrifugation, heat the centrifuge up to room temperature (15–25°C) if the same centrifuge will be used for the next centrifugation steps.**

   After centrifugation, the sample separates into 3 phases: an upper, colorless, aqueous phase containing RNA; a white interphase; and a lower, red, organic phase. For tissues with an especially high fat content, an additional, clear phase may be visible below the red, organic phase. The volume of the aqueous phase should be approximately 350 µl.

   Note: If you want to purify a separate miRNA-enriched fraction, follow the steps in Appendix A (page 31) after performing this step.

8. **Transfer the upper aqueous phase to a new collection tube (supplied). Add 1.5 volumes (usually 525 µl) of 100% ethanol and mix thoroughly by pipetting up and down several times. Do not centrifuge. Continue without delay with step 9.**

   A precipitate may form after addition of ethanol, but this will not affect the RNeasy procedure.

9. **Pipet up to 700 µl of the sample, including any precipitate that may have formed, into an RNeasy Mini spin column in a 2 ml collection tube (supplied). Close the lid gently and centrifuge at ≥8000 x *g* (≥10,000 rpm) for 15 s at room temperature (15–25°C). Discard the flow-through.***

   Reuse the collection tube in step 10.

10. **Repeat step 9 using the remainder of the sample. Discard the flow-through.***

    Reuse the collection tube in step 11.

    Optional: If performing optional on-column DNase digestion (see "Important points before starting"), follow the steps in Appendix B (page 34) after performing this step.

11. **Add 700 µl Buffer RWT to the RNeasy Mini spin column. Close the lid gently and centrifuge for 15 s at ≥8000 x *g* (≥10,000 rpm) to wash the column. Discard the flow-through.†**

    Skip this step if performing the optional on-column DNase digestion (page 34).

    Reuse the collection tube in step 12.

* Flow-through contains QIAzol Lysis Reagent and is therefore not compatible with bleach. See page 5 for safety information.

† Flow-through contains Buffer RWT and is therefore not compatible with bleach. See page 5 for safety information.

12. **Pipet 500 µl Buffer RPE into the RNeasy Mini spin column. Close the lid gently and centrifuge for 15 s at ≥8000 x *g* (≥10,000 rpm) to wash the column. Discard the flow-through.**

    Reuse the collection tube in step 13.

13. **Add another 500 µl Buffer RPE to the RNeasy Mini spin column. Close the lid gently and centrifuge for 2 min at ≥8000 x *g* (≥10,000 rpm) to dry the RNeasy Mini spin column membrane.**

    The long centrifugation dries the spin column membrane, ensuring that no ethanol is carried over during RNA elution. Residual ethanol may interfere with downstream reactions.

    Note: Following centrifugation, remove the RNeasy Mini spin column from the collection tube carefully so the column does not contact the flow-through. Otherwise, carryover of ethanol will occur.

14. **Optional: Place the RNeasy Mini spin column into a new 2 ml collection tube (not supplied), and discard the old collection tube with the flow-through. Centrifuge in a microcentrifuge at full speed for 1 min.**

    Perform this step to eliminate any possible carryover of Buffer RPE or if residual flow-through remains on the outside of the RNeasy Mini spin column after step 13.

15. **Transfer the RNeasy Mini spin column to a new 1.5 ml collection tube (supplied). Pipet 30–50 µl RNase-free water directly onto the RNeasy Mini spin column membrane. Close the lid gently and centrifuge for 1 min at ≥8000 x *g* (≥10,000 rpm) to elute the RNA.**

16. **If the expected RNA yield is >30 µg, repeat step 15 with a second volume of 30–50 µl RNase-free water. Elute into the same collection tube.**

    To obtain a higher total RNA concentration, this second elution step may be performed by using the first eluate (from step 15). The yield will be 15–30% less than the yield obtained using a second volume of RNase-free water, but the final concentration will be higher.

Appendix 7. RNA quantification using Nanodrop Spectrophotometry.

	Sample ID	Nucleic Acid Concentration	Unit	A260	A280	260/280	260/230	Sample Type	Factor
1	MNB	107,7	ng/µl	2,692	1,353	1,99	1,45	RNA	40
2	MNF	86,6	ng/µl	2,165	1,122	1,93	0,48	RNA	40
3	TOB	62,1	ng/µl	1,553	0,803	1,93	1,49	RNA	40
4	TOF	582	ng/µl	14,549	7,043	2,07	1,96	RNA	40
5	PTB	67,3	ng/µl	1,683	0,924	1,82	1,25	RNA	40
6	PTF	332,1	ng/µl	8,303	4,038	2,06	1,76	RNA	40
7	IKB	56,7	ng/µl	1,416	0,746	1,9	1,41	RNA	40
8	IKF	438,1	ng/µl	10,952	5,351	2,05	1,91	RNA	40
9	NMB	74	ng/µl	1,851	0,962	1,92	1,14	RNA	40
10	NMF	985,7	ng/µl	24,642	11,878	2,07	1,47	RNA	40
11	EMB	33,8	ng/µl	0,845	0,449	1,88	1,01	RNA	40
12	EMF	774,6	ng/µl	19,365	9,452	2,05	2,09	RNA	40
13	SCB	99,7	ng/µl	2,493	1,271	1,96	0,3	RNA	40
14	SCF	24,1	ng/µl	0,602	0,388	1,55	0,08	RNA	40
15	PNB	82,2	ng/µl	2,055	1,016	2,02	1,46	RNA	40
16	PNF	502,3	ng/µl	12,558	5,977	2,1	1,95	RNA	40
17	ELB	242,3	ng/µl	6,059	2,972	2,04	0,77	RNA	40
18	ELF	433,1	ng/µl	10,827	5,296	2,04	1,83	RNA	40
19	MDB	66,7	ng/µl	1,668	0,907	1,84	0,26	RNA	40
20	MDF	145,2	ng/µl	3,629	1,779	2,04	1,67	RNA	40
21	RMB	116,4	ng/µl	2,91	1,424	2,04	1,36	RNA	40
22	RMF	454,8	ng/µl	11,37	5,518	2,06	1,83	RNA	40
23	EUMB	179,2	ng/µl	4,481	2,191	2,04	1,81	RNA	40
24	EUMF	1173,4	ng/µl	29,334	14,082	2,08	2,1	RNA	40
25	SHB	72,3	ng/µl	1,808	0,914	1,98	1	RNA	40
26	SHF	295,4	ng/µl	7,385	3,586	2,06	1,84	RNA	40

Appendix 8A. Selected pages from Agilent RNA 6000 Nano Kit.



Agilent
RNA 6000 Nano
Kit Guide

Agilent Technologies

6 Place electrode cleaner in the Agilent 2100 bioanalyzer.

7 Close the lid and leave it closed for about 10 seconds.

8 Open the lid and remove the electrode cleaner. Label it and keep it for further use.

9 Wait another 10 seconds for the water on the electrodes to evaporate before closing the lid.

Preparing the Gel

1 Allow all reagents to equilibrate to room temperature for 30 minutes before use.

2 Place 550 µl of Agilent RNA 6000 Nano gel matrix (red ●) into the top receptacle of a spin filter.

3 Place the spin filter in a microcentrifuge and spin for 10 minutes at 1500 g ± 20 % (for Eppendorf microcentrifuge, this corresponds to 4000 rpm).

4 Aliquot 65 µl filtered gel into 0.5 ml RNase-free microfuge tubes that are included in the kit. Store the aliquots at 4 °C and use them within one month of preparation.

Preparing the Gel-Dye Mix

WARNING *Handling DMSO*

Kit components contain DMSO. Because the dye binds to nucleic acids, it should be treated as a potential mutagen and used with appropriate care.

⇒ Wear hand and eye protection and follow good laboratory practices when preparing and handling reagents and samples.

⇒ Handle the DMSO stock solutions with particular caution as DMSO is known to facilitate the entry of organic molecules into tissues.

1 Allow all reagents to equilibrate to room temperature for 30 minutes before use. Protect the dye concentrate from light while bringing it to room temperature.

2 Vortex RNA 6000 Nano dye concentrate (blue ●) for 10 seconds and spin down.

3 Add 1 µl of RNA 6000 Nano dye concentrate (blue ●) to a 65 µl aliquot of filtered gel (prepared as described in "Preparing the Gel" on page 14).

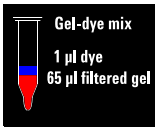

4 Cap the tube, vortex thoroughly and visually inspect proper mixing of gel and dye. Store the dye concentrate at 4 °C in the dark again.

5 Spin tube for 10 minutes at room temperature at 13000 g (for Eppendorf microcentrifuge, this corresponds to 14000 rpm). Use prepared gel-dye mix within one day.

NOTE A larger volume of gel-dye mix can be prepared in multiples of the 65+1 ratio, if more than one chip will be used within one day. Always re-spin the gel-dye mix at 13000 g for 10 minutes before each use.

Loading the Gel-Dye Mix

NOTE Before loading the gel-dye mix, make sure that the base plate of the chip priming station is in position (C) and the adjustable clip is set to the top position. Refer to "Setting up the Chip Priming Station" on page 7 for details.

1 Allow the gel-dye mix to equilibrate to room temperature for 30 minutes before use and protect the gel-dye mix from light during this time.

2 Take a new RNA Nano chip out of its sealed bag .

3 Place the chip on the chip priming station.

4 Pipette 9.0 µl of the gel-dye mix at the bottom of the well marked ⊙ and dispense the gel-dye mix.



NOTE When pipetting the gel-dye mix, make sure not to draw up particles that may sit at the bottom of the gel-dye mix vial. Insert the tip of the pipette to the bottom of the chip well when dispensing. This prevents a large air bubble forming under the gel-dye mix. Placing the pipette at the edge of the well may lead to poor results.

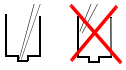

5 Set the timer to 30 seconds, make sure that the plunger is positioned at 1 ml and then close the chip priming station. The lock of the latch will click when the Priming Station is closed correctly.

6 Press the plunger of the syringe down until it is held by the clip.

7 Wait for exactly 30 seconds and then release the plunger with the clip release mechanism.

8 Visually inspect that the plunger moves back at least to the 0.3 ml mark.

9 Wait for 5 seconds, then slowly pull back the plunger to the 1 ml position.

10 Open the chip priming station.

11 Pipette 9.0 µl of the gel-dye mix in each of the wells marked.



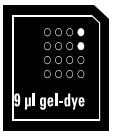

NOTE Please discard the remaining vial with gel-dye mix.

Loading the RNA 6000 Nano Marker

1 Pipette 5 µl of the RNA 6000 Nano marker (green ●) into the well marked with the ladder symbol and each of the 12 sample wells.



NOTE Do not leave any wells empty or the chip will not run properly. Unused wells must be filled with 5 µl of the RNA 6000 Nano marker (green ●) plus 1 µl of the buffer in which the samples are diluted.

Loading the Ladder and Samples

NOTE Always use RNase-free microfuge tubes, pipette tips and water.

1 Before use, thaw ladder aliquots and keep them on ice (avoid extensive warming upon thawing process)

2 To minimize secondary structure, heat denature (70 °C, 2 minutes) the samples before loading on the chip.

3 Pipette 1 µl of the RNA ladder into the well marked with the ladder symbol .

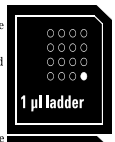

4 Pipette 1 µl of each sample into each of the 12 sample wells.

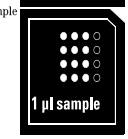

CAUTION *Wrong vortexing speed*

If the vortexing speed is too high, liquid spill that disturbs the analysis may occur .

⇒ Reduce vortexing speed to 2000 rpm!

5 Set the timer to 60 seconds.

6 Place the chip horizontally in the adapter of the IKA vortex mixer and make sure not to damage the buldge that fixes the chip during vortexing.

If there is liquid spill at the top of the chip, carefully remove it with a tissue.

7 Vortex for 60 seconds at 2400 rpm.

8 Refer to the next topic on how to insert the chip in the Agilent 2100 bioanalyzer. Make sure that the run is started within 5 minutes.

NOTE Depending on the RNA isolation protocol, varying results can be expected. Known dependencies include: salt content, cell fixation method and tissue stain. Best results are achieved for samples which are dissolved in deionized and RNase-free water. Avoid genomic DNA contamination by including DNase treatment in the preparation protocol.

Inserting a Chip in the Agilent 2100 Bioanalyzer

1 Open the lid of the Agilent 2100 bioanalyzer.

2 Check that the electrode cartridge is inserted properly and the chip selector is in position (1). Refer to "Setting up the Bioanalyzer" on page 8 for details.

3 Place the chip carefully into the receptacle. The chip fits only one way.

CAUTION *Sensitive electrodes and liquid spills*

Forced closing of the lid may damage the electrodes and dropping the lid may cause liquid spills resulting in bad results.

⇒ Do not use force to close the lid and do not drop the lid onto the inserted chip.

4 Carefully close the lid. The electrodes in the cartridge fit into the wells of the chip.

5 The 2100 expert software screen shows that you have inserted a chip and closed the lid by displaying the chip icon at the top left of the *Instrument* context.

Appendix 8B. RNA quality assessment using Agilent RNA 6000 Nano Kit.
Gel electrophoresis demonstrates inconsistent separation of RNA fragments for the samples (compare samples 2, 7 and 11 versus other samples in Top gel; compare samples 2 and 7 versus the other samples in Lower gel). Sample 1 in Top gel corresponds with sample 1 in Appendix 8C; sample 1 in Lower gel corresponds with sample 13 in Appendix 8C. Gels for samples 25 and 26 in Appendix 8C not shown.

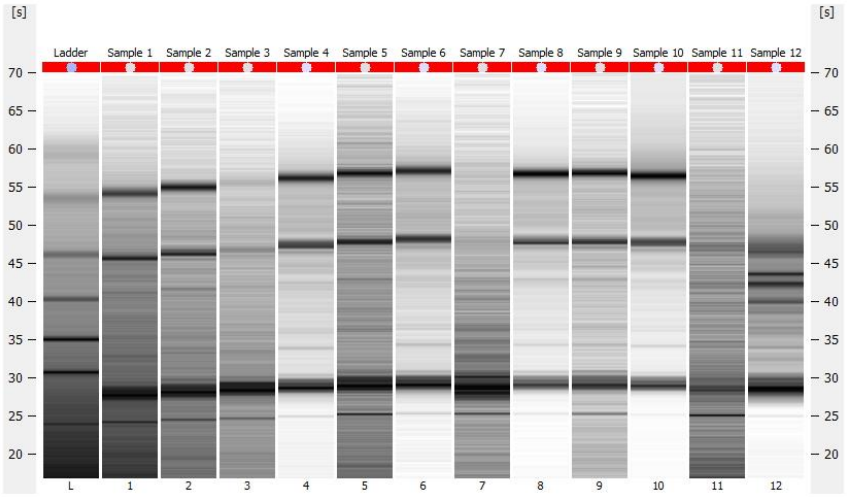

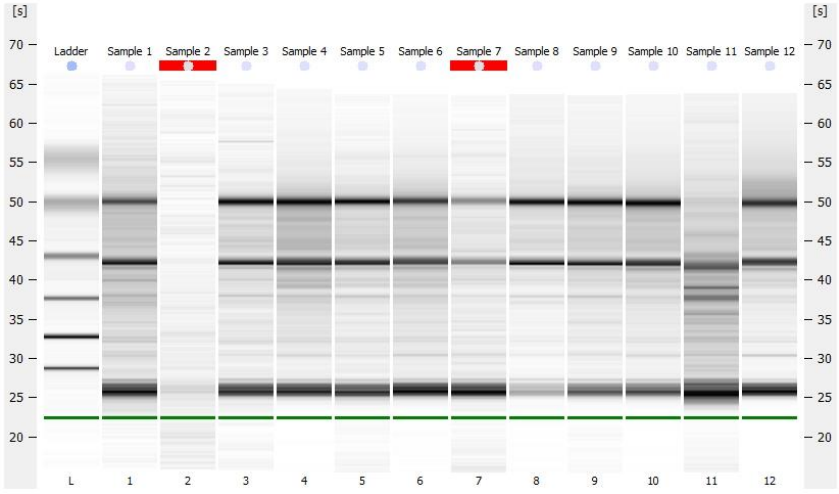

Appendix 8C. Agilent RNA Integrity Analysis.

#	Sample ID	RNA Conc. by Nanodrop	Unit	A260	A280	260/280	RNA Conc. by Bioanalyzer	Unit	RIN
1	**MNB**	107,7	ng/µl	2,692	1,353	1,99	183,65	ng/µl	ND
2	**MNF**	86,6	ng/µl	2,165	1,122	1,93	159,51	ng/µl	ND
3	**TOB**	62,1	ng/µl	1,553	0,803	1,93	177,43	ng/µl	ND
4	**TOF**	582	ng/µl	14,549	7,043	2,07	1142,53	ng/µl	5.5
5	**PTB**	67,3	ng/µl	1,683	0,924	1,82	163,95	ng/µl	ND
6	**PTF**	332,1	ng/µl	8,303	4,038	2,06	773,64	ng/µl	5.0
7	**IKB**	56,7	ng/µl	1,416	0,746	1,9	227,14	ng/µl	ND
8	**IKF**	438,1	ng/µl	10,952	5,351	2,05	1148,17	ng/µl	5.1
9	**NMB**	74	ng/µl	1,851	0,962	1,92	179,53	ng/µl	ND
10	**NMF**	985,7	ng/µl	24,642	11,878	2,07	1932,26	ng/µl	7.4
11	**EMB**	33,8	ng/µl	0,845	0,449	1,88	29,34	ng/µl	ND
12	**EMF**	774,6	ng/µl	19,365	9,452	2,05	1807,7	ng/µl	2.0
13	**SCB**	99,7	ng/µl	2,493	1,271	1,96	125,87	ng/µl	5.9
14	**SCF**	24,1	ng/µl	0,602	0,388	1,55	6,43	ng/µl	ND
15	**PNB**	82,2	ng/µl	2,055	1,016	2,02	94,9	ng/µl	7.4
16	**PNF**	502,3	ng/µl	12,558	5,977	2,1	504,01	ng/µl	6.1
17	**ELB**	242,3	ng/µl	6,059	2,972	2,04	100,58	ng/µl	7.4
18	**ELF**	433,1	ng/µl	10,827	5,296	2,04	486,68	ng/µl	5.6
19	**MDB**	66,7	ng/µl	1,668	0,907	1,84	50,41	ng/µl	ND
20	**MDF**	145,2	ng/µl	3,629	1,779	2,04	155,28	ng/µl	8.4
21	**RMB**	116,4	ng/µl	2,91	1,424	2,04	134,01	ng/µl	7.3
22	**RMF**	454,8	ng/µl	11,37	5,518	2,06	488,41	ng/µl	6.7
23	**EUMB**	179,2	ng/µl	4,481	2,191	2,04	201,31	ng/µl	3.3
24	**EUMF**	1173,4	ng/µl	29,334	14,082	2,08	1091,59	ng/µl	7.1
25	**SHB**	72,3	ng/µl	1,808	0,914	1,98	178,39	ng/µl	ND
26	**SHF**	295,4	ng/µl	7,385	3,586	2,06	227,21	ng/µl	4.4

ND= not determined; RIN = RNA Integrity Number (numbers >7.0 out of a maximum of 10 indicate good RNA integrity); although concentration estimates by the two methods were not identical, the same order of magnitude and direction was detected by both methods.

Appendix 9. Nanostring project report.



nCounter® Evaluation
Gene Expression Assay

SQ-18659

CUSTOMER	Anatech_U Wittwaterstrand
DATE	Dec 22, 2016
ASSAY	nCounter Gene Expression – MRKeir CodeSet

Summary of Project Timeline

SAMPLES RECEIVED	Nov 30, 2016 (29 RNA samples)
TIME TO RUN SAMPLES	2 days
TIME FOR ANALYSIS	<1 day
REPORT DISPATCHED	Dec 22, 2016

nanoString® TECHNOLOGIES

Dear Researcher,

We have completed the nCounter Gene Expression analysis on the samples you provided November, 2016. This report summarizes the results of your NanoString® project and suggests options for further data analysis.

Note: the data analysis presented in this report is for Quality Control purposes and to demonstrate the capabilities of the nSolver® Analysis package. The investigator should perform a thorough analysis before drawing any biological conclusions from this study.

Project Scope

29 total RNA samples were submitted to NanoString, for analysis with the Gene Expression Assay – **MRKeir** CodeSet, using 100ng (5uL) RNA per sample. Assays were performed on the nCounter MAX system.

Raw Data

Raw counts for each assay were collected using the NanoString data analysis software, nSolver, and are provided in the accompanying data file. Raw counts are derived from the RCC data files, also included with this report.

Data Analysis

Normalization of the data was also performed using nSolver for the following two methods:

- Positive control normalization: gene expression data is normalized to the mean of the POS control probes for each assay.
- RNA content normalization: gene expression data is normalized to the geometric mean of housekeeping genes in the CodeSet.

Raw data is also analyzed using the nSolver Advanced Analysis module. More information on the Advanced Analysis package can be found at **http://www.nanostring.com/products/nSolver.**

Results Summary

Based on the positive and negative control probe counts all hybridizations were successful. Gene counts are robust for these samples, and suggest gene expression differences between samples. Sample #14 produced lower than expected raw counts, suggesting low RNA concentration or degradation.

Additional analysis may be performed on your raw data using the **nSolver Analysis tool v3**, which can be downloaded at **www.nanostring.com/products/nSolver**. If you have not done so already, please register as a new customer to download the nSolver tool and manuals.

Included with this Report

- Excel file "SQ-18659 Nanostring_MRKeir-29 sample_Data" - this file contains multiple sheets:
  1. Raw data: unprocessed counts derived from the RCC data files
  2. POS-Gene Normalized data: processed by nSolver following the normalization methods mentioned above (POS control and Reference Gene normalization).
- Compressed folder containing all raw data (RCC) files, which can be analyzed in nSolver

nanoString® TECHNOLOGIES

Assay Setup & Workflow

Gene Expression Assay:

- 100ng of each RNA sample is added to the CodeSet in hybridization buffer and incubated at 65°C for 16 hours. The CodeSet consists of Reporter and Capture probes that hybridize to the target sequences of interest, forming a tripartite complex. Set up time is approximately 10 minutes for 12 assays.

Prep Station and Digital Analyzer (MAX System):

- 5 minute set up, 3 hour automated processing per cartridge on the Prep Station (High Sensitivity Protocol)
- Data acquisition from MAX System Digital Analyzer after 2.5 hour scan per cartridge

Data Analysis:

- Raw data (RCC files) are imported and analyzed in the NanoString data analysis tool nSolver
- Normalizations, Advanced Analysis, and data export to 3rd party software platforms can be performed.

Sample Hybridization



Automated assay purification on Prep Station and imaging on Digital Analyzer



Data analysis: Raw counts are compiled, normalized and analyzed using nSolver

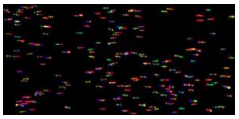

nanoString® TECHNOLOGIES

Analyzing your nCounter Data

nSolver™ Analysis Software

nSolver 3.0 with Advanced Analysis Modules

NanoString offers a free, easy-to-use software package for comprehensive analysis of your nCounter data. Here we demonstrate several examples of data analysis available in the latest update of **nSolver 3 with Universal Advanced Analysis**.

Normalization and Data QC

Pairwise Variance during HK Selection. geNorm is used to calculate a pairwise variation statistic after successive HK genes are removed. The ideal normalization gene set will minimize the pairwise variation statistic.

Normalization Summary: mRNA

The lower the MSE of reference profile the higher quality of normalization. The more positive normalization factor, the higher counts were registered for the sample and vice versa.

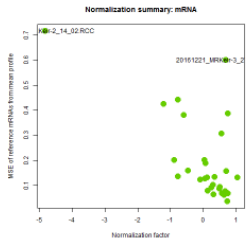

nanoString® TECHNOLOGIES

Heatmap of the normalized data, scaled to give all genes equal variance, generated via unsupervised clustering. Orange indicates high expression; blue indicates low expression. This plot is meant to provide a high level exploratory view of the data.

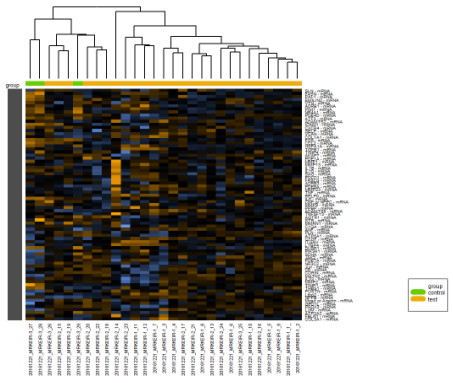

Biological Analysis

Volcano Plot: treatmentTx1

Volcano plot displaying each gene's -log10(p-value) and log2 fold change with the selected covariate. Highly statistically significant genes fall at the top of the plot, and highly differentially expressed genes fall to either side. Green point colors and horizontal lines indicate various False Discovery Rate (FDR) thresholds. The 40 most statistically significant genes are named.

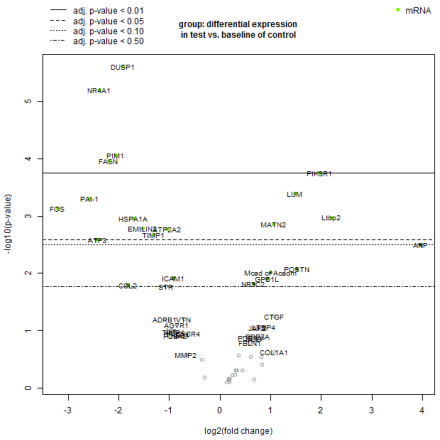

Project Conclusions

Preliminary analysis suggests these sample types produce robust data with the nCounter Gene Expression Assay, and significant gene expression differences are observed for different cell type and treatment groups.

Data can be further analyzed using the nSolver Advanced Analysis Package, as described in this report.

NanoString offers several products that may advance the findings of this proof-of-principle study, including Custom Gene Expression CodeSets, DNA Copy Number, and combined RNA-Protein analysis. We would be pleased to discuss how NanoString can further your research objectives. Please contact us at support@nanostring.com.

Regards,

NanoString Evaluation Project Team

Appendix 10. Genes selected for analysis.

Gene	Accession No	Primary Publication	Name/Alternative name	Major Role	Description (source: www.ncbi.nlm.nih.gov/gene)
ADAMTS2	NM_021599.2	Chen *et al.*[1]	a disintegrin and metalloproteinase with thrombospondin motifs 8	ECM remodelling	Encoded preproprotein is proteolytically processed into the mature procollagen N-proteinase, which proteolytically excises of the N-propeptide of the fibrillar procollagens types I-III and type V.
ADAMTS8	NM_007037.4	Chen *et al.*[1]	ADAMTS 2	ECM remodelling	Preproprotein: mature enzyme, disrupts angiogenesis.
ADRB1	NM_000684.1	Bristow *et al.*[2]	β-adrenergic receptor-1	β-adrenergic signalling	See Chapter 1
ADRB2	NM_000024.3	Engelhardt *et al.*[3]	β-adrenergic receptor-2	β-adrenergic signalling	See Chapter 1
ADRB3	NM_000025.1		β-adrenergic receptor-3	β-adrenergic signalling	See Chapter 1
ADRBK1	NM_001619.2		GRK2 or BARK1 or β adrenergic receptor kinase 1	β-adrenergic signalling	See Chapter 4 and 5 Discussion
ADRBK2	NM_005160.2		GRK3 or BARK2 or β adrenergic receptor kinase 2	β-adrenergic signalling	See Chapter 4 and 5 Discussion
AGT	NM_000029.3	Chen *et al.*[1]	angiotensinogen	Renin-angiotensin aldosterone system (RAAS)	Encodes angiotensinogen precursor protein. The resulting product, angiotensin I, is then cleaved by angiotensin converting enzyme to generate the active enzyme angiotensin II.
AGTR1	NM_000685.3		Angiotensin II receptor 1	RAAS	Encodes the type 1 angiotensin receptor: mediates the major cardiovascular effects of angiotensin II.
AKAP7	NM_016377.3	Zheng et *al.*[4]	A-kinase anchoring protein 7	Cardiac β-AR signalling; cAMP-mediating signaling	Encodes a member of the A-kinase anchoring protein (AKAP) family, a group of functionally related proteins that bind to a regulatory subunit of cAMP-dependent protein kinase A (PKA) and target the enzyme to specific subcellular compartments.
ANF	NM_006172.2	Zheng et al[4]	ANF = NPPA = atrial natriuretic factor/peptide	Heart failure; Atrial mechanical overload	ANP is released by atrial myocytes in response to high blood volume. Result: 1) increased renal excretion of salt and water, 2) vasodilation, and 3) increased vascular permeability.
ARRB1	NM_004041.3	Wisler *et al.*[5]	β-1-Arrestin	β-adrenergic signalling; Anti-apoptosis	See Chapter 5 Discussion
ARRB2	NM_004313.3	Wisler *et al.*[5]	β-2-Arrestin	β-adrenergic signalling; Anti-apoptosis	See Chapter 5 Discussion
ATF3	NM_001674.2	Zheng et *al.*;[4] Zheng et *al.*[6]	activating transcription factor 3 OR cAMP responsive element-binding (CREB)	Cell survival	Encodes a member of the mammalian ATF/CREB protein family of transcription factors. Involved in the complex process of cellular stress response.
ATP2A2	NM_001681.3	Leszek *et al.*;[7] Zheng et *al.*[4]	SERCA 2; ATPase sarcoplasmic/endoplasmic reticulum Ca transporting 2	Myocyte calcium handling	Encodes one of the SERCA Ca^{2+}-ATPases, which are intracellular pumps located in the sarcoplasmic or endoplasmic reticula of muscle cells. It is involved in regulation of the contraction/relaxation cycle.
ATP5A1	NM_001001937.1	Chen *et al.*[1]	ATP synthase, H+ transporting, mitochondrial F1 complex, α subunit 1, cardiac muscle	Cellular bioenergetics	Encodes a subunit of mitochondrial ATP synthase. Mitochondrial ATP synthase catalyzes ATP synthesis, using an electrochemical gradient of protons across the inner membrane during oxidative phosphorylation.
Bcl6	NM_138931.1	Chen *et al.*[1]	B-cell CLL/lymphoma 6	Cell survival	Encodes a transcriptional repressor protein; modulates the transcription of STAT-dependent responses.
C1QA	NM_015991.2	Zheng et *al.*;[6] Chen *et al.*[1]	Complement C1q A chain	Complement activation	Associates with C1r and C1s to yield the first component of the serum complement system.

C6	NM_000065.2	Chen *et al.*;[1] Zheng et *al.*[4]	Complement component 6	Complement activation	It is part of the membrane attack complex that causes cell lysis.
CASP1	NM_001223.3		Cysteine-aspartic acid protease (Caspase)-1	Apoptosis	Sequential activation of caspases plays central role in the execution-phase of cell apoptosis.
CASP10	NM_001230.4		Cysteine-aspartic acid protease (Caspase)-10	Apoptosis	Sequential activation of caspases plays central role in the execution-phase of cell apoptosis.
CCL2	NM_002982.3	Chen *et al.*[1]	C-C motif chemokine ligand 2	Chemotaxis	Encodes a chemokine (secreted proteins involved in immunoregulatory and inflammatory processes). This protein binds to chemokine receptors CCR2 and CCR4.
CNP or NPPC	NM_024409.2		Natriuretic peptide C	Heart failure	Encodes a preproprotein belonging to the natriuretic family of peptides. The encoded peptides exhibit vasorelaxation activity in laboratory animals; elevated levels observed heart failure patients.
COL1A1	NM_000088.3	Chen *et al.*[1]	Collagen type I α 1 chain	ECM protein	Encodes the pro-α1 chains of type I collagen.
COL3A1	NM_000090.3	Chen *et al.*;[1] Zheng et *al.*[6]	Collagen type III α 1 chain	ECM protein	Encodes the pro-α1 chains of type III collagen.
COL4A1	NM_001845.4	Chen *et al.*[1]	Collagen type IV α chain	ECM protein	Encodes a type IV collagen α protein, which are integral components of basement membranes. It interacts with other extracellular matrix components such as perlecans, proteoglycans, and laminins.
COL5A2	NM_000393.3	Zheng et *al.*[6]	Collagen type V α 2 chain	ECM protein	Encodes an α chain of collagen V. Type V collagen is found in tissues containing type I collagen and appears to regulate the assembly of heterotypic fibers composed of both type I and type V collagen.
CORIN	NM_006587.2	Zheng et *al.*[4]	Corin,serine peptidase	Heart failure	Converts pro-ANP to biologically active ANP. It may also function as a pro-BNP convertase.
CSF1R	NM_005211.2	Zheng et *al.*[6]	Colony stimulating factor 1 receptor	Inflammatory cell proliferation and activation	Controls the production, differentiation, and function of macrophages. It is a tyrosine kinase transmembrane receptor and member of the CSF1/PDGF receptor family of tyrosine-protein kinases.
CTGF	NM_001901.2	Zheng et *al.*;[4] Zheng et *al.*;[6] Chen *et al.*[1]	Connective tissue growth factor	Regulation of ECM production	Encodes a mitogen that is secreted by vascular endothelial cells. It plays a role in cell adhesion in many cell types, and is related to platelet derived growth factor.
CXCR4	NM_003467.2	Zheng et *al.*;[6] Chen *et al.*[1]	Chemokine (C-X-C motif) receptor 4	Chemotaxis	Encodes a CXC chemokine receptor specific for stromal cell-derived factor-1.
DCN	NM_001920.3	Zheng et *al.*;[6] Chen *et al.*[1]	Decorin	Non-collagen ECM remodelling; ECM structure	Plays a role in collagen fibril assembly. Binding of this protein to multiple cell surface receptors mediates its role in tumor suppression, including a stimulatory effect on autophagy and inflammation and an inhibitory effect on angiogenesis and tumorigenesis.
DUSP1	NM_004417.2	Zheng et *al.*[4]	dual specificity phosphatase 1	Cell survival	Encodes a protein with structural features similar to members of the non-receptor-type protein-tyrosine phosphatase family, and which has significant amino-acid sequence similarity to a Tyr/Ser-protein phosphatase. DUSP1 can suppress the activation of MAP kinase-1 and 8 (also called p38 and JNK, respectively), and may play an important role in the human cellular response to environmental stress as well as in the negative regulation of cellular proliferation.
EMILIN2	NM_032048.2	Zheng et *al.*[4]	Elastin microfibril interfacer 2	ECM structure; ECM glycoprotein	Extracellular matrix glycoprotein.
FADD	NM_003824.2		Fas associated via death domain	Apoptosis	Encodes an adaptor protein that interacts with various cell surface receptors and mediates cell apoptotic signals. Through its C-terminal death domain, it can be recruited by TNFRSF6/Fas-receptor, TNF receptor, TNFRSF25, and TNFSF10/TRAIL-receptor, and thus it participates in the death signalling initiated by these receptors. Recruits caspase-8 thereby activating the cysteine protease cascade.
FAS	NM_152876.1		Fas cell surface death receptor	Apoptosis	Encodes a member of the TNF-receptor superfamily, and contains a death domain. It plays a central role in the physiological regulation of programmed cell death. The receptor-ligand interaction allows the formation of a death-inducing signalling complex that includes FADD, caspase 8, and caspase 10. It can also activate NF-kappaB, MAPK3/ERK1, and MAPK8/JNK.

FASLG	NM_000639.1		Fas ligand	Apoptosis	Is a member of the TNF superfamily. The primary function of the encoded transmembrane protein is the induction of apoptosis triggered by binding to FAS.
FASN	NM_004104.4	Chen *et al.*[1]	Fatty acid synthase	Cellular bioenergetics	Catalyzes the synthesis of palmitate from acetyl-CoA and malonyl-CoA, in the presence of NADPH, into long-chain saturated fatty acids.
FBLN1	NM_006487.2	Zheng et *al.*;[6] Chen *et al.*[1]	Fibulin 1	ECM structure	ECM glycoprotein.
FBN1	NM_000138.3	Zheng et *al.*;[6] Chen *et al.*[1]	Fibrillin 1	ECM structure	Fibrillin-1 is an ECM glycoprotein that serves as a structural component of Ca^{2+}-binding microfibrils, which provide force-bearing structural support in elastic and nonelastic connective tissue throughout the body.
FOS	NM_005252.2	Zheng et *al.*[4]	Fos	Cell survival; Acute phase response signalling	c-Fos is a proto-oncogene.
GPD1L	NM_015141.3	Zheng et *al.*[4]	glycerol-3-phosphate dehydrogenase 1-like	Myocyte function	Encodes a protein that catalyzes the conversion of sn-glycerol 3-phosphate to glycerone phosphate. It is found in the cytoplasm, associated with the plasma membrane, where it binds the sodium channel, voltage-gated, type V, α subunit (SCN5A). Defects in this gene are a cause of Brugada syndrome type 2 (BRS2) as well as sudden infant death syndrome (SIDS).
HSPA1A	NM_005345.5	Zheng et *al.*[4]	heat shock 70kDa protein 1A	Cellular stress response	Stabilizes existing proteins against aggregation and mediates the folding of newly translated proteins in the cytosol and in organelles. Involved in the ubiquitin-proteasome pathway.
ICAM1	NM_000201.2	Zheng et *al.*;[6] Chen *et al.*[1]	Intercellular adhesion inhibitor type 1	Cell adhesion	Encodes a cell surface glycoprotein, which is typically expressed on endothelial cells and cells of the immune system. It binds to integrins of type CD11a / CD18, or CD11b / CD18.
IL10	NM_000572.2		Interleukin 10	Anti-inflammatory	Encodes a cytokine protein produced primarily by monocytes. Has pleiotropic effects in immunoregulation and inflammation. It down-regulates the expression of Th1 cytokines, MHC class II Ags, and costimulatory molecules on macrophages. It also enhances B cell survival, proliferation, and antibody production. It can block NF-kappa B activity, and is involved in the regulation of the JAK-STAT signalling pathway.
IL1B	NM_000576.2	Chen *et al.*[1]	Interleukin 1 β	Pro-inflammation	This cytokine is an important mediator of the inflammatory response, and is involved in a variety of cellular activities, including cell proliferation, differentiation, and apoptosis.
IL1R1	NM_001320984.1	Shah & Januzzi[8]	ST2	Ventricular biomechanical overload - cardioprotective signalling	Encodes a member of the interleukin 1 receptor family.
IL33	NM_033439.2	Shah & Januzzi[8]	ST2 ligand	Ventricular biomechanical overload - cardioprotective signalling	Encodes a cytokine that binds to the IL1RL1/ST2 receptor. It is involved in the maturation of Th2 cells and the activation of mast cells, basophils, eosinophils and natural killer cells.
IL6	NM_000600.3	Zheng et *al.*[4]	Interleukin 6	Acute phase response signalling	Encodes a pro-inflammatory cytokine that functions in inflammation and the maturation of B cells.
ITGAV	NM_002210.2	Zheng et *al.*[6]	Integrin subunit α 5	ECM structure	Encodes an integrin α chain family member involved in cell surface adhesion and signalling. The heterodimer consisting of αV and β3 subunits is also known as the vitronectin receptor.
JAK2	NM_004972.3	Chen *et al.*[1]	Janus kinase 2	Regulation of inflammatory response	Encodes a protein tyrosine kinase involved in a specific subset of cytokine receptor signalling pathways.
Jun	NM_002228.3	Zheng et *al.*[4]	Jun protooncogene	Cell survival; Acute phase response signalling	In combination with c-Fos, forms the AP-1 early response transcription factor. It is activated through double phosphorylation by the JNK pathway.
KITLG	NM_003994.4	Zheng et *al.*[6]	Stem cell factor (SCF)	Cell survival	KIT-ligand is a pleiotropic factor that acts in hematopoiesis. It promotes mast cell adhesion, migration, proliferation, and survival. Its cardiomyocyte-specific overexpression has been found to improve cardiac function and animal survival after myocardial infarction.

LTBP4	NM_003573.2	Chen *et al.*[1]	Latent transforming growth factor β binding protein 4	Regulation of ECM production	Encodes a protein that binds transforming growth factor β as it is secreted and targeted to the extracellular matrix.
LUM	NM_002345.3	Zheng *et al.*[6]	Lumican	ECM structure	Encodes a member of the small leucine-rich proteoglycan (SLRP) family that includes decorin, biglycan, fibromodulin, keratocan, epiphycan, and osteoglycin. Lumican is the major keratan sulfate proteoglycan of the cornea but is also distributed in interstitial collagenous matrices throughout the body. Lumican may regulate collagen fibril organization and circumferential growth, corneal transparency, and epithelial cell migration and tissue repair.
LTBP2	NM_000428.2	Zheng *et al.*;[6] Chen *et al.*[1]	Latent transforming growth factor β binding protein 2	Regulation of ECM production	Encodes a protein encoded belonging to the family of latent TGF-β binding proteins (LTBP), which are extracellular matrix proteins. It is the largest member of the LTBP family possessing unique regions and with most similarity to the fibrillins.
MAPK1	NM_138957.2		Mitogen-activated protein kinase 1; p38; ERK	B1AR receptor-triggered apoptosis pathway	MAP kinases, also known as extracellular signal-regulated kinases (ERKs), act as an integration point for multiple biochemical signals, and are involved in a wide variety of cellular processes such as proliferation, differentiation, transcription regulation and development. Its activation requires its phosphorylation by upstream kinases, this causes it to phosphorylate nuclear targets.
MAPK8	NM_002750.2		Mitogen-activated protein kinase 8; JNK; JNK1	TNF-α-induced apoptosis	The activation of this kinase by TNF-α is found to be required for TNF-α induced apoptosis.
MATN2	NM_002380.3	Chen *et al.*[1]	Matrilin 2	Non-collagen ECM structure	Involved in the formation of filamentous networks in the extracellular matrices of various tissues.
MMP1	NM_002421.3	Zheng *et al.*[6]	Matrix metalloproteinase 1	ECM remodelling	Matrix metalloproteinases (MMPs) are a heterogeous family of enzymes responsible for the proteolysis of various protein-based extracellular substances. See Chapter 1.
MMP13	NM_002427.2		Matrix metalloproteinase 13	ECM remodelling	See MMP1
MMP2	NM_004530.2	Chen *et al.*[1]	Matrix metalloproteinase 2	ECM remodelling	See MMP1
MMP23	NM_006983.1	Chen *et al.*[1]	Matrix metalloproteinase 23	ECM remodelling	See MMP1
MMP9	NM_004994.2	Zheng *et al.*[6]	Matrix metalloproteinase 9	ECM remodelling	See MMP1
MMRN1	NM_007351.2	Zheng *et al.*[6]	Multimerin 1 or MMRN 1	ECM structure	Is a massive, soluble protein found in platelets and in the endothelium of blood vessels. It may also have functions as an ECM or adhesive protein.
MYD88	NM_002468.3	Chen *et al.*[1]	Myeloid differentiation primary response 88	Positive regulation of IK-B kinase/NFKB cascade	Encodes a cytosolic adapter protein that plays a central role in the innate and adaptive immune response. It functions as an essential signal transducer in the interleukin-1 and Toll-like receptor signalling pathways, which regulate the activation of numerous proinflammatory genes.
Mcad or Acadm	NM_000016.5	Chen *et al.*[1]	acyl-CoA dehydrogenase, C-4 to C-12 straight chain	Faty acid β-oxidation in mitochondria	Encodes the medium-chain specific acyl-Coenzyme A dehydrogenase. The homotetramer enzyme catalyzes the initial step of the mitochondrial fatty acid β-oxidation pathway.
NFKB1	NM_003998.2		nuclear factor kappa B subunit 1	Inflammation	NFKB is a transcription regulator that is activated by various intra- and extra-cellular stimuli such as cytokines, oxidant-free radicals, ultraviolet irradiation, and bacterial or viral products. Activated NFKB translocates into the nucleus and stimulates the expression of genes involved in a wide variety of biological functions.
NPPB	NM_002521.2	Zheng *et al.*[4]	NPPB = BNP = brain natriuretic factor	Heart failure; Ventricular biomechanical overload	BNP secreted by the ventricles of the heart in response to excessive cardiomyocyte stretch. The physiologic actions of BNP are similar to those of ANP.
NR3C2	NM_000901.3	Zheng *et al.*[4]	nuclear receptor subfamily 3, member 2	Mineralocorticoid receptor	Encodes the mineralocorticoid receptor, which mediates aldosterone actions on salt and water balance within restricted target cells.
NR4A1	NM_173157.1	Zheng *et al.*[4]	nuclear receptor subfamily A, group A, member 1	Apoptosis	The encoded protein acts as a nuclear transcription factor. Translocation of the protein from the nucleus to mitochondria induces apoptosis.

PAI-1	NM_000602.4	Zheng et *al.*;[6] Chen et *al.*[1]	Plasminogen activator inhibitor type 1	Positive regulation of immune response; ECM degradation and synthesis	PAI-1 is a serine protease inhibitor that functions as a principal inhibitor of plasminogen activators that promotes fibrosis by preventing MMP activation and ECM degradation by plasminogen activators and plasmin.
PDCD1	NM_005018.2	Zheng et *al.*[4]	Programmed cell death 1	Apoptosis	PD-1 is involved in apoptosis.
PDE1A	NM_005019.3	Zheng et *al.*[4]	phosphodiesterase 1A, calmodulin-dependent	Cardiac β-AR signalling; cAMP-mediating signalling; G-protein couple receptor signalling	Cyclic nucleotide phosphodiesterases (PDEs) regulate intracellular cyclic nucleotide concentrations through hydrolysis of cAMP and/or cGMP to their respective nucleoside 5-prime monophosphates. Members of the PDE1 family, such as PDE1A, are Ca^{2+}/calmodulin-dependent PDEs that are activated by calmodulin in the presence of Ca^{2+}.
PDE4D	NM_006203.4	Zheng et *al.*;[4] Zheng et *al.*[6]	phosphodiesterase 4D	Cardiac β-AR signalling; cAMP-mediating signalling	The encoded protein has 3',5'-cyclic-AMP phosphodiesterase activity and degrades cAMP, which acts as a signal transduction molecule in multiple cell types. See Chapter 5.
PDE6A	NM_000440.2	Zheng et *al.*[4]	phosphodiesterase 6A	Cardiac β-AR signalling; cAMP-mediating signalling; G-protein couple receptor signalling	This gene encodes the cyclic-GMP (cGMP)-specific phosphodiesterase 6A α subunit.
PDE7A	NM_002603.2	Zheng et *al.*[4]	phosphodiesterase 7A	Cardiac β-AR signalling; cAMP-mediating signalling; G-protein couple receptor signalling	By regulating the cellular concentration of cAMP, this protein plays a key role in many important physiological processes.
PDGFA	NM_002607.5		platelet derived growth factor subunit A	Inflammation; Angiogenesis	Binds and activates PDGF receptor tyrosine kinases, which play a role in a wide range of developmental processes.
PIK3R1	NM_181504.2	Zheng et *al.*[4]	Phosphoinositide-3-kinase, regulatory subunit 1	G-protein couple receptor signalling; acute phase response signalling; cell survival	Phosphatidylinositol 3-kinase (PIK3) plays an important role cell survival and proliferation. PIK3R1 encodes a PIK3 regulatory protein.
PIM1	NM_002648.2	Zheng et *al.*[4]	pim-1 oncogene	Cell survival	Encodes a protein belonging to the Ser/Thr protein kinase family, and PIM subfamily. It plays a role in signal transduction in blood cells, contributing to both cell proliferation and survival, and thus provides a selective advantage in tumorigenesis.
PLN	NM_002667.3	Zheng et *al.*[4]	PLN=PLB=Phospholamban;	Myocyte calcium handling	It is a major substrate for the cAMP-dependent PKA in cardiac muscle. It is an inhibitor of SERCA2 in the unphosphorylated state, but inhibition is relieved upon its phosphorylation.
POSTN	NM_001135935.1	Chen et *al.*[1]	Periostin	Matricellular protein	Encodes a secreted ECM protein that functions in ventricular remodelling following myocardial infarction. It binds to integrins to support adhesion and migration of epithelial cells.
PPARA	NM_001001928.2	Chen et *al.*[1]	Peroxisome proliferator activated receptor α	Cellular bioenergetics	PPARs affect the expression of target genes involved in cell proliferation, cell differentiation and in immune and inflammation responses. PPAR-α is a nuclear transcription factor.
PPBP	NM_002704.2	Zheng et *al.*[6]	Proplatelet basic protein (chemokine (CXC motif) ligand 7)	Chemotaxis	Encodes a PDGF that belongs to the CXC chemokine family. It has been shown to stimulate various cellular processes including DNA synthesis, mitosis, glycolysis, intracellular cAMP accumulation, prostaglandin E2 secretion, and synthesis of hyaluronic acid and sulfated glycosaminoglycan.
PRDX3	NM_014098.3	Zheng et *al.*[4]	Peroxiredoxin 3	Cell proliferation and antioxidant function	Regulates apoptotic signalling by mitochondria.
SAG	NM_000541.4		S-antigen visual arrestin	β-adrenergic signalling	See Chapter 5.
SELL	NR_029467.1	Zheng et *al.*[6]	L-selectin	Chemotaxis	Encodes a cell surface adhesion molecule that belongs to a family of adhesion/homing receptors. It is required for binding and subsequent rolling of leucocytes on endothelial cells, facilitating their migration into secondary lymphoid organs and inflammation sites.
SELP	NM_003005.2	Zheng et *al.*[6]	Cell adhesion molecule (GMP 140)	Chemotaxis	Encodes a protein that is stored in the α-granules of platelets and endothelial cells. It mediates the interaction of activated endothelial cells or platelets with leukocytes.

SLN	NM_003063.2	Zheng et *al.*[4]	Sarcolipin - SERCA regulatory protein; predominantly expressed in normal atria	Myocyte calcium handling	This gene encodes a small proteolipid that regulates several sarcoplasmic reticulum Ca^{2+}-ATPases. The transmembrane protein interacts with Ca^{2+}-ATPases and reduces the accumulation of Ca^{2+} in the sarcoplasmic reticulum without affecting the rate of ATP hydrolysis.
STAT1	NM_139266.1	Wagner et *al.*,[9] Wang et *al.*[10]	Signal transducer and activator of transcription 1	Regulation of inflammatory response; cell survival	In response to cytokines and growth factors, STAT family members are phosphorylated by the receptor-associated kinases, and then form homo- or heterodimers that translocate to the cell nucleus where they act as transcription activators. This protein can be activated by various ligands including interferon-α, interferon-gamma, EGF, PDGF and IL6. It mediates the expression of a variety of genes, which is thought to be important for cell viability in response to different cell stimuli.
STAT3	NM_003150.3	Chen et *al.*;[1] Zhang *et al.*[11]	Signal transducer and activator of transcription 3	Regulation of inflammatory response; cell survival	This STAT protein product is activated through phosphorylation in response to various cytokines and growth factors including IFNs, EGF, IL5, IL6, HGF, LIF and BMP2. It mediates the expression of a variety of genes in response to cell stimuli, and thus plays a key role in many cellular processes such as cell growth and apoptosis.
TGFβ1	NM_000660.3	Chen et *al.*[1]	transforming growth factor β 1	Regulation of ECM production; Anti-inflammation	TGF-β1 regulates cell proliferation, differentiation and growth, and can modulate expression and activation of other growth factors including interferon gamma and TNF α.
TGFβ2	NM_003238.2	Zheng et *al.*;[6] Chen et *al.*[1]	transforming growth factor β 2	Regulation of ECM production; regulation of inflammatory response	Encodes a secreted ligand of the TGF-β superfamily of proteins. Ligands of this family bind various TGF-β receptors leading to recruitment and activation of SMAD family transcription factors that regulate gene expression.
TGFβ3	NM_003239.2	Zheng et *al.*[6]	transforming growth factor β 3	Regulation of ECM production; regulation of inflammatory response	This protein is involved in embryogenesis and cell differentiation, and may play a role in wound healing.
TGFβR1	NM_004612.2		transforming growth factor β receptor 1	Regulation of ECM production; regulation of inflammatory response	Important in ECM regulation. Mutations in this gene have been associated with Loeys-Dietz aortic aneurysm syndrome.
TGFβR2	NM_001024847.1		transforming growth factor β receptor 2	ECM regulation; Cell proliferation	Important in ECM regulation. Mutations in this gene have been associated with Marfan Syndrome, Loeys-Deitz Aortic Aneurysm Syndrome, and the development of various types of tumors.
TGFβR3	NM_003243.3		transforming growth factor β receptor 3	ECM regulation	Membrane proteoglycan that often functions as a co-receptor with other TGF-β receptor superfamily members. Decreased expression of this receptor has been observed in various cancers.
THBS1	NM_003246.2	Zheng et *al.*;[4] Zheng et *al.*[6]	thrombospondin 1	ECM remodelling; ECM degradation and synthesis	Encodes an adhesive glycoprotein that mediates cell-to-cell and cell-to-matrix interactions. This protein can bind to fibrinogen, fibronectin, laminin, type V collagen and integrins α-V/β-1.
TIMP1	NM_003254.2	Chen et *al.*[1]		ECM remodelling	Tissue inhibitors of metalloproteinases (TIMPs) are low-molecular-weight proteins that bind to the catalytic domain of active MMPs preventing substrate binding. There are 4 species of TIMPs with overlapping functions within the myocardium, which are not restricted to MMP inhibition.
TIMP2	NM_003255.4	Chen et *al.*[1]		ECM remodelling	TIMP-2 also increases collagen production by fibroblasts.
TIMP3	NM_000362.4	Chen et *al.*[1]		ECM remodelling	TIMP-3 also is responsible for fibroblast apoptosis.
TIMP4	NM_003256.2			ECM remodelling	See TIMP1.
TLR4	NM_138554.2	Chen et *al.*;[1] Zheng et *al.*[6]	Toll like receptor 4	Positive regulation of IK-B kinase/NFKB cascade	TLRs play a fundamental role in pathogen recognition and activation of innate immunity. Involved in signal transduction induced by lipopolysaccharide found in most gram-negative bacteria.
TNF	NM_000594.2		Tumor necrosis factor α	TNF-α signalling	Protein product is mainly secreted by macrophages. It can bind to, and thus functions through its receptors TNFRSF1A/TNFR1 and TNFRSF1B/TNFBR. It is involved in the regulation of a wide spectrum of biological processes including cell proliferation, differentiation, apoptosis, lipid metabolism, and coagulation.

TNFRSF1A	NM_001065.2		TNF receptor superfamily member 1A	TNF-α-induced apoptosis	Encodes a member of the TNF receptor superfamily of proteins. It is found in membrane-bound and soluble forms that interact with membrane-bound and soluble forms, respectively, of its ligand, TNF-α. Binding of membrane-bound TNF-α to the membrane-bound receptor induces receptor trimerization and activation, which plays a role in cell survival, apoptosis, and inflammation.
TNFRSF1B	NM_001066.2		TNF receptor superfamily member 1B	TNF-α-induced apoptosis	The encoded protein is a member of the TNF-receptor superfamily. It forms a heterocomplex with TNF-receptor 1 that mediates the recruitment of two anti-apoptotic proteins, c-IAP1 and c-IAP2. c-IAP1 is thought to potentiate TNF-induced apoptosis.
TNFSF13	NM_003808.3	Chen *et al.*[1]	Tumor necrosis factor superfamily member 13	Inflammatory cell proliferation and activation	It is a ligand for TNFRSF17/BCMA, a member of the TNF receptor family. It may induce apoptosis through its interaction with other TNF receptor family proteins.
VCAN	NM_004385.3	Zheng et *al.*[6]	Versican	ECM structure	Major component of the ECM. It is involved in cell adhesion, proliferation, proliferation, migration and angiogenesis and plays a central role in tissue morphogenesis and maintenance.
VTN	NM_000638.3	Zheng et *al.*[6]	Vitronectin	ECM structure & regulation	Vitronectin binds glycosaminoglycans, collagen, plasminogen and the urokinase-receptor. It also stabilizes the inhibitory conformation of PAI-1. By its localization in the extracellular matrix and its binding to PAI-1, vitronectin can potentially regulate the proteolytic degradation of this matrix.

ECM=extra cellular matrix.

References for Appendix 10.

1. Chen YW, Pat B, Gladden JD, et al. Dynamic molecular and histopathological changes in the extracellular matrix and inflammation in the transition to heart failure in isolated volume overload. *Am J Physiol Heart Circ Physiol* 2011; **300**(6): H2251-60.
2. Bristow MR, Minobe WA, Raynolds MV, et al. Reduced beta 1 receptor messenger RNA abundance in the failing human heart. *J Clin Invest* 1993; **92**(6): 2737-45.
3. Engelhardt S, Bohm M, Erdmann E, Lohse MJ. Analysis of beta-adrenergic receptor mRNA levels in human ventricular biopsy specimens by quantitative polymerase chain reactions: progressive reduction of beta 1-adrenergic receptor mRNA in heart failure. *Journal of the American College of Cardiology* 1996; **27**(1): 146-54.
4. Zheng J, Yancey DM, Ahmed MI, et al. Increased Sarcolipin Expression and Adrenergic Drive in Humans With Preserved Left Ventricular Ejection Fraction and Chronic Isolated Mitral Regurgitation. *Circulation: Heart Failure* 2014; **7**(1): 194-202.
5. Wisler JW, DeWire SM, Whalen EJ, et al. A unique mechanism of beta-blocker action: carvedilol stimulates beta-arrestin signaling. *Proceedings of the National Academy of Sciences of the United States of America* 2007; **104**(42): 16657-62.
6. Zheng J, Chen Y, Pat B, et al. Microarray identifies extensive downregulation of noncollagen extracellular matrix and profibrotic growth factor genes in chronic isolated mitral regurgitation in the dog. *Circulation* 2009; **119**(15): 2086-95.
7. Leszek P, Korewicki J, Klisiewicz A, et al. Reduced myocardial expression of calcium handling protein in patients with severe chronic mitral regurgitation. *Eur J Cardiothorac Surg* 2006; **30**(5): 737-43.
8. Shah RV, Januzzi JL, Jr. ST2: a novel remodeling biomarker in acute and chronic heart failure. *Curr Heart Fail Rep* 2010; **7**(1): 9-14.
9. Wagner MA, Siddiqui MA. The JAK-STAT pathway in hypertrophic stress signaling and genomic stress response. *Jakstat* 2012; **1**(2): 131-41.
10. Wang TL, Yang YH, Chang H, Hung CR. Angiotensin II signals mechanical stretch-induced cardiac matrix metalloproteinase expression via JAK-STAT pathway. *J Mol Cell Cardiol* 2004; **37**(3): 785-94.
11. Zhang W, Qu X, Chen B, et al. Critical Roles of STAT3 in beta-Adrenergic Functions in the Heart. *Circulation* 2016; **133**(1): 48-61.

Appendix 11. Genes selected from Zheng *et al.* (2014).[1]

Gene	Accession No	Description	Role	Fold change in CPMR patients
AKAP7	NM_016377.3	A-kinase anchoring protein 7	Beta-adrenergic signalling	up (exact value not published)
ANF	NM_006172.2	Atrial natriuretic factor	Volume overload	21.87
ATF3	NM_001674.2	Activating transciption factor 3	Apoptosis inhibition	-3.27
C6	NM_000065.2	Complement component 6	Complement activation	3.67
CORIN	NM_006587.2	Corin	Natriuretic peptide activation	2.3
CTGF	NM_001901.2	Connective tissue growth factor	ECM regulation	2.28
DUSP1	NM_004417.2	Dual specificity phosphatase 1	Beta-adrenergic signalling	-3.43
EMILIN2	NM_032048.2	Elastin microfibril interfacer 2	ECM glycoprotein	-3.21
FOS	NM_005252.2	Fos proto-oncogene	Cell survival	-14.95
GPD1L	NM_015141.3	Glycerol-3-phosphate dehydrogenase 1-like	Cardiomyocyte function	2.22
HSPA1A	NM_005345.5	Heat shock 70kDa protein 1A	Cellular stress response	-3.1
Jun	NM_002228.3	Jun proto-oncogene	Cell survival	-2.22
NPPB	NM_002521.2	Brain natriuretic factor	Volume overload	5.13
NR3C2	NM_000901.3	Nuclear receptor subfamily 3, member 2	Mineralocorticoid receptor	2.07
NR4A1	NM_173157.1	Nuclear receptor subfamily A, group A, member 1	Apoptosis	-4.42
PDCD1	NM_005018.2	Programmed cell death 1	Apoptosis	2.65
PDE1A	NM_005019.3	Phosphodiesterase 1A	Beta-adrenergic signalling	2.17
PDE4D	NM_006203.4	Phosphodiesterase 4D	Beta-adrenergic signalling	-2.64
PIK3R1	NM_181504.2	Phosphoinositide-3-kinase, regulatory subunit 1	Beta-adrenergic signalling	2.2
PIM1	NM_002648.2	Pim-1 oncogene	Cell survival	-4.88
PLN	NM_002667.3	Phospholamban	Myocyte calcium handling	2.54
PRDX3	NM_014098.3	Peroxiredoxin 3	Cell survival	2.75
SLN	NM_003063.2	Sarcolipin	Myocyte calcium handling	12.42
THBS1	NM_003246.2	Thrombospondin 1	ECM regulation	-2.18

Reference

1. Zheng J, Yancey DM, Ahmed MI, et al. Increased Sarcolipin Expression and Adrenergic Drive in Humans With Preserved Left Ventricular Ejection Fraction and Chronic Isolated Mitral Regurgitation. *Circulation: Heart Failure* 2014; **7**(1): 194-202.

Appendix 12. Gene expression in patients with chronic primary mitral regurgitation (CPMR) compared with normal hearts.

Gene Name	Accession #	Description	CPMR	Normal	Fold Change	P value
Extra cellular matrix remodelling						
ADAMTS2	NM_021599.2	A disintegrin and metalloproteinase with thrombospondin motifs 8	61,85	54,73	1,13	0,8193
ADAMTS8	NM_007037.4	ADAMTS 2	20,5	19,62	1,04	0,9297
COL1A1	NM_000088.3	Collagen type I α 1 chain	195,68	80,43	2,43	0,4159
COL3A1	NM_000090.3	Collagen type III α 1 chain	3234,38	2211,26	1,46	0,6059
COL4A1	NM_001845.4	Collagen type IV α chain	1597,38	1585,9	1,01	0,9851
COL5A2	NM_000393.3	Collagen type V α 2 chain	385,5	203,72	1,89	0,1082
CTGF	**NM_001901.2**	**Connective tissue growth factor**	**930,37**	**404,86**	**2,3**	**0,0802**
DCN	NM_001920.3	Decorin	8965,3	8220,64	1,09	0,7011
EMILIN2	**NM_032048.2**	**Elastin microfibril interfacer 2**	**62,25**	**218,83**	**-3,52**	**0,0160**
FBLN1	NM_006487.2	Fibulin 1	2527,52	1610,98	1,57	0,2101
FBN1	NM_000138.3	Fibrillin 1	682,62	405,69	1,68	0,2740
ITGAV	NM_002210.2	Integrin subunit α 5	1178,58	974,77	1,21	0,7152
LTBP2	**NM_000428.2**	**Latent transforming growth factor β binding protein 2**	**559,53**	**97,91**	**5,71**	**0,0070**
LTBP4	**NM_003573.2**	**Latent transforming growth factor β binding protein 4**	**1533,32**	**763,31**	**2,01**	**0,0105**
LUM	**NM_002345.3**	**Lumican**	**5898,93**	**1889,64**	**3,12**	**0,0454**
MATN2	**NM_002380.3**	**Matrilin 2**	**511,29**	**249,96**	**2,05**	**0,0677**
MMP2	NM_004530.2	Matrix metalloproteinase 2	479,69	771,2	-1,61	0,2173
MMP23	**NM_006983.1**	**Matrix metalloproteinase 23**	**8,88**	**4,04**	**2,2**	**0,0419**
MMP9	NM_004994.2	Matrix metalloproteinase 9	7,43	23,17	-3,12	0,1226
MMRN1	NM_007351.2	Multimerin 1 or MMRN 1	16,11	40,95	-2,54	0,2173
PAI-1	**NM_000602.4**	**Plasminogen activator inhibitor type 1**	**55,52**	**318,58**	**-5,74**	**0,0498**
POSTN	**NM_001135935.1**	**Periostin**	**608,64**	**193,48**	**3,15**	**0,0991**
TGFB1	NM_000660.3	Transforming growth factor β 1	192,58	144,4	1,33	0,6070
TGFB2	NM_003238.2	Transforming growth factor β 2	111,62	184,36	-1,65	0,4783
TGFB3	NM_003239.2	Transforming growth factor β 3	137,23	212,22	-1,55	0,4750
TGFBR1	NM_004612.2	Transforming growth factor β receptor 1	297,91	240,99	1,24	0,2701
TGFBR2	**NM_001024847.1**	**Transforming growth factor β receptor 2**	**986,27**	**1307,71**	**-1,33**	**0,0295**
TGFBR3	NM_003243.3	Transforming growth factor β receptor 3	173,24	229,81	-1,33	0,4627
THBS1	NM_003246.2	Thrombospondin 1	650,3	926,06	-1,42	0,6831
TIMP1	NM_003254.2	Tissue inhibitor of metalloproteinase 1	788,78	1794,36	-2,27	0,4305
TIMP2	NM_003255.4	Tissue inhibitor of metalloproteinase 2	871,76	847,35	1,03	0,8695
TIMP3	NM_000362.4	Tissue inhibitor of metalloproteinase 3	5427,95	5035,65	1,08	0,7774
TIMP4	NM_003256.2	Tissue inhibitor of metalloproteinase 4	127,31	285,85	-2,25	0,1991
VCAN	NM_004385.3	Versican	120,66	98,52	1,22	0,7732
VTN	NM_000638.3	Vitronectin	87,67	147,51	-1,68	0,1275
Beta-adrenergic signalling						
ADRB1	**NM_000684.1**	**β-adrenergic receptor-1**	**90,28**	**210,89**	**-2,34**	**0,0022**
ADRB2	NM_000024.3	β -adrenergic receptor-2	57,7	58,25	-1,01	0,9461
ADRBK1	NM_001619.2	GRK2 or BARK1 or β adrenergic receptor kinase 1	594,04	768,95	-1,29	0,1124
ADRBK2	**NM_005160.2**	**GRK3 or BARK2 or β adrenergic receptor kinase 2**	**136,37**	**91,12**	**1,5**	**0,0177**
ARRB1	NM_004041.3	β -1-Arrestin	331,88	308,57	1,08	0,8058
ARRB2	**NM_004313.3**	**β -2-Arrestin**	**22,35**	**40,22**	**-1,8**	**0,0022**
PDE1A	NM_005019.3	Phosphodiesterase 1A, calmodulin-dependent	138,75	102,85	1,35	0,3446
PDE4D	**NM_006203.4**	**Phosphodiesterase 4D**	**70,11**	**168,17**	**-2,4**	**0,0146**

PDE6A	NM_000440.2	Phosphodiesterase 6A	9,96	2,04	4,88	0,1374
PDE7A	NM_002603.2	Phosphodiesterase 7A	962,34	566,9	1,7	0,3381
		Renin-angiotensin-aldosterone system				
AGT	NM_000029.3	Angiotensinogen	478,04	397,3	1,2	0,3018
AGTR1	**NM_000685.3**	**Angiotensin II receptor 1**	**18,56**	**64,4**	**-3,47**	**0,0133**
NR3C2	**NM_000901.3**	**Nuclear receptor subfamily 3, member 2**	**289,41**	**182,45**	**1,59**	**0,0008**
		Calcium regulation				
AKAP7	NM_016377.3	A-kinase anchoring protein 7	135,48	134,71	1,01	0,9865
ATP2A2	**NM_001681.3**	**SERCA 2; ATPase sarcoplasmic/endoplasmic reticulum Ca transporting 2**	**2198,87**	**4440,61**	**-2,02**	**0,0010**
PLN	NM_002667.3	PLN=PLB=Phospholamban	37250,14	28929,08	1,29	0,4375
SLN	NM_003063.2	Sarcolipin - SERCA regulatory protein	87,25	34,07	2,56	0,5282
		Heart failure				
ANF	NM_006172.2	ANF = NPPA = atrial natriuretic factor/peptide	60990,1	2640,86	23,09	0,1772
CNP or NPPC	NM_024409.2	Natriuretic peptide C	9,39	19	-2,02	0,1018
CORIN	NM_006587.2	Corin,serine peptidase	548,73	581,48	-1,06	0,8599
IL1R1	NM_001320984.1	ST2	91,34	169,76	-1,86	0,3614
IL33	NM_033439.2	ST2 ligand	320,13	256,52	1,25	0,7200
NPPB	NM_002521.2	NPPB = BNP = brain natriuretic factor	2188,68	1077,94	2,03	0,7630
		Cell survival and apoptosis				
ATF3	**NM_001674.2**	**Activating transcription factor 3 OR cAMP responsive element-binding (CREB)**	**51,47**	**422,84**	**-8,21**	**0,0017**
BCL6	NM_138931.1	B-cell CLL/lymphoma 6	269,81	505,61	-1,87	0,2649
CASP1	NM_001223.3	Cysteine-aspartic acid protease (Caspase)-1	83,58	62,53	1,34	0,4813
CASP10	**NM_001230.4**	**Cysteine-aspartic acid protease (Caspase)-10**	**220,2**	**138,81**	**1,59**	**0,0233**
DUSP1	**NM_004417.2**	**Dual specificity phosphatase 1**	**972,92**	**3808,08**	**-3,91**	**0,0006**
FADD	NM_003824.2	Fas associated via death domain	14,72	17,04	-1,16	0,6894
FAS	NM_152876.1	Fas cell surface death receptor	70,42	50,03	1,41	0,3143
FOS	**NM_005252.2**	**Fos proto-oncogene**	**146,3**	**1249,94**	**-8,54**	**0,0015**
JAK2	NM_004972.3	Janus kinase 2	779,22	484,36	1,61	0,2600
JUN	**NM_002228.3**	**Jun proto-oncogene**	**289,2**	**599**	**-2,07**	**0,0101**
KITLG	**NM_003994.4**	**Stem cell factor (SCF)**	**253,17**	**111,1**	**2,28**	**0,0712**
MAPK1	**NM_138957.2**	**Mitogen-activated protein kinase 1; p38; ERK**	**715,41**	**916,27**	**-1,28**	**0,0113**
MAPK8	NM_002750.2	Mitogen-activated protein kinase 8; JNK; JNK1	225,74	221,77	1,02	0,8975
NR4A1	**NM_173157.1**	**Nuclear receptor subfamily A, group A, member 1**	**92,4**	**501,74**	**-5,43**	**0,0004**
PDGFA	NM_002607.5	Platelet derived growth factor subunit A	14,89	11,3	1,32	0,1506
PIK3R1	NM_181504.2	Phosphoinositide-3-kinase, regulatory subunit 1	1372,36	363,24	3,78	0,1309
PIM1	**NM_002648.2**	**Pim-1 oncogene**	**88,63**	**345,71**	**-3,9**	**1E-05**
PRDX3	NM_014098.3	Peroxiredoxin 3	4139,15	4043,44	1,02	0,9333
STAT1	NM_139266.1	Signal transducer and activator of transcription 1	816,38	611,36	1,34	0,1571
STAT3	NM_003150.3	Signal transducer and activator of transcription 3	993,13	2205,34	-2,22	0,1457
TNFRSF1A	NM_001065.2	TNF receptor superfamily member 1A	478,14	861,85	-1,8	0,3227
TNFRSF1B	NM_001066.2	TNF receptor superfamily member 1B	90,72	113,35	-1,25	0,5520
TNFSF13	NM_003808.3	TNF superfamily member 13	29,87	19,54	1,53	0,3942
		Cellular bioenergetics and stress				
ATP5A1	NM_001001937.1	ATP synthase, H+ transporting, mitochondrial F1 complex, α subunit 1, cardiac muscle	18052,84	16099,11	1,12	0,7257
FASN	NM_004104.4	Fatty acid synthase	40,89	194,94	-4,77	0,1142
GPD1L	NM_015141.3	Glycerol-3-phosphate dehydrogenase 1-like	3175,99	1763,62	1,8	0,2613
HSPA1A	**NM_005345.5**	**Heat shock 70kDa protein 1A**	**197,62**	**576,47**	**-2,92**	**0,0119**
MCAD or ACADM	NM_000016.5	Acyl-CoA dehydrogenase, C-4 to C-12 straight chain	5183,76	2546,27	2,04	0,2139
PPARA	NM_001001928.2	Peroxisome proliferator activated receptor α	490,01	523,39	-1,07	0,5069

Inflammation						
C1QA	NM_015991.2	Complement C1q A chain	18,71	17,21	1,09	0,8307
C6	NM_000065.2	Complement component 6	565,84	304,88	1,86	0,1765
CCL2	NM_002982.3	C-C motif chemokine ligand 2	160,92	567,06	-3,52	0,2898
CSF1R	NM_005211.2	Colony stimulating factor 1 receptor	22,61	14,91	1,52	0,3520
CXCR4	NM_003467.2	Chemokine (C-X-C motif) receptor 4	104,06	171,39	-1,65	0,2137
ICAM1	NM_000201.2	Intercellular adhesion inhibitor type 1	94,39	178,33	-1,89	0,3266
IL6	**NM_000600.3**	**Interleukin 6**	**3,61**	**55,65**	**-15,4**	**0,0429**
MYD88	NM_002468.3	Myeloid differentiation primary response 88	83,38	109,19	-1,31	0,5816
NFKB1	NM_003998.2	Nuclear factor kappa B subunit 1	118,06	135,5	-1,15	0,4225
PPBP	**NM_002704.2**	**Proplatelet basic protein (chemokine (CXC motif) ligand 7)**	**40,27**	**7,94**	**5,07**	**0,0904**
SELL	NR_029467.1	L-selectin	13,14	21,53	-1,64	0,1832
SELP	NM_003005.2	Cell adhesion molecule (GMP 140)	125,17	63,21	1,98	0,1282
TLR4	**NM_138554.2**	**Toll like receptor 4**	**188,87**	**114,32**	**1,65**	**0,0406**
TNF	NM_000594.2	Tumor necrosis factor-α	3,41	3,37	1,01	0,9786

Appendix 13. Gene Ontology analysis with DAVID bioinformatics.

Figure 1 A **Molecular functions (top 10)**

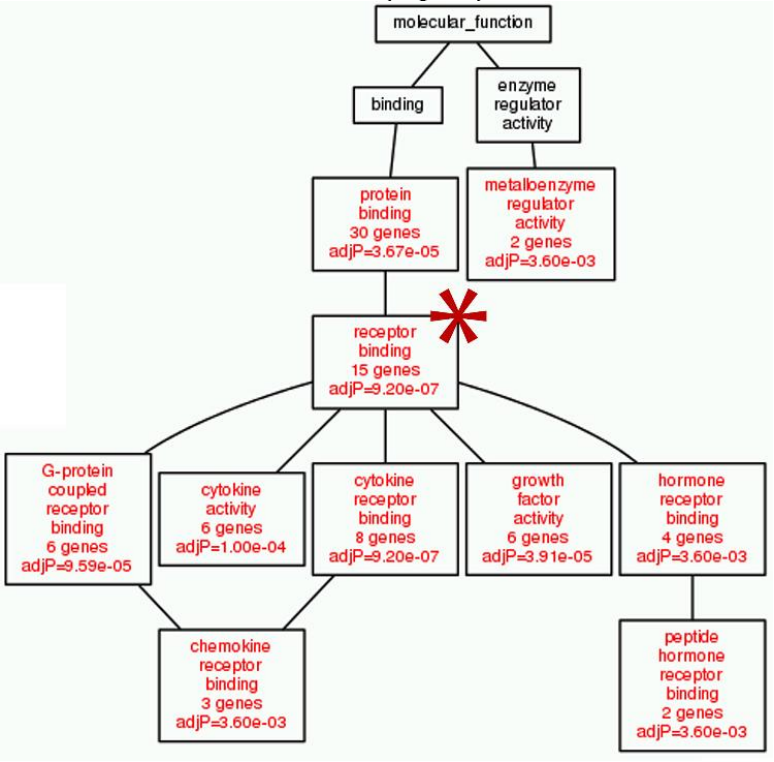

Database: molecular function Name: receptor binding ID: GO:0005102

n=15 adjP=9.20e-07

Gene Symbol	Gene Name
LTBP4	latent transforming growth factor beta binding protein 4
AGTR1	angiotensin II receptor, type 1
ATP2A2	ATPase, Ca++ transporting, cardiac muscle, slow twitch 2
CTGF	connective tissue growth factor
CCL2	chemokine (C-C motif) ligand 2
IL6	interleukin 6 (interferon, beta 2)
PIK3R1	phosphoinositide-3-kinase, regulatory subunit 1 (alpha)
ADRB1	adrenoceptor beta 1
KITLG	KIT ligand
NPPB	natriuretic peptide B
IL10	interleukin 10
IL1B	interleukin 1, beta
STAT3	signal transducer and activator of transcription 3 (acute-phase response factor)
NPPC	natriuretic peptide C
PPBP	pro-platelet basic protein (chemokine (C-X-C motif) ligand 7)

Figure 1 B **Biological processes (top 10)**

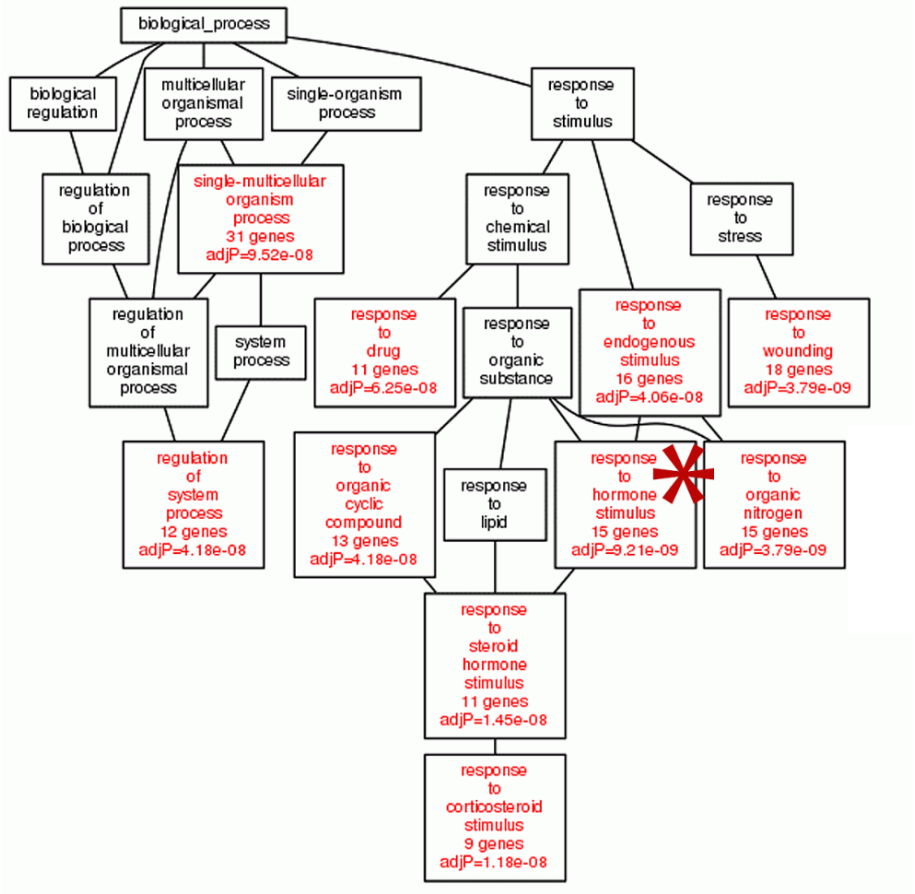

Database: biological process Name: response to hormone stimulus ID: GO:0009725; n=15; adjP=9.21e-09

Gene Symbol	Gene Name
MMP9	matrix metallopeptidase 9 (gelatinase B)
TIMP1	TIMP metallopeptidase inhibitor 1
ATP2A2	ATPase, Ca++ transporting, cardiac muscle, slow twitch 2
CTGF	connective tissue growth factor
CCL2	chemokine (C-C motif) ligand 2
IL6	interleukin 6 (interferon, beta 2)
COL1A1	collagen, type I, alpha 1
PIK3R1	phosphoinositide-3-kinase, regulatory subunit 1 (alpha)
TIMP4	TIMP metallopeptidase inhibitor 4
NPPB	natriuretic peptide B
IL10	interleukin 10
FOS	FBJ murine osteosarcoma viral oncogene homolog
IL1B	interleukin 1, beta
STAT3	signal transducer and activator of transcription 3
DUSP1	dual specificity phosphatase 1

Figure 1 C **Cellular components (top 10)**

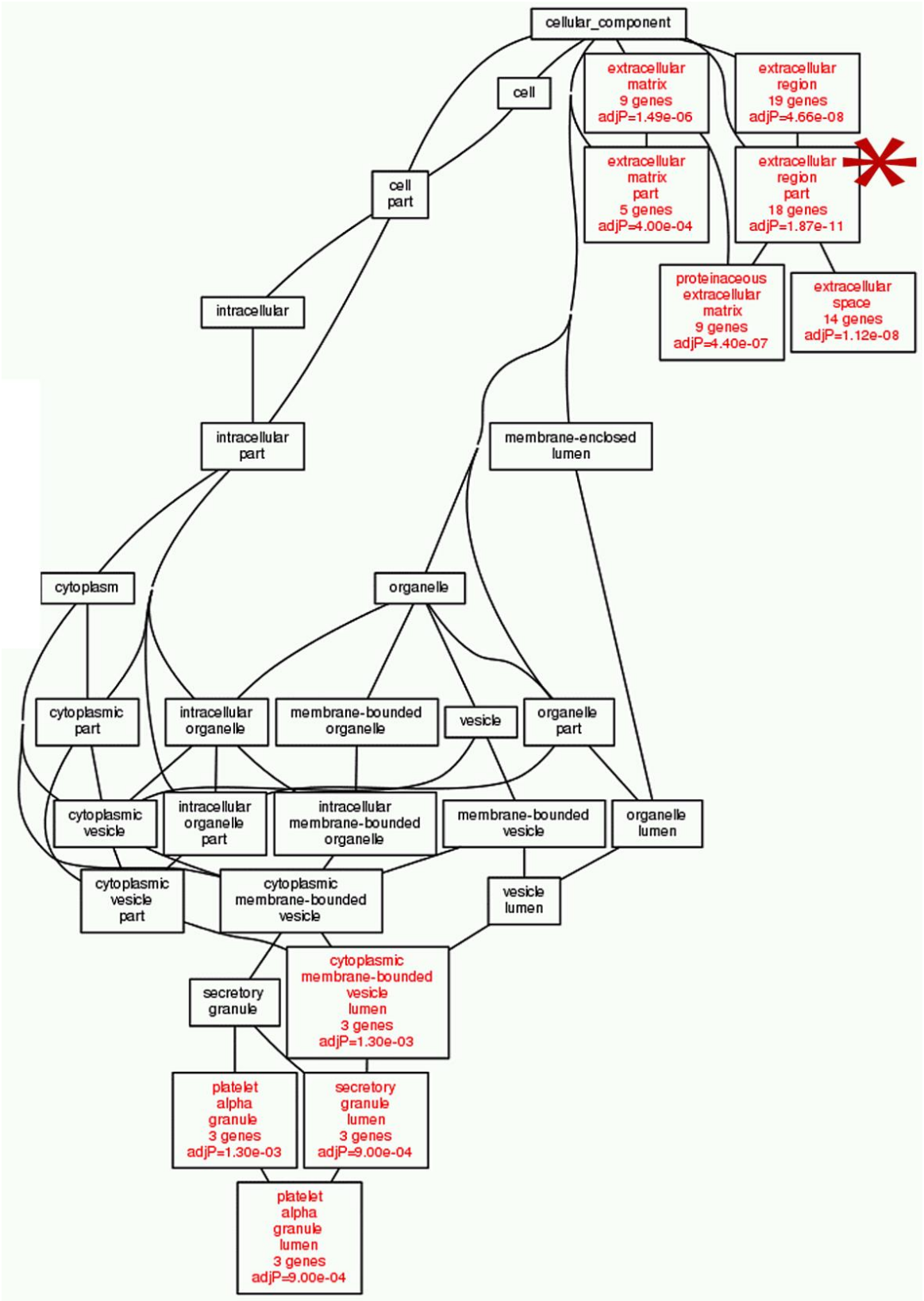

Figure 1 C (continued) Cellular components (top 10)

Database: cellular component Name: extracellular region part ID: GO:0044421
n=18 adjP=1.87e-11

Gene Symbol	Gene Name
MMP9	matrix metallopeptidase 9 (gelatinase B)
CCL2	chemokine (C-C motif) ligand 2
LUM	lumican
COL1A1	collagen, type I, alpha 1
TIMP4	TIMP metallopeptidase inhibitor 4
IL10	interleukin 10
IL1B	interleukin 1, beta
CTGF	connective tissue growth factor
TIMP1	TIMP metallopeptidase inhibitor 1
LTBP4	latent transforming growth factor beta binding protein 4
POSTN	periostin, osteoblast specific factor
IL6	interleukin 6 (interferon, beta 2)
EMILIN2	elastin microfibril interfacer 2
MATN2	matrilin 2
KITLG	KIT ligand
NPPB	natriuretic peptide B
NPPC	natriuretic peptide C
PPBP	pro-platelet basic protein (chemokine (C-X-C motif) ligand 7)

Figure 1 D Diseases (top 10)

Disease	n	adjP	Gene symbol
Disease Progression	11	1.10e-14	MMP9, PDCD1, POSTN, LTBP4, AGTR1, TIMP1, CTGF, CCL2, IL6, IL10, IL1B
Aortic Aneurysm, Abdominal	7	2.68e-13	MMP9, IL10, LTBP4, AGTR1, TIMP1, IL1B, IL6
Pathologic Processes	12	2.84e-12	MMP9, PDCD1, POSTN, AGTR1, TIMP1, CTGF, CCL2, IL6, NPPB, PDE4D, IL10, IL1B
Chronic Disease	10	6.73e-12	MMP9, PDCD1, AGTR1, TIMP1, CTGF, CCL2, IL6, NPPB, IL10, IL1B
Arterial Occlusive Diseases	9	1.37e-11	MMP9, AGTR1, TIMP1, CCL2, IL6, NR4A1, NPPB, PDE4D, PPBP
Vascular Diseases	10	1.73e-11	MMP9, AGTR1, TIMP1, CCL2, IL6, NPPB, PDE4D, IL10, IL1B
Lung Diseases	10	1.73e-11	MMP9, POSTN, TIMP1, CCL2, IL6, NPPB, IL10, IL1B, STAT3, DUSP1
Ischemia	8	1.91e-11	MMP9, AGTR1, CCL2, IL6, ADRB1, NPPB, PDE4D, IL1B
Heart Diseases	10	1.91e-11	MMP9, AGTR1, ATP2A2, CCL2, IL6, SLN, ADRB1, TIMP4, NPPB, NPPC
Aortic Aneurysm	6	3.02e-11	MMP9, IL10, LTBP4, AGTR1, TIMP1, IL6

Appendix 13 Legend. Bioinformatic analysis using DAVID.[1]

Gene Ontology (GO) analysis using DAVID revealed enrichment of genes coding for several important molecular processes, biological processes and cellular components. Each figure shows the Top 10 processes identified by GO analysis. Results are displayed as trees (Figures 1A-C) showing most significantly enriched (Top) processes in red. Statistical ranking was based on number of (differentially expressed) genes (=n) uploaded and number of genes in the pathway, making corrections for multiple comparison (adjusted P value). The P value provides an estimate of the probability that a given enrichment is present by chance alone and are derived using corrections for multiple comparisons (Benjamini and Hochberg false discovery rates). For each of the three Gene Ontology aspects, the most significant process is indicated by a red asterisk and the genes related to this process are listed below the tree. These results suggest that the changes in gene expression are not by chance but are related to changes in a number of molecular, biological and cellular processes. Furthermore, the results confirm that changes in gene expression in the CPMR patients are consistent with findings in previous studies, including abdominal aortic aneurysm pathology, arterial occlusive disease, vascular disease and heart disease (Supplementary figure 1D).

Figure 1A: Top 10 Molecular functions

Figure 1B: Top 10 Biological processes

Figure 1C: Top 10 Cellular components

Figure 1D: Top 10 Diseases

Reference

1. Dennis G, Jr., Sherman BT, Hosack DA, et al. DAVID: Database for Annotation, Visualization, and Integrated Discovery. *Genome biology* 2003; **4**(5): P3.

Appendix 14. Gene expression in patients with chronic primary mitral regurgitation versus normal hearts: comparison with previously published data.

Gene	Accession number	Fold change in Zheng *et al.*[1]: CPMR versus Normal	Fold change in current study: CPMR versus Normal
AKAP7	NM_016377.3	up (no value given in original paper)	-1,07
ANF	NM_006172.2	21,87	21,56
SLN	NM_003063.2	12,42	2,39
NPPB	NM_002521.2	5,13	1,90
C6	NM_000065.2	3,67	1,73
PRDX3	NM_014098.3	2,75	-1,05
PDCD1	NM_005018.2	2,65	2,19
PLN	NM_002667.3	2,54	1,20
CORIN	NM_006587.2	2,3	-1,14
CTGF	NM_001901.2	2,28	2,15
GPD1L	NM_015141.3	2,22	1,68
PIK3R1	NM_181504.2	2,2	3,53
PDE1A	NM_005019.3	2,17	1,26
NR3C2	NM_000901.3	2,07	1,48
THBS1	NM_003246.2	-2,18	-1,53
Jun	NM_002228.3	-2,22	-2,22
PDE4D	NM_006203.4	-2,64	-2,57
HSPA1A	NM_005345.5	-3,1	-3,13
EMILIN2	NM_032048.2	-3,21	-3,77
ATF3	NM_001674.2	-3,27	-8,80
DUSP1	NM_004417.2	-3,43	-4,19
NR4A1	NM_173157.1	-4,42	-5,82
PIM1	NM_002648.2	-4,88	-4,18
FOS	NM_005252.2	-14,95	-9,15
IL6	NM_000600.3	down (no value given in original paper)	-16,57

Reference

1. Zheng J, Yancey DM, Ahmed MI, Wei C-C, Powell PC, Shanmugam M, Gupta H, Lloyd SG, McGiffin DC, Schiros CG, Denney TS, Babu GJ, Dell'Italia LJ. Increased Sarcolipin Expression and Adrenergic Drive in Humans With Preserved Left Ventricular Ejection Fraction and Chronic Isolated Mitral Regurgitation. *Circulation: Heart Failure* 2014; **7**(1): 194-202.

Appendix 15. Correlation between animal and human studies.

	Zheng *et al*[1]	Chen *et al*[2]	Zheng *et al*[3]	Current study	Correlation
Model:	**Dog**	**Rat**	**Human**	**Human**	
Number of subjects:	**4**	**5**	**35**	**13**	
Mechanism of VO:	**Experimental MR**	**ACF**	**CPMR**	**CPMR**	
ADAMTS2		down		1.13	No
ADAMTS8		up		1.04	NA
ADRB1				-2.34	NA
ADRB2				-1.01	NA
ADRBK1				-1.29	NA
ADRBK2				1.5	NA
AGT				1.2	NA
AGTR1				-3.47	NA
AKAP7			up	1.01	NA
ANF	3,74		21.87	23.09	Yes
ARRB1				1.08	NA
ARRB2				-1.8	NA
ATF3	2,58		-3.27	-8.21	No
ATP2A2	down			-2.02	Yes
ATP5A1		down		1.12	No
Bcl6		up		-1.87	No
C1QA	-1,89	up		1,09	No
C6			3.67	1,86	NA
CASP1				1,34	NA
CASP10				**1,59**	NA
CCL2				-3,52	NA
CNP or NPPC	2,49			-2,02	No
COL1A1		down		2,43	No
COL3A1	1,51	up		1,46	Yes
COL4A1		up		1,01	Yes
COL5A2	-1,6	up		1,89	No
CORIN			2.3	-1,06	NA
CSF1R	-3,76			1,52	No
CTGF	-1,56	up	2.28	**2,3**	No
CXCR4	1,75	up		-1,65	No
DCN	-1,8	up		1,09	No
DUSP1			-3.43	**-3,91**	NA
EMILIN2			-3.21	**-3,52**	NA
FADD				-1,16	NA
FAS				1,41	NA
FASN		up		-4,77	No
FBLN1	-1,78	up		1,57	No
FBN1	-1,79	up		1,68	No
FOS			-14.95	**-8,54**	NA
GPD1L			2.22	1,8	NA
HSPA1A		up	-3.1	**-2,92**	No
ICAM1	-2,65			-1,89	Yes

IL1R1				-1,86	NA
IL33				1,25	NA
IL6			down	**-15,4**	NA
ITGAV	-1,6			1,21	No
JAK2		up		1,61	Yes
JUN			-2.22	**-2,07**	NA
KITLG	1,93			**2,28**	Yes
LTBP4		up		**2,01**	Yes
LUM	-1,63			**3,12**	No
LTBP2	-1,87			**5,71**	No
MAPK1				**-1,28**	NA
MAPK8				1,02	NA
MATN2	-2,11			**2,05**	No
MMP2				-1,61	NA
MMP23				**2,2**	NA
MMP9	10,13			-3,12	No
MMRN1	-6,14			-2,54	Yes
MYD88		up		-1,31	No
Mcad or Acadm		down		2,04	No
NFKB1				-1,15	NA
NPPB	3,68		5.13	2,03	Yes
NR3C2			2.07	**1,59**	NA
NR4A1			-4.42	**-5,43**	NA
PAI-1	-2,99			**-5,74**	Yes
PDE1A			2.17	1,35	NA
PDE4D	2		-2.64	**-2,4**	No
PDE6A				4,88	NA
PDE7A				1,7	NA
PDGFA				1,32	NA
PIK3R1			2.2	3,78	NA
PIM1			-4.88	**-3,9**	NA
PLN			2.54	1,29	NA
POSTN				**3,15**	NA
PPARA		down		-1,07	No
PPBP	13,03			**5,07**	Yes
PRDX3			2.75	1,02	NA
SELL	6,1			-1,64	No
SELP	3,96			1,98	Yes
SLN			12.42	2,56	NA
STAT1				1,34	NA
STAT3		up		-2,22	No
TGFB1		up		1,33	Yes
TGFB2		up		-1,65	No
TGFB3				-1,55	NA
TGFBR1				1,24	NA
TGFBR2	-1,68			**-1,33**	Yes
TGFBR3	-1,52			-1,33	Yes
THBS1	-2,41		-2.18	-1,42	Yes

TIMP1		up		-2,27	No
TIMP2		up		1,03	NA
TIMP3		up		1,08	NA
TIMP4				-2,25	NA
TLR4	-1,77	up		**1,65**	No
TNF				1,01	NA
TNFRSF1A				-1,8	NA
TNFRSF1B				-1,25	NA
TNFSF13				1,53	NA
VCAN	-1,67			1,22	No
VTN	-2,19			-1,68	Yes

VO=volume overload; MR=mitral regurgitation; ACF=aorto-caval fistula; CPMR=chronic primary mitral regurgitation.

References

1. Zheng J, Chen Y, Pat B, et al. Microarray identifies extensive downregulation of noncollagen extracellular matrix and profibrotic growth factor genes in chronic isolated mitral regurgitation in the dog. *Circulation* 2009; **119**(15): 2086-95.
2. Chen YW, Pat B, Gladden JD, et al. Dynamic molecular and histopathological changes in the extracellular matrix and inflammation in the transition to heart failure in isolated volume overload. *Am J Physiol Heart Circ Physiol* 2011; **300**(6): H2251-60.
3. Zheng J, Yancey DM, Ahmed MI, et al. Increased Sarcolipin Expression and Adrenergic Drive in Humans With Preserved Left Ventricular Ejection Fraction and Chronic Isolated Mitral Regurgitation. *Circulation: Heart Failure* 2014; **7**(1): 194-202.

Appendix 16. Baseline expression of genes in the two CPMR groups.

Gene Name	Accession #	CRV	Nil	Baseline CRV vs. Nil fold change	P value	Lower 95% CI of fold change	Upper 95% CI of fold change	FDR
Extra cellular matrix remodelling								
ADAMTS2	NM_021599.2	68,99	39,02	1,77	0,2480	-1,66	5,19	1
ADAMTS8	NM_007037.4	33,74	8,76	3,85	0,0539	-1,05	15,52	1
COL1A1	NM_000088.3	292,45	92,13	3,17	0,1937	-2,24	22,61	1
COL3A1	NM_000090.3	3767,82	1953,64	1,93	0,2080	-1,63	6,06	1
COL4A1	NM_001845.4	1667,74	1076,57	1,55	0,2052	-1,39	3,33	1
COL5A2	NM_000393.3	387,3	269,99	1,43	0,2760	-1,44	2,97	1
CTGF	NM_001901.2	1250,27	487,15	2,57	0,0442	1,02	6,47	1
DCN	NM_001920.3	7477,17	7563,92	-1,01	0,9686	-1,95	1,9	1
EMILIN2	NM_032048.2	57,95	47,05	1,23	0,6082	-1,98	3	1
FBLN1	NM_006487.2	2476,37	1815,21	1,36	0,3791	-1,69	3,14	1
FBN1	NM_000138.3	701,92	467,11	1,5	0,3026	-1,58	3,57	1
ITGAV	NM_002210.2	1153,47	847,36	1,36	0,5182	-2,08	3,85	1
LTBP2	NM_000428.2	864,16	254,92	3,39	0,0240	1,22	9,45	1
LTBP4	NM_003573.2	1730,89	955,77	1,81	0,1778	-1,39	4,55	1
LUM	NM_002345.3	5798,32	4222,78	1,37	0,3683	-1,55	2,93	1
MATN2	NM_002380.3	431,4	426,4	1,01	0,9560	-1,57	1,61	1
MMP2	NM_004530.2	451,37	358,71	1,26	0,6778	-2,68	4,24	1
MMP23	NM_006983.1	11,83	4,69	2,52	0,1081	-1,29	8,23	1
MMP9	NM_004994.2	5,24	7,41	-1,41	0,7274	-13,03	6,51	1
MMRN1	NM_007351.2	9,82	18,59	-1,89	0,3781	-9,91	2,77	1
PAI-1	NM_000602.4	66,96	32,39	2,07	0,2343	-1,8	7,67	1
POSTN	NM_001135935.1	485,68	536,69	-1,11	0,8408	-3,57	2,92	1
TGFB1	NM_000660.3	190,23	137,19	1,39	0,5386	-2,34	4,51	1
TGFB2	NM_003238.2	108,76	80,61	1,35	0,4067	-1,66	3,02	1
TGFB3	NM_003239.2	145,38	91,15	1,59	0,1011	-1,15	2,91	1
TGFBR1	NM_004612.2	259,97	240,22	1,08	0,6778	-1,47	1,72	1
TGFBR2	NM_001024847.1	837,62	817,14	1,03	0,8581	-1,35	1,42	1
TGFBR3	NM_003243.3	144,04	146,61	-1,02	0,9224	-1,52	1,46	1
THBS1	NM_003246.2	582,96	510,44	1,14	0,7002	-1,89	2,46	1
TIMP1	NM_003254.2	712,1	614,79	1,16	0,6225	-1,68	2,25	1
TIMP2	NM_003255.4	901,32	593,29	1,52	0,0865	-1,1	2,53	1
TIMP3	NM_000362.4	5477,3	3784,94	1,45	0,0542	-1,01	2,12	1
TIMP4	NM_003256.2	161,25	70,73	2,28	0,1068	-1,26	6,54	1
VCAN	NM_004385.3	145,39	70,46	2,06	0,1183	-1,26	5,38	1
VTN	NM_000638.3	87,96	61,49	1,43	0,2278	-1,38	2,82	1
Beta-adrenergic signalling								

ADRB1	NM_000684.1	77,87	73,64	1,06	0,8940	-2,38	2,66	1
ADRB2	NM_000024.3	48,69	48,12	1,01	0,9596	-1,66	1,7	1
ADRBK1	NM_001619.2	493,79	502,85	-1,02	0,8803	-1,33	1,28	1
ADRBK2	NM_005160.2	129,37	101,14	1,28	0,4063	-1,48	2,43	1
ARRB1	NM_004041.3	288,66	268,49	1,08	0,8095	-1,8	2,08	1
ARRB2	NM_004313.3	22,59	15,56	1,45	0,1985	-1,31	2,75	1
PDE1A	NM_005019.3	131,23	103,22	1,27	0,3446	-1,37	2,21	1
PDE4D	NM_006203.4	60,64	57,03	1,06	0,9040	-2,88	3,26	1
PDE6A	NM_000440.2	18,33	3,83	4,78	0,0386	1,09	21,06	1
PDE7A	NM_002603.2	860,87	756,96	1,14	0,4460	-1,27	1,65	1
Renin-angiotensin-aldosterone system								
AGT	NM_000029.3	449,93	357,39	1,26	0,1865	-1,15	1,82	1
AGTR1	NM_000685.3	14,12	17,65	-1,25	0,7559	-6,19	3,96	1
NR3C2	NM_000901.3	217,31	271,21	-1,25	0,2631	-1,9	1,22	1
Heart Failure								
ANF	NM_006172.2	74361,89	35198,35	2,11	0,2917	-2,15	9,61	1
CNP or NPPC	NM_024409.2	5,96	10,4	-1,74	0,3116	-5,73	1,89	1
CORIN	NM_006587.2	369,34	573,65	-1,55	0,3175	-4,11	1,7	1
IL1R1	NM_001320984.1	78,26	75,02	1,04	0,8958	-2,05	2,23	1
IL33	NM_033439.2	294,55	244,83	1,2	0,7698	-3,41	4,94	1
NPPB	NM_002521.2	4995,8	674,71	7,4	0,1882	-4,31	236,38	1
Cell survival and apoptosis								
ATF3	NM_001674.2	41,64	44,77	-1,08	0,9226	-5,93	5,12	1
BCL6	NM_138931.1	237,7	215,49	1,1	0,5657	-1,32	1,6	1
CASP1	NM_001223.3	72,43	67,86	1,07	0,8060	-1,7	1,93	1
CASP10	NM_001230.4	183,2	186,23	-1,02	0,9368	-1,62	1,57	1
DUSP1	NM_004417.2	878,32	758,32	1,16	0,5046	-1,39	1,87	1
FADD	NM_003824.2	12,32	12,38	-1	0,9885	-1,94	1,92	1
FAS	NM_152876.1	66,75	52,27	1,28	0,4079	-1,48	2,42	1
FOS	NM_005252.2	76,05	198,03	-2,6	0,1920	-12,09	1,78	1
JAK2	NM_004972.3	610,24	700,12	-1,15	0,5385	-1,92	1,46	1
JUN	NM_002228.3	253,96	231,73	1,1	0,8527	-2,75	3,31	1
KITLG	NM_003994.4	202,9	222,27	-1,1	0,7399	-2,02	1,69	1
MAPK1	NM_138957.2	597,97	602,26	-1,01	0,9608	-1,4	1,38	1
MAPK8	NM_002750.2	186,29	192,47	-1,03	0,8118	-1,4	1,31	1
NR4A1	NM_173157.1	79,11	75,94	1,04	0,8967	-1,94	2,11	1
PDGFA	NM_002607.5	17,64	8,84	2	0,0349	1,06	3,76	1
PIK3R1	NM_181504.2	1190,16	1113,48	1,07	0,7272	-1,42	1,63	1
PIM1	NM_002648.2	93,81	58,92	1,59	0,2176	-1,39	3,53	1
PRDX3	NM_014098.3	3111,1	3874,91	-1,25	0,5893	-3,03	1,95	1
STAT1	NM_139266.1	709,25	661,21	1,07	0,7077	-1,45	1,66	1

STAT3	NM_003150.3	939,9	738,38	1,27	0,2210	-1,21	1,95	1
TNFRSF1A	NM_001065.2	425,44	378,11	1,13	0,6770	-1,67	2,12	1
TNFRSF1B	NM_001066.2	87,24	66,38	1,31	0,4147	-1,57	2,72	1
TNFSF13	NM_003808.3	28,76	21,83	1,32	0,5511	-2,16	3,74	1
Calcium regulation								
AKAP7	NM_016377.3	110,99	116,37	-1,05	0,8915	-2,25	2,05	1
ATP2A2	NM_001681.3	1878,65	1810,95	1,04	0,8157	-1,36	1,47	1
PLN	NM_002667.3	28896,7	33787,92	-1,17	0,2744	-1,59	1,16	1
SLN	NM_003063.2	81,97	65,35	1,25	0,7618	-4,22	6,64	1
Cellular bioenergetics and stress								
ATP5A1	NM_001001937.1	13523,75	16956,96	-1,25	0,1150	-1,68	1,07	1
FASN	NM_004104.4	43,4	27,11	1,6	0,3635	-1,91	4,89	1
GPD1L	NM_015141.3	2582,93	2747,89	-1,06	0,6892	-1,51	1,34	1
HSPA1A	NM_005345.5	178,6	153,87	1,16	0,6914	-1,96	2,65	1
MCAD or ACADM	NM_000016.5	4013,19	4711,45	-1,17	0,2236	-1,55	1,13	1
PPARA	NM_001001928.2	438,29	385,49	1,14	0,2754	-1,14	1,47	1
Inflammation								
C1QA	NM_015991.2	16,02	15,38	1,04	0,9465	-3,7	4,02	1
C6	NM_000065.2	365,07	617,11	-1,69	0,4041	-7,14	2,5	1
CCL2	NM_002982.3	104,76	173,93	-1,66	0,3675	-5,59	2,03	1
CSF1R	NM_005211.2	21,37	16,83	1,27	0,5303	-1,86	3	1
CXCR4	NM_003467.2	95,13	80,09	1,19	0,5763	-1,65	2,33	1
ICAM1	NM_000201.2	69,15	90,66	-1,31	0,4178	-2,73	1,59	1
IL6	NM_000600.3	2,48	3,93	-1,59	0,4947	-6,96	2,76	1
MYD88	NM_002468.3	80,53	60,75	1,33	0,3305	-1,43	2,52	1
NFKB1	NM_003998.2	106,91	91,74	1,17	0,4642	-1,35	1,83	1
PPBP	NM_002704.2	23,43	50,14	-2,14	0,4586	-22,78	4,98	1
SELL	NR_029467.1	9,5	12,8	-1,35	0,4687	-3,34	1,84	1
SELP	NM_003005.2	100,79	109,39	-1,09	0,7628	-2,05	1,74	1
TLR4	NM_138554.2	157,59	159,26	-1,01	0,9715	-1,98	1,94	1
TNF	NM_000594.2	3,55	2,38	1,49	0,3383	-1,72	3,82	1

FDR = false discovery rate.

Appendix 17. Changes in expression of genes in response to treatment with carvedilol.

		Carvedilol-treated group			Nil group			
Gene	**Accession #**	**Baseline**	**Final**	**Change**	**Baseline**	**Final**	**Change**	**P value**
Extra cellular matrix remodelling								
ADAMTS2	NM_021599.2	48,27	75,32	10,38	45,46	48,915	4,61	0,7488
ADAMTS8	NM_007037.4	30,09	32,705	-6,84	16,78	12,02	-1,54	0,8728
COL1A1	NM_000088.3	364,695	182,925	3,17	107,425	92,105	4,44	0,5218
COL3A1	NM_000090.3	3284,93	2362,67	-1685,065	2415,315	2196,49	114,78	0,3367
COL4A1	NM_001845.4	1507,78	1456,17	43,65	1171,775	1200,865	-30,97	0,7488
COL5A2	NM_000393.3	332,285	338,38	-17,255	359,92	336,335	40,575	0,0374
CTGF	NM_001901.2	1295,595	1251,295	-143,315	498,355	588,94	-22,24	0,5218
DCN	NM_001920.3	7886,345	7668,275	-1986,01	10686,25	8109,65	-758,505	0,8728
EMILIN2	NM_032048.2	69,27	65,405	-7,065	54,69	92,655	27,63	0,1495
FBLN1	NM_006487.2	2355,345	2391,6	-207,12	2337,665	1679,385	-526,86	1.0000
FBN1	NM_000138.3	543,37	526,42	-132,875	537,905	452,88	-89,17	0,7488
ITGAV	NM_002210.2	1349,255	904,34	10,635	813,71	861,305	222,13	0,7488
LTBP2	NM_000428.2	1215,75	534,62	-480,61	255,285	252,065	-57,6	0,3367
LTBP4	NM_003573.2	1963,825	1234,3	-134,845	864,525	946,225	-32,075	0,6310
LUM	NM_002345.3	5528,985	5425,395	-341,455	5668,83	3805,74	-1429,045	0,8728
MATN2	NM_002380.3	483,255	536,99	-13,835	553,27	545,935	44,835	0,7488
MMP2	NM_004530.2	596,59	514,15	-147,565	582,345	547,425	-28,665	0,1495
MMP23	NM_006983.1	12,255	15,035	-5,9	4,485	3,255	-1,6	0,8728
MMP9	NM_004994.2	4,145	12,035	5,87	9,12	5,495	-2,085	0,2623
MMRN1	NM_007351.2	9,915	23,39	13,925	24,135	23,005	-1,69	0,7488
PAI-1	NM_000602.4	83,265	47,775	-7,12	33,175	41,38	2,96	0,5218
POSTN	NM_001135935.1	562,665	424,875	-134,03	649,51	565,085	-56,395	0,8728
TGFB1	NM_000660.3	256,64	132,08	16,72	130,68	98,055	-9,365	0,7488
TGFB2	NM_003238.2	111,065	130,185	13,01	82,115	92,775	-1,12	0,6310
TGFB3	NM_003239.2	159,335	170,3	-18,61	106,065	138,805	21,32	0,4233
TGFBR1	NM_004612.2	284,165	300,495	-37,085	286,86	292,08	0,135	0,6310
TGFBR2	NM_001024847.1	890,08	832,56	-101,165	981,09	988,615	37,275	0,4233
TGFBR3	NM_003243.3	155,47	152,275	-5,855	186,3	164,695	1,105	0,8728
THBS1	NM_003246.2	610,705	572,46	-63,91	636,485	370,425	-314,875	0,2002
TIMP1	NM_003254.2	617,125	711,385	-73,36	649,35	554,97	-54,1	0,8728
TIMP2	NM_003255.4	934,92	783,595	-104,915	717,265	682,79	-82,6	0,4233
TIMP3	NM_000362.4	6014,555	5684,275	-318,735	4596,77	5403,475	149,155	0,6310
TIMP4	NM_003256.2	175,33	139,025	-10,065	125,915	193,2	94,985	0,1495
VCAN	NM_004385.3	135,705	120,45	-41,195	66,085	77,225	10,58	0,2002
VTN	NM_000638.3	108,185	92,06	-21,9	70,575	95,005	24,27	0,7488
Beta-adrenergic signalling								
ADRB1	NM_000684.1	79,28	70,725	-0,245	82,165	83,275	10,84	0,8728

ADRB2	NM_000024.3	53,12	68,525	-3,39	55,295	58,015	11,63	0,7488
ADRBK1	NM_001619.2	614,53	646,83	31,68	591,41	614,49	38,82	0,7488
ADRBK2	NM_005160.2	157,53	118,23	-37,285	147,305	119,1	1,5	0,3367
ARRB1	NM_004041.3	259,915	287,65	-18,78	269,08	234,495	-60,57	0,5218
ARRB2	NM_004313.3	22,435	15,23	-6,96	18,78	25,925	9,255	0,0250
PDE1A	NM_005019.3	127,975	158,56	-10,535	120,45	223,53	108,265	0,0163
PDE4D	NM_006203.4	100,06	71,95	-26,045	93,495	123,74	58,365	0,0782
PDE6A	NM_000440.2	19,435	14,475	-11,96	5,42	1,915	-1,275	0,3367
PDE7A	NM_002603.2	1028,435	1045,775	7,53	964,335	1128,83	71,235	0,7488
Renin-angiotensin-aldosterone system								
AGT	NM_000029.3	508,62	402,28	-101,4	419,78	310,235	-30,425	0,4233
AGTR1	NM_000685.3	28,69	33,155	5,955	23,93	46,105	31,92	0,3367
NR3C2	NM_000901.3	261,3	283,3	-25,84	336,47	319,45	-36,815	0,6310
Calcium regulation								
AKAP7	NM_016377.3	169,18	176,78	7,6	189,65	191,895	12,555	0,7488
ATP2A2	NM_001681.3	2284,58	2303,575	189,935	2226,765	2413,8	172,13	1.0000
PLN	NM_002667.3	32173,065	44138,225	5325,96	40965,345	39251,865	-849,78	0,0374
SLN	NM_003063.2	120,68	61,785	-17,89	131,56	49,52	-86,52	0,5218
Heart failure								
ANF	NM_006172.2	72433,275	51421,805	-9025,43	48179,57	7990,835	-35667,91	0,6310
CNP or NPPC	NM_024409.2	5,6	5,415	-1,37	11,525	7,965	-0,185	0,5218
CORIN	NM_006587.2	607,955	498,76	-16,475	758,755	563,995	-187,16	0,4233
IL1R1	NM_001320984.1	71,79	97,09	33,575	99,05	72,085	-13,45	0,4233
IL33	NM_033439.2	407,7	453,065	-17,235	464,825	309,055	-88,16	0,5218
NPPB	NM_002521.2	7431,39	7175,855	-108,725	2963,78	287,11	-2802,515	0,1495
Cell survival and apoptosis								
ATF3	NM_001674.2	56,795	70,22	16,075	82,865	93,64	45,89	0,3367
BCL6	NM_138931.1	269,515	185,78	-66,045	229,22	258,015	1,4	0,2623
CASP1	NM_001223.3	109,925	92,815	-15,24	91,43	59,56	-19,345	0,5218
CASP10	NM_001230.4	206,455	166,375	-16,555	214,835	173,085	-36,63	0,8728
DUSP1	NM_004417.2	914,945	1064,43	-75,825	805,87	1144,125	283,805	0,3367
FADD	NM_003824.2	11,935	13,29	1,235	14,345	10,975	0,165	0,5218
FAS	NM_152876.1	67,245	74,58	-11,055	70,425	72,34	1,72	0,3367
FOS	NM_005252.2	74,955	68,505	14,05	220,905	97,81	-157,92	0,3367
JAK2	NM_004972.3	773,575	807,75	35,5	726,585	1015,805	329,85	0,7488
JUN	NM_002228.3	347,47	359,61	-20,77	372,55	405,4	32,495	1.0000
KITLG	NM_003994.4	232,54	245,605	-24,265	281,815	198,49	-91,835	0,7488
MAPK1	NM_138957.2	797,32	769,46	24,08	761,645	842,235	114,36	0,3367
MAPK8	NM_002750.2	233,24	220,42	-25,27	242,34	241,82	19,24	0,3367
NR4A1	NM_173157.1	99,84	107,81	-12,02	81,86	92,045	-7,01	1.0000
PDGFA	NM_002607.5	21,195	11,6	-16,545	9,535	15,94	5,58	0,0163
PIK3R1	NM_181504.2	1370,435	1427,275	224,125	1326,735	1518,46	268,22	1.0000

PIM1	NM_002648.2	95,29	69,975	-25,275	73,2	46,355	-18,535	0,6310
PRDX3	NM_014098.3	5265,61	5314,225	-143,83	6201,42	6535,01	1056,09	0,2623
STAT1	NM_139266.1	897,745	821	-67,475	797,325	715,375	4,95	0,3367
STAT3	NM_003150.3	1005,2	839,315	-30,61	835,625	830,12	27,835	0,5218
TNFRSF1A	NM_001065.2	400,565	379,2	-8,655	420,675	332,95	-62,57	1.0000
TNFRSF1B	NM_001066.2	87,225	80,075	-12,975	66,335	64,03	1,705	0,7488
TNFSF13	NM_003808.3	21,56	30,77	-2,48	27,115	18,395	-3,74	0,8728
Cellular bioenergetics and stress								
ATP5A1	NM_001001937.1	15955,94	19340,055	633,825	21466,485	22086,655	2227,715	0,6310
FASN	NM_004104.4	56,24	40,33	0,89	25,88	28,905	3,025	1.0000
GPD1L	NM_015141.3	3223,34	3292,75	461,055	3360,93	3763,885	160,55	0,5218
HSPA1A	NM_005345.5	209,08	130,38	-24,585	137,495	123,585	-0,69	0,7488
MCAD or ACADM	NM_000016.5	4465,81	5204,37	397,635	5402,855	5448,17	2	0,4233
PPARA	NM_001001928.2	503,845	593,38	23,16	483,05	503,115	44,12	1.0000
Inflammation								
C1QA	NM_015991.2	19,43	17,665	-1,84	26,45	24,24	-1,095	0,8728
C6	NM_000065.2	756,87	456,855	-300,575	861,79	643,825	-187,025	0,5218
CCL2	NM_002982.3	121,02	238,7	22,92	253,245	75,75	-143,14	0,3367
CSF1R	NM_005211.2	18,42	13,995	-5,165	19,715	18,245	0,675	0,1727
CXCR4	NM_003467.2	96,485	125,865	-9,165	89,55	94,635	22,565	0,3367
ICAM1	NM_000201.2	73,935	103,095	3,415	99,895	69,565	-24,96	0,4233
IL6	NM_000600.3	2,29	3,34	0,59	3,36	6,98	0,675	0,8726
MYD88	NM_002468.3	93,75	84,045	-4,485	79,015	65,745	4,985	0,5218
NFKB1	NM_003998.2	134,135	141,855	-8,105	123,35	114,74	2,38	0,6310
PPBP	NM_002704.2	30,455	7,345	-17,16	41,185	9,12	-34,645	0,3367
SELL	NR_029467.1	10,775	18,425	2,875	14,905	17,235	2,94	0,6310
SELP	NM_003005.2	96,945	101,375	-25,665	133,375	68,975	-57,51	0,4233
TLR4	NM_138554.2	172,675	158,72	-23,73	189,195	138,735	-57,915	0,8728
TNF	NM_000594.2	5,24	9,63	7,055	2,92	6,085	3,085	0,4233

Appendix 18. Turnitin report (first page only).

Document Viewer

Turnitin Originality Report

Processed on: 25-Mar-2018 11:48 AM SAST
ID: 935714934
Word Count: 30449
Submitted: 1

9408520j:All_chapters_for_Turnitin_25032018.d...
By Keir McCutcheon

21% match (publications)
Keir McCutcheon, Pravin Manga, "Left ventricular remodelling in chronic primary mitral regurgitation: implications for medical therapy", Cardiovascular Journal of Africa, 2018

Similarity Index
32%

Similarity by Source

Internet Sources:	7%
Publications:	30%
Student Papers:	2%

1% match (publications)
"Abstracts", European Heart Journal, 09/02/2001

1% match (Internet from 09-Dec-2017)
http://www.journals.ac.za

<1% match (publications)
"Abstracts", European Heart Journal, 2000.

<1% match (Internet from 29-Aug-2017)
https://doaj.org/article/0e972d481b924a23a1adad3614aed8b0

<1% match (publications)
"Sunday, 30 August 2009", European Heart Journal, 09/02/2009

<1% match (publications)
"Abstracts", European Heart Journal, 1998.

<1% match (publications)
Pediatric and Congenital Cardiology Cardiac Surgery and Intensive Care, 2014.

<1% match (publications)
Xin, H., and W. Jianan. "UP-REGULATION OF ENDOGENOUS LEPTIN IMPROVES HUMAN MESENCHYMAL STEM CELL SURVIVAL ABILITY IN VITRO AND THIS CELLS PROTECT FATAL CARDIAL MYOCYTES FROM APOPTOSIS", Heart, 2012.

<1% match (Internet from 02-Jun-2017)
http://medfac.tbzmed.ac.ir

<1% match (publications)
Davies, Julie M., Rebeca Santaolalla, Richard J. von Furstenberg, Susan J. Henning, and Maria T. Abreu. "The Viral Mimetic Polyinosinic:Polycytidylic Acid Alters the Growth Characteristics of Small Intestinal and Colonic Crypt Cultures", PLoS ONE, 2015.

<1% match (publications)
H KASAHARA. "Biochemical analyses of eight NKX2.5 homeodomain missense mutations causing atrioventricular block and cardiac anomalies", Cardiovascular Research, 10/2004

Appendix 19.

8. Habara M, Terashima M, Nasu K, Kaneda H, Yokota D, Ito T *et al.* Morphological differences of tissue characteristics between early, late, and very late restenosis lesions after first generation drug-eluting stent implantation: an optical coherence tomography study. *Eur Heart J Cardiovasc Imaging* 2013;**14**:276–84.
9. Nagoshi R, Shinke T, Otake H, Shite J, Matsumoto D, Kawamori H *et al.* Qualitative and quantitative assessment of stent restenosis by optical coherence tomography—comparison between drug-eluting and bare-metal stents. *Circ J* 2013;**77**:652–60.
10. Yabushita H, Bouma BE, Houser SL, Aretz HT, Jang IK, Schlendorf KH *et al.* Characterization of human atherosclerosis by optical coherence tomography. *Circulation* 2002;**106**:1640–5.
11. Jang IK, Bouma BE, Kang DH, Park SJ, Park SW, Seung KB *et al.* Visualization of coronary atherosclerotic plaques in patients using optical coherence tomography: comparison with intravascular ultrasound. *J Am Coll Cardiol* 2002;**39**:604–9.
12. Kume T, Akasaka T, Kawamoto T, Watanabe N, Toyota E, Neishi Y *et al.* Assessment of coronary arterial plaque by optical coherence tomography. *Am J Cardiol* 2006;**97**:1172–5.
13. Takano M, Yamamoto M, Inami S, Murakami D, Ohba T, Seino Y *et al.* Appearance of lipid-laden intima and neovascularization after implantation of bare-metal stents extended late-phase observation by intracoronary optical coherence tomography. *J Am Coll Cardiol* 2009;**55**:26–32.
14. Kume T, Akasaka T, Kawamoto T, Watanabe N, Toyota E, Sukmawan R *et al.* Visualization of neointima formation by optical coherence tomography. *Int Heart J* 2005;**46**:1133–6.
15. Axel DI, Kunert W, Göggelmann C, Oberhoff M, Herdeg C, Küttner A *et al.* Paclitaxel inhibits arterial smooth muscle cell proliferation and migration in vitro and in vivo using local drug delivery. *Circulation* 1997;**96**:636–45.
16. Nakano M, Vorpahl M, Otsuka F, Taniwaki M, Yazdani SK, Finn AV *et al.* Ex vivo assessment of vascular response to coronary stents by optical frequency domain imaging. *J Am Coll Cardiol Intv* 2012;**5**:71–82.
17. Otake H, Shite J, Ikeno F, Shinke T, Teramoto T, Miyoshi N *et al.* Evaluation of the peri-strut low intensity area following sirolimus-and paclitaxel-eluting stents implantation: Insights from an optical coherence tomography study in humans. *Int J Cardiol* 2010;**157**:38–42.
18. Teramoto T, Ikeno F, Otake H, Lyons JK, van Beusekom HM, Fearon WF *et al.* Intriguing peri-strut low-intensity area detected by optical coherence tomography after coronary stent deployment. *Circ J* 2010;**74**:1257–9.
19. Nagai H, Ishibashi-Ueda H, Fujii K. Histology of highly echolucent regions in optical coherence tomography images from two patients with sirolimus-eluting stent restenosis. *Catheter Cardiovasc Interv* 2010;**75**:961–3.

IMAGE FOCUS

doi:10.1093/ehjci/jet153
Online publish-ahead-of-print 18 October 2013

Delayed heart failure due to mitral valve perforation after stab chest

Keir R.G. McCutcheon* and Pravin Manga

Division of Cardiology, Charlotte Maxeke Johannesburg Academic Hospital, 7 York Road, Parktown, Johannesburg 2193, South Africa

* Corresponding author. Tel: +27(0)827808982; Fax: +27(0)116429041. Email: keir_mccutcheon@hotmail.com

A 30-year-old male presented to our hospital with signs and symptoms of biventricular failure. He had no significant past medical history. However, he reported having been stabbed in the chest ~18 months prior to the development of symptoms. He was stabbed with a screwdriver-like implement and underwent primary suturing of the superficial wound and insertion of an intercostal drain at a peripheral hospital at that time. During assessment at our hospital, we determined that the cause of the heart failure was severe mitral regurgitation through a 1 cm defect in the anterior mitral leaflet (*Panels A* and *B*). There was no evidence of a pericardial effusion or a ventricular septal defect. Three-dimensional transoesophgeal confirmed a well-circumscribed defect measuring 1.2 × 0.9 cm (*Panels C* and *D*; Supplementary data online, *Videos*).

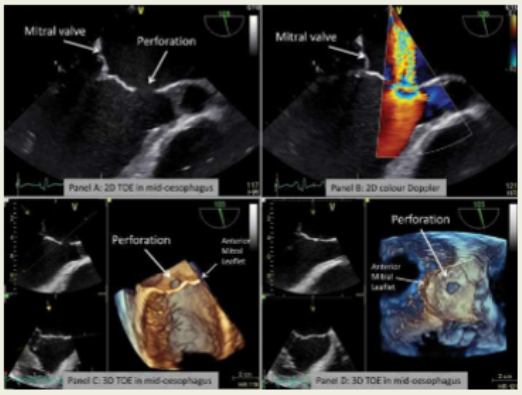

This case highlights the importance of a thorough cardiology assessment in any patient with a stab chest in the proximity of the heart and the need for later examination as cardiac sequelae of trauma to the heart may present much later than the initial traumatic event. Furthermore, this case highlights the usefulness of 3D echocardiography in better delineating traumatic cardiac lesions.

Supplementary data are available at *European Heart Journal – Cardiovascular Imaging* online.

Published on behalf of the European Society of Cardiology. All rights reserved. © The Author 2013. For permissions please email: journals.permissions@oup.com

Downloaded from https://academic.oup.com/ehjcimaging/article-abstract/15/3/315/2299739
by KU Leuven Libraries user
on 27 March 2018

Appendix 20.

CVJAFRICA CARDIOVASCULAR JOURNAL OF AFRICA • Advance Online Publication, February 2018 1

Review Article

Left ventricular remodelling in chronic primary mitral regurgitation: implications for medical therapy

Keir McCutcheon, Pravin Manga

Abstract

Surgical repair or replacement of the mitral valve is currently the only recommended therapy for severe primary mitral regurgitation. The chronic elevation of wall stress caused by the resulting volume overload leads to structural remodelling of the muscular, vascular and extracellular matrix components of the myocardium. These changes are initially compensatory but in the long term have detrimental effects, which ultimately result in heart failure. Understanding the changes that occur in the myocardium due to volume overload at the molecular and cellular level may lead to medical interventions, which potentially could delay or prevent the adverse left ventricular remodelling associated with primary mitral regurgitation. The pathophysiological changes involved in left ventricular remodelling in response to chronic primary mitral regurgitation and the evidence for potential medical therapy, in particular beta-adrenergic blockers, are the focus of this review.

Keywords: mitral regurgitation, left ventricular remodelling, medical therapy, beta-blocker

Submitted 30/5/16, accepted 12/1/17
Cardiovasc J Afr 2017; **28**: 00–00 www.cvja.co.za

DOI: 10.5830/CVJA-2017-009

Mitral regurgitation (MR) is caused by failure of adequate coaptation of the anterior and posterior mitral leaflets during left ventricular contraction, resulting in various degrees of regurgitation of blood from the left ventricle (LV) into the left atrium (LA). The result of this regurgitation is twofold. Firstly, there is a reduction in forward stroke volume (FSV) into the aorta, with subsequent reduction in perfusion. Secondly, there is an increase in LA blood volume during ventricular systole, which results in an increase in left ventricular preload, the so-called 'volume overloaded' state.

Division of Cardiology, Department of Internal Medicine, Charlotte Maxeke Johannesburg Academic Hospital and University of the Witwatersrand, Johannesburg, South Africa
Keir McCutcheon, BSc (Hons), MSc, MB BCh, FCP (SA), Cert Cardiol (SA), keir_mccutcheon@hotmail.com
Pravin Manga, MBBCh, FCP (SA), PhD, FRCP (UK)

MR is classified as either primary (organic) or secondary (functional), and acute or chronic.[1] Causes of acute MR include infective endocarditis and spontaneous cordal rupture and will not be discussed further in this review. Chronic secondary MR can be ischaemic and/or non-ischaemic in nature and therapies for secondary MR range from medical to surgical.[2] By contrast, chronic primary MR is predominantly caused by degenerative disease in developed countries,[3] and rheumatic heart disease (RHD) in developing countries.[4] RHD is one of the major contributors to the aetiology of heart failure in Africa, where it remains the most common form of acquired cardiovascular disease in children and adults.[4]

Current therapy for patients with severe chronic primary MR, as recommended by the European Society of Cardiology guidelines,[1] comprises surgical repair or replacement in patients who are surgical candidates, or conservative (i.e. palliative) therapy in patients with very poor left ventricular function who are deemed to be poor surgical candidates. At present, there is no recommendation for drug therapy in patients with any degree of chronic primary MR. However, once heart failure develops, angiotensin converting enzyme inhibitors (ACE inhibitors), beta-blockers and spironolactone may be considered.[5]

Although there have been several recent reviews focusing on ventricular remodelling in ischaemic heart disease, hypertensive heart disease and aortic stenosis, there have been few recent reviews on pathological left ventricular remodelling in patients with primary MR.[6-8] In this review we focus in particular on the pathophysiological changes seen in the myocardium of the LV due to volume overload caused by chronic primary MR. We also discuss medical interventions that may attenuate or reverse the adverse changes seen in chronic primary MR, focusing on data related to the use of beta-blockers in these patients.

Pathophysiological changes in the LV in chronic primary MR

Primary MR may present acutely, as a slowly progressive disease, or as chronic progressive MR with sudden deterioration related to acute changes in mitral valve anatomy such as a ruptured cord. Acute MR is usually a medical emergency requiring emergent surgery and is not the focus of this review.

Patients with chronic primary MR are often asymptomatic for long periods of time before presenting at a late stage in heart failure. During this period, there is development of progressive left ventricular dysfunction as the LV is remodelled in an attempt to produce an adequate forward stroke volume.[9,10] Five- to

10-year cardiovascular mortality rates vary between 10 and 15%, with a worse prognosis for patients with severe MR.[11,12]

Alterations in the global structure of the LV in response to primary MR have been reviewed in detail previously.[3] Briefly, MR results in increases in LA volume, a reduction in FSV and an increase in left ventricular preload. By mechanisms that are unclear but are discussed in more detail below, the LV responds to the increased preload by eccentric hypertrophy, with a serial increase in myocyte sarcomeres and myofibril slippage (Fig. 1).[13-18]

Eccentric hypertrophy normalises afterload, as estimated by mean systolic stress, compared to patients with AR leading to a period of so-called 'compensation'.[19] However, the hypertrophy that develops is actually insufficient to fully compensate for the wall stress that develops. This is due to inadequate protein synthesis triggered by MR compared to pressure overload[14,20] and progressive deterioration in myocardial function.[21]

There is no clear explanation for this phenomenon but it has been proposed that the lower systolic load in the case of MR may result in a reduced hypertrophic response at a time when there is a marked demand for an increased stroke volume.[21] Altered cytoskeletal changes, such as microtubular density, may also play a role.[22] With time, in the face of inadequate hypertrophy and a dilating LV, systolic wall stress increases [based on the Laplace effect where wall stress (σ) is directly related to the pressure within the ventricle and its radius (Pr), and inversely related to the wall thickness (2h); $\sigma = Pr/2h$] due to the increases in LV dimensions and inadequate hypertrophy.[21,23,24]

Chronic increases in wall stress are detrimental to the myocardium, resulting in activation of a number of complex inflammatory and apoptotic pathways, in a similar manner to heart failure from other causes. Ultimately, there is myocyte loss and sliding displacement of cardiomyocytes, or cell slippage, caused by disruption of the myocardial extracellular matrix (ECM)–integrin linkages.[7,25]

Various lines of evidence point to time-dependent changes in the up- and downregulation of remodelling pathways in chronic primary MR.[26] This process is initiated by diastolic mechanical stretch due to an increase in end-diastolic wall stress, leading to an early increase in reactive oxygen species (ROS) generation, inflammatory cytokine expression and neurohormonal activation, with increases in angiotensin II and catecholamine levels. Early in the remodelling process there is interstitial collagen loss and cell slippage but with time there is myocyte apoptosis and pathological ECM fibrosis.[27] Chronic decompensated MR ensues, and the LV resembles end-stage dilated cardiomyopathy.

MR causes mechanical stretch, which triggers mechanoreceptors and activates signal-transduction pathways

Myocardial mechanoreception is currently poorly understood.[28-30] There is no evidence that specialised mechanosensory cells exist in the myocardium and the role of stretch-activated channels in sensing stretch is debatable.[29] Two systems appear to be particularly important in mechanoreception in the cardiomyocyte: the collagen–integrin–cytoskeleton connections[25,31] and sarcomere-related signalling.[30]

The contraction–relaxation cycle of the myocyte depends on coordinated interaction between the thin actin filament and the thick myosin filament within the myocyte sarcomere.[32] Actin is bound directly to the Z-disc while myosin is bound indirectly to the Z-disc via the giant elastic protein, titin.[33,34] In the normal heart, titin is responsible for restoring the stretched sarcomere to its resting length following active contraction.[33,34] However, another important role for titin is in mechanoreception and the activation of a number of signal-transduction pathways when there is chronic myocyte stretch.[28,29,33,35-37] It does this by changes

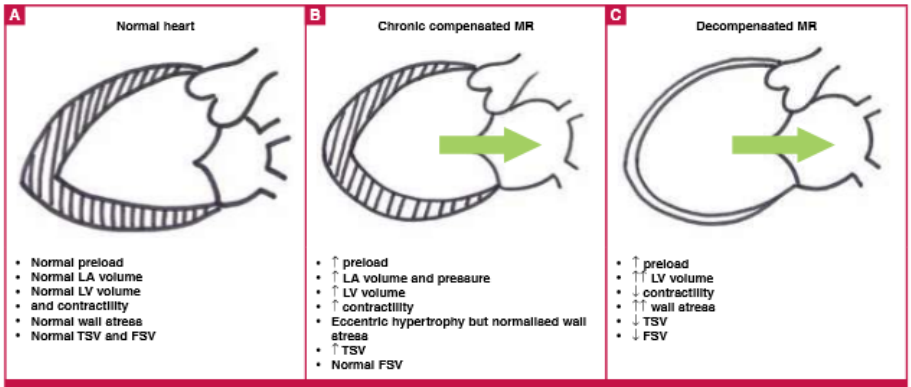

Fig. 1. Left ventricular remodelling in chronic primary mitral regurgitation. A: Normal LV is represented on the left. Wall stress is normal. B: Chronic compensation with eccentric hypertrophy and dilatation. The increase in LV volume is compensated for by the increase in wall thickness. Wall stress appears to be normalised by the eccentric hypertrophy. FSV is normal because of increased LV filling. C: Adversely remodelled LV of decompensated chronic MR. The myocardial wall is thin resulting in an increase in wall stress. The arrow indicates severe MR, which becomes more severe with a dilating LV. LA = left atrium; LV = left ventricle; TSV = total stroke volume; FSV = forward stroke volume; MR = mitral regurgitation.

in the expression of various genes involved in adaptation to the increased load and, ultimately, to the activation of various maladaptive pathways.[38-40]

Titin complexes with a number of potential 'signalosomes' (a mechanosensative signalling complex), including the Z-disc-localised protein MLP (muscle LIM protein), which has been shown to be responsible for hypertrophy and cardiomyopathy in MLP-deficient animals.[41,42] MLP, aside from its structural role in the Z-disk and its interaction with signal transduction proteins, is able to translocate to the nucleus and thereby act as a transcription factor modifying gene expression, depending on mechanical stretch.[43] MLP may be responsible for control of other transcription factors coordinating alterations in the expression of genes responsible for ventricular remodelling. Another important titin signalosome that controls muscle gene expression is the sarcomere M-band-associated protein titin kinase (TK), which is activated by myocyte stretch.[38,40] TK may primarily respond to diastolic stretch,[39] which is particularly relevant in the case of pathological volume overload caused by chronic MR (Fig. 2).

Pathological volume overload-induced mechanical stretch has a number of other effects on the cardiomyocyte. For example, in *in vitro*[44] and *in vivo*[45] rat experiments, TNF-α is produced by cardiomyocytes, resulting in an inflammatory response to stretch, suggesting that TNF-α is an important component in the pathophysiological response of the myocardium to volume overload. Mechanical stretch also results in the local production of angiotensin II[46] and ROS,[47] which, via transcription factors, such as TRAIL (TNF-related apoptosis-inducing ligand) and NFκB,[47] result in local increases in pro-inflammatory cytokines, further contributing to activation of remodelling signal-transduction pathways.[48,49] Finally, as discussed in more detail below, mechanical stretch is transmitted through the ECM to cardiomyocyte integrins, which trigger a number of intracellular signal-transduction pathways involved in hypertrophy and apoptosis.[21,22]

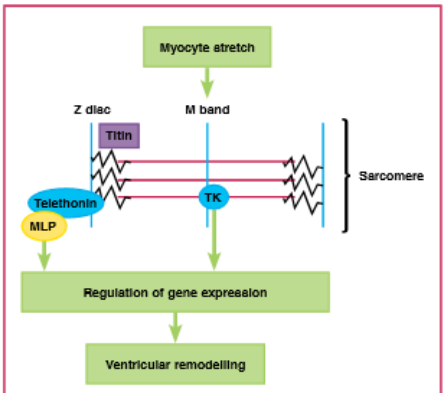

Fig. 2. Schematic representation of gene regulation in response to myocyte sarcomere stretch via signal transduction through MLP and TK (see text for details). MLP – muscle LIM protein; TK – titin kinase.

Chronic primary MR increases cardiac reactive oxidative stress

ROS play an important role in signal transduction and physiological regulation in vascular and myocardial cells. However, under pathological conditions, such as excessive myocyte stretch or excessive inflammatory signals, ROS have been shown to activate maladaptive remodelling signal-transduction pathways.[50,51] These signal-transduction pathways include (but are not limited to) protein phosphorylation pathways leading to cell growth or apoptosis (depending on ROS levels and other factors); matrix metalloproteinase activation;[52] cell cycle protein pathways leading to apoptosis; and pathways leading to the activation of inflammatory transcription factors such as NFκB.[53]

ROS are increased in patients with congestive heart failure,[54] and there is evidence of pathological increases in ROS in patients with chronic isolated MR who still have left ventricular ejection fractions (LVEF) above 60%.[55] These data suggest that there is an increase in oxidative stress even before the LV starts to develop systolic dysfunction, which supports the notion that wall stress is present throughout the evolution of left ventricular remodelling in primary MR. This oxidative stress appears to be present as long as the volume overload persists (Fig. 3).[56]

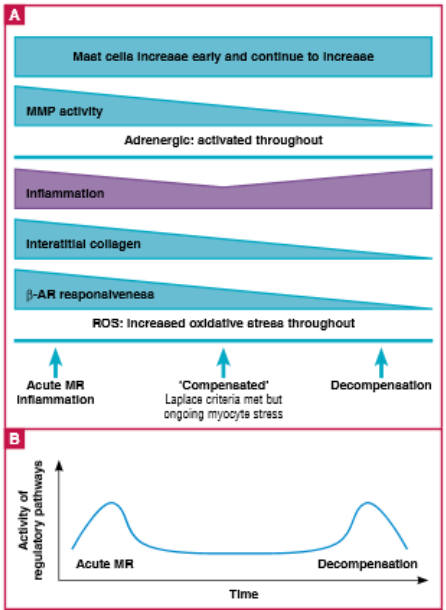

Fig. 3. A. Proposed time-dependent changes in various remodelling pathways including changes in measured prevalence of mast cells. B. Proposed overall time-dependent changes in remodelling pathway activation MMP – matrix metalloproteinases; β-AR – β-adrenergic; ROS – reactive oxidative species. See text for details.

Chronic primary MR triggers an inflammatory response

Tumour necrosis factor (TNF), interleukin-1 (IL-1) and interleukin-6 (IL-6) are produced by all nucleated cells, including cardiac myocytes.[57] Cytokines are responsible for beneficial adaptation to short-term stresses, such as haemodynamic overload, within the myocardium. These molecules may play an important role in protecting the heart from oxidative injury and there are several lines of evidence supporting their beneficial role in short-term stress.[58] However, the role of cytokines in remodelling is complicated and not easily predictable. For example, TNF can have both a protective and an adverse effect on the myocardium, depending on which TNF receptors are activated.[59] Furthermore, prolonged elevation of tissue cytokines has been found to have deleterious effects on the LV.[60,61]

Chronic elevation of cytokines has an effect on left ventricular remodelling by blunting of β-adrenergic signalling[62] and activation of apoptotic pathways.[63-66] TNF-α also increases cardiomyocyte apoptosis[63,65] by activating p38 MAP kinase and NFκB and by down-regulating ERK 1/2 MAP kinase.[66] Overexpression of TNF has also been shown to increase tissue matrix metalloproteinase (MMP) activity, with the resultant acute loss in myocardial fibrillar collagen and left ventricular dilatation.[67-69] However, with continuing TNF overexpression, there is an increase in tissue inhibitors of metalloproteinase (TIMP-1) expression and reduction in MMP expression, leading to abnormal increases in fibrillar collagen,[67,68] suggesting a time-dependent effect of chronic exposure to elevated myocardial TNF.

Cytokines are elevated in patients with heart failure,[70] in patients with pressure and volume overload,[71] and in other forms of heart disease.[72,73] Several lines of evidence suggest that the myocardial response to TNFα is similar regardless of aetiology. Gene expression analysis by micro-array suggests that there is a time-dependent inflammatory response to volume overload (Fig. 3).[24,65] Very early after the initiation of volume overload in aorto-caval fistula rats, there is a marked increase in the expression of inflammatory pathway genes, followed by relative normalisation during the chronic 'compensated' period of volume overload.[24] This is supported by earlier studies that demonstrate that myocyte stretch induces TNFα secretion from myocytes,[44,74] and mast cell-deficient rats with volume overload were protected from TNFα-dependent left ventricular remodelling.[69] Furthermore, in humans with compensated chronic primary MR and normal LVEF, there is a down-regulation of inflammatory pathways.[56]

As the LV becomes dilated and dysfunctional, there is an increase in inflammatory pathway gene expression,[24] which is supported by clinical work in patients with severe chronic primary MR[71,75] and severe rheumatic aortic regurgitation.[76] Overall, there appears to be a biphasic elevation in the inflammatory response to mitral regurgitation, with early volume overload activating the expression of numerous inflammatory pathways, and decompensation triggering a second inflammatory response (Fig. 3).

Myocyte loss in chronic primary MR

Apoptosis is activated by several extracellular death signals, including myocyte stretch,[77] catecholamines[25,78-80] and inflammatory cytokines,[57] and various intracellular death signals.[81-85] These death signals[25] activate transcription factors,[86] ultimately resulting in activation of the caspase cascade.[87] Loss of myocytes will increase the stress on remaining myocytes. This leads to further increases in ROS,[88] cytokine release,[44] increases in adrenergic activation,[89] perpetuating loss of myocytes in a downward spiraling process. Time-dependent apoptosis of non-myocyte cells has been described in volume-loaded rats[24] and there is evidence that chronic primary MR causes a reduction in contractile elements.[21,82,90] Based on this evidence and evidence from studies in myocardial remodelling due to other causes, it is probable that cell loss is an important component in left ventricular dilatation and dysfunction in chronic primary MR.

ECM changes in chronic primary MR

Myocyte arrangement and myocardial integrity is highly organised to enable the continuously moving myocardium to produce coordinated contraction, resulting in stroke volume.[91] The structural integrity is provided by the ECM, which comprises a basement membrane, proteoglycans and glycosaminoglycans, and ECM proteins such as type I, III and V collagen, of which approximately 85% is type I collagen.[7] This collagen framework serves to maintain cardiac myocyte alignment, without which the myocytes would 'slip', altering the shape and size of the cardiac chambers.[91]

The ECM is a highly dynamic part of the myocardium that changes depending on the degree and type of mechanical stress, neurohormonal activation, inflammation and oxidative stress. These stressors on the ECM result in changes in the expression and activation of the proteins responsible for ECM turnover and, ultimately, alterations in collagen deposition and degradation.

MMPs are a heterogeous family of enzymes responsible for the proteolysis of various protein-based extracellular substances. They include the collagenases (MMP-1, MMP-8 and MMP-13), stromelysins (MMP-3 and MMP-10) and the gelatinases (MMP-2 and MMP-9). They are expressed and secreted into the extracellular space by a variety of cells, including cardiac myocytes, cardiac fibroblasts and macrophages.[92] However, the roles of each MMP and the control of their activity are not yet clearly elucidated and this is an area of on-going research.[7] Some studies have demonstrated a correlation between MMP expression and cardiomyopathy phenotypes,[93-95] and others have demonstrated that serum levels of MMPs have prognostic value in heart failure.[96,97]

TIMPs are low-molecular-weight proteins that bind to the catalytic domain of active MMPs, preventing substrate binding. There are four species of TIMPs with overlapping functions within the myocardium, which are not restricted to MMP inhibition. Other pleomorphic effects have been described. For example, TIMP-2 increases collagen production by fibroblasts, whereas TIMP-3 is responsible for fibroblast apoptosis.[98]

Biological and/or mechanical stimuli trigger various signal-transduction pathways, resulting in the production of MMP transcription factors and the secretion of these enzymes into the ECM.[92,99-101] Mechanical stimuli, such as stretch,[102] are transduced through the ECM, which, via collagen–integrin–cytoskeleton connections, are connected to and activate a number of intra-myocyte signal-transduction pathways involved in ECM remodelling.[21,66,103-106] Local ROS, endothelin-1, angiotensin II and catecholamines, via α- and β-receptors, are also responsible for increases in MMP expression.[92,99,107,108]

Cytokines, such as TNFα and IL-1, have been found to increase MMP expression,[97,102] promoting matrix degradation and ventricular dilatation.[7] On the other hand, MMP-9 production can be suppressed by TGF-β-activated NFκB binding in some experiments,[109] whereas its expression was up-regulated by angiotensin II-activated NFκB in other experiments.[110] Angiotensin II[107] and aldosterone both increase ECM remodelling, mainly through TGF-β,[111] although the effects of this protein are multiple and often opposing, depending on circumstances.[112]

TGF-β stimulation induces maturation of fibroblasts to myofibroblasts and enhances ECM protein synthesis via induction of TIMP expression and inhibition of certain MMPs expression.[111] However, this is dependent on the load on the myocardium and there is clear evidence that volume overload results in reduction in TGF-β level and loss of interstitial collagen,[113] whereas pressure overload increases TGF-β.[114] The result is increased detection of markers of collagen types I and III turnover in the serum,[115] pathological decreases in interstitial collagen[15,116,117] and left ventricular dilatation.

In response to different haemodynamic overloads (pressure versus volume), the ECM undergoes different patterns of remodelling.[27] Volume overload produces a distinctive loss of collagen fibrils surrounding individual myocytes,[15,116,118] with the resultant wall thinning and ventricular dilatation changing the geometrical shape of the LV, whereas excess matrix deposition is observed in pressure overload.[119,120] Despite similar fibrotic molecular pathways and cellular effectors, the pathophysiological mechanisms leading to fibrotic remodelling are different, depending on the load on the heart.[7] For example, ACE inhibitors reduce remodelling and collagen accumulation in pressure overload,[121] but not in chronic MR.[15,122] Furthermore, the expression of integrins, which are important in ECM–myocyte connectivity and ECM remodelling, are reduced in MR[123] but increased in pressure overload.[124] Similarly, profibrotic TGF-β expression was increased in mice with pressure overload[114] but was decreased in dogs with experimental MR,[113] and expression of PAI-1, which is fibrogenic, was increased in a swine model of early pressure overload[124] but decreased in chronic MR.[113]

There appears to be a time-dependent increase and decrease in MMP activity during the evolution of left ventricular remodelling in response to primary MR (Fig. 3).[26,117] Myocardial mast cells have been found to be instrumental in increases in MMP activity in early volume overload,[49,117,125,126] and are increased in number in response to volume overload-induced increases in myocardial TNFα.[45] In animal models there is an early rise in myocardial MMP levels after the volume-loaded state is created but this seems to normalise after the acute phase.[127,128]

MMP gene expression in dogs with isolated MR has confirmed that, at four months, there was down-regulation of a number of non-collagen genes important in ECM structure, down-regulation of pro-fibrotic connective tissue growth factor and plasminogen activator, and down-regulation of numerous genes in the TGF-β pathway.[113] However, MMP-1 and MMP-9 gene expression was still markedly increased in these dogs with compensated MR compared with controls.[113] As the LV started to dilate in dogs with chronic myxomatous mitral valve disease, MMP-9 levels decreased.[129]

Over time, there are characteristic changes in the MMP/TIMP ratio, enabling the ventricle to initially increase compliance in the acute and compensated phases of MR. However, at some point (the 'transition' point) there is excessive degradation of the ECM, leading to the decompensated and dilated LV.[27,130] What controls the steady deterioration in the myocardium in response to volume overload is not clear and appears to be complex. In the early stages of volume overload, there are decreases in ECM deposition (which contrasts with the picture in pressure overload),[113] but late in the progression of the dilating volume-loaded heart, an increase in perivascular collagen deposition has been noted,[26,126] which may reduce ventricular compliance and promote systolic dysfunction.[27]

Chronic primary MR activates the neurohormonal system: implications for beta-blocker therapy

Patients with chronic primary MR demonstrate LV systolic dysfunction even before a reduction in LVEF occurs.[121,122] As with heart failure due to any other cause, chronic MR results in activation of the neurohormonal system and inflammatory cascade at both systemic and local levels.[122–125] With neurohormonal activation, myocardial angiotensin II plays an important role in the regulation of cell proliferation, apoptosis, inflammation and production of mediators of remodelling such as platelet-derived growth factor and MMPs.[126] Persistent angiotensin receptor-1 activation by angiotensin II not only results in the generation of ROS but also alterations in protein synthesis via tyrosine kinase receptor activation and MAP kinase signalling.[127] Furthermore, angiotensin II-activated ROS act as second messengers that also have effects on inflammation and cell growth.[128] Angiotensin II also acts on the sympathetic nerve endings in the myocardium to facilitate catecholamine release.[129,140]

Long-term increases in myocardial angiotensin II levels increase local TGFβ, with the resultant increases in activation of genes involved in ECM production via nuclear translocation of NFκB.[110,141] Unlike the pressure-overloaded heart where there is progressive fibrosis,[142] the increase in myocardial angiotensin II in volume overload results in an increase in ECM turnover with loss of interstitial ECM.[143] Despite the clear link between angiotensin and remodelling in heart failure, to date there has been little clinical evidence to support the role of medical therapy directed against angiotensin in subjects with chronic organic MR.[15,144–146] This may be explained by the fact that ACE inhibitors reduce the breakdown of bradykinin, which has been implicated in the initial increase in MMP activity and collagen breakdown seen in volume overload.[143]

Three types of β-adrenergic receptors (β-ARs) are known to exist in the myocardium: β_1, β_2 and β_3, with an approximate ratio of 80:17:3.[147] β_1 and β_2 are important in the regulation of myocyte excitation–contraction coupling.[80] β_1-AR is the predominant receptor subtype expressed in the heart and, like other β-ARs, its stimulation results in G-protein-coupled activation of the adenyl cyclase–cAMP–protein kinase A (PKA) signalling cascade. This leads to activation of a number of subcellular pathways important in cardiomyocyte contractile function, including calcium channel activation and troponin I phosphorylation. By contrast, β_2-AR signalling has negative effects on adenyl cyclase activation and the subsequent G-protein-activated ionotropic response.[80] β_2AR appears to be important in protection from hypertrophic and fibrotic remodelling by preserving NO/cGMP signalling during cardiac stress.[148]

The β-adrenergic receptor system plays an important role in the pathogenesis of myocardial remodelling and heart failure.[84] The exact mechanisms are unclear but it has been known for decades that chronically increased plasma catecholamines can lead to heart failure.[149,150] In dogs with chronic primary MR, there is activation of the adrenergic system,[89,108] and recent gene array data in chronic primary MR patients with preserved LVEF demonstrate increased expression of genes involved in β-adrenergic signalling.[84] This indicates that the adrenergic system is activated during the compensatory phase of MR and supports the concept that blocking these pathways may reduce their adverse consequences. However, with transition to decompensation there is a reduction in adrenergic responsiveness.

In patients with systolic heart failure (HF), several studies in the last three decades show that β_1-receptor density[151] and its mRNA[152,153] are reduced while β_2-receptor density remains unchanged.[154] Similarly, in animals with HF due to chronic volume overload, β_1-AR responsiveness is reduced due to neurohormonal activation (Fig. 3).[47,155] These changes in β_1-AR expression are caused by sustained adrenergic activity, causing an increase in the expression and activity of GRK 2 (G-protein-coupled receptor kinase; formerly called β-ARK or β-agonist receptor kinase), resulting in β_1-AR being phosphorylated and labelled for desensitisation, internalisation and recycling.[156] The result is a reduction in the density of β_1-ARs and a reduced propensity for myocyte activation by chronic β_1-receptor activation, which may protect the myocyte from long-term catecholamine toxicity.[82]

Beta-blocker therapy improves β_1-AR signalling and clinical outcomes in HF

Chronic β_1-AR activation causes a number of detrimental effects, ultimately resulting in changes in the ECM and cell loss from necrosis and apoptosis,[25] which in turn leads to cardiac dilatation and failure.[157] However, the intracellular pathways responsible for these final acts are unclear.[25] What is clear is that β_1-AR antagonists improve clinical outcomes in patients with systolic heart failure and improve cardiac function and myocardial remodelling.[158]

Most β-adrenergic blockers are antagonistic to β-ARs (whether β-1, β-2 or β-3) by occupying the receptor and preventing signal transduction via G-protein activation. Importantly, there is an up-regulation of β_1-AR expression and improvements in receptor sensitivity, resulting in reversal of cardiac remodelling.[147] However, the pharmacological and clinical effects of these agents vary quite considerably. Cardioselective beta-blockers (metoprolol, bisoprolol and atenolol, for example) have a greater affinity for β_1-ARs than β_2-ARs, whereas carvedilol binds β_1-ARs more than β_2-ARs and has vasodilatory effects, via nitric oxide and α_1 receptor blockade.

There are other important differences between carvedilol and other beta-blockers. For example, metoprolol upregulates cardioprotective β_2-AR expression, whereas carvedilol does not.[159,160] Carvedilol has antioxidant and antiproliferative properties[161-163] and differs from metoprolol in its effects on haemodynamics, left ventricular function and β_1-AR expression.[164,165] Carvedilol[166] and bisoprolol[167] have also been shown to improve right ventricular (RV) ejection fraction, attenuate RV dilatation and reduce pulmonary artery hypertension in patients with ischaemic and non-ischaemic dilated cardiomyopathy. Although there are no recent confirmatory studies, these improvements in RV function may be related to reductions in RV afterload and/or improvements in RV contractility.[166,167] By contrast, short-term (two-week) metoprolol did not improve RV function in patients with moderate-to-severe degenerative MR.[168]

Clinical support for β-adrenergic receptor blocker therapy in patients with heart failure is well known,[158,169,170] with some data suggesting that patient outcomes are better with carvedilol than the immediate-release form of metoprolol.[171]

Several mechanisms for the improvement in outcomes with β_1-receptor blockade have been proposed,[84] including anti-arrhythmic properties;[172] improved β-adrenergic signalling by cardiac β-AR upregulation;[82] free-radical scavenging;[161] improvements in calcium cycling by the sarcoplasmic reticulum;[83,173] bradycardia reducing myocardial work, mechanical stress,[174] and prolonging diastolic calcium uptake and cycling by the sarcoplasmic reticulum; inhibition of the renin–angiotensin–aldosterone system; and there is growing evidence that β-antagonists, in particular carvedilol,[162,163] directly reduce apoptosis[78,175-177] and collagen loss by MMP activation.[178]

β_1-AR blockade in MR counters adverse adrenergic effects

Since MR leads to a reduction in forward stroke volume, it is hypothesised that the adrenergic system is activated to maintain systemic blood pressure and perfusion, and blockade of the adrenergic system should limit adverse left ventricular remodelling. There is evidence that chronic primary MR results in excessive activation of the sympathetic nervous system, with increases in myocardial catecholamine levels,[89,118,124] similar to heart failure from other causes.[179]

Tallaj *et al.*[118] demonstrated that β-AR blockade with extended-release metoprolol succinate attenuated angiotensin II-mediated norepinephrine and epinephrine release in the myocardium of dogs with 'subacute' (two to four weeks' duration) isolated MR. Similarly, Hankes *et al.*[89] demonstrated that norepinephrine release into the cardiac interstitium was significantly higher in dogs with subacute MR, which was reduced by β_1-AR blockade. In an earlier study by Tsutsui *et al.*[95] in 'chronic' (three months) canine MR, the β_1- AR blocker atenolol improved left ventricular function, which was associated with improvement in contractile function of isolated cardiocytes and an increase in the number of contractile elements. This was supported by a similar study by Nemoto *et al.*,[165] which showed that only when a β_1-AR blocker was added to an ACE inhibitor did forward stroke volume and cardiac contractility return to normal. Recently, Trappanese *et al.*[180] demonstrated an improvement in β_2-AR expression and β_2-NO-cGMP coupling with chronic therapy with metoprolol in dogs with primary MR. Since β_2-AR is cardioprotective, this may partially explain the potential beneficial effects of β_1-AR blockade in primary MR.[159]

Beta-blockade therapy for chronic primary MR

At present there is no proven medical therapy for chronic primary MR. Surgery is the mainstay of treatment for severe MR[1] but carries peri-operative risk, and patients are potentially subjected to a life-time risk of anticoagulation if they undergo

mitral valve replacement. Many patients in the developing world are from poor and rural backgrounds where access to regular medication and regular anti-coagulation assessment is difficult. A medication that could limit or even reverse left ventricular dysfunction associated with the volume-loaded state of chronic severe MR would be extremely beneficial to these patients even if only to delay the need for surgical intervention. This would especially be true in women of child-bearing age. Warfarin is teratogenic and many women with prosthetic valves have complicated pregnancies related to the teratogenic effects of warfarin or the risks related to bleeding during pregnancy.

Persistent, and often worsened, postoperative left ventricular dysfunction is a major cause of morbidity and mortality in these patients,[122] although this is not a universal finding, especially when patients are referred for early surgery.[181-182] Nevertheless, a means to improve left ventricular function in the peri-operative period might improve the postoperative morbidity and mortality rates associated with left ventricular dysfunction.

Current guidelines[1,184] recommend surgery for patients with severe pulmonary hypertension on presentation or a progressively dilating LV, even if they are asymptomatic. However, timing of surgery is uncertain[185,186] and there is no clear guideline as to the urgency of the surgery in asymptomatic patients without overt left ventricular systolic dysfunction (LVEF < 60%). Several studies support early surgery for chronic primary MR.[187-189] Enriquez-Sarano *et al.*[12] showed that patients with an effective regurgitant orifice area of at least 40 mm² as assessed by echocardiography should promptly be considered for cardiac surgery. Barbieri *et al.*[190] found that asymptomatic patients with evidence of pulmonary hypertension (> 50 mmHg at rest) should undergo prompt surgery. However, there is also evidence that asymptomatic patients with severe MR can be followed until they become symptomatic or demonstrate echocardiographic signs of left ventricular dysfunction.[122,191]

How these patients should be managed in the interim is unclear but it is important that patients are not left untreated until irreversible left ventricular remodelling has taken place. In resource-limited hospitals, patients who do not need emergency surgery often wait several months before they undergo surgery, by which time there has been progressive advancement of ventricular remodelling, leading to permanent impairment of function. Medical therapy that could reverse or at least attenuate LV remodelling may improve outcomes in these patients.

To date, there is little evidence to support medical therapy in the treatment of patients with organic valve disease,[1,119,192] or in the reversal or attenuation of LV remodelling, which may delay the need for surgery in asymptomatic patients.[192] Vasodilator therapy, which reduces peripheral vascular resistance and left ventricular afterload,[119] has generally not improved outcomes in patients with MR or in experimental MR canine models.[15,122,145,194] Although several small studies from the 1970s to the 1990s showed benefit of vasodilator therapy in acute MR,[144] small human studies from the same period failed to show long-term benefit.[195] One retrospective study, however, demonstrated an improvement in echocardiographic LVEF in patients treated with afterload-reducing agents.[146] However, there are no large randomised studies assessing long-term vasodilator therapy, including ACE inhibitors, in humans.

There is some clinical evidence to support the concept that β-AR blockade may attenuate remodelling in patients with primary MR (Table 1). Stewart *et al.*[196] recruited 25 patients with moderate or severe degenerative MR and randomly assigned the participants to the β_1-AR blocker metoprolol or placebo for approximately two weeks. Left ventricular function was assessed at baseline and on study completion by cardiac magnetic resonance imaging. They found that the β_1-AR blocker resulted in a decrease in left ventricular work and an increase in forward stroke volume.[196] Mitral annular dimensions also appeared to improve over the two-week period in the same cohort of patients.[197]

A retrospective observational study involving 895 patients in California showed that participants on β_1-AR blocker therapy with severe MR and normal left ventricular function had a significantly lowered mortality hazard, regardless of the presence of hypertension or coronary artery disease.[198] Ahmed *et al.*[199] published the results of the first randomised, controlled phase IIb trial of beta-blockade in patients with chronic degenerative MR. Thirty-eight asymptomatic patients with moderate-to-severe isolated MR were randomised to either placebo or long-acting metoprolol for two years. Cardiac magnetic resonance analysis showed that patients randomised to the β-AR blocker had significantly better LVEFs after two years of therapy.

By contrast, there are several pre-clinical and clinical studies demonstrating that beta-blocker therapy actually worsens left ventricular dimensions and function in chronic primary MR (Table 1).[108,146,197,200,201] A recent, longer-term (23 to 35 weeks) study in rats found that echocardiographic measures of left ventricular remodelling were not improved by carvedilol.[201] In fact, left ventricular dimensions, ejection fraction and survival were significantly lower with long-term carvedilol use.

Similarly, in a four-month dog model, extended-release metoprolol succinate failed to attenuate the adverse global left ventricular remodelling and ECM loss, but did preserve cardiomyocyte function.[200] Interestingly, all dogs treated with β-1-receptor blocker (n = 6) survived to four months, whereas only five out of nine of the untreated dogs survived to four months. Similarly, Sabri *et al.*[108] found that, despite reductions in interstitial collagen degradation and reductions in adverse remodelling-related intracellular signalling, extended-release metoprolol succinate failed to attenuate left ventricular dilatation or decline in left ventricular function.

A retrospective echocardiographic study in 134 human subjects with moderate-to-severe MR (67% degenerative and 20% 'non-specific thickening') found that patients exposed to beta-adrenergic blockade developed worsening of their ejection fraction over a mean of 20 months of follow up.[146] Finally, despite improvements in left ventricular work and annular dimensions,[197] in patients treated over a short period with metoprolol, there were significant increases in left ventricular end-systolic and end-diastolic volume with no significant change in LVEF or regurgitant volume.[196]

At the present time, there are no recommendations regarding medical therapy in chronic primary MR. Afterload reduction has not consistently been shown to improve long-term outcomes.[15,122,145,146,195] Data from heart failure trials[168,169,170] as well as from animal models[80] and human trials[199] suggest a role for beta-blockade in MR, however, other studies do not support this.[108,146,197,200,201] The reasons for the discrepancies in these findings are unclear but some explanations can be proposed.

Firstly, the studies have been performed in different experimental models and at different stages in the evolution

Table 1. Studies of beta-blocker therapy and left ventricular function in primary MR

Authors	*Year*	*Subject*	*Cause of MR*	*Number treated with BB*	*Type of study*	*Control*	*Type of BB*	*Duration of BB*	*Outcome measures*	*Favours BB*
Tsutsui *et al.*[88]	1994	Dog	Experimental chordal rupture	$n = 6$	Case controlled	$n = 6$	Atenolol 50mg daily	3 months	Cardiocytc contractility, myofibrillar density	+
Nemoto *et al.*[144]	2002	Dog	Experimental chordal rupture	$n = 11$	Longitudinal	NA	Atenolol 100mg daily	3 months	Hemodynamics, LV function	+
Tallaj *et al.*[127]	2003	Dog	Experimental chordal rupture	2 weeks MR+BB: $n = 6$ 4 weeks MR+BB: $n = 8$	Case controlled	Normal: $n = 8$ 2 weeks MR: $n = 8$ 4 weeks MR: $n = 6$	Metoprolol succinate 100mg daily	4 weeks	RAAS activation	+
Hankes *et al.*[83]	2006	Dog	Experimental chordal rupture	4 weeks of MR+BB = 8	Case controlled	Normal = 6 Untreated MR = 6	Metoprolol succinate 100mg daily	4 weeks	NE release into cardiac interstitium	+
Oh *et al.*[145]	2007	Human	71% degenerative	$n = 134$	Retrospective cohort	NA	Not ascertained	1–88 months	Echo LVEF	–
Pat *et al.*[109]	2008	Dog	Experimental chordal rupture	$n = 11$	Case controlled	$n = 10$	Metoprolol succinate 100mg twice daily	4 months	LV remodelling by MRI and echo; cardiomyocytc function	Improved cardiomyocytc function and BB receptiveness but failure to attenuate remodelling
Sabri *et al.*[125]	2008	Dog	Experimental chordal rupture	$n = 6$	Case controlled	Normal = 6 Untreated MR = 6	Metoprolol succinate 100 mg daily	4 weeks	LV remodelling by echo; interstitial collagen quantification; FAK signalling (integrin signalling)	BB reduced FAK tyrosine phosphorylation but no change in remodeling parameters; BB reduced epicardial collagen loss but not endocardial collagen loss
Varadarajan *et al.*[187]	2008	Human	LVEF > 55% + 'severe MR'	$n = 218$	Retrospective observational cohort study	$n = 614$	Not stated	8 years	Mortality	+
Stewart *et al.*[164]	2008	Human	MVP	$n = 25$	Double-blind cross-over study	NA	Metoprolol to a maximum 190mg/d	14 days	• MRI • EF • LVEDV • LVESV • LV 'work' (CO)	 – – – +
Ahmed *et al.*[155]	2012	Human	MVP	$n = 19$	RCT	$n = 19$	Toprol XL 25-100mg daily		• MRI LVEF • MRI LVESV • LV longitudinal strain rate	+ – –
Pu *et al.*[200]	2013	Rat	Experimental leaflet disruption	$n = 43$ 'Long-term' BB in 19	RCT	$n = 44$	Carvedilol (1200 PPM)	36 weeks	• Echo only • LV dimensions • LVESV and mass index • FS and EF • Survival probability	–
Trappanese *et al.*[178]	2015	Dog	Experimental chordal rupture	$n = 8$ (MR + BB)	Case controlled	Normal = 10 Untreated MR = 8	Metoprolol succinate 100 mg daily	4 weeks	• Activation of β3AR/NO-cGMP signalling • β3AR expression	+ +

BB = beta-blocker; MVP = mitral valve prolapse; RCT = randomised controlled trial; MR = mitral regurgitation; NE = norepinephrine; + indicates that the study favoured BB therapy in primary MR; - indicates that the study did not favour BB therapy in primary MR; LV = left ventricle; LVEF = left ventricular ejection fraction; LVEDV = left ventricular end-diastolic volume; LVESV = left ventricular end-systolic volume; CO = cardiac output; RAAS = renin–angiotensin–aldosterone system; echo = echocardiogram; MRI = magnetic resonance imaging.

of MR-related left ventricular remodelling. Many of the experiments performed thus far have been in animal models with controlled formation of volume overload showing that early introduction of beta-blocker therapy[89,90,118] may be beneficial, and this is supported to some extent by the work of Ahmed *et al.*[155] in humans. However, there appears to be a time-dependent pattern during remodelling of the LV in chronic primary MR.

Early after the development of MR there is a marked increase in inflammatory and neurohormonal response to the acute volume overload.[26,118] A period of compensation and a relatively normal inflammatory response appears to follow until the late decompensated stage is reached, when adverse pathway activation seems to increase.[26] Depending on when in this evolution of left ventricular remodelling the studies to date have been performed, there may be discrepancies in the findings with regard to the impact of beta-blockade on left ventricular remodelling. Beta-blockade may have more impressive effects if used early in the evolution of volume overload-related left ventricular remodeling but it may be less effective later on.

Secondly, various beta-adrenergic agents have been tested under different circumstances. Compared to the impressive beneficial results in heart failure patients with the mixed adrenergic blocker, carvedilol,[158,202] Pu *et al.*[201] demonstrated that this drug caused worsening left ventricular dimensions and function in animal subjects with primary MR. By contrast, treatment of dogs with the selective beta-blocker atenolol

improved left ventricular remodelling,[95] whereas treatment with metoprolol in animals and humans have had mixed results.[108,180,196,197,199,200]

Thirdly, an important question is whether patients presenting in more advanced stages of left ventricular remodelling will respond to anti-remodelling therapy or whether the wall stresses determined by the Laplace law will outweigh any potential beta-blocker effect. In this regard, the findings of Pat *et al.* [200] are interesting because although there were improvements in cardiomyocyte contractility and beta-receptor responsiveness, left ventricular remodelling was not attenuated by metoprolol. It was postulated that β-AR blockade failed to preserve interstitial collagen loss and therefore failed to prevent ongoing myocyte slippage. There appears to be a strong early adrenergic response to chronic primary MR,[56] and beta-blocker therapy before onset of left ventricular dilatation may have more benefit.

Lastly, in patients with rheumatic mitral valve disease, there is a possibility that rheumatic fever causing rheumatic carditis may have long-lasting effects on the myocardium, attenuating reverse remodelling by beta-blockers.

Conclusion

Left ventricular remodelling in response to the volume load created by chronic primary MR is a complex process that stems from excessive diastolic stretch of myocytes. Excessive stretch triggers activation of numerous signal transduction pathways, resulting in an initial adaptive remodelling process in the form of eccentric hypertrophy. However, chronic activation of these pathways results in abnormal increases in ROS, catecholamines, angiotensin II and inflammatory cytokines. This is followed by a transition to adverse remodelling involving cardiomyocyte apoptosis and interstitial collagen loss, common to all forms of heart failure.

Limited data do not support the routine long-term use of afterload-reducing agents for the treatment of chronic primary MR. By contrast, there is pre-clinical data demonstrating that β-AR blockade reverses remodelling caused by the volume overload of chronic primary MR, and there are some recent clinical data to support this hypothesis. However, some studies demonstrated worsening left ventricular remodelling with beta-blocker therapy. Whether these contrasting outcomes are related to differences in beta-blockers, varying experimental models or differences in timing of therapy will need clarification. Ultimately, further studies are required to elucidate the exact mechanisms involved, and large randomised clinical trials are needed to clarify the role of these agents for patients with chronic primary MR.

References

1. Vahanian A, Alfieri O, Andreotti F, *et al.* Guidelines on the management of valvular heart disease (version 2012): the Joint Task Force on the Management of Valvular Heart Disease of the European Society of Cardiology (ESC) and the European Association for Cardio-Thoracic Surgery (EACTS). *Eur J Cardiothorac Surg* 2012; **42**(4): S1–44.
2. Ciarka A, van de Veire N. Secondary mitral regurgitation: pathophysiology, diagnosis, and treatment. *Heart* 2011; **97**(12): 1012–1023.
3. Foster E. Clinical practice. Mitral regurgitation due to degenerative mitral-valve disease. *N Engl J Med* 2010; **363**(2): 156–165.
4. Sliwa K, Mocumbi AO. Forgotten cardiovascular diseases in Africa. *Clin Res Cardiol* 2010; **99**(2): 65–74.
5. McMurray JJ, Adamopoulos S, Anker SD, *et al.* ESC guidelines for the diagnosis and treatment of acute and chronic heart failure 2012: The Task Force for the Diagnosis and Treatment of Acute and Chronic Heart Failure 2012 of the European Society of Cardiology. Developed in collaboration with the Heart Failure Association (HFA) of the ESC. *Eur Heart J* 2012; **33**(14): 1787–1847.
6. Burchfield JS, Xie M, Hill JA. Pathological ventricular remodeling: mechanisms: part 1 of 2. *Circulation* 2013; **128**(4): 388–400.
7. Kong P, Christia P, Frangogiannis NG. The pathogenesis of cardiac fibrosis. *Cell Mol Life Sci* 2014; **71**(4): 549–574.
8. Otto CM, Prendergast B. Aortic-valve stenosis – from patients at risk to severe valve obstruction. *N Engl J Med* 2014; **371**(8): 744–756.
9. Carabello BA, Crawford FA. Valvular heart disease. *New Engl J Med* 1997; **337**(1): 32–41.
10. Enriquez-Sarano M, Akins CW, Vahanian A. Mitral regurgitation. *Lancet* 2009; **373**(9672): 1382–1394.
11. Avierinos JF, Gersh BJ, Melton LJ, 3rd, *et al.* Natural history of asymptomatic mitral valve prolapse in the community. *Circulation* 2002; **106**(11): 1355–1361.
12. Enriquez-Sarano M, Avierinos JF, Messika-Zeitoun D, *et al.* Quantitative determinants of the outcome of asymptomatic mitral regurgitation. *N Engl J Med* 2005; **352**(9): 875–883.
13. Ross J Jr, Sonnenblick EH, Taylor RR, Spotnitz HM, Covell JW. Diastolic geometry and sarcomere lengths in the chronically dilated canine left ventricle. *Circ Res* 1971; **28**(1): 49–61.
14. Grossman W, Jones D, McLaurin LP. Wall stress and patterns of hypertrophy in the human left ventricle. *J Clin Invest* 1975; **56**(1): 56–64.
15. Dell'italia LJ, Balcells E, Meng QC, *et al.* Volume-overload cardiac hypertrophy is unaffected by ACE inhibitor treatment in dogs. *Am J Physiol* 1997; **273**(2 Pt 2): H961–970.
16. Matsuo T, Carabello BA, Nagatomo Y, *et al.* Mechanisms of cardiac hypertrophy in canine volume overload. *Am J Physiol* 1998; **275**(1 Pt 2): H65–74.
17. Kerckhoffs RC, Omens J, McCulloch AD. A single strain-based growth law predicts concentric and eccentric cardiac growth during pressure and volume overload. *Mech Res Commun* 2012; **42**: 40–50.
18. Spinale FG, Ishihra K, Zile M, DeFryte G, Crawford FA, Carabello BA. Structural basis for changes in left ventricular function and geometry because of chronic mitral regurgitation and after correction of volume overload. *J Thorac Cardiovasc Surg* 1993; **106**(6): 1147–1157.
19. Wisenbaugh T, Spann JF, Carabello BA. Differences in myocardial performance and load between patients with similar amounts of chronic aortic versus chronic mitral regurgitation. *J Am Coll Cardiol* 1984; **3**(4): 916–923.
20. Imamura T, McDermott PJ, Kent RL, Nagatsu M, Cooper Gt, Carabello BA. Acute changes in myosin heavy chain synthesis rate in pressure versus volume overload. *Circ Res* 1994; **75**(3): 418–425.
21. Urabe Y, Mann DL, Kent RL, *et al.* Cellular and ventricular contractile dysfunction in experimental canine mitral regurgitation. *Circ Res* 1992; **70**(1): 131–147.
22. Tsutsui H, Ishihara K, Cooper Gt. Cytoskeletal role in the contractile dysfunction of hypertrophied myocardium. *Science* 1993; **260**(5108): 682–687.
23. Carabello BA. Progress in mitral and aortic regurgitation. *Prog Cardiovasc Dis* 1988; **43**(6): 457–475.
24. O'Gara P, Sugeng L, Lang R, *et al.* The role of imaging in chronic degenerative mitral regurgitation. *JACC Cardiovasc Imaging* 2008; **1**(2): 221–237.

25. Amin P, Singh M, Singh K. Beta-Adrenergic receptor-stimulated cardiac myocyte apoptosis: role of beta1 integrins. *J Signal Transduct* 2011; **2011**: 179057.
26. Chen YW, Pat B, Gladden JD, *et al.* Dynamic molecular and histopathological changes in the extracellular matrix and inflammation in the transition to heart failure in isolated volume overload. *Am J Physiol Heart Circ Physiol* 2011; **300**(6): H2251–2260.
27. Hutchinson KR, Stewart JA Jr, Lucchesi PA. Extracellular matrix remodeling during the progression of volume overload-induced heart failure. *J Mol Cell Cardiol* 2010; **48**(3): 564–569.
28. Knoll R, Marston S. On mechanosensation, acto/myosin interaction, and hypertrophy. *Trends Cardiovasc Med* 2012; **22**(1): 17–22.
29. Buyandelger B, Mansfield C, Knoll R. Mechano-signaling in heart failure. *Pflugers Arch* 2014; **466**(6): 1093–1099.
30. Lyon RC, Zanella F, Omens JH, Sheikh F. Mechanotransduction in cardiac hypertrophy and failure. *Circ Res* 2015; **116**(8): 1462–1476.
31. Israeli-Rosenberg S, Manso AM, Okada H, Ross RS. Integrins and integrin-associated proteins in the cardiac myocyte. *Circ Res* 2014; **114**(3): 572–586.
32. Opie LH BD. *Mechanisms of Cardiac Contraction and Relaxation*. 10th edn. Philadelphia: Saunders Elsevier, 2015.
33. Miller MK, Granzier H, Ehler E, Gregorio CC. The sensitive giant: the role of titin-based stretch sensing complexes in the heart. *Trends Cell Biol* 2004; **14**(3): 119–126.
34. Zou P, Pinotsis N, Lange S, *et al.* Palindromic assembly of the giant muscle protein titin in the sarcomeric Z-disk. *Nature* 2006; **439**(7073): 229–233.
35. Knoll R, Hoshijima M, Hoffman HM, *et al.* The cardiac mechanical stretch sensor machinery involves a Z disc complex that is defective in a subset of human dilated cardiomyopathy. *Cell* 2002; **111**(7): 943–955.
36. Hishiya A, Kitazawa T, Takayama S. BAG3 and Hsc70 interact with actin capping protein CapZ to maintain myofibrillar integrity under mechanical stress. *Circ Res* 2010; **107**(10): 1220–1231.
37. Kuwahara K, Kinoshita H, Kuwabara Y, *et al.* Myocardin-related transcription factor A is a common mediator of mechanical stress- and neurohumoral stimulation-induced cardiac hypertrophic signaling leading to activation of brain natriuretic peptide gene expression. *Mol Cell Biol* 2010; **30**(17): 4134–4148.
38. Lange S, Xiang F, Yakovenko A, *et al.* The kinase domain of titin controls muscle gene expression and protein turnover. *Science* 2005; **308**(5728): 1599–1603.
39. Wagner MA, Siddiqui MA. The JAK-STAT pathway in hypertrophic stress signaling and genomic stress response. *Jakstat* 2012; **1**(2): 131–141.
40. Puchner EM, Alexandrovich A, Kho AL, *et al.* Mechanoenzymatics of titin kinase. *Proc Natl Acad Sci USA* 2008; **105**(36): 13385–13390.
41. Arber S, Hunter JJ, Ross J Jr, *et al.* MLP-deficient mice exhibit a disruption of cardiac cytoarchitectural organization, dilated cardiomyopathy, and heart failure. *Cell* 1997; **88**(3): 393–403.
42. Knoll R, Kostin S, Klede S, et al. A common MLP (muscle LIM protein) variant is associated with cardiomyopathy. *Circ Res* 2010; **106**(4): 695–704.
43. Boateng SY, Senyo SE, Qi L, Goldspink PH, Russell B. Myocyte remodeling in response to hypertrophic stimuli requires nucleocytoplasmic shuttling of muscle LIM protein. *J Mol Cell Cardiol* 2009; **47**(4): 426–435.
44. Wang BW, Hung HF, Chang H, Kuan P, Shyu KG. Mechanical stretch enhances the expression of resistin gene in cultured cardiomyocytes via tumor necrosis factor-alpha. *Am J Physiol Heart Circ Physiol* 2007; **293**(4): H2305–2312.
45. Chen Y, Pat B, Zheng J, *et al.* Tumor necrosis factor-alpha produced in cardiomyocytes mediates a predominant myocardial inflammatory response to stretch in early volume overload. *J Mol Cell Cardiol* 2010; **49**(1): 70–78.
46. Wang TL, Yang YH, Chang H, Hung CR. Angiotensin II signals mechanical stretch-induced cardiac matrix metalloproteinase expression via JAK-STAT pathway. *J Mol Cell Cardiol* 2004; **37**(3): 785–794.
47. Gealekman O, Abassi Z, Rubinstein I, Winaver J, Binah O. Role of myocardial inducible nitric oxide synthase in contractile dysfunction and beta-adrenergic hyporesponsiveness in rats with experimental volume-overload heart failure. *Circulation* 2002; **105**(2): 236–243.
48. Baud V, Karin M. Signal transduction by tumor necrosis factor and its relatives. *Trends Cell Biol* 2001; **11**(9): 372–377.
49. Lebrec H, Ponce R, Preston BD, Iles J, Born TL, Hooper M. Tumor necrosis factor, tumor necrosis factor inhibition, and cancer risk. *Curr Med Res Opin* 2015; **31**(3): 557–574.
50. Griendling KK, Sorescu D, Lassegue B, Ushio-Fukai M. Modulation of protein kinase activity and gene expression by reactive oxygen species and their role in vascular physiology and pathophysiology. *Arterioscler Thromb Vasc Biol* 2000; **20**(10): 2175–2183.
51. Grote K, Flach I, Luchtefeld M, *et al.* Mechanical stretch enhances mRNA expression and proenzyme release of matrix metalloproteinase-2 (MMP-2) via NAD(P)H oxidase-derived reactive oxygen species. *Circ Res* 2003; **92**(11): e80–86.
52. Siwik DA, Pagano PJ, Colucci WS. Oxidative stress regulates collagen synthesis and matrix metalloproteinase activity in cardiac fibroblasts. *Am J Physiol Cell Physiol* 2001; **280**(1): C53–60.
53. Birukov KG. Cyclic stretch, reactive oxygen species, and vascular remodeling. *Antioxid Redox Signal* 2009; **11**(7): 1651–1667.
54. Keith M, Geranmayegan A, Sole MJ, *et al.* Increased oxidative stress in patients with congestive heart failure. *J Am Coll Cardiol* 1998; **31**(6): 1352–1356.
55. Ahmed MI, Gladden JD, Litovsky SH, *et al.* Increased oxidative stress and cardiomyocyte myofibrillar degeneration in patients with chronic isolated mitral regurgitation and ejection fraction > 60%. *J Am Coll Cardiol* 2010; **55**(7): 671–679.
56. Zheng J, Yancey DM, Ahmed MI, *et al.* Increased sarcolipin expression and adrenergic drive in humans with preserved left ventricular ejection fraction and chronic isolated mitral regurgitation. *Circulation: Heart Failure* 2014; 7(1): 194–202.
57. Mann DL. Innate immunity and the failing heart: the cytokine hypothesis revisited. *Circ Res* 2015; **116**(7): 1254–1268.
58. Nakano M, Knowlton AA, Dibbs Z, Mann DL. Tumor necrosis factor-alpha confers resistance to hypoxic injury in the adult mammalian cardiac myocyte. *Circulation* 1998; **97**(14): 1392–1400.
59. Hamid T, Gu Y, Ortines RV, *et al.* Divergent tumor necrosis factor receptor-related remodeling responses in heart failure: role of nuclear factor-kappaB and inflammatory activation. *Circulation* 2009; **119**(10): 1386–1397.
60. Pagani FD, Baker LS, Hsi C, Knox M, Fink MP, Visner MS. Left ventricular systolic and diastolic dysfunction after infusion of tumor necrosis factor-alpha in conscious dogs. *J Clin Invest* 1992; **90**(2): 389–398.
61. Franco F, Thomas GD, Giroir B, *et al.* Magnetic resonance imaging and invasive evaluation of development of heart failure in transgenic mice with myocardial expression of tumor necrosis factor-alpha. *Circulation* 1999; **99**(3): 448–454.
62. Krown KA, Page MT, Nguyen C, *et al.* Tumor necrosis factor alpha-induced apoptosis in cardiac myocytes. Involvement of the sphingolipid signaling cascade in cardiac cell death. *J Clin Invest* 1996; **98**(12): 2854–2865.

63. Haudek SB, Taffet GE, Schneider MD, Mann DL. TNF provokes cardiomyocyte apoptosis and cardiac remodeling through activation of multiple cell death pathways. *J Clin Invest* 2007; **117**(9): 2692–2701.
64. Dhingra S, Bagchi AK, Ludke AL, Sharma AK, Singal PK. Akt regulates IL-10 mediated suppression of TNFalpha-induced cardiomyocyte apoptosis by upregulating Stat3 phosphorylation. *PLoS One* 2011; **6**(9): e25009.
65. Engel D, Peshock R, Armstong RC, Sivasubramanian N, Mann DL. Cardiac myocyte apoptosis provokes adverse cardiac remodeling in transgenic mice with targeted TNF overexpression. *Am J Physiol Heart Circ Physiol* 2004; **287**(3): H1303–1311.
66. Dhingra S, Sharma AK, Arora RC, Slezak J, Singal PK. IL-10 attenuates TNF-alpha-induced NF kappaB pathway activation and cardiomyocyte apoptosis. *Cardiovasc Res* 2009; **82**(1): 59–66.
67. Sivasubramanian N, Coker ML, Kurrelmeyer KM, *et al.* Left ventricular remodeling in transgenic mice with cardiac restricted overexpression of tumor necrosis factor. *Circulation* 2001; **104**(7): 826–831.
68. Diwan A, Dibbs Z, Nemoto S, *et al.* Targeted overexpression of noncleavable and secreted forms of tumor necrosis factor provokes disparate cardiac phenotypes. *Circulation* 2004; **109**(2): 262–268.
69. Levick SP, Gardner JD, Holland M, Hauer-Jensen M, Janicki JS, Brower GL. Protection from adverse myocardial remodeling secondary to chronic volume overload in mast cell deficient rats. *J Mol Cell Cardiol* 2008; **45**(1): 56–61.
70. Levine B, Kalman J, Mayer L, Fillit HM, Packer M. Elevated circulating levels of tumor necrosis factor in severe chronic heart failure. *N Engl J Med* 1990; **323**(4): 236–241.
71. Kapadia SR, Yakoob K, Nader S, Thomas JD, Mann DL, Griffin BP. Elevated circulating levels of serum tumor necrosis factor-alpha in patients with hemodynamically significant pressure and volume overload. *J Am Coll Cardiol* 2000; **36**(1): 208–212.
72. Sliwa K, Skudicky D, Bergemann A, Candy G, Puren A, Sareli P. Peripartum cardiomyopathy: analysis of clinical outcome, left ventricular function, plasma levels of cytokines and Fas/APO-1. *J Am Coll Cardiol* 2000; **35**(3): 701–705.
73. Bujak M, Frangogiannis NG. The role of IL-1 in the pathogenesis of heart disease. *Arch Immunol Ther Exp (Warsz)* 2009; **57**(3): 165–176.
74. Palmieri EA, Benincasa G, Di Rella F, *et al.* Differential expression of TNF-alpha, IL-6, and IGF-1 by graded mechanical stress in normal rat myocardium. *Am J Physiol Heart Circ Physiol* 2002; **282**(3): H926–934.
75. Oral H, Sivasubramanian N, Dyke DB, *et al.* Myocardial proinflammatory cytokine expression and left ventricular remodeling in patients with chronic mitral regurgitation. *Circulation* 2003; **107**(6): 831–837.
76. Spina GS, Tarasoutchi F, Sampaio RO, *et al.* Neurohormonal profile of rheumatic patients with significant chronic aortic regurgitation. *Arq Bras Cardiol* 2009; **92**(2): 143-56.
77. Cheng W, Li B, Kajstura J, et al. Stretch-induced programmed myocyte cell death. *J Clin Invest* 1995; **96**(5): 2247–2259.
78. Communal C, Singh K, Pimentel DR, Colucci WS. Norepinephrine stimulates apoptosis in adult rat ventricular myocytes by activation of the beta-adrenergic pathway. *Circulation* 1998; **98**(13): 1329–1334.
79. Geng YJ, Ishikawa Y, Vatner DE, *et al.* Apoptosis of cardiac myocytes in Gsalpha transgenic mice. *Circ Res* 1999; **84**(1): 34–42.
80. Lymperopoulos A, Rengo G, Koch WJ. Adrenergic nervous system in heart failure: pathophysiology and therapy. *Circ Res* 2013; **113**(6): 739–753.
81. Orrenius S, McConkey DJ, Bellomo G, Nicotera P. Role of Ca^{2+} in toxic cell killing. *Trends Pharmacol Sci* 1989; **10**(7): 281–285.
82. Mulieri LA, Tischler MD, Martin BJ, *et al.* Regional differences in the force-frequency relation of human left ventricular myocardium in mitral regurgitation: implications for ventricular shape. *Am J Physiol Heart Circ Physiol* 2005; **288**(5): H2185–2191.
83. Gupta RC, Mishra S, Mishima T, Goldstein S, Sabbah HN. Reduced sarcoplasmic reticulum Ca(2+)-uptake and expression of phospholamban in left ventricular myocardium of dogs with heart failure. *J Mol Cell Cardiol* 1999; **31**(7): 1381–1389.
84. Sabbah HN. Biologic rationale for the use of beta-blockers in the treatment of heart failure. *Heart Fail Rev* 2004; **9**(2): 91–97.
85. Leszek P, Korewicki J, Klisiewicz A, *et al.* Reduced myocardial expression of calcium handling protein in patients with severe chronic mitral regurgitation. *Eur J Cardiothorac Surg* 2006; **30**(5): 737–743.
86. Dorn GW, 2nd. Apoptotic and non-apoptotic programmed cardiomyocyte death in ventricular remodelling. *Cardiovasc Res* 2009; **81**(3): 465–473.
87. Foo RS, Mani K, Kitsis RN. Death begets failure in the heart. *J Clin Invest* 2005; **115**(3): 565–571.
88. Remondino A, Kwon SH, Communal C, *et al.* Beta-adrenergic receptor-stimulated apoptosis in cardiac myocytes is mediated by reactive oxygen species/c-Jun NH2-terminal kinase-dependent activation of the mitochondrial pathway. *Circ Res* 2003; **92**(2): 136-8.
89. Hankes GH, Ardell JL, Tallaj J, *et al.* Beta1-adrenoceptor blockade mitigates excessive norepinephrine release into cardiac interstitium in mitral regurgitation in dog. *Am J Physiol Heart Circ Physiol* 2006; **291**(1): H147–151.
90. Tsutsui H, Spinale FG, Nagatsu M, *et al.* Effects of chronic beta-adrenergic blockade on the left ventricular and cardiocyte abnormalities of chronic canine mitral regurgitation. *J Clin Invest* 1994; **93**(6): 2639–2648.
91. Janicki JS, Brower GL. The role of myocardial fibrillar collagen in ventricular remodeling and function. *J Card Fail* 2002; **8**(6 Suppl): S319–325.
92. Spinale FG. Myocardial matrix remodeling and the matrix metalloproteinases: influence on cardiac form and function. *Physiol Rev* 2007; **87**(4): 1285–1342.
93. Spinale FG, Coker ML, Heung LJ, *et al.* A matrix metalloproteinase induction/activation system exists in the human left ventricular myocardium and is upregulated in heart failure. *Circulation* 2000; **102**(16): 1944–1949.
94. King MK, Coker ML, Goldberg A, *et al.* Selective matrix metalloproteinase inhibition with developing heart failure: effects on left ventricular function and structure. *Circ Res* 2003; **92**(2): 177–185.
95. Ahmed SH, Clark LL, Pennington WR, *et al.* Matrix metalloproteinases/tissue inhibitors of metalloproteinases: relationship between changes in proteolytic determinants of matrix composition and structural, functional, and clinical manifestations of hypertensive heart disease. *Circulation* 2006; **113**(17): 2089–2096.
96. George J, Patal S, Wexler D, Roth A, Sheps D, Keren G. Circulating matrix metalloproteinase-2 but not matrix metalloproteinase-3, matrix metalloproteinase-9, or tissue inhibitor of metalloproteinase-1 predicts outcome in patients with congestive heart failure. *Am Heart J* 2005; **150**(3): 484–487.
97. Buralli S, Dini FL, Ballo P, *et al.* Circulating matrix metalloproteinase-3 and metalloproteinase-9 and tissue Doppler measures of diastolic dysfunction to risk stratify patients with systolic heart failure. *Am J Cardiol* 2010; **105**(6): 853–856.
98. Lovelock JD, Baker AH, Gao F, et al. Heterogeneous effects of tissue inhibitors of matrix metalloproteinases on cardiac fibroblasts. *Am J Physiol Heart Circ Physiol* 2005; **288**(2): H461–468.
99. Chakraborti S, Mandal M, Das S, Mandal A, Chakraborti T. Regulation of matrix metalloproteinases: an overview. *Mol Cell Biochem* 2003; **253**(1–2): 269–285.

100. Vincenti MP, Brinckerhoff CE. Signal transduction and cell-type specific regulation of matrix metalloproteinase gene expression: can MMPs be good for you? *J Cell Physiol* 2007; **213**(2): 355–364.
101. Klein T, Bischoff R. Physiology and pathophysiology of matrix metalloproteases. *Amino Acids* 2011; **41**(2): 271–290.
102. Siwik DA, Chang DL, Colucci WS. Interleukin-1beta and tumor necrosis factor-alpha decrease collagen synthesis and increase matrix metalloproteinase activity in cardiac fibroblasts in vitro. *Circ Res* 2000; **86**(12): 1259–1265.
103. MacKenna DA, Dolfi F, Vuori K, Ruoslahti E. Extracellular signal-regulated kinase and c-Jun NH2-terminal kinase activation by mechanical stretch is integrin-dependent and matrix-specific in rat cardiac fibroblasts. *J Clin Invest* 1998; **101**(2): 301–310.
104. MacKenna D, Summerour SR, Villarreal FJ. Role of mechanical factors in modulating cardiac fibroblast function and extracellular matrix synthesis. *Cardiovasc Res* 2000; **46**(2): 257–263.
105. Manso AM, Elshrif L, Kang SM, Ross RS. Integrins, membrane-type matrix metalloproteinases and ADAMs: potential implications for cardiac remodeling. *Cardiovasc Res* 2006; **69**(3): 574–584.
106. Ross RS. The extracellular connections: the role of integrins in myocardial remodeling. *J Card Fail* 2002; **8**(6 Suppl): S326–331.
107. Coker ML, Jolly JR, Joffs C, *et al.* Matrix metalloproteinase expression and activity in isolated myocytes after neurohormonal stimulation. *Am J Physiol Heart Circ Physiol* 2001; **281**(2): H543–551.
108. Sabri A, Rafiq K, Seqqat R, Kolpakov MA, Dillon R, Dell'Italia LJ. Sympathetic activation causes focal adhesion signaling alteration in early compensated volume overload attributable to isolated mitral regurgitation in the dog. *Circ Res* 2008; **102**(9): 1127–1136.
109. Ogawa K, Chen F, Kuang C, Chen Y. Suppression of matrix metalloproteinase-9 transcription by transforming growth factor-beta is mediated by a nuclear factor-kappaB site. *Biochem J* 2004; **381**(Pt 2): 413–422.
110. Rouet-Benzineb P, Gontero B, Dreyfus P, Lafuma C. Angiotensin II induces nuclear factor- kappa B activation in cultured neonatal rat cardiomyocytes through protein kinase C signaling pathway. *J Mol Cell Cardiol* 2000; **32**(10): 1767–1778.
111. Seeland U, Haeuseler C, Hinrichs R, *et al.* Myocardial fibrosis in transforming growth factor-beta(1) (TGF-beta(1)) transgenic mice is associated with inhibition of interstitial collagenase. *Eur J Clin Invest* 2002; **32**(5): 295–303.
112. Bujak M, Frangogiannis NG. The role of TGF-beta signaling in myocardial infarction and cardiac remodeling. *Cardiovasc Res* 2007; **74**(2): 184–195.
113. Zheng J, Chen Y, Pat B, *et al.* Microarray identifies extensive downregulation of noncollagen extracellular matrix and profibrotic growth factor genes in chronic isolated mitral regurgitation in the dog. *Circulation* 2009; **119**(15): 2086–2095.
114. Zhang YM, Bo J, Taffet GE, *et al.* Targeted deletion of ROCK1 protects the heart against pressure overload by inhibiting reactive fibrosis. *FASEB J* 2006; **20**(7): 916–125.
115. Jellis C, Martin J, Narula J, Marwick TH. Assessment of nonischemic myocardial fibrosis. *J Am Coll Cardiol* 2010; **56**(2): 89–97.
116. Dell'Italia LJ, Meng QC, Balcells E, *et al.* Increased ACE and chymase-like activity in cardiac tissue of dogs with chronic mitral regurgitation. *Am J Physiol* 1995; **269**(6 Pt 2): H2065–2073.
117. Stewart JA, Jr., Wei CC, Brower GL, *et al.* Cardiac mast cell- and chymase-mediated matrix metalloproteinase activity and left ventricular remodeling in mitral regurgitation in the dog. *J Mol Cell Cardiol* 2003; **35**(3): 311–319.
118. Tallaj J, Wei CC, Hankes GH, *et al.* Beta1-adrenergic receptor blockade attenuates angiotensin II-mediated catecholamine release into the cardiac interstitium in mitral regurgitation. *Circulation* 2003; **108**(2): 225–230.
119. Lin A, Stewart R. Medical treatment of asymptomatic chronic aortic regurgitation. *Expert Rev Cardiovasc Ther* 2011; **9**(9): 1249–1254.
120. Weidemann F, Herrmann S, Stork S, *et al.* Impact of myocardial fibrosis in patients with symptomatic severe aortic stenosis. *Circulation* 2009; **120**(7): 577–584.
121. Weinberg EO, Schoen FJ, George D, *et al.* Angiotensin-converting enzyme inhibition prolongs survival and modifies the transition to heart failure in rats with pressure overload hypertrophy due to ascending aortic stenosis. *Circulation* 1994; **90**(3): 1410–1422.
122. Perry GJ, Wei CC, Hankes GH, *et al.* Angiotensin II receptor blockade does not improve left ventricular function and remodeling in subacute mitral regurgitation in the dog. *J Am Coll Cardiol* 2002; **39**(8): 1374–1379.
123. Babbitt CJ, Shai SY, Harpf AE, Pham CG, Ross RS. Modulation of integrins and integrin signaling molecules in the pressure-loaded murine ventricle. *Histochem Cell Biol* 2002; **118**(6): 431–439.
124. Bloor CM, Nimmo L, McKirnan MD, Zhang Y, White FC. Increased gene expression of plasminogen activators and inhibitors in left ventricular hypertrophy. *Mol Cell Biochem* 1997; **176**(1–2): 265–71.
125. Brower GL, Chancey AL, Thanigaraj S, Matsubara BB, Janicki JS. Cause and effect relationship between myocardial mast cell number and matrix metalloproteinase activity. *Am J Physiol Heart Circ Physiol* 2002; **283**(2): H518–525.
126. Janicki JS, Brower GL, Gardner JD, *et al.* Cardiac mast cell regulation of matrix metalloproteinase-related ventricular remodeling in chronic pressure or volume overload. *Cardiovasc Res* 2006; **69**(3): 657–665.
127. Nagatomo Y, Carabello BA, Coker ML, *et al.* Differential effects of pressure or volume overload on myocardial MMP levels and inhibitory control. *Am J Physiol Heart Circ Physiol* 2000; **278**(1): H151–161.
128. Chancey AL, Brower GL, Peterson JT, Janicki JS. Effects of matrix metalloproteinase inhibition on ventricular remodeling due to volume overload. *Circulation* 2002; **105**(16): 1983–1988.
129. Ljungvall I, Rajamaki MM, Crosara S, *et al.* Evaluation of plasma activity of matrix metalloproteinase-2 and -9 in dogs with myxomatous mitral valve disease. *Am J Vet Res* 2011; **72**(8): 1022–1028.
130. Iwanaga Y, Aoyama T, Kihara Y, Onozawa Y, Yoneda T, Sasayama S. Excessive activation of matrix metalloproteinases coincides with left ventricular remodeling during transition from hypertrophy to heart failure in hypertensive rats. *J Am Coll Cardiol* 2002; **39**(8): 1384–1391.
131. Moustafa SE, Kansal M, Alharthi M, Deng Y, Chandrasekaran K, Mookadam F. Prediction of incipient left ventricular dysfunction in patients with chronic primary mitral regurgitation: a velocity vector imaging study. *Eur J Echocardiogr* 2011; **12**(4): 291–298.
132. Magne J, Mahjoub H, Dulgheru R, Pibarot P, Pierard LA, Lancellotti P. Left ventricular contractile reserve in asymptomatic primary mitral regurgitation. *Eur Heart J* 2014; **35**(24): 1608–1616.
133. Le Tourneau T, de Groote P, Millaire A, *et al.* Effect of mitral valve surgery on exercise capacity, ventricular ejection fraction and neurohormonal activation in patients with severe mitral regurgitation. *J Am Coll Cardiol* 2000; **36**(7): 2263–2269.
134. Mehta RH, Supiano MA, Oral H, *et al.* Compared with control subjects, the systemic sympathetic nervous system is activated in patients with mitral regurgitation. *Am Heart J* 2003; **145**(6): 1078–1085.
135. Nagatsu M, Zile MR, Tsutsui H, *et al.* Native beta-adrenergic support for left ventricular dysfunction in experimental mitral regurgitation normalizes indexes of pump and contractile function. *Circulation* 1994; **89**(2): 818–826.
136. Touyz RM, Schiffrin EL. Signal transduction mechanisms mediating the physiological and pathophysiological actions of angiotensin II in vascu-

lar smooth muscle cells. *Pharmacol Rev* 2000; **52**(4): 639–672.
137. Schieffer B, Bernstein KE, Marrero MB. The role of tyrosine phosphorylation in angiotensin II mediated intracellular signaling and cell growth. *J Mol Med (Berl)* 1996; **74**(2): 85–91.
138. Abe J, Berk BC. Reactive oxygen species as mediators of signal transduction in cardiovascular disease. *Trends Cardiovasc Med* 1998; **8**(2): 59–64.
139. Brasch H, Sicrosławski L, Dominiak P. Angiotensin II increases norepinephrine release from atria by acting on angiotensin subtype 1 receptors. *Hypertension* 1993; **22**(5): 699–704.
140. Farrell DM, Wei CC, Tallaj J, *et al.* Angiotensin II modulates catecholamine release into interstitial fluid of canine myocardium in vivo. *Am J Physiol Heart Circ Physiol* 2001; **281**(2): H813–822.
141. Kagami S, Border WA, Miller DE, Noble NA. Angiotensin II stimulates extracellular matrix protein synthesis through induction of transforming growth factor-beta expression in rat glomerular mesangial cells. *J Clin Invest* 1994; **93**(6): 2431–2437.
142. Goldsmith EC, Bradshaw AD, Spinale FG. Cellular mechanisms of tissue fibrosis. 2. Contributory pathways leading to myocardial fibrosis: moving beyond collagen expression. *Am J Physiol Cell Physiol* 2013; **304**(5): C393–402.
143. Ryan TD, Rothstein EC, Aban I, *et al.* Left ventricular eccentric remodeling and matrix loss are mediated by bradykinin and precede cardiomyocyte elongation in rats with volume overload. *J Am Coll Cardiol* 2007; **49**(7): 811–821.
144. Levine HJ, Gaasch WH. Vasoactive drugs in chronic regurgitant lesions of the mitral and aortic valves. *J Am Coll Cardiol* 1996; **28**(5): 1083–1091.
145. Nemoto S, Hamawaki M, De Freitas G, Carabello BA. Differential effects of the angiotensin-converting enzyme inhibitor lisinopril versus the beta-adrenergic receptor blocker atenolol on hemodynamics and left ventricular contractile function in experimental mitral regurgitation. *J Am Coll Cardiol* 2002; **40**(1): 149–154.
146. Oh SH, Meyers DG. Afterload reduction may halt and beta-adrenergic blockade may worsen progression of left ventricular dysfunction in patients with chronic compensated mitral regurgitation: a retrospective cohort study. *Angiology* 2007; **58**(2): 196–202.
147. Woo AY, Xiao RP. Beta-adrenergic receptor subtype signaling in heart: from bench to bedside. *Acta Pharmacol Sin* 2012; **33**(3): 335–341.
148. Belge C, Hammond J, Dubois-Deruy E, *et al.* Enhanced expression of β3-adrenoceptors in cardiac myocytes attenuates neurohormone-induced hypertrophic remodeling through nitric oxide synthase. *Circulation* 2014; **129**(4): 451–462.
149. Chidsey CA, Braunwald E, Morrow AG, Mason DT. Myocardial norepinephrine concentration in man. Effects of reserpine and of congestive heart failure. *N Engl J Med* 1963; **269**: 653–658.
150. Fowler MB, Bristow MR. Rationale for beta-adrenergic blocking drugs in cardiomyopathy. *Am J Cardiol* 1985; **55**(10): 120d–124d.
151. Bristow MR, Ginsburg R, Minobe W, *et al.* Decreased catecholamine sensitivity and beta-adrenergic-receptor density in failing human hearts. *N Engl J Med* 1982; **307**(4): 205–211.
152. Lowes BD, Minobe W, Abraham WT, *et al.* Changes in gene expression in the intact human heart. Downregulation of alpha-myosin heavy chain in hypertrophied, failing ventricular myocardium. *J Clin Invest* 1997; **100**(9): 2315–2324.
153. Lowes BD, Gilbert EM, Abraham WT, *et al.* Myocardial gene expression in dilated cardiomyopathy treated with beta-blocking agents. *N Engl J Med* 2002; **346**(18): 1357–1365.
154. Engelhardt S, Bohm M, Erdmann E, Lohse MJ. Analysis of beta-adrenergic receptor mRNA levels in human ventricular biopsy specimens by quantitative polymerase chain reactions: progressive reduction of beta 1-adrenergic receptor mRNA in heart failure. *J Am Coll Cardiol* 1996; **27**(1): 146–154.
155. Hammond HK, Roth DA, Insel PA, *et al.* Myocardial beta-adrenergic receptor expression and signal transduction after chronic volume-overload hypertrophy and circulatory congestion. *Circulation* 1992; **85**(1): 269–80.
156. Choi DJ, Koch WJ, Hunter JJ, Rockman HA. Mechanism of beta-adrenergic receptor desensitization in cardiac hypertrophy is increased beta-adrenergic receptor kinase. *J Biol Chem* 1997; **272**(27): 17223–17229.
157. Osadchii OE, Norton GR, McKechnie R, Defterevos D, Woodiwiss AJ. Cardiac dilatation and pump dysfunction without intrinsic myocardial systolic failure following chronic beta-adrenoreceptor activation. *Am J Physiol Heart Circ Physiol* 2007; **292**(4): H1898–1905.
158. Packer M, Fowler MB, Roecker EB, *et al.* Effect of carvedilol on the morbidity of patients with severe chronic heart failure: results of the carvedilol prospective randomized cumulative survival (COPERNICUS) study. *Circulation* 2002; **106**(17): 2194–2199.
159. Kohout TA, Takaoka H, McDonald PH, *et al.* Augmentation of cardiac contractility mediated by the human beta(3)-adrenergic receptor overexpressed in the hearts of transgenic mice. *Circulation* 2001; **104**(20): 2485–2491.
160. Zhao Q, Wu TG, Jiang ZF, Chen GW, Lin Y, Wang LX. Effect of beta-blockers on beta3-adrenoceptor expression in chronic heart failure. *Cardiovasc Drugs Ther* 2007; **21**(2): 85–90.
161. Yue TL, Cheng HY, Lysko PG, *et al.* Carvedilol, a new vasodilator and beta adrenoceptor antagonist, is an antioxidant and free radical scavenger. *J Pharmacol Exp Ther* 1992; **263**(1): 92–98.
162. Ohlstein EH, Douglas SA, Sung CP, *et al.* Carvedilol, a cardiovascular drug, prevents vascular smooth muscle cell proliferation, migration, and neointimal formation following vascular injury. *Proc Natl Acad Sci U S A* 1993; **90**(13): 6189–6193.
163. Wisler JW, DeWire SM, Whalen EJ, *et al.* A unique mechanism of beta-blocker action: carvedilol stimulates beta-arrestin signaling. *Proc Natl Acad Sci USA* 2007; **104**(42): 16657–16662.
164. Gilbert EM, Abraham WT, Olsen S, *et al.* Comparative hemodynamic, left ventricular functional, and antiadrenergic effects of chronic treatment with metoprolol versus carvedilol in the failing heart. *Circulation* 1996; **94**(11): 2817–2825.
165. Stoschitzky K, Koshucharova G, Zweiker R, *et al.* Differing beta-blocking effects of carvedilol and metoprolol. *Eur J Heart Fail* 2001; **3**(3): 343–349.
166. Quaife RA, Christian PE, Gilbert EM, Datz FL, Volkman K, Bristow MR. Effects of carvedilol on right ventricular function in chronic heart failure. *Am J Cardiol* 1998; **81**(2): 247–250.
167. Beck-da-Silva L, de Bold A, Davies R, *et al.* Effect of bisoprolol on right ventricular function and brain natriuretic peptide in patients with heart failure. *Congest Heart Fail* 2004; **10**(3): 127–132.
168. Hongning Y, Stewart RA, Whalley GA. The impact of beta-blockade on right ventricular function in mitral regurgitation. *Heart Lung Circ* 2014; **23**(4): 378–380.
169. The Cardiac Insufficiency Bisoprolol Study II (CIBIS-II): a randomised trial. *Lancet* 1999; **353**(9146): 9–13.
170. Effect of metoprolol CR/XL in chronic heart failure: Metoprolol CR/XL Randomised Intervention Trial in Congestive Heart Failure (MERIT-HF). *Lancet* 1999; **353**(9169): 2001–2007.
171. Poole-Wilson PA, Swedberg K, Cleland JG, *et al.* Comparison of carvedilol and metoprolol on clinical outcomes in patients with chronic heart failure in the Carvedilol Or Metoprolol European Trial (COMET):

randomised controlled trial. *Lancet* 2003; **362**(9377): 7–13.
172. Naccarelli GV, Lukas MA. Carvedilol's antiarrhythmic properties: therapeutic implications in patients with left ventricular dysfunction. *Clin Cardiol* 2005; **28**(4): 165–173.
173. Bristow MR. beta-adrenergic receptor blockade in chronic heart failure. *Circulation* 2000; **101**(5): 558–569.
174. Nagatsu M, Spinale FG, Koide M, *et al.* Bradycardia and the role of beta-blockade in the amelioration of left ventricular dysfunction. *Circulation* 2000; **101**(6): 653–659.
175. Communal C, Singh K, Sawyer DB, Colucci WS. Opposing effects of beta(1)- and beta(2)-adrenergic receptors on cardiac myocyte apoptosis: role of a pertussis toxin-sensitive G protein. *Circulation* 1999; **100**(22): 2210–2212.
176. Mason RP, Giles TD, Sowers JR. Evolving mechanisms of action of beta blockers: focus on nebivolol. *J Cardiovasc Pharmacol* 2009; **54**(2): 123–128.
177. Saini-Chohan HK, Hatch GM. Biological actions and metabolism of currently used pharmacological agents for the treatment of congestive heart failure. *Curr Drug Metab* 2009; **10**(3): 206–219.
178. Wu TC, Chen YH, Leu HB, *et al.* Carvedilol, a pharmacological antioxidant, inhibits neointimal matrix metalloproteinase-2 and -9 in experimental atherosclerosis. *Free Radic Biol Med* 2007; **43**(11): 1508–1522.
179. Lohse MJ, Engelhardt S, Eschenhagen T. What is the role of beta-adrenergic signaling in heart failure? *Circ Res* 2003; **93**(10): 896–906.
180. Trappanese DM, Liu Y, McCormick RC, *et al.* Chronic beta1-adrenergic blockade enhances myocardial beta3-adrenergic coupling with nitric oxide-cGMP signaling in a canine model of chronic volume overload: new insight into mechanisms of cardiac benefit with selective beta1-blocker therapy. *Basic Res Cardiol* 2015; **110**(1): 456.
181. Starling MR. Effects of valve surgery on left ventricular contractile function in patients with long-term mitral regurgitation. *Circulation* 1995; **92**(4): 811–818.
182. Witkowski TG, Thomas JD, Delgado V, *et al.* Changes in left ventricular function after mitral valve repair for severe organic mitral regurgitation. *Ann Thorac Surg* 2012; **93**(3): 754–760.
183. Kainuma S, Taniguchi K, Toda K, *et al.* B-type natriuretic peptide response and reverse left ventricular remodeling after surgical correction of functional mitral regurgitation in patients with advanced cardiomyopathy. *J Cardiol* 2015; **66**(4): 279–285.
184. Bonow RO, Carabello BA, Chatterjee K, *et al.* 2008 focused update incorporated into the ACC/AHA 2006 guidelines for the management of patients with valvular heart disease: a report of the American College of Cardiology/American Heart Association Task Force on Practice Guidelines (Writing Committee to revise the 1998 guidelines for the management of patients with valvular heart disease). Endorsed by the Society of Cardiovascular Anesthesiologists, Society for Cardiovascular Angiography and Interventions, and Society of Thoracic Surgeons. *J Am Coll Cardiol* 2008; **52**(13): e1–142.
185. Hetzer R, Dandel M. Early detection of left ventricular dysfunction in patients with mitral regurgitation due to flail leaflet is still a challenge. *Eur Heart J* 2011; **32**(6): 665–667.
186. Carabello BA. Beta-blockade for mitral regurgitation: could the management of valvular heart disease actually be moving into the 21st century? *J Am Coll Cardiol* 2012; **60**(9): 839–840.
187. Samad Z, Kaul P, Shaw LK, et al. Impact of early surgery on survival of patients with severe mitral regurgitation. *Heart* 2011; **97**(3): 221–224.
188. Kang DH, Park SJ, Sun BJ, *et al.* Early surgery versus conventional treatment for asymptomatic severe mitral regurgitation: a propensity analysis. *J Am Coll Cardiol* 2014; **63**(22): 2398–2407.
189. Yazdchi F, Koch CG, Mihaljevic T, *et al.* Increasing disadvantage of 'watchful waiting' for repairing degenerative mitral valve disease. *Ann Thorac Surg* 2015; **99**(6): 1992–2000.
190. Barbieri A, Bursi F, Grigioni F, *et al.* Prognostic and therapeutic implications of pulmonary hypertension complicating degenerative mitral regurgitation due to flail leaflet: a multicenter long-term international study. *Eur Heart J* 2011; **32**(6): 751–759.
191. Rosenhek R, Rader F, Klaar U, *et al.* Outcome of watchful waiting in asymptomatic severe mitral regurgitation. *Circulation* 2006; **113**(18): 2238–2244.
192. Eskesen K, Olsen NT, Dimaano VL, Fritz-Hansen T, Sogaard P, Abraham TP. Effects of early and late-onset treatment with carvedilol in an experimental model of aortic regurgitation. *Springerplus* 2015; **4**: 52.
193. Carabello BA. The current therapy for mitral regurgitation. *J Am Coll Cardiol* 2008; **52**(5): 319–326.
194. Wisenbaugh T. Vasoactive medications in the treatment of severe mitral regurgitation. *Coron Artery Dis* 2000; **11**(1): 19–22.
195. Wisenbaugh T, Sinovich V, Dullabh A, Sareli P. Six month pilot study of captopril for mildly symptomatic, severe isolated mitral and isolated aortic regurgitation. *J Heart Valve Dis* 1994; **3**(2): 197–204.
196. Stewart RA, Raffel OC, Kerr AJ, *et al.* Pilot study to assess the influence of beta-blockade on mitral regurgitant volume and left ventricular work in degenerative mitral valve disease. *Circulation* 2008; **118**(10): 1041–1046.
197. Ennis DB, Rudd-Barnard GR, Li B, *et al.* Changes in mitral annular geometry and dynamics with ss-blockade in patients with degenerative mitral valve disease. *Circ Cardiovasc Imaging* 2010; **3**(6): 687–693.
198. Varadarajan P, Joshi N, Appel D, Duvvuri L, Pai RG. Effect of Beta-blocker therapy on survival in patients with severe mitral regurgitation and normal left ventricular ejection fraction. *Am J Cardiol* 2008; **102**(5): 611–615.
199. Ahmed MI, Aban I, Lloyd SG, *et al.* A Randomized controlled phase IIb trial of beta1-receptor blockade for chronic degenerative mitral regurgitation. *J Am Coll Cardiol* 2012; **60**(9): 833–838.
200. Pat B, Killingsworth C, Denney T, *et al.* Dissociation between cardiomyocyte function and remodeling with beta-adrenergic receptor blockade in isolated canine mitral regurgitation. *Am J Physiol Heart Circ Physiol* 2008; **295**(6): H2321–2327.
201. Pu M, Gao Z, Pu DK, Davidson WR Jr. Effects of early, late, and long-term nonselective beta-blockade on left ventricular remodeling, function, and survival in chronic organic mitral regurgitation. *Circ Heart Fail* 2013; **6**(4): 756–762.
202. Capomolla S, Febo O, Gnemmi M, *et al.* Beta-blockade therapy in chronic heart failure: diastolic function and mitral regurgitation improvement by carvedilol. *Am Heart J* 2000; **139**(4): 596–608.